

**THE CHARACTERIZATION OF GELATINASE INHIBITION AND THE
INVOLVEMENT OF THE MATRIX METALLOPROTEINASES AND THEIR
INHIBITORS IN GLAUCOMA AND A RETINAL DEGENERATION**

by

Janice A. Vranka

A DISSERTATION

Presented to the Department of Biochemistry and Molecular Biology

and the Oregon Health Sciences University

School of Medicine

in partial fulfillment of

the requirements for the degree of

Doctor of Philosophy

April 1997

School of Medicine
Oregon Health Sciences University

CERTIFICATE OF APPROVAL


This is certify that the Ph.D. thesis of

Janice A. Vranka

has been approved



Professor in charge of thesis



Member



Member



Member



Member

Associate Dean for Graduate Studies

TABLE OF CONTENTS

	<u>Page</u>
I. Introduction	1
II. Expression and Purification of TIMP-1, -2, -3, and Purification of Gelatinase A and B.	
A. Introduction	23
B. Materials and Methods	28
C. Results	48
D. Discussion	75
III. Gelatinase A and B Inhibition Kinetics; A Glaucoma Model System	
A. Introduction	79
B. Materials and Methods	90
C. Results	99
D. Discussion	145
IV. Patterns of Expression of human TIMP-3	
A. Introduction	154
B. Materials and Methods	158

C.	Results	165
D.	Discussion	188
V.	Conclusions	194
VI.	References	199

LIST OF FIGURES

<u>Figures</u>	<u>Page</u>
Figure 1. The Domain Structure of the Matrix Metalloproteinases.	5
Figure 2. The Catalytic Domain of Fibroblast Collagenase.	7
Figure 3. Comparison of Promoter Regions of the MMPs.	10
Figure 4. The Cysteine Switch.	12
Figure 5. Schematic of TIMP-1 Domain Structure.	16
Figure 6. The Structure of the N-Terminal Domain of TIMP-2.	18
Figure 7. Interference of Multiple Viral Infections.	25
Figure 8. Ping-Pong Amplification.	27
Figure 9. The Bacterial Expression Vectors, pMAL and pGEX.	31
Figure 10. The pSFF Expression Vector.	37
Figure 11. The pCEP4 Expression Vector.	43
Figure 12. PCR Amplification of TIMP-1 cDNA.	49
Figure 13. Restriction Digestions of pMAL.	50
Figure 14. PCR Amplification of pMAL-TIMP-1 Clones.	51
Figure 15. Southern Blot of pMAL-TIMP-1 Clones.	52
Figure 16. Western Immunoblot of MBP-TIMP-1 Protein.	53
Figure 17. Restriction Digestion of pGEX.	55
Figure 18. Restriction Digestion of pGEX-TIMP-1 Clones.	56
Figure 19. Coomassie Gel and Western blot of GST-TIMP-1 Protein.	58

Figure 20. Restriction Digestion of pSFF and TIMP-1 for Cloning.	60
Figure 21. PCR Amplification of pSFF-TIMP-1 Clones.	61
Figure 22. RT-PCR of pSFF-TIMP-1-Transfected Cells.	62
Figure 23. Western Immunoblot of Purified MBP-TIMP-2.	64
Figure 24. Restriction Digestions of pCEP4 and TIMP-3 for Cloning.	66
Figure 25. Restriction Digestions of pCEP4-TIMP-3 Clones.	67
Figure 26. Western Immunoblots of pCEP4-TIMP-3-Transfected Cells.	68
Figure 27. Western Immunoblot of TIMP-3 Purification.	70
Figure 28. Silver Stained Gel of Purified TIMP-3.	71
Figure 29. Reverse Zymogram of TIMP-3.	72
Figure 30. Gelatin Zymogram and Western Blot of Gelatinase A and B.	74
Figure 31. The $\alpha 1$ Type I Collagen Cleavage Site.	83
Figure 32. Structure of the Right-Hand Side Inhibitors and a Hydroxamate Inhibitor.	84
Figure 33. Anatomical Structure of the Eye.	88
Figure 34. The ECMs of the Human Trabecular Meshwork.	89
Figure 35. Structures of the Matrix Metalloproteinase Inhibitors.	93
Figure 36. Structure of the Matrix Metalloproteinase Inhibitors.	94
Figure 37. Graphical Representation of Various Inhibition Mechanisms.	96
Figure 38. Perfused Anterior Segment Explant Organ Culture.	98
Figure 39. Gelatinase A Activity on FITC-Gelatin Substrate.	102
Figure 40. Gelatinase B Activity on FITC-Gelatin Substrate	103

Figure 41. Kinetics of Gelatinase A and B Activity on FITC-Gelatin.	104
Figure 42. IC ₅₀ Graphs of Gelatinase A Inhibition.	109
Figure 43. IC ₅₀ Graphs of Gelatinase B Inhibition.	110
Figure 44. Gelatinase A, B Inhibition with Minocycline on FITC-Gelatin.	112
Figure 45. Gelatinase A and B Inhibition with Trp-Hydroxamate.	113
Figure 46. Gelatinase A and B Inhibition with Collagenase Inhibitor.	114
Figure 47. Gelatinase A Inhibition with p-Hydroxybenzoyl-Ala-Phe.	115
Figure 48. Gelatinase A and B Inhibition with RCGVP Propeptide.	116
Figure 49. Gelatinase A and B Inhibition with RCGVPD Propeptide.	117
Figure 50. Gelatinase A and B Inhibition with RCGNPD Propeptide.	118
Figure 51. Table: Inhibition Constants of Gelatinase A on FITC-Gelatin.	119
Figure 52. Table: Inhibition Constants of Gelatinase B on FITC-Gelatin.	120
Figure 53. Gelatinase A in the Presence of EDTA, PMSFor Phenan.	123
Figure 54. Gelatin Zymogram of Gelatinase A and B.	124
Figure 55. Graph of Gelatinase A and B Concentration Curve on Mca-Peptide Substrate.	126
Figure 56. Gelatinase A Activity on Mca-Peptide Substrate.	127
Figure 57. Gelatinase B Activity on Mca-Peptide Substrate.	128
Figure 58. Kinetics of Gelatinase A and B Activity on Mca-Peptide.	129
Figure 59. IC ₅₀ Graphs of Gelatinase A Inhibition.	130.
Figure 60. IC ₅₀ Graphs of Gelatinase B Inhibition.	132
Figure 61. Gelatinase A and B Inhibition with Minocycline.	133

Figure 62. Gelatinase A and B Inhibition with Trp-Hydroxamate.	134
Figure 63. Gelatinase A and B Inhibition with Collagenase Inhibitor.	135
Figure 64. Gelatinase A and B Inhibition with RCGVPD Propeptide.	136
Figure 65. Gelatinase A and B Inhibition with RCGNPD Propeptide.	137
Figure 66. Gelatinase A and B Inhibition with rhTIMP-1.	139
Figure 67. Gelatinase A Inhibition with TIMP-3.	140
Figure 68. Dixon and Cornish Bowen Plots of Gelatinase B Inhibition.	142
Figure 69. Table of Inhibition Constants of Gelatinase A on Mca-Peptide.	143
Figure 70. Table of Inhibition Constants of Gelatinase B on Mca-Peptide.	144
Figure 71. Outflow Rate Changes in Response to Various Modulators.	146
Figure 72. Outflow Rate Changes in Response to Various Modulators.	147
Figure 73. Schematic of Human Retina.	155
Figure 74. RT-PCR of TIMP mRNA Expression.	166
Figure 75. Northern Analysis of TIMP mRNA Expression.	168
Figure 76. Restriction Digestion of TIMP-3 PCR Product.	169
Figure 77. RT-PCR of TIMP mRNA Expression from RPE Cells.	170
Figure 78. Immunohistochemistry of TIMP Expression in the Retina.	172
Figure 79. Confocal Microscopy of TIMPs in RPE Cells.	174
Figure 80. Confocal Microscopy of TIMP-3 in RPE Cells.	176
Figure 81. Western Immunoblot of TIMP Expression in RPE Cells.	178
Figure 82. Restriction Digestion of TIMP-3 PCR Product from Cells.	179
Figure 83. Western Blot of TIMP-3 from Normal and Mutant Cells.	181

Figure 84. Confocal Microscopy of TIMP-3 in Normal and Mutant Cells.	182
Figure 85. Photomicrograph of TIMP-3 Protein in Monolayers of Cells.	183
Figure 86. Photomicrograph of TIMP-3 Protein in Multilayers of Cells.	185
Figure 87. Confocal Microscopy of TIMP-3 in Multilayers of Cells.	186
Figure 88. Confocal Microscopy of TIMP-3 in Unfixed Cells.	187

ACKNOWLEDGEMENTS

I would like to thank Dr. Ted Acott for his insightful advising, his never-ending enthusiasm in science, and his sense of humor through all of the ups and downs of the ongoing projects. I would also like to thank the all of the people in the Acott lab who supported me, discussed ideas, made helpful suggestions along the way, and made it a good environment in which to work. They are: Christine Colvis, John Bradley, Aurelie Snyder, Xianghong Zhu, Amy Shepardson, Lisa Parshley, Preston Alexander, Dennis Schultz, and all of the others not mentioned.

My research advisory committee has been extremely helpful in their comments, suggestions and directions. They are: Dr. Caroline Enns, Dr. Lynn Sakai, and Dr. Hans Peter Bachinger.

I would also like to thank my family for their unerring support along the way. Thanks to my good friend Anne Lee for her encouragement and thanks to Kennedy Wambalaba for his patience, understanding and support.

ABSTRACT

The extracellular matrix plays a pivotal role in maintaining the structural integrity of tissues, as well as possessing the ability to modulate the behavior of the cells with which it is associated. The extracellular matrix (ECM) is made up of various structural components and exists in a dynamic equilibrium of degradation and synthesis that is required for cellular homeostasis. The matrix metalloproteinases (MMPs) are a family of zinc-dependent, calcium-stabilized enzymes that degrade various components of the extracellular matrix in a strictly regulated manner. The interaction of the matrix metalloproteinases with their natural tissue inhibitors, the tissue inhibitors of metalloproteinases (TIMPs), is a key event in the regulation of the matrix-degrading activity of these enzymes. Uncontrolled MMP activity has been shown to lead to various pathological states, as is the case for arthritis, and an imbalance in the net MMP/TIMP activity is thought to be a primary factor in the development of various diseases, including cancer cell invasion and metastasis.

Although the MMP and TIMP interactions have been studied recently, specific details on the mechanism of action of the MMPS, as well as the mode by which the TIMPS inhibit their enzymatic activity remain to be elucidated. One of the goals of these studies was to analyze the inhibition of gelatinase A and B, two members of the MMP family, in the presence of various selected inhibitors in order to determine their efficacy, specificity, and possible mechanism of inhibition. Two distinct enzymatic assays were utilized for the study of the kinetics of gelatinase A and B activity and their inhibition,

including a protein-substrate-based tube assay, and a continuously-recording fluorescent peptide substrate assay. The inhibitors selected for analysis were shown to selectively inhibit the gelatinases via different mechanisms of action.

A second goal of these studies was to determine the involvement of the gelatinases and the TIMPs in primary open-angle glaucoma. Although the cause of primary open-angle glaucoma is unclear, our working hypothesis is that the balance of MMP/TIMP activity in the ECM of the trabecular meshwork may be disrupted causing a build-up of ECM components at the point of aqueous humor outflow in the eye. This then may lead to the increase in intraocular pressure seen in primary open-angle glaucoma. In order to test this hypothesis, the same inhibitors that had been shown to inhibit the gelatinases were put into a glaucoma model system developed in the Acott lab where the changes in the outflow rate versus time can be measured. Purified MMPs, when added to the outflow system, were shown to increase the flow rate gradually over time. In contrast, when a MMP inhibitor was added to the perfusion medium, the outflow rate decreased gradually over time, causing a “glaucomatous” state. These results have shown that the MMPs and TIMPs may be involved in the development of this disease.

The final goal of these studies was to characterize the expression of TIMP-3 in various eye tissues, as well as characterize the expression of a mutant TIMP-3 from skin fibroblasts. Mutations in TIMP-3 have been shown to be associated with an autosomal dominant disorder called Sorsby’s fundus dystrophy (SFD). SFD shares similar clinical features with age-related macular degeneration (AMD), where affected patients develop lipid- and ECM-containing deposits, thickening of Bruch’s membrane, and subsequent

neovascularization and atrophy of the choroid, RPE and retina. The TIMP-3 mutations that have been found thus far in SFD patients are single mutations to a cysteine, although how such mutations may lead to the development of the disease remains unclear.

Therefore, the aim of these studies was to determine the expression and localization of the TIMPs, especially that of TIMP-3, in various eye tissues.

The TIMPs were found to have discrete distribution and expression patterns within the retina and choroid. Interestingly, TIMP-3 was the predominant TIMP found localized to Bruch's membrane. These results suggest a possible role for TIMP-3 in the retina and Bruch's membrane as possible localized "protection" against MMP proteolytic activity. The mutation in TIMP-3 may alter the proper folding of the inhibitor thereby affecting the protein's ability to properly inhibit an active MMP molecule. Alternative possibilities exist for the function and role of the TIMPs in the retina and choroid. Additionally, mutant cells were obtained from SFD patients and the TIMP-3 protein expression was analyzed between the mutant and normal cells. In summary, no significant differences of TIMP-3 protein expression or localization were observed between the mutant and the normal. The effects of the TIMP-3 mutations may be relatively subtle and these results are in agreement with the clinical development of the disease, which has a relatively late age of onset.

I. Introduction

Overview - Normal tissue architecture is maintained by interactions between cells and the extracellular matrix (ECM). The ECM not only stabilizes the physical structure of the tissues, but also modulates the behavior of cells, as well as serving as a barrier in order to maintain the integrity of each cell and tissue with which it is associated. The ECM contains primary structural components such as collagen, elastin and several proteoglycans, as well as tissue-specific complexes of proteins such as laminin, type IV collagen and fibronectin, that ultimately determine specific cellular properties. The ECM plays a critical role in maintaining the structural integrity of tissues by influencing cellular processes such as proliferation, differentiation, migration, adhesion, and embryo development and morphogenesis. Cells produce and assemble the components of the ECM, while simultaneously retaining the ability to produce and secrete the proteolytic enzymes necessary for molecular disassembly of the same matrix macromolecules. Clearly, a dynamic equilibrium exists between the synthesis and degradation of ECM macromolecules for matrix maintenance and tissue integrity.

Collectively, the matrix metalloproteinases (MMPs) have the combined ability to degrade the various protein components of connective tissue matrices in a controlled manner. Although many proteinases can cleave specific ECM molecules, the MMPs are believed to be the normal, physiologically-relevant mediators of matrix degradation. Under normal circumstances, the enzymes are therefore important in such processes as development and tissue remodeling, including uterine involution, wound healing, bone

morphogenesis and angiogenesis [1]. The activity of the MMPs is strictly regulated and required for the continuation of normal processes (see reviews) [2-4]. In addition to their roles in normal physiologic processes, and perhaps as a consequence of uncontrolled MMP activity, the MMPs have been found to be associated with various pathological processes such as rheumatoid arthritis [5-7], osteoarthritis [8, 9], periodontitis [10-14], cancer cell invasion and metastasis [15-18].

The Matrix Metalloproteinases - The matrix metalloproteinases are a family of zinc-dependent, calcium-stabilized endopeptidases, whose natural substrates are various ECM macromolecules. This family consists of fibroblast, neutrophil and breast carcinoma-derived collagenases [19-21], stromelysin-1, -2, and -3 [22, 23], 92 kDa and 72 kDa gelatinases (gelatinases B and A, respectively) [24-26], macrophage metalloelastase (MME) [27], matrilysin [28], and the recently-described membrane-type metalloproteinase-1 and -2 [29, 30].

The interstitial collagenases are the most specific of the MMPs, cleaving the native helix of the fibrillar collagens (types I, II, and III) at a single locus. Neutrophil collagenase is expressed by neutrophil granules and is a considerably more efficient enzyme than the fibroblast collagenase on most substrates except for type III collagen [31, 32]. Fibroblast collagenase is expressed by many different cell types. The proteolytic activity of the collagenases is not limited to types I, II and III collagen, but includes other collagens, gelatin, and proteoglycan core proteins, although their specific activities are lower on these substrates [32]. Collagenase-3 is expressed by breast tumors and preferentially

cleaves type II collagen [33].

The stromelysins cleave a broad range of ECM protein substrates, including proteoglycans, types IV and V collagen, fibronectin, laminin, elastin, and the propeptides of collagenase and 92 kDa gelatinase [34-38]. Stromelysin-1 is expressed by fibroblasts, macrophages, endothelial cells, and cartilage [22, 39]. Stromelysin-2 has been found to be expressed less abundantly, but is active in normal keratinocytes and is expressed in some human carcinomas [35, 40]. Stromelysin-3 was identified through its expression in stromal cells surrounding invasive breast carcinomas and later in other human carcinomas, and has therefore been implicated in tumor progression [23, 41]. It was found to have a restricted substrate specificity and some sequence differences that make it distinct from all other MMPs [42-44].

The gelatinases, otherwise known as the type IV collagenases, have a high affinity for gelatin (denatured collagens), types IV, V, VII, X, and XI collagen, and elastin. Gelatinase A (the 72 kDa gelatinase) is widely distributed and has been identified in most normal cell types studied, as well as in some transformed cells [45-47]. Expression of gelatinase B (the 92 kDa gelatinase) has been observed in keratinocytes, monocytes, and in a number of malignant or transformed cell types [26, 48, 49]. There are some differences in the gelatinase substrate specificities, though both enzymes have similar affinities for types IV and V collagen, gelatin, and elastin. However the activity against other substrates, including fibronectin, laminin, and types I and III collagen was different between the two metalloproteinases [50, 51].

Other members of the MMP family include matrilysin (or PUMP, a putative

metalloproteinase), macrophage metalloelastase (MME), and the membrane-type metalloproteinases. Matrilysin is normally expressed in the human endometrium and in mononuclear phagocytes [52, 53], and has been isolated from rectal carcinoma cells [54]. Matrilysin cleaves a wide range of substrates including fibronectin, laminin, casein, gelatin and elastin [28, 55]. Macrophage metalloelastase was first cloned from mouse macrophages and was found to degrade many matrix molecules, including insoluble elastin [27, 56]. Finally, the membrane-type matrix metalloproteinase (MT-MMP-1) has been found recently and is expressed in stromal cells of human colon, breast, and head and neck carcinomas [29, 57]. MT-MMP-1 was found to have gelatinolytic activity and had the ability of degrading other matrix molecules such as fibronectin, laminin, vitronectin, casein, and elastin, as well as being capable of activating progelatinase A [58-61].

The predicted amino acid sequences of all of the MMPs, when aligned, demonstrate a high degree of conservation among the various members, and the MMPs may be broadly divided into distinct domains (Fig. 1) [2-4, 16]. The MMP sequences all contain a hydrophobic signal sequence as all of the MMPs are secreted proteins. This is then followed by a propeptide sequence of 77-87 amino acids that makes up the amino terminal domain of the secreted MMP precursor. The propeptide domain, and more specifically a highly-conserved region of this domain PRCGXPD, is important in maintaining the enzyme in a catalytically inactive form. This propeptide domain, consisting of approximately 80 amino acids, is lost upon activation of the enzyme [62-64]. Once the enzymes have undergone initial activation, they slowly truncate themselves within the C-terminal domains generating small molecular weight enzymes that have

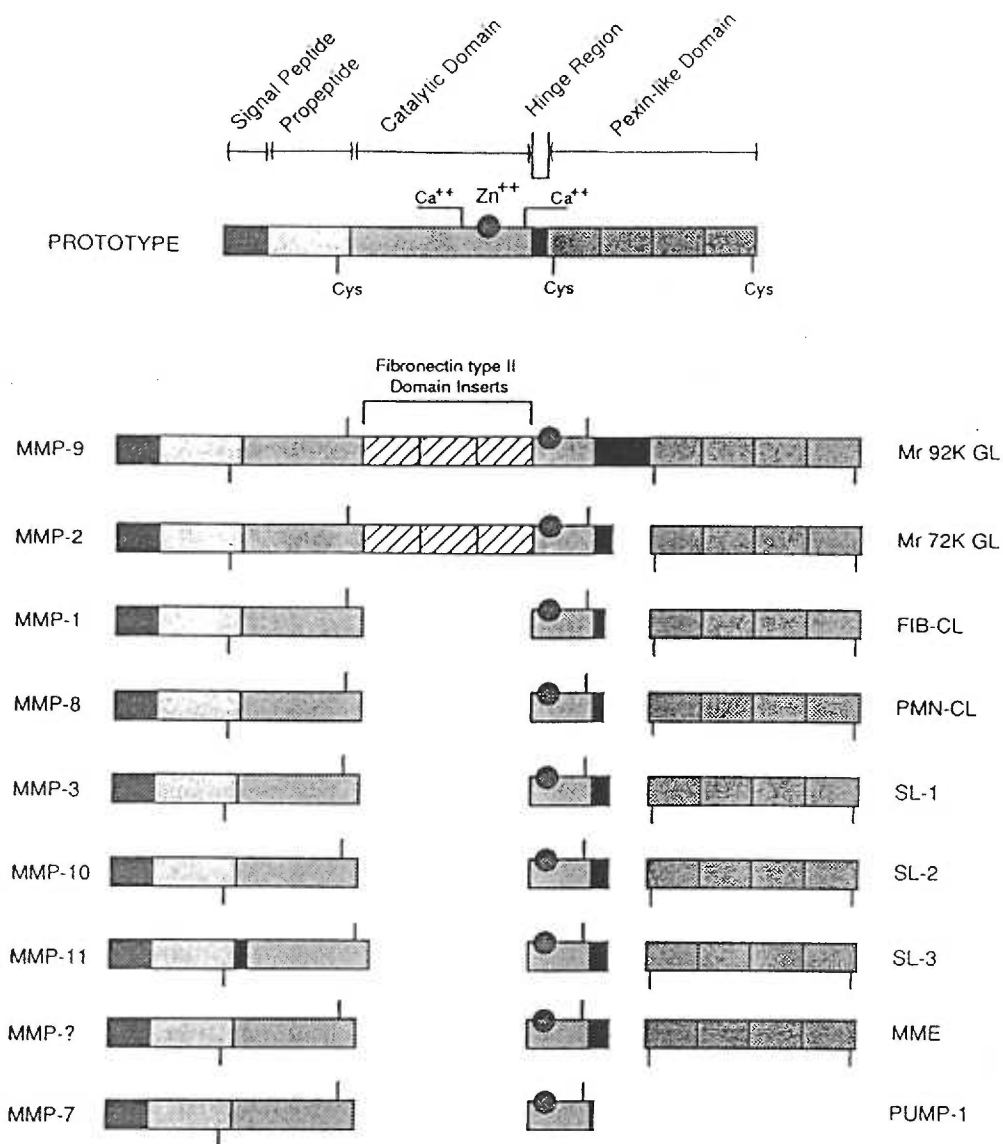


Figure 1: Domain Structure of the Matrix Metalloproteinases. MMP-9 and MMP-2 are gelatinase B and A, respectively. MMP-1 and MMP-8 are fibroblast and neutrophil collagenase, respectively. MMP-3, MMP-10, and MMP-11 are the three stromelysins. MME is the macrophage metalloelastase, and MMP-7 is matrilysin. (from: H. Birkedal-Hansen, "Matrix Metalloproteinases: A Review", *Crit. Rev. Oral Biol. Med.*, 4(2): 197, 1993.)

retained catalytic activity against their substrates [65].

The MMPs all have a catalytic domain, which contains a conserved zinc-binding site at its core. The crystal or NMR structures have recently been solved for matrilysin, the catalytic domains of stromelysin, collagenase, and previously for the bacterial endoproteinase, thermolysin [66-72]. This has provided information on the tertiary structure of the catalytic domain of the MMPs and possible reaction mechanisms at the active site have been proposed. The global fold of the catalytic domain for matrilysin, stromelysin, neutrophil collagenase, and fibroblast collagenase consists of three helices and a five-stranded β -sheet. The diagram in figure 2 is the catalytic domain of fibroblast collagenase complexed with a hydroxamate peptide inhibitor, and is representative of the MMP catalytic domains. The β -sheet consists of four parallel strands (A, B, C, and E) and one antiparallel strand (D). The long N-terminal α -helix (I) runs along the line of β -strand B, which is twisted relative to the β -sheet. The central helix (II) lies under the β -sheet, at approximately a 20° rotation relative to helix I. The third helix (III) lies on the outer surface perpendicular to helix I. The active site lies in the cleft between the β -sheet and helix II. The catalytic zinc is located at the bottom of the cleft, and the three His residues in the sequence HEXGHXXGXXH are the three ligands responsible for binding to the catalytic zinc. The fourth ligand is either a H_2O molecule or a single unpaired Cys residue in the propeptide, when the enzyme is either active or latent, respectively [69]. A second zinc located above the β -sheet is tetrahedrally coordinated by three His residues, and is inaccessible to solvent, suggesting its importance in stabilization of the active enzyme [67, 70, 73].

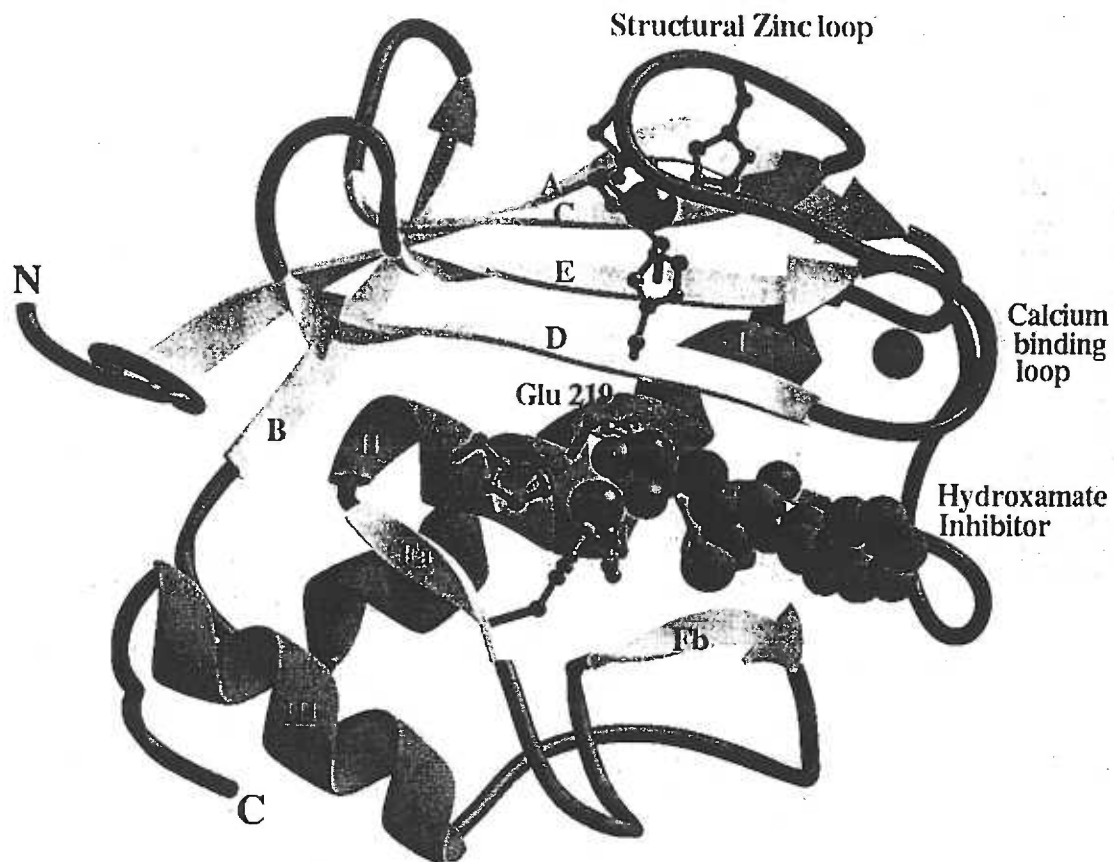


Figure 2: Catalytic Domain of Human Fibroblast Collagenase Complexed to a Hydroxamate Inhibitor. The β - sheets are represented by the letters A-E, and the α -helices are represented by the Roman numerals I-III. The bound metal ions (two zincs and one calcium) are indicated in the figure, as is the bound hydroxamate inhibitor. The Fa and Fb regions represent proposed extensions of the substrate binding cleft of the enzyme.
 (from: J.C. Spurlino, "1.56 Å Structure of Mature Truncated Human Fibroblast Collagenase" Proteins: Structure, Function and Genetics, 19: 98-109, 1994.)

Biochemical experiments have shown that, in addition to the catalytic requirement for zinc, MMPs are stabilized by the presence of both zinc and calcium [74-76]. Additional metal binding sites exist within the N-terminal half of the MMPs, as either one calcium ion [69, 70, 72] or two calcium ions [66, 77] are packed against the top of the β -sheet and presumably function to stabilize the catalytic domain. A conserved Glu- and Asp-rich region between the structural Zn^{2+} site and the hinge region constitutes one hexa- or octacoordinate Ca^{2+} binding site. Both sites shown for calcium ion binding are on top of, and on either side of the β -sheet. Finally, the MMPs have a proline-rich region that marks the transition to the carboxyl-terminal domain. With the exception of matrilysin, all of the MMPs contain a C-terminal domain that consists of four repeats that share some homology with sequences found in hemopexin and vitronectin. The C-terminal domain has been found to play a role in substrate specificity and matrix binding [76, 78, 79]. This domain mediates the interaction of collagenase and stromelysin to collagen [78, 79]. The C-terminal domain in the proenzyme form of the gelatinases has been found to interact with the specific inhibitors, the tissue inhibitors of metalloproteinase (TIMPs), which will be described in detail below. Gelatinase A, in its proform, interacts at the carboxyl-terminus with TIMP-2, and the proform of gelatinase B interacts with TIMP-1 [80-86]. More recently, the C-terminus of gelatinase A has been found to be involved in a binding event at the cell surface involving MT-MMP-1, which results in activation of gelatinase A [59, 87].

Gelatinase A and B are larger than the other MMPs and contain three additional exons, which encode the three fibronectin type II domains inserted upstream of the

catalytic zinc binding site. The presence of these domains coincides with the ability of the proenzyme forms of both gelatinases to bind gelatin [84, 88, 89]. Previously it had been shown that collagenase and stromelysin bind to collagen through the hemopexin- or vitronectin-like C-terminal domain [78], however, gelatinase A was found to interact with collagen through its fibronectin-like domain [90, 91]. Furthermore, the fibronectin-like domains have been shown to be required for the elastolytic activity of both gelatinase A and B [92]. Gelatinase B has an extended hinge region that contains sequences similar to the $\alpha 2$ -chain of type V collagen. It is not clear if this additional type V collagen-like domain plays any role in substrate specificity, since only subtle differences between the activities of gelatinase A and B have been detected against the substrates tested thus far [4, 93].

Given that the MMPs can degrade a broad array of substrates, their regulation is necessarily stringent and occurs at several different levels. At the level of gene expression, many of the MMPs are often coordinately regulated. Promoter regions of the genes for stromelysin and collagenase share common features such as TATA elements, tumor promoter-responsive elements (TRE) that bind the transcription factor AP-1, and PEA-3 sites, that interact with proto-oncogene product c-ets (Fig. 3) [94, 95]. In general, the following factors are stimulatory for expression of the MMPs: 12-O-tetradecanoyl-phorbol-13-acetate (TPA), interleukin-1 (IL-1) and tumor necrosis factor- α (TNF- α) [94, 96-98]. The promoter regions of gelatinase and neutrophil collagenase are different from that of stromelysin by the absence of a TATA box and AP-1 site [4, 99], and the presence of several SP-1 sites. Other structural features include an adenovirus E1A

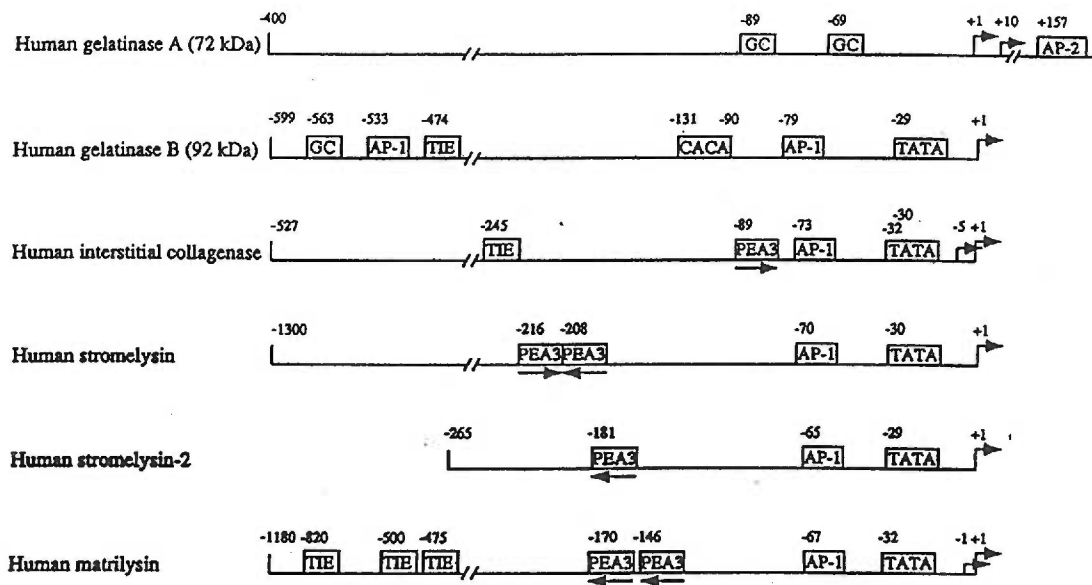


Figure 3: Comparison of the Promoter Regions of the Matrix Metalloproteinases. TATA boxes, AP-1 motifs, PEA3 elements, TGF- β 1 inhibitory element-like sequences (TIE), AP-2 sites, and GC box/SP-1 binding site (GC) are indicated. (from: M. Gaire, "Structure and Expression of the Human Gene for the Matrix Metalloproteinase Matrilysin", *J. Biol. Chem.*, 269(3): 2032, 1994.)

oncogene-repressible enhancer element [100] and a strong silencer downstream. IL-1 β and TNF- α are capable of inducing the expression of gelatinase B [94, 101].

An additional regulatory mechanism for controlling the activity of the MMPs is the stepwise process of activation of the proenzymes to a fully processed and active form of the enzyme [102]. As mentioned above, latency of the proenzyme is maintained through a Cys-Zn²⁺ interaction that links the unpaired propeptide Cys residue to the active site Zn²⁺ displacing the H₂O molecule necessary for catalysis [64, 103, 104]. This is referred to as a “cysteine-switch” mode of activation [103, 105]. Activation of the proenzyme occurs when the H₂O molecule gains access to the zinc ion as the cysteine interaction is disturbed (Fig. 4) [106]. Disruption of the Cys-Zn²⁺ bond is achieved by chemical and physical means such as exposure to organomercurials, metal ions, thiol reagents and detergents, and also by proteolytic enzymes that excise portions of the propeptide, thereby changing the conformation of the polypeptide surrounding the active site zinc. The enzyme can then catalyze autolytic cleavage of the remaining propeptide to generate the fully active and processed form [102, 107-109]. Site-directed mutations of the Cys residue in the conserved propeptide sequence RCGV/NPD has been shown to result in autocatalytically active enzymes [110, 111]. Potential physiologic activators of the MMPs include plasmin, trypsin, chymotrypsin, neutrophil elastase, and cathepsins B and G [5, 62]. Additionally, some latent MMPs have been found to have different susceptibilities to various active MMPs. For example, activation of gelatinase B may be mediated by gelatinase A or by stromelysin [38, 50, 112, 113]. Gelatinase A does not contain some of the proteinase cleavage sites that the are in the other MMPs. However, it can be

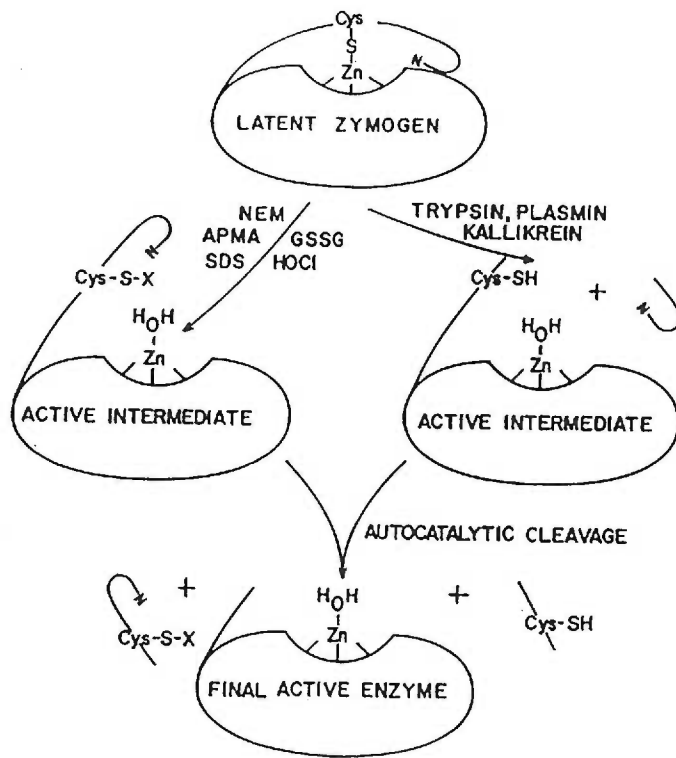


Figure 4: The Cysteine Switch Mechanism of MMP Activation. Cysteine in the proenzyme domain contacts zinc to maintain latency of the enzymes. Physical agents such as sodium dodecyl sulfate (SDS), chaotropic agents, reagents that react with sulfhydryl groups can unfold the structure or inactivate the cysteine to expose zinc. Alternatively, proteolytic enzymes can cleave the propeptide. In a second step, the active forms can be autolytically cleaved by the activated MMP to remove the propeptide and confer permanent activity. (from: J. Woessner, "Matrix Metalloproteinases and Their Inhibitors in Connective Tissue Remodeling", *FASEB J.*, 5:2145, 1991.)

activated by MT-MMP at the surface of cells and can undergo autocatalytic cleavage to obtain the fully processed form of the enzyme [108, 109, 114, 115]. The binding interactions of the pro-forms of gelatinase A and B and the TIMPs appear to regulate the activation process as the TIMPs can prevent or slow down the autocatalytic cleavages that occur after the activation has been initiated by other proteinases [80, 114, 116].

A final means of regulating the overall MMP proteolytic activity that will be discussed here is via the specific interactions of the tissue inhibitors of metalloproteinases (TIMPs) and the MMPs. (The TIMPs will be described in detail below). TIMPs form noncovalent bimolecular complexes with the active forms of MMPs and with the latent forms of gelatinase A and B (as mentioned previously). Except in the latter case, the inhibitors are thought to bind at the active site of the MMPs and to block access to substrate. Binding is generally tight, with a K_d of 10^{-9} to 10^{-10} M and the inhibitor binds to the active MMP in a 1:1 molar ratio [117, 118]. The regulation of ECM degradation at this level, therefore, is tightly controlled considering the selective inhibition of either autoactivation or substrate catalysis by different TIMP family members, as well as differences in specificity for different MMPs [2, 4, 106, 119].

The Tissue Inhibitors of Metalloproteinases - The TIMPs are secreted, multi-functional proteins that play an important role in the regulation of ECM metabolism. Four members of the TIMP family of proteins have been cloned and sequenced from human cells [120-127]. The proteins are classified based on their structural similarities, as well as their ability to inhibit the MMPs, as all have closely related structures and similar

inhibitory properties. The four human TIMP sequences share a 22% identity, although between individual members, the identity can be as high as 50%, for example, between TIMP-2 and TIMP-4. TIMP-1, -2, and -3 appear to be distributed widely in tissues and fluids, and expressed by many normal and transformed cell types [2, 47, 125, 127-135].

TIMP-1 expression is stimulated by a variety of agents including growth factors (epidermal growth factor (EGF), TNF- α , IL-1, TGF- β), phorbol esters, retinoids, and glucocorticoids (as reviewed [2, 99, 136]). The human TIMP-1 gene is located on the X chromosome [137]. TIMP-1 is a glycosylated protein containing two N-glycosylation sites. However, non-glycosylated, recombinant forms of TIMP-1 have been shown to have similar inhibitory properties to the wild-type TIMP-1 suggesting that the carbohydrate moiety is not involved in the inhibition of MMPs [119]. The wild-type TIMP-1 (glycosylated) migrates as a 28-kDa protein on SDS polyacrylamide gels. TIMP-1 binds reversibly to the active forms of the MMPs in a 1:1 stoichiometric complex, and TIMP-1 binds to the proenzyme form of gelatinase B [84].

TIMP-2 expression is regulated differently from that of TIMP-1 and is largely constitutive. TIMP-2 expression is down regulated by TGF- β and does not respond to phorbol esters or other cytokines [138-140]. The human TIMP-2 gene has been localized to chromosome 17 [141]. TIMP-2 is a nonglycosylated protein that migrates as a 20-21 kDa protein. TIMP-2 binds to and inhibits the active forms of the MMPs, as well as selectively forming a complex with the proform of gelatinase A [80, 81]. TIMP-2 is secreted as a complex with progelatinase A by human fibroblasts, where alveolar macrophages secrete it uncomplexed [142].

Regulation of expression of the human TIMP-3 gene has not been studied extensively, however, the murine gene has been shown to be stimulated by TPA and TGF- β [143]. The human TIMP-3 gene has been localized to chromosome 22 [124]. TIMP-3 protein has been found to have both a nonglycosylated form and an N-glycosylated form that migrate as 24 kDa and 27 kDa proteins, respectively [144]. Interestingly, TIMP-3 was found to be associated with the extracellular matrix of cultured cells and not secreted out into the medium, showing its localization to be distinct from that of the other TIMP proteins [143, 145]. TIMP-3 has been shown to have inhibitory activity similar to that of TIMP-1 against both gelatinases, collagenase, and stromelysin [144].

TIMP-4 has only recently been cloned and sequenced from a human heart cDNA library [127]. Its predicted sequence shows high conservation with the other members of the TIMP family. In contrast to the findings for the other three TIMPs, tissue expression was limited as TIMP-4 mRNA was found only in adult heart. It was shown to migrate as a 24 kDa protein and to have general MMP inhibitory activity in a reverse gelatin zymogram [127].

Based on the existing knowledge of TIMP-1, -2, and the limited information on TIMP-3 and TIMP-4, there are several characteristics common to all members of the TIMP family. The first is their conserved gene structure. The structure of the protein coding exons is similar in the Timp-1, -2, and -3 genes, although the actual sizes of exons appear to be less conserved than their exon-intron boundaries within the mRNA [140, 144]. Secondly, the TIMPs are secreted extracellularly and all have inhibitory activities specifically against MMPs. Thirdly, twelve cysteine residues as well as their relative

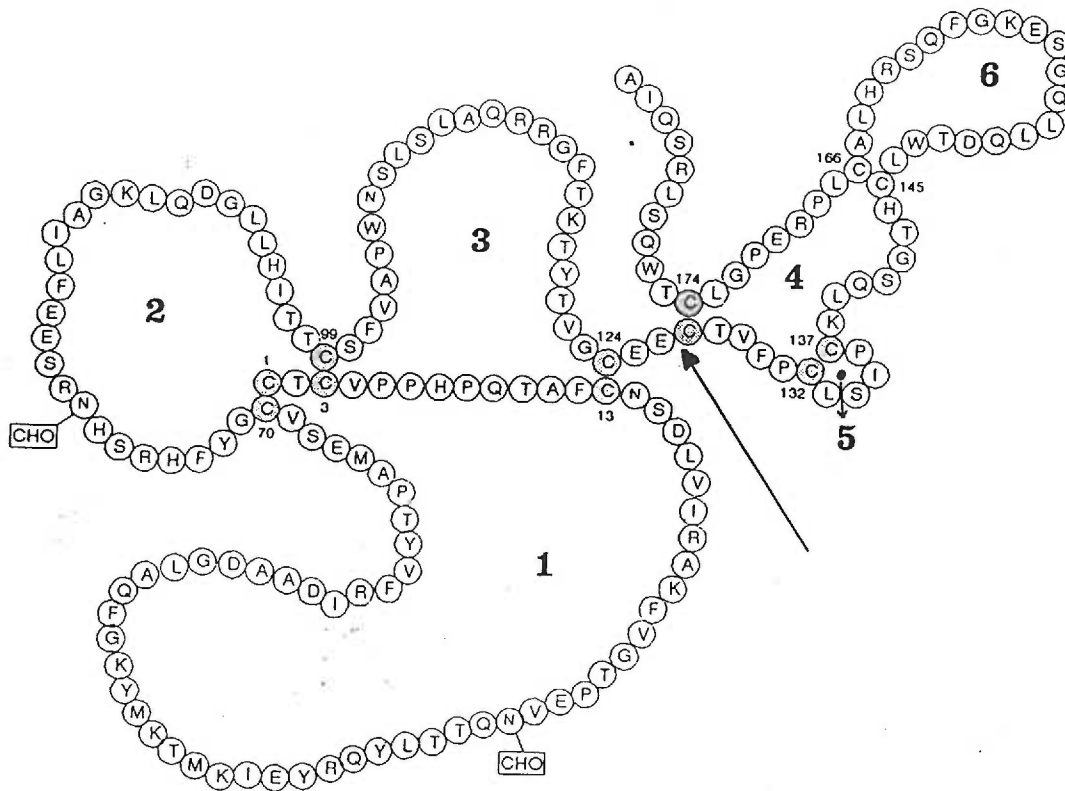


Figure 5: Schematic of TIMP-1 Domain Structure.
 The depiction of the six-loop structure is based on the assignment of the disulfide bonds. The arrow indicates the approximate location of the division of the C- and N-terminal domains.
 (from: F. Willenbrock, "Structure-Function Relationships in the Tissue Inhibitors of Metalloproteinases", *Am J Respir Crit Care Med*, 150: S165, 1994.)

spacing are conserved among the primary sequences of the TIMP proteins. In TIMP-1 the 12 cysteine residues have been shown to form six intra-chain disulfide bonds [146], and presumably the same disulfide bonds are formed in the other TIMPs and all share the same gross structural features. The disulfide bonds appear to be essential in maintaining a highly compact tertiary structure and two structurally distinct domains can be defined within the molecule. The N-terminal domain-consists of loops 1-3 and the C-terminal domain of loops 4-6 (Fig. 5) [119].

Finally, the TIMPs all share a highly conserved N-terminal domain which has been shown, for TIMP-1 and TIMP-2, to not only fold independently of the C-terminal domain but also to be adequate for inhibition of the MMPs [147-150]. Various mutations have been made to determine key residues involved in inhibition, but no single amino acid residue was found to be essential for TIMP activity [151]. The solution structure has been solved for the N-terminal domain of TIMP-2 and consists of a five-stranded anti-parallel β sheet that is rolled over on itself to form a closed β -barrel (Fig. 6) [152]. The tertiary structure of the N-terminal three loops of the TIMPs are expected to be similar to TIMP-2 based on their sequence similarities. The C-terminal domain has been shown to be responsible for the interactions of TIMP-1 and TIMP-2 with the proenzyme forms of gelatinase B and A, respectively [83, 148, 149, 153].

Although MMP inhibition is the defining feature of the TIMPs, they have also been shown to have other properties independent of their inhibitory activity, such as growth factor activity [154-158]. TIMP-3 has been shown to be involved in the transformation of chick embryo fibroblasts [145] and in the progression of the cell cycle [159]. It is unclear

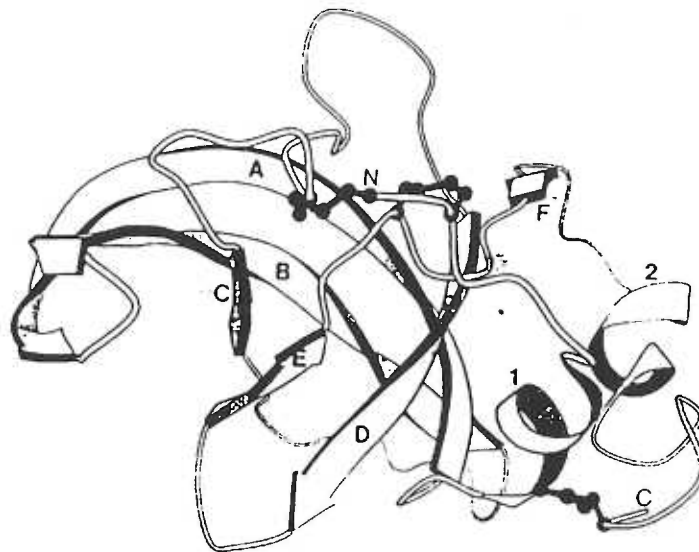


Figure 6: The Structure of the N-Terminal Domain of TIMP-2.
The backbone topology of the truncated protein is defined by a five-stranded antiparallel β -sheet that is rolled over on itself to form a closed β -barrel, and two short helices which pack close to one another on the same barrel face.
(from: R. Williamson, "Solution Structure of the Active Domain of Tissue Inhibitor of Metalloproteinases-2", *Biochemistry*, 33: 11745, 1994.)

what roles the growth stimulatory activity of the TIMPs may play in vivo. It is possible that in situations of tissue remodeling, the inhibitory functions of the TIMPs regulate matrix breakdown, while the stimulatory function may contribute to cell growth in a specific manner to promote tissue rebuilding.

MMP-TIMP Interactions - As stated above, the C-terminal domains of the gelatinases are involved in TIMP binding events. The interactions of TIMP-1 with the C-terminal domain of progelatinase B seem to enhance the rate of inhibition, whereas the interactions of TIMP-2 and gelatinase B do not involve the C-terminal domain of the enzyme [86]. In the case of TIMP-2, deletion mutants have shown that a charged C-terminal peptide “tail”, located at the extreme end of the protein and which is nonexistent in TIMP-1, is important for its association with progelatinase A [148]. Thus, the C-terminal domains of enzyme and inhibitor interact together and this interaction greatly increases the rate of inhibition. The site on TIMP-2 that forms the complex with the progelatinase is distinct from the binding site for inhibition, thus permitting the formation of higher order complexes where one or two molecules of inhibitor are associated with two molecules of proteinase [82]. A progelatinase A-TIMP-2 complex can act as an inhibitor of active MMPs forming a ternary complex that can then be activated [160]. The rate of inhibition by TIMP-2 was found to be approximately five-fold faster than that by TIMP-1 on several of the MMPs tested [119]. Interestingly, TIMP-2 has been suggested to have a different binding site for stromelysin than for gelatinase A, as the C-terminal domain of stromelysin does not appear to be involved in TIMP binding, and the C-terminal

domain of TIMP-1 or -2 does not have a significant effect on the reaction rate [83].

Clearly, the binding interactions between the TIMPs and the MMPs are complex. Inhibition has been suggested to occur as a result of binding at the active site of the enzyme, although the mechanism of inhibition has only been determined recently for inhibition of collagenase. TIMP-1 was found to inhibit collagenase as a noncompetitive inhibitor in a two-step mechanism, in which an inactive, rapidly formed, reversible complex slowly forms an inactive, tight complex [161]. As has been suggested for the inhibition of other MMPs, the carboxyl-terminal domain of the MMP, in this case of fibroblast collagenase, is important for the initial complex and this contributes to the overall binding. This will be discussed in more detail in later chapters.

Clearly, though the MMPs are tightly regulated at the transcriptional level, their interactions as degradative enzymes with cellular activators, substrate molecules, and finally, with the TIMPs are complex and only partially understood. However, the involvement of MMPs and the TIMPs in matrix degradation and remodeling has been shown to be important in many normal and in some pathological processes. Degradation and resynthesis of the extracellular matrix components depend on the net activity of the MMPs and TIMPs. Therefore, coordinated expression and the specific interactions of the MMPs and their tissue inhibitors, the TIMPs, mediate cellular processes involving the active turnover of extracellular matrix. It follows that the balance between the activities of the two components (MMPs and TIMPs) is necessary in maintaining a healthy state, and that this balance may be upset in some disease states in which the MMPs have been implicated.

MMP activity has been implicated in tumor invasion and metastasis, as studies have clearly demonstrated a positive correlation between MMP expression, invasive behavior, and metastatic potential (as reviewed [17, 162, 163]). TIMP-1 has been shown to inhibit *in vivo* metastasis in animal models [162, 164]. TIMP-2 has been shown to successfully inhibit *in vitro* tumor cell invasion of ECM [141, 162]. Down-regulation of the TIMP-1 gene in embryonic stem cells significantly increases their invasive capacity [165]. Thus, TIMPs can suppress tumor invasion and metastasis and they have been shown to have potent anti-angiogenic properties [166]. Imbalances in the extracellular activities of MMPs and TIMPs have been linked with the pathological tissue destruction seen not only in cancer, but also in arthritis and cardiovascular disease [166].

Arthritis is characterized by the irreversible loss of collagen matrix in cartilaginous surfaces of joints. In osteoarthritic cartilage, it has been shown that TIMP levels rise, but do not compensate for the much larger increase in degradative activity of MMPs [167]. Increased collagenase activity has been shown to exist in rheumatoid synovial fluids, and also in human periodontal diseases. In the case of the latter disease, enzyme activity generally increases with disease severity [2, 10]. In these cases, the apparent imbalance of MMP-TIMP activity, or the overall net activity, may be involved in the development of a pathological state. Given the importance of MMPs in a variety of normal and pathological processes, it is clear that inhibitors of metalloproteinases are of considerable clinical relevance in diseases where MMPs play a major role. Much attention has recently been focused on elucidating the mechanism of inhibition of the TIMPs on the various MMPs, as well as on the synthesis and testing of small, synthetic metalloproteinase

inhibitors that may eventually be used in clinical applications for various diseases.

This body of work focuses not only on the involvement of MMPs and the TIMPs in two distinct disease processes in the eye, but also investigates the specific interactions of gelatinase A and B with the TIMPs, as well as with several synthetic metalloproteinase inhibitors.

II. Expression and Purification of TIMP-1, -2, -3, and Purification of Gelatinase A and B

A. Introduction

The TIMP family of proteins are important for tissue homeostasis and for the remodelling that is essential for normal development and repair [2, 136, 166]. TIMPs block the activities of the extracellular matrix-degrading metalloproteinases. TIMP-1, -2 and -3 are able to inhibit the active forms of all MMPs, and TIMP-1 and -2 are able to form complexes with progelatinase B and A, respectively [3, 166]. The question of whether there is differential MMP inhibition by the TIMPs still exists. One study has shown that TIMP-2 was 10-times more effective than TIMP-1 in inhibiting active gelatinase A [168]. In contrast, TIMP-1 was twice as effective as TIMP-2 in inhibiting fibroblast collagenase. TIMP-3 was shown to be a superior inhibitor of gelatinase B as compared to either TIMP-1 or -2 by reverse zymography [166]. As for the MMP binding interactions, several studies have shown that multiple sites on the TIMPs are involved in contact with and inhibition of MMPs [83, 151, 153, 169].

The purpose of these studies was to obtain recombinant, purified TIMP proteins for various biochemical, inhibitory, and kinetic analyses, in order to gain insight into their mode of action, especially pertaining to two distinct eye disorders, which will be discussed in more detail below. This was done by subcloning the TIMPs into various bacterial and eukaryotic expression vectors for protein expression and subsequent purification. TIMP-

1 cDNA was subcloned into the pMal bacterial expression vector for expression as a fusion protein with maltose binding protein. Additionally, TIMP-1 was cloned into the pGEX1 λ T expression vector. Human TIMP-1 cDNA was also cloned into the retroviral expression vector pSFF and transfected into cocultured cells where the provirus is stably incorporated into the host cell's genomic DNA, a system developed by the Kabat lab [170]. The purpose of expressing TIMP-1 protein in such a manner was primarily to obtain permanent cell lines constitutively expressing a fully glycosylated, mature TIMP-1 that could be purified and used in further in vitro studies. In addition, the virions expressing the TIMP-1 could be used to infect other cell lines allowing the establishment of cell cultures constitutively expressing TIMP-1. This would allow studies to be done on cell lines where there would be an over abundance of TIMP-1 protein expressed.

Retroviruses contain their genomic information as RNA and the virions contain reverse transcriptase to produce a DNA copy [171]. Retroviruses have broad host and tissue ranges and relatively mild effects on cells in culture so they are often chosen for gene transfer studies [172]. Typically, a cell will be infected only once by a particular retrovirus, which stably inserts itself into the host cell's genome. The host cell's transcriptional machinery is then utilized to produce the viral proteins encoded by the gag, pol and env genes, proteins which are required for the assembly of infectious virions. In order to infect a cell, the virion uses the env proteins on its surface to bind and interact with cell surface receptors. An infected cell will express some of the retroviral env protein on its surface, where it appears to prevent further infection of that cell by virions using the same type of receptors. Consequently, cells that release retrovirions cannot be super-

infected by those virions (Fig. 7). This process is called viral interference where in figure 7 the open circles represent the virions released by the host cell [173]. Retroviruses are often classified according to the host-range of their env proteins, for example, ecotropic viruses are capable of infecting only murine cells, whereas amphotropic viruses infect murine cells and most other species [174, 175]. Retroviral vectors become amplified when they are added as calcium phosphate precipitates to cocultures of cells whose env proteins on their surfaces have two distinct host ranges. The Kabat lab developed a means of avoiding the interference that results from expression of the env protein on the cell surface, thus allowing multiple infections of cells (Fig. 8). This is called ping-pong amplification [170, 176]. With the increased multiplicity of infection the amount of retrovirally encoded protein rises, as compared with that of total cellular protein, to become as high as 4-6 % of total cellular protein synthesis [170]. Obtaining permanent cell lines which stably over-express TIMP-1 would aid in the characterization of the expressed TIMP-1 cDNA. The cell lines could provide a means of studying cellular responses to constitutive synthesis of TIMP-1.

Gelatinase A and B, also known as type IV collagenases, are members of the matrix metalloproteinase family of proteins. The gelatinases hydrolyze denatured and nonhelical collagens, and native type IV and V collagens, and are thought to interact synergistically with collagenase in the degradation of collagens [3, 26, 51]. Many studies have been performed to determine cleavage site requirements for the gelatinases and different specificities for the two enzymes using small synthetic peptide substrates [24, 51, 93, 177]. Although the substrate specificities of gelatinase A and B seem similar, the two

enzymes are known to be synthesized by different cells in vitro. Gelatinase A is synthesized primarily by skin and gingival fibroblasts, endothelial cells, osteoblasts, and many other normal and transformed cells, whereas gelatinase B is produced mainly by inflammatory cells, by various tumor cells such as fibrosarcoma HT1080 or leukemic HL-60 cells, and by normal cells such as cytotrophoblasts, keratinocytes, and osteoclasts [12, 26, 45, 48, 50, 178-184].

The purpose of purifying the gelatinases from various cell types was to analyze their mechanism of action against a protein or peptide substrate in vitro. This was followed by an analysis of the inhibitory action of the recombinant purified TIMPs and several synthetic inhibitors on gelatinase A and B in order to determine specificity of the inhibitors and their mechanism of inhibition. Gelatinase A was purified from the media of cultured human skin fibroblasts (HS27 cells) and gelatinase B was purified from cultured human fibrosarcoma cells (HT1080 cells) for further analysis. Enzyme assays using the purified enzymes and various inhibitors will be described in the next chapter.

B. Materials and Methods

TIMP-1 Cloning and Expression - Human TIMP-1 cDNA was originally cloned in the plasmid vector p-Alter-1 (Promega) by Linda Lund from the Acott lab (unpublished data). E.coli XL1Blue cells were transformed with 100 ng of p-Alter-TIMP-1 and grown overnight on luria-agar plates in the presence of 50 µg/ml ampicillin and 15 µg/ml tetracycline [185]. Two colonies were selected and grown overnight in 100 ml liquid luria

broth cultures. Total cellular nucleic acids were extracted from the cells using the alkaline-lysis method [186, 187]. Briefly, overnight liquid cultures were centrifuged at 4000 x g for 10 minutes and the supernatant was discarded. The cell pellets were resuspended in 15% sucrose, 25 mM Tris-HCl, 10 mM EDTA, pH 8.0. Cells were lysed by adding a freshly-made solution of 0.2 N NaOH and 1% sodium dodecyl sulfate (SDS). A 3 M stock solution of potassium acetate, pH 5.6 was added to the lysed cells and the mix was incubated on ice for 30 minutes. The tube was centrifuged at 14,000 x g for 15 minutes at 4°C and the supernatant transferred to a new tube. DNA was precipitated from the supernatant by the addition of 1 volume of 100 % isopropanol. Tubes were centrifuged at 10000 x g for 10 minutes at room temperature to collect the DNA pellet. After completely decanting the tube, the pellet was resuspended in 10 mM NaCl, 10 mM Tris-HCl, 1 mM EDTA, pH 8.0. Rnase, Dnase-free (Boehringer Mannheim) was added and the solution was incubated at 37°C for 30 minutes. The solution was then extracted with an equal volume of a 1:1 mix of TE (pH8)-saturated phenol:chloroform. After centrifugation at 12,000 x g, the aqueous phase was transferred to a clean tube containing 3 M sodium acetate, pH 5.2 and 100 % isopropanol and the tubes were centrifuged at room temperature for 5 minutes. The DNA pellet was then washed in 70 % EtOH and allowed to dry before resuspending it in deionized H₂O. The concentration and purity of recovered DNA was determined by measuring the absorbance of the solution at 260 and 280 nm. Plasmid DNA was brought to a final concentration of 1 mg/ml, digested with several restriction enzymes and subjected to agarose gel electrophoresis to verify restriction sites and purity.

For the purpose of expressing high levels of recombinant TIMP-1 protein in bacterial cells, TIMP-1 cDNA was ligated into the pMAL C2 expression vector (New England Biolabs) (Fig. 9a). In brief, 1 μ g pMAL plasmid DNA was digested with the restriction enzymes Eco RI and Xmn I and electrophoresed on a 1 % agarose gel. The expected size of the linearized plasmid was 6.64 Kb. The digested product was then excised out of the gel and purified using the GeneClean Kit from Bio101, Inc. Briefly, the gel slice was incubated in 6M NaI at 45°C to dissolve the gel. Glassmilk was added to the solution and the solution was vortexed and centrifuged to pellet the glassmilk beads with bound DNA. The beads were then washed three times in New Wash and finally, the beads were resuspended in water and incubated at 45°C for 5 minutes to dissociate the DNA from the beads. After centrifugation the DNA was removed from the beads in the supernatant, as described above for the ligation reactions. The TIMP-1 cDNA was PCR-amplified using 36-mer mutagenic oligonucleotides that created novel restriction sites in the amplified DNA. The restriction sites for Nae I and Eco RI were mutated into the 5' and 3' ends, respectively, on the amplified TIMP-1 cDNA as follows. TIMP-1 cDNA (100 ng) was amplified by PCR using Tfi DNA polymerase (2 Units in 100 μ l; Epicentre, Madison, WI), but with the following changes: 125 nM of each (sense and antisense) PCR primer, 0.2 mM each dNTP, 50 mM Tris (pH 9.0), 2 mM (NH₄)₂SO₄ and 1.75 mM MgCl₂ were used. Thirty-five PCR cycles (95°C, 15 sec ; 55°C, 1 min; 72°C, 2 min) were used with a final extension of 5 minutes at 72°C. PCR products were electrophoresed on 3% agarose gels in TAE buffer (40 mM Tris-acetate, 1 mM EDTA, pH 8) with ethidium bromide staining and using a 123 bp DNA ladder for size standards

(GIBCO/BRL). The appropriately sized PCR product of 616 bp was excised from the gel and extracted from the agarose gel using the GeneClean kit, as described above. The final product was then digested with the restriction enzymes Nae I and Eco RI (Boehringer Mannheim) simultaneously for 1 hour at 37°C in order to create the compatible 5' and 3' ends for ligation into the pMAL C2 vector. The digested products were electrophoresed on a 3 % agarose and the band, at the expected size of 578 bp, was excised from the gel and purified using the GeneClean Kit, as described above. The final products were ligated in a reaction with T4-DNA Ligase (Boehringer Mannheim) as described above. Ligation reactions were then transformed into competent XLIBLue E.coli cells as described above [185] and plated out onto luria-agar plates with 100 µg/ml ampicillin and 15 µg/ml tetracycline. Several transformant colonies were picked from the plates and grown up as overnight cultures in luria broth with 100 µg/ml ampicillin and 15 µg/ml tetracycline. Plasmid DNA was extracted and purified from the cells using the miniprep procedure described above [188]. DNA was subjected to restriction digestion analysis with the enzymes Xmn I and Eco RI and the products were electrophoresed on a 1 % agarose gel. The resulting band sizes were 578 bp (TIMP-1) and 6.64 kb (pMAL). Large scale overnight cultures were grown with the transformants of interest and DNA was extracted and purified as described above for DNA sequencing [187]. In addition to identifying positive tranformant clones by their restriction digestion patterns, they were also subjected to southern blotting and hybridization [189]. In brief, the full length, purified pMal-TIMP-1 plasmid was run on a 1% agarose gel and a positive control for TIMP-1 plasmid was run in an adjacent lane. The gel was stained with ethidium bromide and photographed. Then

it was denatured in 1.5 M NaCl and 0.5 M NaOH for 45 minutes. It was then neutralized in 1 M Tris (pH 7.4) and 1.5 M NaCl for 30 minutes. The DNA was transferred overnight to nitrocellulose using 10x SSC as transfer buffer. The filter was then dried and the DNA fixed to the membrane by baking at 80°C for 90 minutes. The filter was wet in 6x SSC and then put into prehybridization buffer: 40 % formamide, 5x SSC, 5x Denhardt's solution, 0.5 % SDS, and herring sperm DNA, for 60 minutes at 42°C. The TIMP-1 cDNA probe was synthesized by PCR (as described previously) and labeled with ³²P-dATP using the random primer extension kit from Boehringer Mannheim for 2 hours at room temperature [189]. The probe was boiled and added to the membrane in the prehybridization buffer and incubated overnight at 42°C. The filter was washed extensively with 1x SSC and 0.1 % SDS and then exposed to film overnight.

In order to determine relative protein expression levels, XLI Blue E.coli cells expressing the pMAL C2-TIMP-1 plasmid were analyzed for the presence of the maltose binding protein-TIMP-1 fusion protein [189]. In brief, a 10 ml overnight culture, containing a single colony with the fusion plasmid construct, was grown in luria broth with 100 µg/ml ampicillin and 15 µg/ml tetracycline overnight at 37°C with shaking. The overnight culture was then used to inoculate 500 mls luria broth with 1% glucose and ampicillin/tetracycline. Cultures were grown 37°C with shaking to a cell density of 2x10⁸ cells/ml or to an OD₆₀₀ = 0.4 to 0.6. In order to induce high levels of fusion protein expression, isopropyl-β-D-thiogalactopyranoside (IPTG) was added to a final concentration of 1 mM and cultures were incubated again for 2 hours at 37°C with shaking. Cells were then centrifuged for 20 minutes at 4000 x g. Cells were resuspended

in a sodium phosphate lysis buffer (10 mM NaPO₄ buffer, pH 7.2, 0.5 M NaCl, 0.25 % Tween 20, 10 mM EDTA, 10 mM EGTA) and frozen overnight at -20°C. Cells were thawed on ice and sonicated in short bursts to lyse the cells. Sonicated cells were then centrifuged for 20 minutes at 14,000 x g, 4°C. The supernatant was then subjected to affinity chromatography using an amylose resin column (New England Biolabs, Inc) at a rate of 1 ml/min in the same buffer [189]. After the sample was bound to the column and the flow through collected, the column was washed with 3-5 column volumes of the same buffer. The maltose binding protein was then eluted with the column buffer and 10 mM maltose in 3-ml fractions. Fusion protein yield and purity were analyzed by SDS-PAGE and Western Blot analysis [189-191]. Proteins were electrophoresed on SDS-PAGE (12% or 15% acrylamide gels) and were electro-transferred to nitrocellulose filters (Schleicher and Schuell). Filters were blocked in 2 % non-fat skimmed milk and probed with primary antibodies to TIMP-1 overnight at 4°C with shaking. The antibody used to detect the TIMP-1 fusion protein was a polyclonal peptide antibody (Triple Point Biologics). The blots were then washed four times for 15 mins at room temperature with 1x PBS and incubated for 2 hrs at room temperature with a goat anti-rabbit secondary antibody conjugated to alkaline phosphatase (Sigma). The immunoblot was washed four times in PBS for 15 minutes at room temperature and developed by addition of 5-bromo-4-chloro-3-indolylphosphate/nitroblue tetrazolium substrate for alkaline phosphatase as recommended by the manufacturers (Sigma).

For the purpose of ligating TIMP-1 into the pGEX1λT expression vector from Pharmacia, 1 µg of the pGEX vector (Fig. 9b) was digested with the restriction enzymes

Bam HI and Eco RI (Boehringer Mannheim) simultaneously at 37°C for 1 hour. The reaction was then electrophoresed on a 0.8% agarose gel. The linearized product was 4.89 kb. The TIMP-1 cDNA was PCR amplified using mutagenic oligonucleotides in order to create restriction sites compatible for ligation into the multiple cloning site of pGEX1λT. The restriction sites Bam HI and Eco RI were created at the 5' and 3' ends of the TIMP-1 cDNA, respectively, with PCR amplification. The PCR product was subjected to restriction digestion analysis with Bam HI and Eco RI simultaneously for 1 hour at 37°C. The products were electrophoresed on a 3% agarose gel. The digested product of 580 bp was excised out of the gel and extracted with the GeneClean kit from (Bio101) as described above. The pGex vector and the TIMP-1 insert were ligated with T4-DNA Ligase (Boehringer Mannheim) as described above. Ligation reactions were then put into transformation reactions with competent XLI Blue E.coli cells (as previously described) and transformed cells were plated out on luria-agar plates with 100 µg/ml ampicillin and 15 µg/ml tetracycline and grown overnight at 37°C. Colonies were selected and placed into overnight luria broth liquid cultures with 100 µg/ml ampicillin and 15 µg/ml tetracycline. The miniprep protocol described above was used to extract the plasmid DNA from the selected cultures. The plasmid DNA was then subjected to restriction digestion analysis with the enzymes Bam HI and Eco RI. The digested products were electrophoresed on a 1 % agarose gel. The resulting bands were 4.89 kb (pGex) and 580 bp (TIMP-1). Selected transformants were then grown up in large overnight liquid cultures and a large scale plasmid preparation and purification was performed in order to sequence the plasmid DNA. The sequence data verified the

presence of the TIMP-1 insert. In order to determine glutathione-s-transferase-TIMP-1 fusion protein levels, a similar procedure was followed as that described above for the maltose binding protein fusion protein expression and analysis, except for the following changes: the sonicated cells were applied to a glutathione-sepharose column in order to bind the glutathione-s-transferase-TIMP-1 fusion protein. After washing several times with PBS, the fusion protein was eluted by adding 5 mM reduced glutathione in 50 mM Tris buffer, pH 8.0. The eluted fractions were analyzed by SDS-PAGE and Western immunoblot, as described previously, to look for presence of GST-TIMP-1 fusion protein [189]. Additional steps were taken to purify the GST-TIMP-1 fusion protein using anion exchange chromatography [191, 192]. DE52 resin (Whatman) was washed alternately in 0.5N HCl and water several times. The resin was then washed in binding buffer: 10 mM sodium phosphate (pH 7.2), 1 mM NaCl and a slurry of the resin was added to soluble extracts from transformant cells. Protein was bound overnight at 4°C. The resin with bound protein was then washed in several volumes of binding buffer with increasing NaCl concentrations and the eluted fractions were analyzed by SDS-PAGE and Western analysis as described previously.

For the purpose of expressing the recombinant TIMP-1 in a mammalian expression system, the procedure began with ligating TIMP-1 cDNA into the pSFF expression vector (Fig. 10). Briefly, 1 µg of pAlter-TIMP-1 was digested simultaneously with the restriction enzymes Bam HI and Eco RI (Boehringer Mannheim) at 37°C for 1 hour. The digested product was electrophoresed on a 2 % agarose gel with ethidium bromide at a final concentration of 100 ng/ml in TAE buffer. The digested product was a linear DNA

fragment of 680 bp in length. The vector pSFF was also digested with Bam HI and Eco RI simultaneously, which cleave the 5' and 3' ends of a multiple cloning site located in the env gene region [170, 176]. The restriction digestion products were electrophoresed on a 0.8 % agarose gel with ethidium bromide. A linear band was observed at approximately 9 kb containing compatible sites (5' and 3') for ligation with the TIMP-1 fragment described above. The appropriate bands were excised out of the gel and the DNA was eluted from the gel slices using the GeneClean Kit from Bio101, Inc, as was described above.

TIMP-1 cDNA was ligated into pSFF using T4-DNA Ligase (Boehringer Mannheim, Inc.) overnight at 16°C [185]. DK-1 E. coli cells were made competent using the CaCl₂ method [185], frozen at -70°C, and thawed on ice immediately prior to use for transformation. To transform the competent cells with the ligated DNA, an estimated 10-50 ng of ligated plasmid DNA was added to 100 µl of DK-1 cells, incubated on ice for 30 minutes, heat shocked for 90 seconds at 42°C and put onto ice for 2 minutes. Then 900 µl of luria broth was added to the cells and incubated for 1 hour at 37°C. After incubation, cells were spread onto luria-agar plates containing 100 µg/ml ampicillin and grown overnight at 37°C [185].

Several of the colonies growing on the plates were selected and grown up in overnight luria broth liquid cultures and the plasmid DNA was isolated using a mini-prep protocol [188, 189]. Plasmid DNA from the mini-preps was digested with Eco RI and Bam HI and electrophoresed on a 1 % agarose gel. Of the colonies that yielded bands of the expected sizes (ie 9 kb for pSFF and 0.68 kb for TIMP-1), two were selected for further analysis by restriction digestion, grown up in larger quantities and the plasmid

DNA was purified using the alkaline lysis method as previously described. Additionally, the selected clones were analyzed using PCR amplification to detect the presence of the TIMP-1 insert. Purified plasmids were used as the cDNA template and PCR amplification was conducted as described above. The products were electrophoresed on a 2 % agarose gel containing ethidium bromide and photographed. A negative control, the pSFF vector without the TIMP-1 insert, was run in the PCR reaction and in an adjacent lane on the gel.

In order to make cocultures for transfections, Ψ -2 and PA-12 packaging cell lines [170, 176] were trypsinized, counted with a hemocytometer and seeded 1:1 in T-25 flasks at a final cell density of 50,000 cells per flask. Cocultures were grown for 48 hours in 5 mls Dulbecco's Modified Eagle Medium (DMEM) before transfecting. DNA for transfection was precipitated as a calcium phosphate aggregate by mixing 10 μ g plasmid DNA with 0.5 ml of 250 mM CaCl_2 and adding 0.5 ml phosphate buffer (50 mM HEPES, 250 mM NaCl, 1 mM NaH_2PO_4 , pH 7.1) dropwise, with mixing, to the solution. Medium was aspirated from flasks, 1 ml of DNA precipitate was added per flask and flasks were incubated at room temperature for 20 minutes. Three ml of transfection medium (DMEM, 10 mM HEPES, 10 % FBS, 0.12 % NaH_2CO_2 , pH 7.1) was added, flasks were tightly capped and incubated for 4 hours at 37°C. The cells were glycerol-shocked by aspirating off the medium, rinsing with phosphate buffered saline (10x solution: 10 mM NaH_2PO_4 , 1.3 M NaCl, 30 mM KCl, 0.3 M HEPES, 0.1 M glucose) and incubating with 10 % glycerol in phosphate buffered saline at room temperature for 2 minutes. The glycerol solution was removed, growth medium added back to the cells and they were grown for several days before passaging [193, 194]. Mock transfected cells were transfected in the

absence of any retroviral vector as a negative control.

In order to establish clonal cell lines of retrovirally infected cells, cocultures were limit-dilution cloned. To achieve this, they were trypsinized as for passaging, the cells were counted with a hemocytometer and then diluted to a final concentration of 30 cells per 20 mls of media. The diluted cells were then plated into a 96-well tissue culture plate (Falcon, Inc.) at 0.2 ml media per well and incubated for ten days. At the end of that time, wells with colonies growing in them (typically 10-20 % of all wells) were trypsinized, reseeded into 24 well tissue culture plates, incubated for 1-2 days, and then passaged into T-25 flasks.

RT-PCR was used to screen transfected cocultures for SFF-TIMP-1 positive cocultures. Total RNA was isolated and purified from cultured cells [195]. In brief, monolayers of cells were washed in PBS and then a solution of 4 M guanidinium isothiocyanate was added to lyse the cells. Lysed cells were transferred to 1.7 ml tubes and β -mercaptoethanol and sodium acetate, pH 4 were added. Phenol and chloroform were added to the tubes and tubes were vortexed and incubated on ice. After centrifugation the upper aqueous phase, containing nucleic acids, was removed to a new tube and isopropanol was added to precipitate the RNA. Tubes were centrifuged again to pellet the RNA, which was then washed in 70 % EtOH, resuspended in deionized H₂O and subjected to reverse transcription with MMLV reverse transcriptase (Gibco BRL, Inc.). RNA was reverse transcribed for 90 minutes at 37°C in 50 mM Tris-HCl (pH 8.3), 75 mM KCl, 10 mM dithiothreitol, 3mM MgCl₂ and 0.5 mM of each dNTP. Specific fragments of TIMP-1 cDNA (100 ng) were amplified by PCR using Tfi DNA polymerase

(2 Units in 100 μ l; Epicentre, Madison, WI), as follows: 125 nM of each (sense and antisense) PCR primer, 0.2 mM each dNTP, 50 mM Tris (pH 9.0), 2 mM $(\text{NH}_4)_2\text{SO}_4$ and 1.75 mM MgCl_2 were used. Thirty-five PCR cycles (95°C, 15 sec ; 55°C, 1 min; 72°C, 2 min) were used with a final extension of 5 minutes at 72°C. PCR products were electrophoresed on 3% agarose gels in TAE buffer with ethidium bromide staining and using a 123 bp DNA ladder for size standards (GIBCO/BRL).

Positive clones were grown up in T-25 flasks until confluent and passaged to T75-flasks. Cells were grown in DMEM without serum for 2-3 weeks. Medium was collected and concentrated 10-100x by centrifuging at 3000 x g using a centricon-10 (Amicon), and analyzed by SDS-PAGE and Western blotting in order to detect recombinant TIMP-1 protein.

TIMP-2 Expression - Human TIMP-2 cDNA was originally cloned into the pMALC2 expression vector (New England Biolabs) by Lisa Parshley (unpublished data). The pMAL-TIMP-2 construct was transformed into XLI Blue E. coli cells and the maltose binding protein-TIMP-2 fusion protein was expressed in the cytoplasm of the bacterial cells upon induction with isopropyl- β -D-thiogalactopyranosid (IPTG). The procedure described above for the expression and purification of the MBP-TIMP-1 protein is the same that was followed for the purification of the MBP-TIMP-2 fusion protein [189]. At this stage the purified fusion protein was detectable on Western Blots using a polyclonal rabbit anti-TIMP-2 peptide antibody (Triple Point Biologics) and was detectable on SDS-denaturing polyacrylamide gels by Coomassie Blue staining. Attempts were made to cleave the maltose binding protein moiety from TIMP-2 by Factor Xa

cleavage [189, 191, 196]. The Factor Xa was purchased from Boehringer Mannheim, Inc. Briefly, the recombinant protein sample was dialyzed overnight at 4°C against the following cleavage buffer: 20 mM Tris-Cl, pH 8.0, 100 mM NaCl, 2 mM CaCl₂, and 1 mM sodium azide. Then the Factor Xa was added to the dialyzed sample at a final concentration of 200 µg/ml and incubated overnight at room temperature. The products were then electrophoresed on an SDS-PAGE gel and analyzed by Coomassie Blue staining and by Western analysis. This procedure was also performed on recombinant protein samples that had previously been denatured in 8 M, 6M, 4M, or 2M urea, or 6 M guanidinium-HCl, and renatured, prior to dialysis against the cleavage buffer and cleavage with the Factor Xa.

TIMP-3 Cloning and Expression - For the purpose of ligating the human TIMP-3 cDNA into the eukaryotic expression vector pCEP4 (In Vitrogen) (Fig. 11), 1 µg pCEP4 was digested with the restriction enzymes Bam HI and Eco RI (Boehringer Mannheim) simultaneously at 37°C for 1 hour. The digested product was electrophoresed on a 1% agarose gel and the size was 10.35 kb. The band was excised out of the gel and extracted from the agarose using the GeneClean kit as described previously. The human TIMP-3 was originally obtained as a gift from S. Apte [124, 144]. The TIMP-3 cDNA was PCR amplified using mutagenic oligonucleotides that created novel restriction sites in the amplified cDNA. The sites NheI and BamHI were created at the 5' and 3' ends, respectively, of the PCR-amplified DNA. The products were electrophoresed on a 2 % agarose gel with ethidium bromide and the fragment at the expected size of 747 bp was excised from the gel and purified with the GeneClean kit. The TIMP-3 cDNA was the

subjected to restriction digestion with the enzymes Nhe I and Bam HI (Boehringer Mannheim) simultaneously and the digested products were electrophoresed on a 2 % agarose gel with ethidium bromide. The fragment, at the expected size of 714 bp, was excised from the gel and purified as described previously for ligation into the pCEP4 vector. The ligation reactions and subsequent transformations into competent DH5 α cells (from Gibco BRL, Inc.) were performed as described previously. Transformant colonies were selected and grown overnight at 37°C in liquid cultures of luria broth with 100 μ g/ml ampicillin. Plasmid DNA was extracted and purified using the miniprep procedure, as described above [188], and was then subjected to restriction digestion analysis with Nhe I and Bam HI. The resulting bands were 10.35 kb (pCEP4) and 714 bp (TIMP-3) as expected. Further restriction digestion analysis (with Pst I or Bgl II) was performed with the plasmid in order to verify the correct orientation of the TIMP-3 insert. Using these criteria two colonies were further selected and grown in overnight liquid cultures with ampicillin. The plasmid DNA was purified as described previously and sequenced.

In order to express the recombinant protein in mammalian cells, the DNA was then prepared for transfection into the mammalian cell cultures 293-EBNA (InVitrogen, Inc.). Transfections were performed as described previously [193, 194]. Transfected cells were grown for up to 30 days in serum-free medium and the medium was analyzed regularly for the presence of TIMP-3 protein. The extracellular matrix (ECM) of the transfected cells was also tested for the presence of the TIMP-3 protein. TIMP-3 protein appeared in the media at around 10 days post-transfection, however by approximately day 21 the TIMP-3 protein was localized in the ECM of the transfected cells and was no longer detectable by

Western Blot analysis in the media of the cells [197]. The TIMP-3 protein was detected using a polyclonal, rabbit anti-TIMP-3 peptide antibody (Triple Point Biologics). The TIMP-3 protein was purified from the media of the cells by binding to cation exchange chromatography [192]. Carboxy-methyl support is a weak cationic exchanger and was purchased from BioRad, Inc. The TIMP-3 protein has a $pI = 9.07$ allowing for separation of TIMP-3 from the other TIMPs based on the charge of the protein. For purification, batches of media were concentrated 10-100x on centricon-10 concentrators (Amicon, Inc.) and then dialyzed overnight in binding buffer: 20 mM Bicine, 50 mM NaCl, 0.05% Brij, pH 8.5 at 4°C. Then a slurry of buffer-equilibrated carboxy-methyl matrix was added to the dialyzed samples and incubated with shaking 2-4 hours at 4°C. The tubes were centrifuged for 1 minute, the supernatant collected for analysis, and the beads were washed several times with the Bicine binding buffer. The TIMP-3 protein was eluted in binding buffer with increasing concentrations of salt up to 1M NaCl. Eluted fractions were electrophoresed on a 13 % acrylamide SDS-PAGE gel and detected by Western immunoblot analysis using a polyclonal antibody against the TIMP-3 protein. Fractions containing the highest concentrations of TIMP-3 were subjected to reverse zymogram analysis in order to detect TIMP-3 inhibitory activity [197, 198]. SDS-PAGE gels were prepared with the incorporation of purified matrix metalloproteinases and substrate (gelatin) into the acrylamide matrix of the gel. SDS (0.1%), 12% polyacrylamide gels were prepared, except that a semi-purified sample containing several matrix metalloproteinases was also added into the acrylamide mix and the water volume was reduced accordingly. Gelatin substrate was added to a final concentration of 0.1 mg/ml

prior to polymerization of the gels. Samples were electrophoresed at 4°C, gels were washed in 2.5% Triton X-100, 50 mM Tris-HCl (pH 7.5), and 5 mM CaCl₂ once for 15 min and then again overnight at room temperature with shaking. Gels were then rinsed three times in deionized H₂O, incubated in 50 mM Tris-HCl (pH 7.5) and 5 mM CaCl₂, 10 μM ZnCl₂ for 24 hrs at 37°C with shaking and then stained with Coomassie blue stain.

Gelatinase A and B Purification - Several cell lines were cultured for the sole purpose of purifying the gelatinases from their media. It had been shown previously that various cell lines express relatively high levels of secreted matrix metalloproteinases [50, 199, 200]. HT1080 cells (from ATCC) were found to express predominantly gelatinase B, into the media of the cells, whereas HS27 cells (from ATCC) expressed mainly gelatinase A (also secreted into the media of the cells). Both cell lines were grown in Dulbecco's modified eagle medium (DMEM) supplemented with 10 % fetal calf serum until 80-90 % confluence. The cells were then made serum-free, and the media was collected from the cells 24-48 hours later for purification. The media was concentrated 10-100x by centrifugation at 5000 x g on Centricon-10 concentrators (Amicon, Inc.) The concentrate was then subjected to affinity chromatography by applying to a gelatin-agarose matrix (Sigma). The gelatin-agarose with bound enzyme was washed extensively with PBS and the gelatinases were eluted with 10 % dimethyl sulfoxide (DMSO). Gelatinolytic activity of fractions was analyzed by gelatin zymography (described below) and fractions with peak activity were pooled and dialyzed extensively against 20 mM Tris-Cl (pH 7.5), 150 mM NaCl and 5 mM CaCl₂, to remove all traces of DMSO.

Gelatin zymograms were prepared like standard SDS-PAGE gels but with the

following changes: 0.1 mg/ml gelatin substrate (final concentration) was added in with the acrylamide and volume of water was decreased accordingly prior to polymerization [201-203]. Enzyme samples to be electrophoresed were boiled in SDS-PAGE loading buffer without reducing agents and loaded on to gel. The gel was run as usual but then put into a 2.5 % Triton X-100 solution and washed with shaking at room temperature twice for 15 minutes. The gel was then washed in deionized H₂O twice for 15 minutes and finally the gel was incubated overnight at 37°C with shaking in 50 mM Tris-Cl (pH 7.5), 5 mM CaCl₂, and 10 μM ZnCl₂ buffer. The gel was then briefly washed in deionized H₂O and then put into Coomassie blue stain.

Further purification steps were made in order to separate the gelatinases from each other. Concanavalin A is used in the purification of glycoproteins and will bind reversibly to glycosylated proteins [204-206]. A Con A Sepharose 4B (from Pharmacia) column was prepared and a sample containing a mixed population of gelatinases was added to the matrix. Gelatinase A was expected to flow through and gelatinase B, because of its glycosylations, was bound to the Con A Sepharose. The flow through was collected and the column washed in 20 mM Tris pH 7.4 buffer with 0.5 M NaCl. Elution of bound protein was achieved using 0.5 M methyl- α -D-mannopyranoside in Tris buffer. Lentil Lectin-Sepharose 4B (Pharmacia) binds α -D-glucose and α -D-mannose residues and is used for the purification of glycoproteins [207, 208]. A lentil lectin sepharose column was prepared and a sample containing a mixed population of gelatinases was added to the matrix. Some gelatinase B was bound to the column and eluted in a similar manner as with the Con A Sepharose. Partially-purified gelatinases were analyzed by Western

analysis using polyclonal rabbit antibodies to gelatinase A and gelatinase B (Biogenesis) [191].

C. Results

TIMP-1 Cloning and Expression in Bacterial Expression Systems -TIMP-1

cDNA was cloned into the maltose binding protein fusion protein expression vector by PCR amplification of the TIMP-1 cDNA and subsequent restriction digestion with Eco RI and Nae I (Fig. 12). The pMAL C2 expression vector was digested with Eco RI and Xmn I creating compatible ends for ligation of the TIMP-1 insert into the vector (Fig. 13). After ligation reactions, XL1-Blue E.coli cells were transformed with the recombinant plasmid containing the TIMP-1 insert and resultant colonies were screened for TIMP-1 expression by PCR amplification with specific TIMP-1 primers (Fig. 14). Several positive clones were chosen and screened by restriction digestion analysis in order to verify correct orientation of the insert (data not shown). Additionally, plasmids were electrophoresed on an agarose gel, transferred to nitrocellulose, and probed with a TIMP-1 probe to detect positive clones (Fig. 15). Plasmid DNA from selected individual clones were also purified and then sequenced for verification of the full-length TIMP-1 insert.

Large scale cultures were grown up with the selected colonies and recombinant MBP-TIMP-1 protein was detected in the bacterial soluble extracts by Western analysis with a TIMP-1 antibody (Fig. 16). The observed size of the MBP-TIMP-1 fusion protein was approximately 69-70 kDa, as expected, however, there was an additional unidentified,

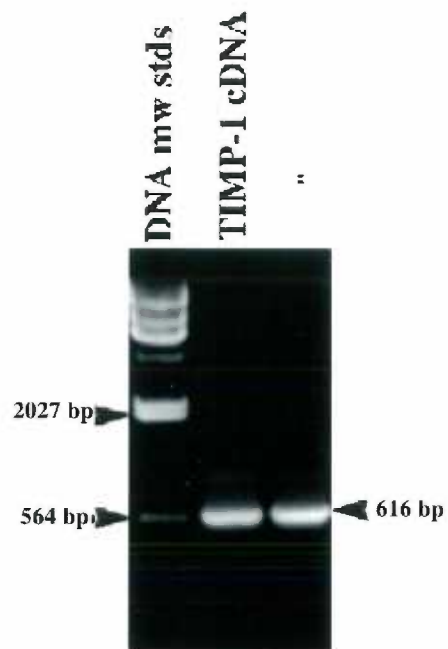


Figure 12: PCR amplification of TIMP-1 cDNA for the purpose of subcloning. The two lanes are identical samples of the 616 bp PCR product. DNA molecular weight standards are in the first lane.

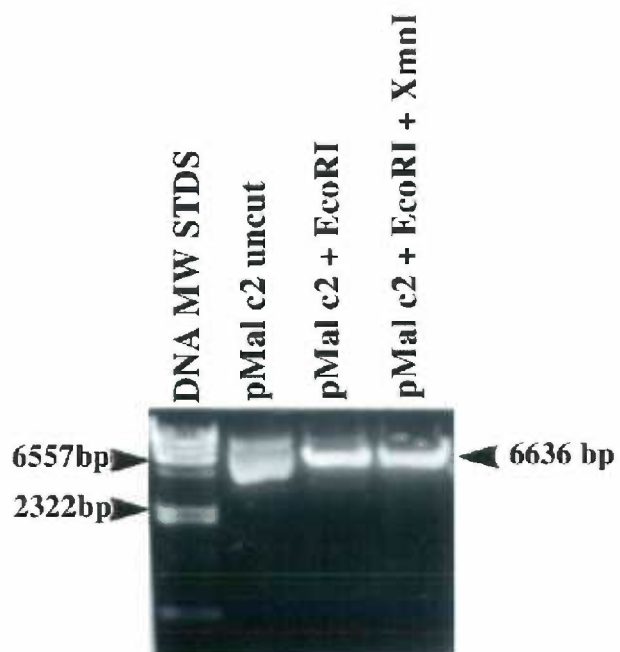


Figure 13: Restriction digestions of the pMAL vector with EcoRI and/or XmnI or uncut vector, as indicated, for the purpose of cloning.

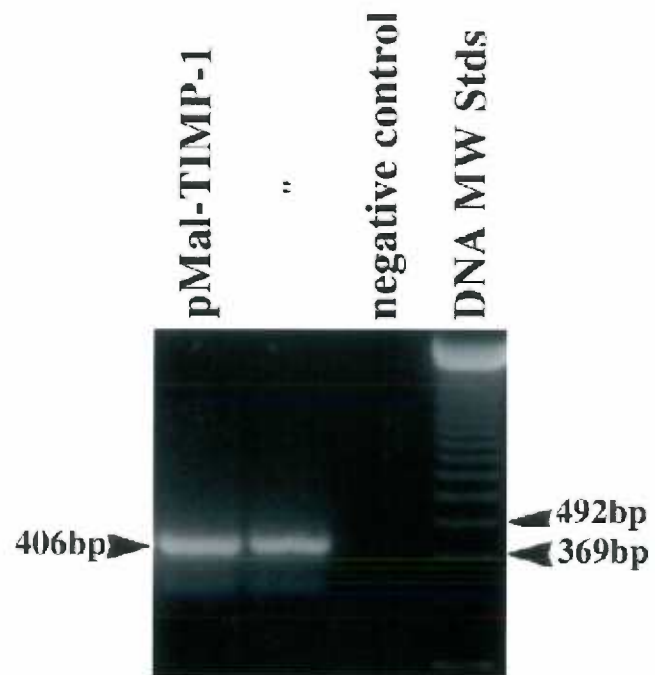


Figure 14: PCR-screening of selected pMAL-TIMP-1 transformants with primers specific for the TIMP-1 sequence. The first two lanes are from different clones.

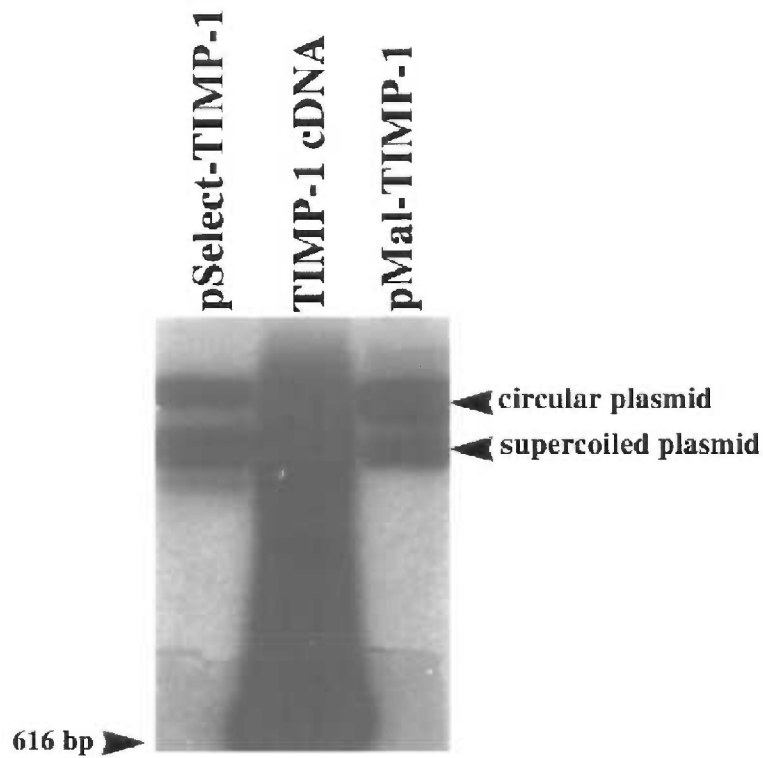


Figure 15: Detection of TIMP-1 by southern blot analysis with a radiolabeled TIMP-1 DNA probe. The first lane is a positive control of an uncut plasmid of pSelect-TIMP-1, the second lane is a positive control of the TIMP-1 PCR product, and the third lane is the selected pMAL-TIMP-1 plasmid which migrates as a circular plasmid (upper band) and a supercoiled plasmid (lower band).

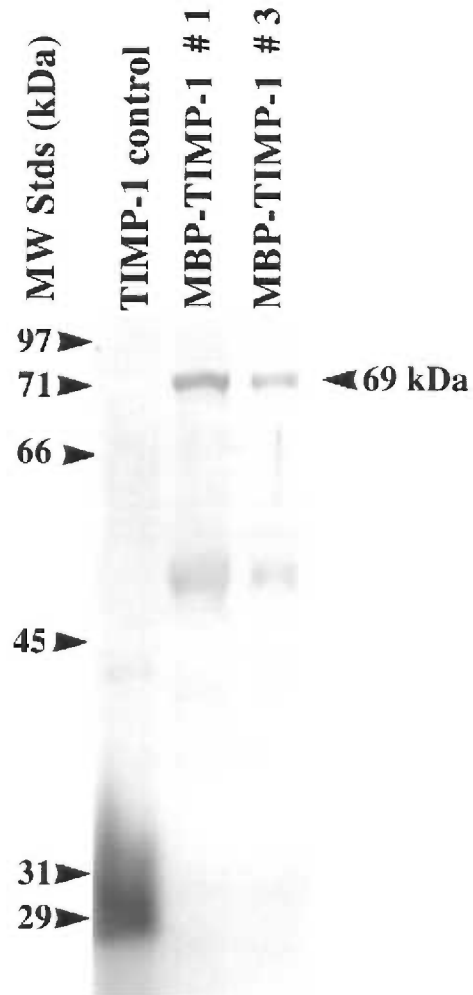


Figure 16: Western immunoblot of MBP-TIMP-1-expressing cells. A positive TIMP-1 control was loaded in the first lane, the soluble fraction of the cell lysate with the MBP-TIMP-1 fusion protein from two separate clones in the second and third lanes.

lower molecular weight band at 50 kDa. The recombinant protein did not appear to be inducible with IPTG (data not shown). The fusion protein was then subjected to purification by harvesting the soluble extract from the lysates and applying to amylose affinity resin. Flow-through and eluted fractions were collected and analyzed by western analysis to determine relative purity of the TIMP-1 fusion protein. Insoluble extracts from the bacterial cells were also analyzed for the presence of the fusion protein. Nearly equal amounts of the recombinant protein were detected in the soluble and insoluble extracts from cell lysates by western analysis (data not shown), however, only soluble extracts were used for purification attempts of the fusion protein. The recombinant MBP-TIMP-1 fusion protein did not appear to bind to the amylose matrix. In an attempt to improve fusion protein binding with the amylose resin, the recombinant protein was denatured and slowly renatured in binding buffer prior to column binding [209]. This did not help in the purification of the fusion protein. The approximate yield of crude, recombinant protein from this expression system was 0.2-2mg per 1 liter culture, as estimated from Coomassie blue staining of the fusion protein.

TIMP-1 cDNA was also cloned into the glutathione-s-transferase fusion protein vector, by the same methods described above except that the restriction enzymes used for cloning were Bam HI and Eco RI (Fig. 17). XL1-Blue cells were transformed with the recombinant plasmid and clones were selected based on restriction digestion analyses in order to verify correct orientation and sequence of the TIMP-1 insert. pGex1-TIMP-1 clones were digested with Pst I (Fig. 18a) and with Eco RI and Bam HI (Fig. 18b) yielding the expected fragment sizes. Individual clones were grown in large overnight cultures for

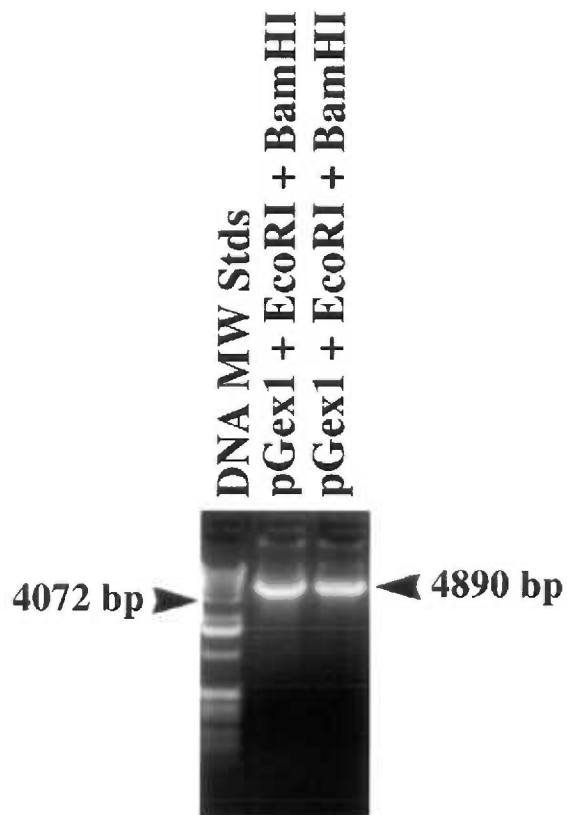


Figure 17: Restriction digests of the pGEX vector with EcoRI and BamHI.

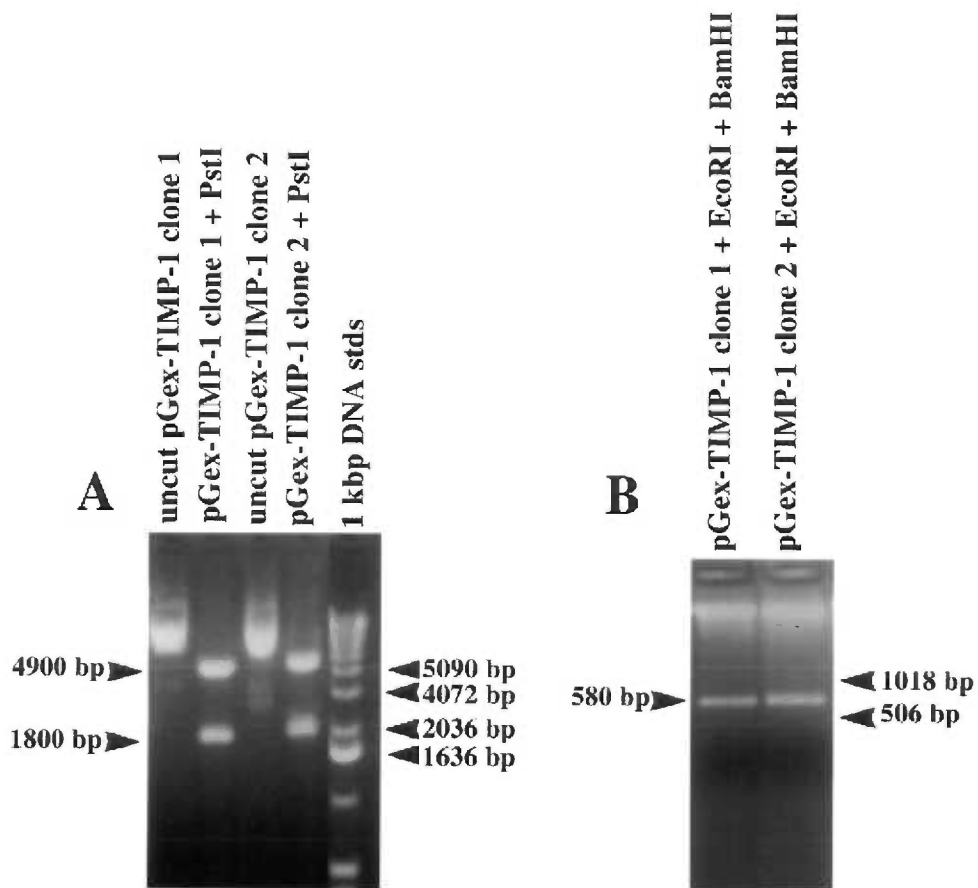


Figure 18: Restriction digests of selected pGEX-TIMP-1 transformants with either Pst I (panel A) or with EcoRI and BamHI (panel B).

recombinant protein expression. Cultures were analyzed by SDS-PAGE and Coomassie blue staining to determine relative levels of induced fusion protein expression. The recombinant protein did not appear to be inducible with IPTG (not shown).

In order to purify the GST fusion protein, crude cell lysates from the soluble fraction were applied to the glutathione column. The insoluble fraction was also analyzed for the presence of TIMP-1 fusion protein. Again it appeared that roughly half of the recombinant protein was found in the insoluble extract, however, only the soluble fraction was used for affinity purification. Flow through and eluted fractions were collected from the glutathione column and analyzed for the presence of GST-TIMP-1 fusion protein by Western immunoblot analysis. The fusion protein only appeared in the flow through and, although conditions were optimized for binding interactions, the GST-TIMP-1 fusion protein did not bind to the glutathione-sepharose for purification (data not shown). However, it was possible to achieve partial purification of the GST-TIMP-1 fusion protein by subjecting the soluble extracts to anion exchange chromatography on a DE 52 column. Increasing concentrations of NaCl were used to elute the protein. Fractions were analyzed by SDS-PAGE, Coomassie blue staining (Fig. 19a), and Western analysis using an anti-TIMP-1 antibody (Fig. 19b). The recombinant protein eluted at salt concentrations of approximately 200-300 mM NaCl and migrated at an approximate molecular weight of 55 kDa. There was an additional unidentified band detected at approximately 97 kDa in the Western blot (Fig. 19b). The final yield of partially pure recombinant protein was 0.2 mg per liter of culture, as estimated by Coomassie blue staining.

TIMP-1 Cloning and Expression in the Retroviral expression system - TIMP1

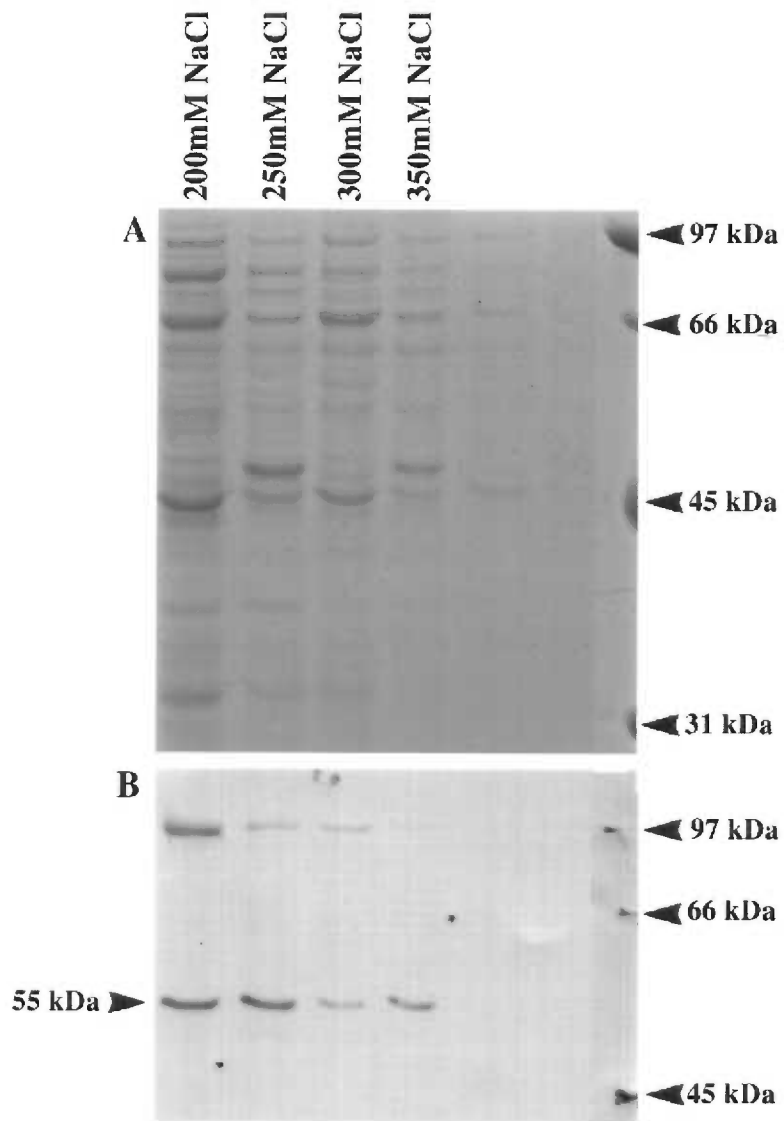


Figure 19: Purification of GST-TIMP-1 fusion protein by DE52 chromatography. Eluted fractions at increasing NaCl concentrations are in lanes 1-6. (A) Coomassie stained gel, (B) Western immunoblot with TIMP-1 antibody. Fusion protein migrates at a molecular weight of 55 kDa.

protein was also expressed in a retroviral expression vector in a mammalian cell culture system [170, 176]. The TIMP-1 cDNA was cloned into the expression vector pSFF by initially PCR-amplifying the TIMP-1 cDNA and then digesting the TIMP-1 cDNA with BamHI and EcoRI (Fig. 20). The pSFF vector was constructed so that the gag, pol and env genes are no longer capable of producing functional retroviral gene products. The multiple cloning site is localized to the env gene region. The pSFF vector was digested with BamHI and EcoRI to create compatible ends for ligation with the TIMP-1 insert (Fig. 20). Following ligation of the excised TIMP-1 cDNA into pSFF, DK-1 cells were transformed and several individual clones were selected for further analysis by restriction digestion and sequencing in order to determine the proper orientation and sequence of the TIMP-1 insert. In addition, plasmids from selected clones were purified and then subjected to PCR amplification using primers specific for TIMP-1 sequences. The pSFF vector was used as a negative control in the reactions. Two distinct TIMP-1 primer sets were used to amplify two fragments of approximately 406 bp and 711 bp (Fig. 21).

Cocultures of the packaging-defective cell lines, Ψ -2 cells and PA-12, cells were seeded at the appropriate density 48 hours prior to transfection. They were then transfected with the recombinant plasmid as a calcium phosphate precipitate. Mock transfected controls did not receive any vector DNA. After transfection, the cocultures were grown and maintained for several weeks to allow the infection process to continue. The infection process was stopped, typically 3-4 weeks later when high levels of TIMP-1 mRNA expression could be detected by RT-PCR (Fig. 22) To stop the cross-infection process, the cells were limit-dilution cloned in 96-well tissue culture plates.

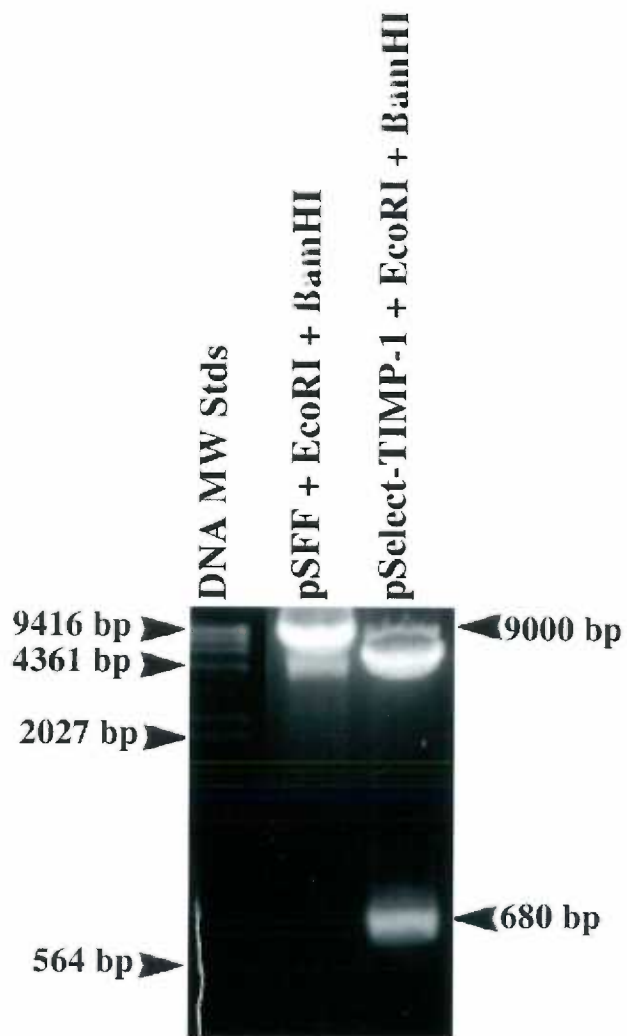


Figure 20: Restriction digestion of the pSFF vector (lane two) and of pSelect-TIMP-1 (lane three) with EcoRI and BamHI for cloning.

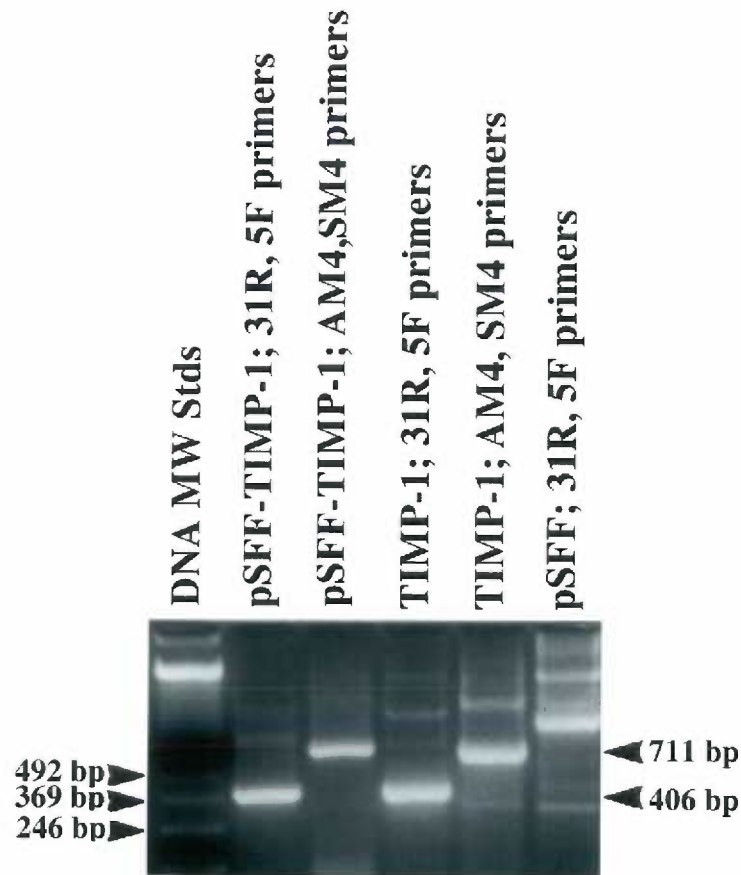


Figure 21: PCR amplification of pSFF-TIMP-1 transformants with primer pairs specific for TIMP-1 DNA sequences, as indicated. A negative control of the pSFF plasmid without the TIMP-1 insert is in the lane on the far right.

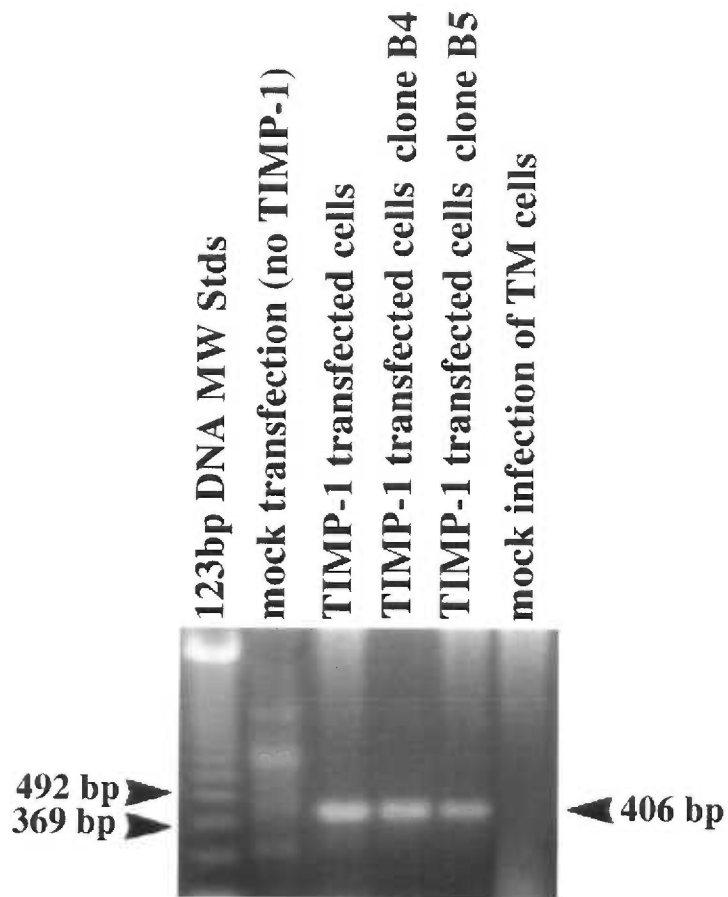


Figure 22: RT-PCR of mRNA from selected cells transfected with the pSFF-TIMP-1 plasmid. Primer pairs were specific for the TIMP-1 sequence.

Approximately 15 wells per plate contained single cells which were grown up as clonal cell lines. Established clonal cell lines expressing TIMP-1 at reasonable levels were used to characterize the production of TIMP-1 at both the mRNA level and the protein level. Endogenous TIMP-1 from the mock transfected cells was not detectable by either RT-PCR or Western blot analysis. However, when the media from the TIMP-1 transfected cell lines was concentrated 10-100x, TIMP-1 protein was only faintly detectable (data not shown). Purification by TIMP-1 binding to heparin sepharose [198] was attempted, but levels of TIMP-1 protein expressed in this system were low and yield was not enough for further protein analysis.

TIMP-2 Fusion protein expression and purification - The TIMP-2 cDNA was cloned into the pMAL C vector and expressed in XL1-Blue cells by Lisa Parshley in the Acott lab (data not shown). Individual clones expressing high levels of the recombinant MBP-TIMP-2 were selected and grown in large overnight cultures for purification. Soluble cellular extracts were collected and applied to the amylose affinity resin. Fractions were collected and analyzed by SDS-PAGE and Western analysis using an antibody to TIMP-2. The recombinant protein was purified to >85% homogeneity as determined by Coomassie blue staining (data not shown). In order to cleave the maltose binding protein from the TIMP-2, the purified protein was incubated with Factor Xa and later analyzed by Western analysis. Although the cleavage reaction was optimized, and the MBP-TIMP-2 fusion protein was partially unfolded in urea in order to make the Factor Xa cleavage site more accessible to the enzyme, it was not possible to obtain cleavage of the MBP-TIMP-2 fusion protein with the Factor Xa enzyme (Fig. 23). The yield of the fusion protein was

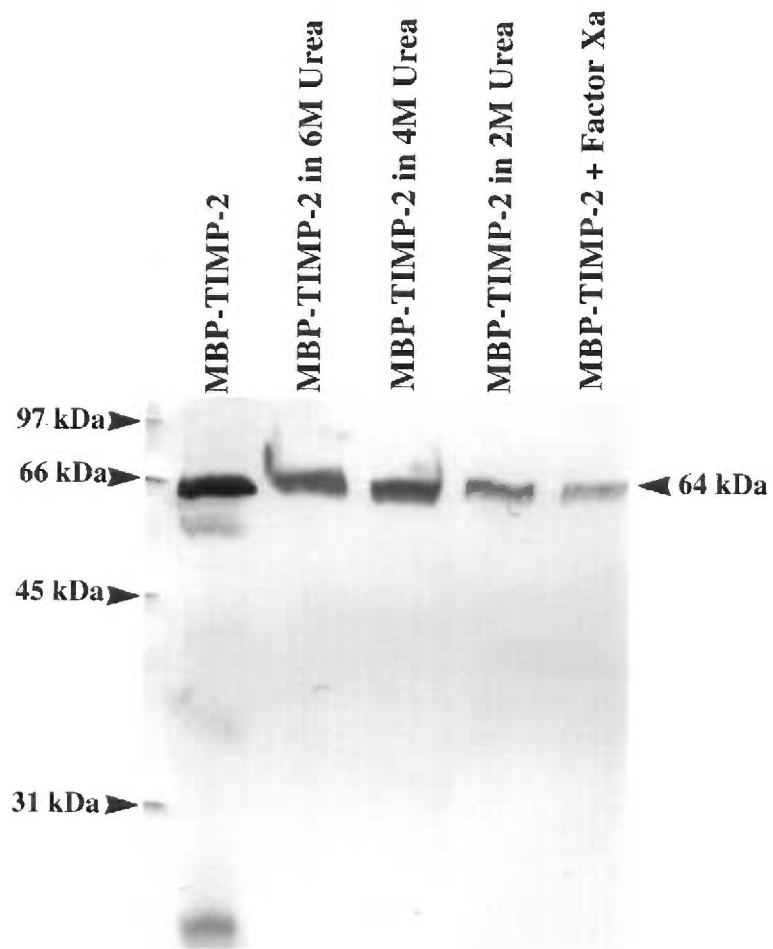


Figure 23: Western immunoblot of purified MBP-TIMP-2 in varying urea concentrations with an antibody to TIMP-2. MBP-TIMP-2 cut with 200 ug/ml Factor Xa is in the far right lane.

approximately 20 mg per liter, and purified fusion protein was subsequently analyzed for inhibitory activity in enzyme kinetic assays (see below).

TIMP-3 Cloning, Expression and Purification - TIMP-3 cDNA was originally obtained from S. Apte and consisted of a mouse/human DNA chimeric construct in which the expressed protein retains all of the correct amino acids as in the endogenous human sequence [124, 144]. The cDNA was PCR-amplified and restriction digested with *NheI* and *BamHI* for ligation into the pCEP4 vector (InVitrogen) (Fig. 24a). The pCEP4 vector was digested with the same restriction enzymes (Fig. 24b) and the excised fragments were ligated together and transformed into competent DH5 α cells. Transformed colonies were selected and analyzed by restriction digestion with either *Pst* I (Fig. 25a) or *Sal* I (Fig. 25b). In addition, the correct orientation of the TIMP-3 insert was verified by DNA sequencing. Individual clones were selected and large amounts of the plasmid were purified for transfection. For transfections, 293-EBNA (InVitrogen) cells were seeded at the appropriate density and the plasmid was transfected in a calcium phosphate precipitate. As a positive control for transfection and expression, cells were transfected with a pCEP4-CAT construct. Cells expressing the plasmid were selected based on resistance to hygromycin B. Surviving cells were then cultured in DMEM and 10 % fetal calf serum for several weeks and analyzed for TIMP-3 mRNA expression levels by RT-PCR (data not shown) and for TIMP-3 protein levels (Fig. 26a), or CAT protein for the control (Fig. 26b), by western analysis. TIMP-3 protein was found secreted into the media of the transfected cells at approximately three weeks post transfection in both its nonglycosylated form (24 kDa) and glycosylated form (27 kDa) in a 2:1 ratio.

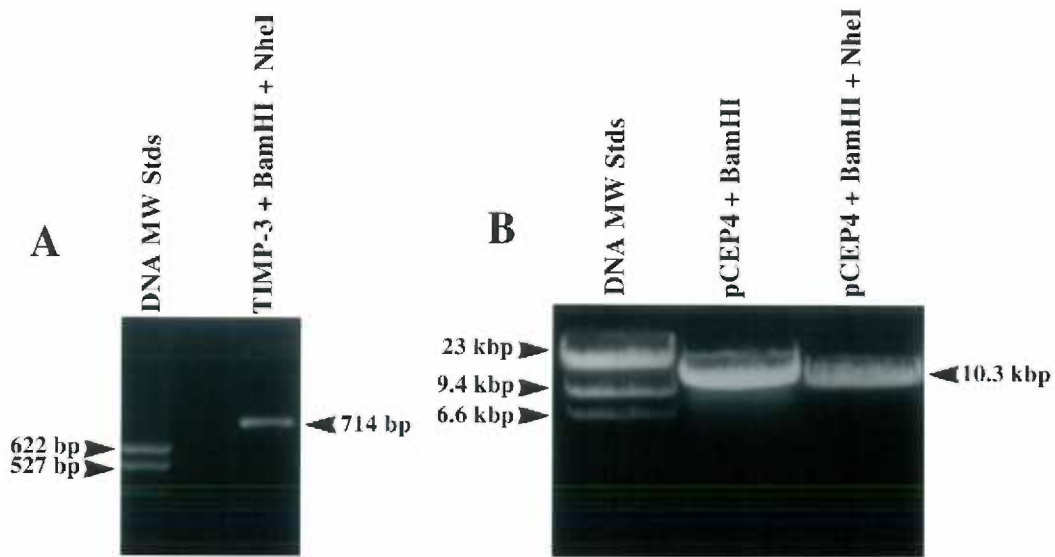


Figure 24: Restriction digestions of TIMP-3 (panel A) or the pCEP4 vector (panel B) with BamHI and NheI for cloning.

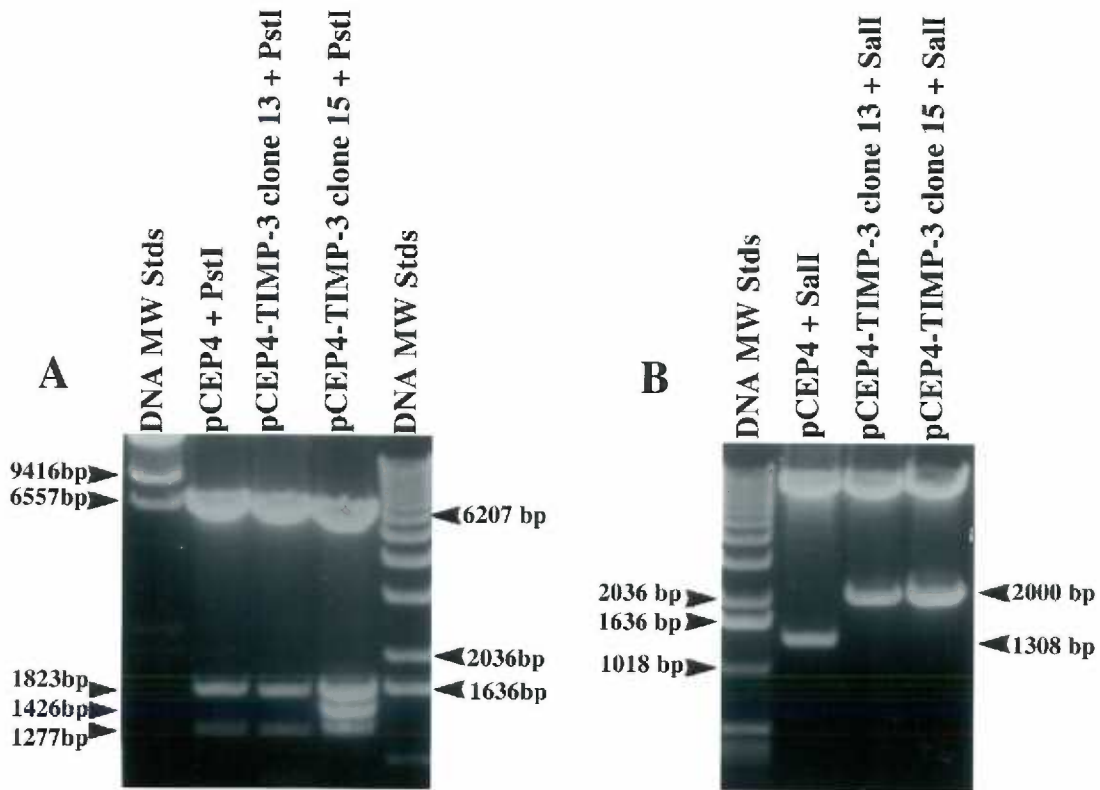


Figure 25: Restriction digestions of pCEP4 or pCEP4-TIMP-3 clones with either PstI (A) or Sal I (B) to determine the orientation of the TIMP-3 insert. Clone 13 and clone 15 have different orientations based on the digestion patterns.

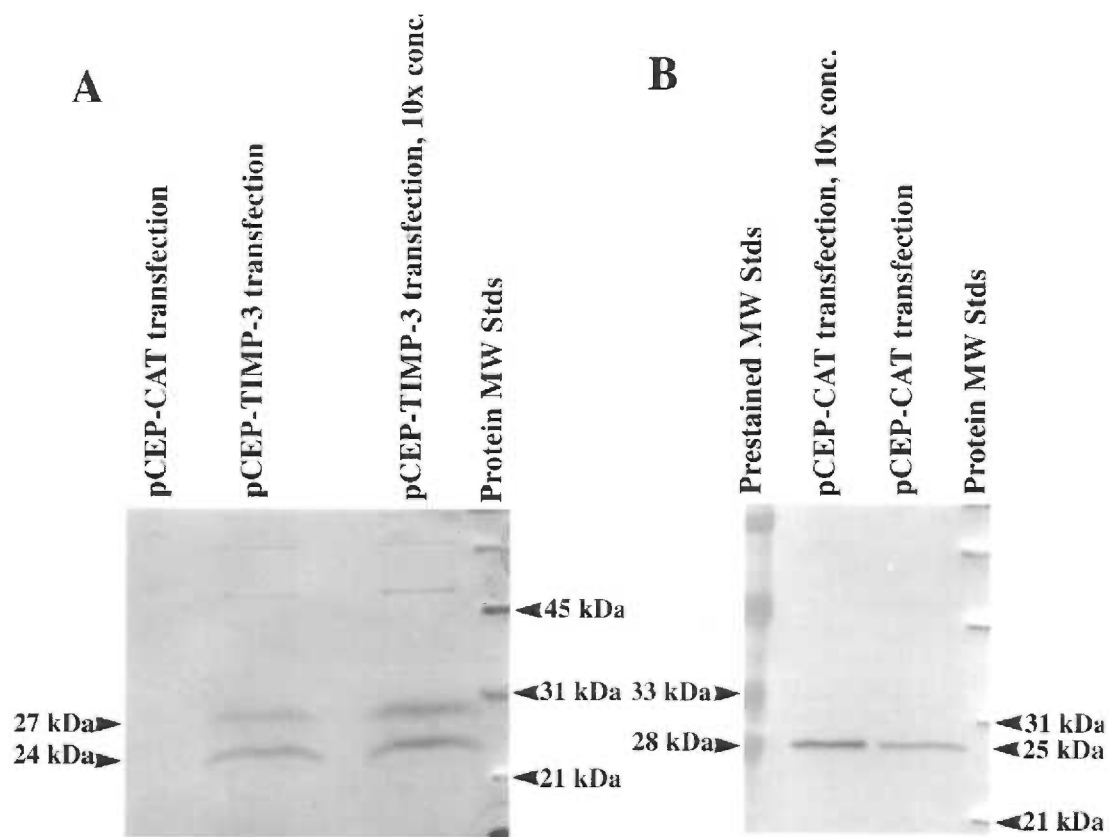


Figure 26: Western immunoblots of the media from cells transfected with a pCEP4-TIMP-3 construct or with a pCEP4-CAT construct, with either an antibody to the TIMP-3 protein (A) or an antibody to the CAT protein (B).

Unidentified, high molecular weight bands were detected as well (Fig. 26a). The CAT protein was detected as a 25 kDa band (Fig. 26b). The media was collected from cells grown serum- free for concentration and purification of the TIMP-3 protein. Beyond four weeks post transfection, the levels of TIMP-3 protein in the media decreased dramatically, however, the protein was still detectable at reasonable levels in the extracellular matrix of the transfected cells. TIMP-3 was purified from the media by binding the protein to a carboxy-methyl support (a cationic exchanger from BioRad, Inc.) The isoelectric point of TIMP-3 (pI = 9.1) is higher than that of TIMP-1 (pI = 8.0) or TIMP-2 (pI = 7.4), and it can therefore be purified away from the other TIMPs based on charge alone. TIMP-3 protein binds at low NaCl concentrations to the cation exchange resin, and elutes at 0.5-1M NaCl (Fig. 27), although approximately half of the TIMP-3 protein did not bind to the cation exchange column under the conditions tested. The purity and concentration of the TIMP-3 protein was determined by silver staining of SDS-PAGE gels (Fig. 28) and Western analysis, however, only the 27 kDa band was detected by silver stain. The protein was estimated to be 70% pure and the approximate yield was 500 ng partially-purified TIMP-3 protein per liter of media. The TIMP-3 protein could also be extracted from the extracellular matrix of the transfected cells using 1 % SDS in buffer and electrophoresed on an SDS-PAGE gel. The recombinant TIMP-3 was analyzed for its inhibitory activity against the MMPs in a reverse zymogram (Fig. 29). TIMP-3 extracted from the ECM, in both its glycosylated and nonglycosylated forms, was active on the reverse zymogram. Mock transfected cells showed approximately five fold less inhibitory activity, suggesting the presence of endogenous TIMP activity in the cells.

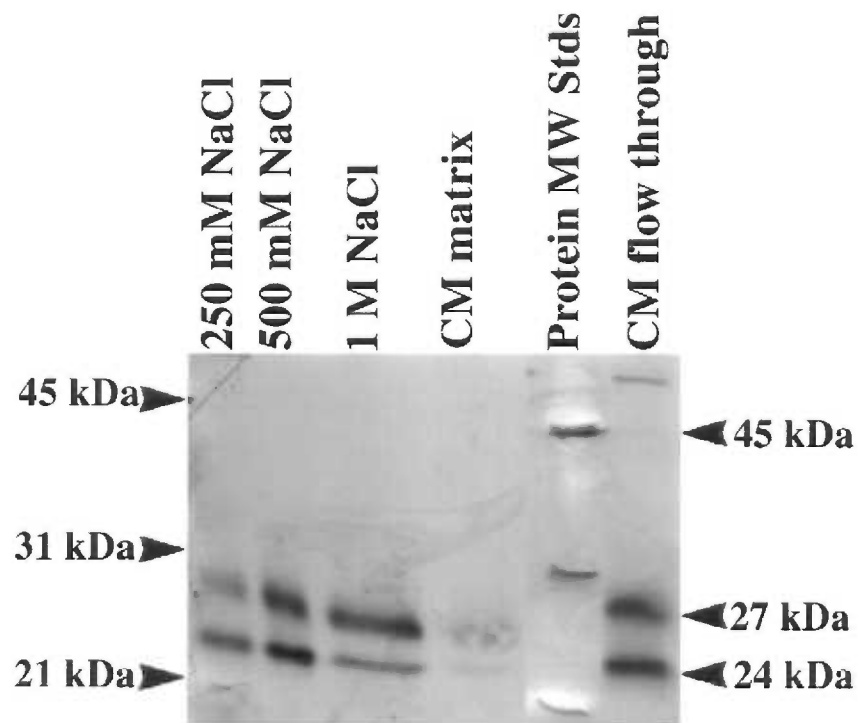


Figure 27: Western immunoblot of the purification of TIMP-3 protein by cation exchange chromatography with a carboxy-methyl (CM) resin. Proteins were eluted with increasing concentrations of NaCl. The far right lane represents the portion of the TIMP-3 sample that did not bind to the CM resin.

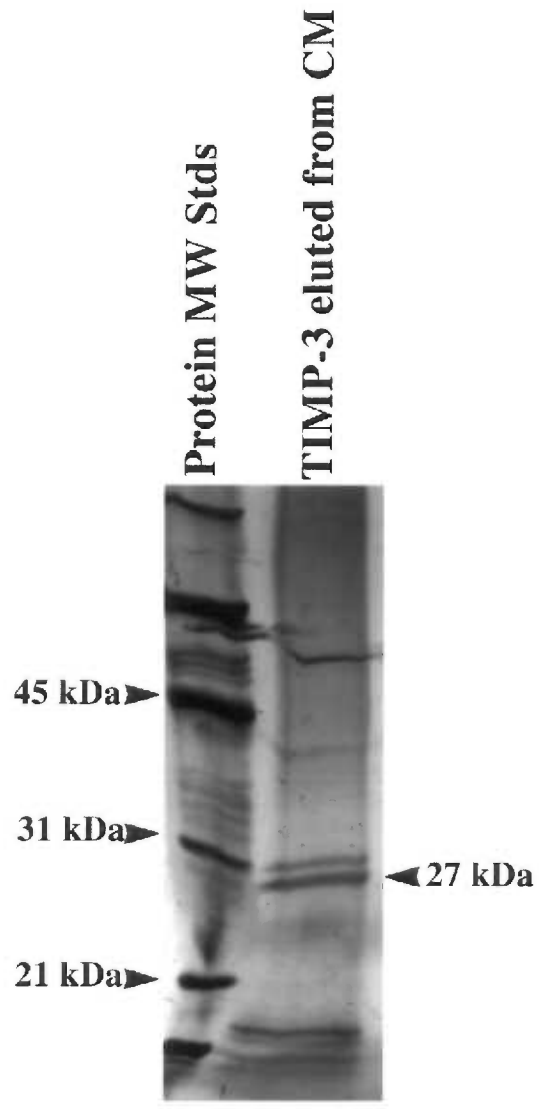


Figure 28: Silver stained SDS-PAGE of purified TIMP-3 from the media of transfected cells. Glycosylated TIMP-3 migrates at 27 kDa.

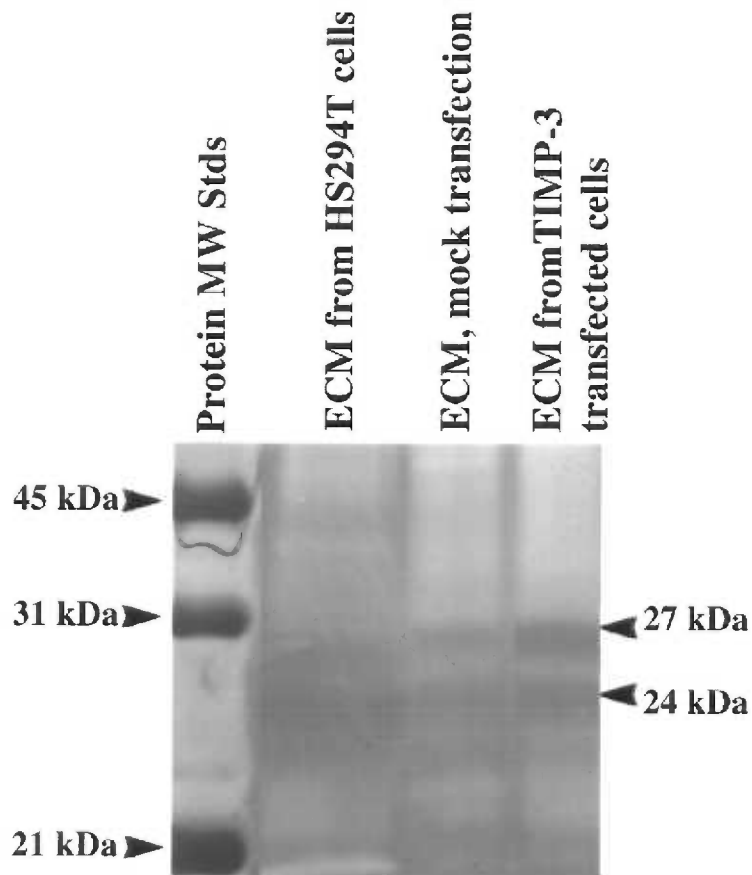


Figure 29: Reverse zymogram to determine levels of TIMP-3 inhibition in ECM samples. ECM from a tumor cell line (HS294T) that expresses TIMP-3 in lane two, ECM from mock-transfected cells in lane three, and ECM from TIMP-3 transfected cells in lane four.

Gelatinase A and B purification from cultured cells - In order to purify gelatinase B and A for use in enzymatic assays and for kinetic analysis, HT1080 cells (human fibro- sarcoma cells from ATCC) and HS27 cells (human foreskin fibroblasts from ATCC) were cultured. The HT1080 cells have been shown to express high levels of gelatinase B, and gelatinase A was expressed at much higher levels than gelatinase B in the HS27 cells allowing purification of the individual gelatinases from the different cell lines [50, 199, 200]. The media was collected from the cells and concentrated 10-100x prior to applying it to gelatin-agarose. Concentrated media was then applied to gelatin-agarose and washed extensively before eluting the gelatinases with 10% dimethyl sulfoxide. The eluted fractions were analyzed by gelatin zymography (Fig. 30a) and Western analysis of gelatinase A (Fig. 30b) and gelatinase B (Fig. 30c) to determine relative enzymatic activity and yield. At this stage of purification the peak fractions contained predominantly gelatinase A or gelatinase B with no detectable contamination of other matrix metalloproteinases. Though the gelatinases were purified from cells that predominantly expressed either gelatinase A or gelatinase B, often it was difficult to obtain a completely homogeneous sample of either one or the other enzyme. Therefore, other methods were employed in order to separate the two gelatinases from each other based on their differences in glycosylations. Gelatinase B is a glycosylated protein, whereas gelatinase A has no glycosylations. Concanavalin A-sepharose is used in the purification of glycoproteins. Lentil-Lectin Sepharose binds α -D-glucose and α -D-mannose residues and, like Con A, is used for purification of glycoproteins. Both resins were used in order to bind to gelatinase B and separate it from gelatinase A (data not shown). Although

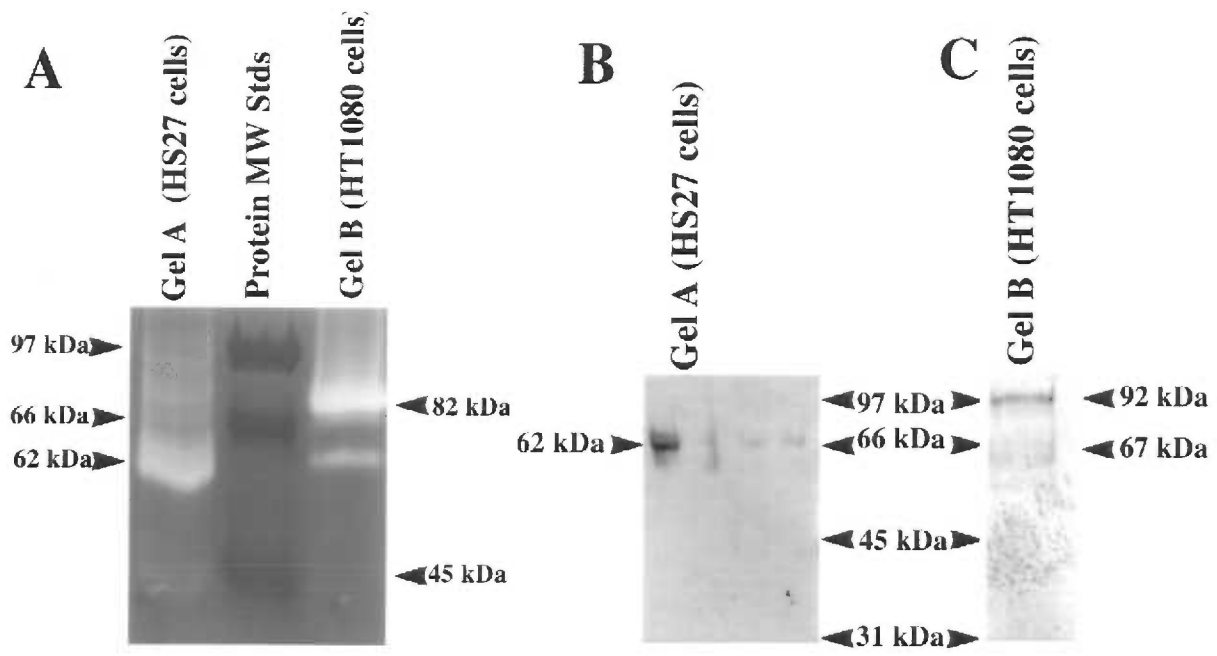


Figure 30: Gelatin zymogram (A) and Western immunoblot (B) of gelatinase A and B purified from cultured cells by gelatin affinity chromatography.

gelatinase B appeared to bind to both affinity columns and could later be eluted off the columns, gelatinase A was also bound at lower levels to both column matrices. It has been difficult to distinguish between the gelatinases by zymography because of the presence of the active forms of the enzymes and their multiple breakdown products, whose sizes have not been unambiguously assigned. The sizes of the lower molecular weight forms that exist for gelatinase A are 62-65 kDa, 43-45 kDa and 36-38 kDa [108, 109, 114]. The sizes of the lower molecular weight forms that exist for gelatinase B are 80-82 kDa, 66-68 kDa or 62 kDa, and 50-53 kDa or 45 kDa [38, 113, 210].

However, gelatinase A and B were able to be separated from each other based on their differences in activation [206]. Gelatinase A has been shown to have maximum enzymatic activity after a 2 hour incubation with APMA at 37°C, whereas gelatinase B activity is undetectable after a 2 hour incubation with APMA at 37°C. In contrast, gelatinase B has maximum enzymatic activity after an 18-24 hour incubation with APMA at 37°C and gelatinase A activity is nonexistent after more than 4 hours incubation under the same conditions. Although both enzymes were purified simultaneously using gelatin-agarose affinity chromatography, it was possible to separate the gelatinase A and B enzymatic activities using different conditions for their activation, prior to kinetic analysis in subsequent enzymatic assays.

D. Discussion

The tissue inhibitors of metalloproteinases are a family of secreted proteins that are

recognized for their inhibitory activity against the matrix metalloproteinases. Based on their inhibitory action, the TIMPs play pivotal roles in controlling the rate of extracellular matrix metabolism in both normal physiologic processes, as well as in disease states [136, 166]. It has therefore been of interest to clone and express the various TIMPs in expression systems in order to further study their modes of action.

The data presented above demonstrate that human TIMP-1, TIMP-2 and TIMP-3 have been expressed in various prokaryotic and eukaryotic expression systems at differing levels. The expressed TIMP proteins have been partially purified with varying levels of success. TIMP-1 was expressed as a fusion protein in two distinct prokaryotic expression vectors, the maltose binding protein and the glutathione-s-transferase fusion protein, and was detected as an expressed protein in the cell lysates. However it was not possible to purify the protein using affinity chromatography in either system. The TIMPs normally form a highly compact tertiary structure containing six disulfide bonding interactions. The TIMP-1 portion of the fusion protein may have been incorrectly folded during protein synthesis and this may have interfered with the ability of the maltose binding protein or glutathione-s-transferase protein to interact with their appropriate affinity resins. In spite of these difficulties, it was possible to obtain a partially purified TIMP-1 fusion protein by anion exchange chromatography. This fusion protein was not analyzed for inhibitory activity.

TIMP-2 was previously expressed as a fusion protein with the maltose binding protein in prokaryotic cells at relatively high levels (unpublished data). The fusion protein was purified by adding the soluble cell extracts to an amylose affinity column and eluting

in 25 mM maltose. The purified fusion protein was subjected to cleavage by Factor Xa, in order to obtain purified TIMP-2 protein lacking the maltose binding protein. Although conditions were optimized for cleavage, the proteinase was unable to cleave the fusion protein away from TIMP-2. Various strategies were used to denature and renature the fusion protein in order to improve Factor Xa cleavage, however the enzyme did not cleave the fusion protein. The fusion protein was analyzed and shown to have inhibitory activity in an enzymatic assay with gelatinase A, as will be described below.

TIMP-3 was cloned and expressed in a mammalian expression system. The protein has been shown to exist in a glycosylated and non glycosylated form [144, 211], and in this expression system both forms were expressed simultaneously in the transfected cells in a 2:1 ratio. The recombinant TIMP-3 protein was secreted out into the media of the transfected cells for up to approximately 4 weeks, after which it was only detectable in the ECM of the same cells. TIMP-3 has an unusually high isoelectric point ($pI = 9.1$) as compared with either TIMP-2 ($pI = 7.4$) or TIMP-1 ($pI = 8.0$), which allowed for separation of the three inhibitory activities. TIMP-3 protein was bound to a cationic exchange matrix and eluted at high salt concentrations and the eluted, partially-purified TIMP-3 protein was detected by silver stain. The TIMP-3 protein localized to the ECM of the cells was extractable with 1 % SDS and contained predominantly the nonglycosylated form of the protein. The partially purified TIMP-3 was then analyzed for inhibitory activity against the MMPs on a reverse gelatin zymogram.

Gelatinase A and B are two members of the MMP family of proteins. The expression of both gelatinase A and gelatinase B has been shown to be upregulated in

tumor cells or the stroma surrounding tumor cells, and their expression and activity correlate with the invasive potential of various tumor cells [46, 49, 182, 184, 212]. Their activities against various protein and peptide substrates have been investigated, although no mechanisms have been proposed for their mode of action [24, 177, 213, 214]. Additionally, the mode of inhibitory action of the TIMPs on the gelatinases is unknown.

In order to better understand the enzymatic activity of the gelatinases and the mode of action of various inhibitors on the gelatinase activity, it was necessary to purify gelatinase A and B from cultured cells. Various cell lines had been shown previously to express moderate to high levels of either gelatinase A or gelatinase B [50, 199, 200]. Gelatinases were partially purified from the medium of the cultured cells by binding to, and eluting from gelatin-agarose chromatography [206]. The enzymes were both shown to have enzymatic activity on a gelatin zymogram, prior to their use in the enzymatic assays that will be described in the following chapter. As will be discussed, the gelatinase A and B activities were analyzed using gelatin as a substrate. In order to avoid possible contaminating gelatinase activity, for example, either gelatinase A contaminating the gelatinase B preparation, or vice versa, the enzymes were activated differentially. As mentioned previously, the enzymes have different requirements for their activation steps where gelatinase A is activated within a two-hour incubation period with APMA, but gelatinase B requires an eighteen to twenty-hour incubation for optimal enzyme activity [38, 90, 114, 210]. In this way it was possible to assign gelatinolytic activity unambiguously as either gelatinase A or gelatinase B activity in enzymatic assays that will be described below.

III. Gelatinase A and B Inhibition Kinetics; A Glaucoma Model System

A. Introduction

Gelatinase A (72 kDa gelatinase) and gelatinase B (92 kDa gelatinase) are two members of the matrix metalloproteinase family. The gelatinases share several common features with other members of the MMP family, including an N-terminal domain responsible for the maintenance of the proenzyme state, a zinc-binding domain that comprises the active center of the enzyme, and finally a hemopexin-like C-terminal domain. Unique to gelatinase A and B is an additional domain composed of three fibronectin type II-like repeats inserted in tandem within the zinc-binding catalytic domain [25]. Gelatinase B also contains an $\alpha 2(V)$ collagen-like domain not found in any of the other family members [26].

Both enzymes hydrolyze type IV, type V, type VII, and type X collagens, fibronectin, elastin, and a variety of gelatins [25, 26, 215, 216]. The C-terminal domain of the gelatinases has been shown to differ from collagenase and stromelysin in that it has no collagen binding properties [80]. Several recent studies have demonstrated the importance of the fibronectin-like domains in gelatin binding. Recombinant proteins corresponding to the fibronectin-related regions of gelatinase A and B were found to have high affinity for gelatin and elastin, as well as for native type I collagen [88, 91, 216, 217]. Conversely, recombinant gelatinase A lacking the fibronectin type II units was shown to lack affinity for gelatin or type I and type IV collagens and its ability to degrade gelatin

was impaired, indicating that the fibronectin-like domain is the site of collagen and gelatin binding [90]. A catalytic domain of gelatinase A with deletion of the fibronectin-like repeats was constructed and shown to be functionally active against a peptide substrate and had reduced activity; against gelatin and casein [218]. Additionally, these domains have been shown to be crucial for elastin binding and elastolytic activity [92]. The fibronectin-like domains of the gelatinases have been proposed to form an extension of the substrate binding cleft in which all three type II units contribute to gelatin binding [219].

Substrate specificities of many of the MMPs have been investigated using short synthetic peptides as model substrates. Cleavage site specificity of gelatinase was determined using small collagenous peptides with varied sequences around Gly-Leu or Gly-Ile [24]. Subsite specificities of gelatinase A and B were systematically examined using synthetic oligopeptides covering the P_3 through P_3' subsites of the substrate, where P_n and P_n' represent the amino acid residues in the substrate on either side of the scissile bond. The reference peptide was modeled after the collagenase cleavage site in the $\alpha 1$ (I) chain of collagen (Gly-Pro-Gln-Gly-Ile-Ala-Gly-Gln) [93, 213, 214]. With respect to amino acid preferences in peptide substrates, gelatinase A and B are very similar [93]. They both prefer hydrophobic residues in subsites P_2 and P_2' , and Pro is preferred by both in subsite P_3 . The largest differences in the subsite specificities of the MMPs occur at subsites P_1 , P_1' , and P_3' . The gelatinases tolerate only small amino acids in subsite P_1 and Ile appears to be the best amino acid at subsite P_1' , and may be replaced only by Met. As for the P_3' subsite, the only replacement for Gly that was tolerated was Ala or Ser [93].

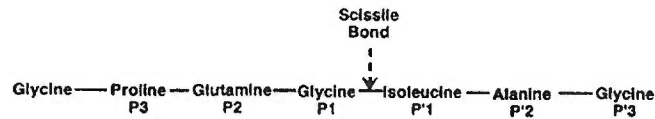
Optimization of substrate structure has provided a convenient method for studying

enzyme mechanisms of action as well as affording information of inhibitor design. In order to facilitate kinetic studies of the MMPs, quenched fluorescent substrates have been created. These substrates consist of a short sequence of amino acids containing the scissile peptide bond which separates the naturally fluorescent amino acid tryptophan from a dinitrophenyl (Dnp) group that acts as an internal quencher [177, 213]. Quenching occurs by resonance energy transfer and is mostly unaffected by the intervening amino acids. More recently, an MMP substrate was developed and tested on various MMPs where the tryptophan was replaced by derivatives of 7-methoxycoumarin, which are highly fluorescent and efficiently quenched by the Dnp group. The substrate, (7-methoxycoumarin-4-yl)Acetyl-Pro-Leu-Gly-Leu-(3-[2,4-dinitrophenyl]-l-2,3-diaminopropionyl)-Ala-Arg-NH₂, was used to analyze enzymatic activity of collagenase, stromelysin, gelatinase A and matrilysin in continuous assays [220]. In addition to a fluorescently-labeled gelatin protein substrate, this peptide substrate has been used in enzymatic assays to characterize the activity of the gelatinases and the inhibitory activity of various inhibitors of the gelatinases, as will be described later in this chapter.

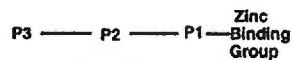
The MMPs play a fundamental role in the pathophysiology of rheumatic disease and are involved in tumor cell invasion and metastasis [8, 9, 16, 221, 222]. As a result, considerable effort has been devoted to the development of synthetic peptides designed to specifically inhibit metalloproteinases [223]. Natural inhibitors of the MMPs exist and are known as the tissue inhibitors of metalloproteinases (TIMPs), as described previously. Efforts to produce active fragments of the TIMPs have not succeeded and little has been known about their mechanism of action [224]. Only recently has there been proposed a

mechanism of inhibition of collagenase by TIMP-1 involving a noncompetitive two-step process in which an inactive, rapidly formed, reversible complex slowly forms an inactive, tight complex [161]. However, much work has been focused on the search for synthetic, low molecular weight MMP inhibitors as drug targets. In vivo inhibition of the MMPs using small, potent, synthetic inhibitors has become a therapeutic goal for modulation of connective tissue degradation in various disorders. Several antibiotics and synthetic peptides have been shown to specifically inhibit various matrix metalloproteinases. Of the antibiotics, tetracycline and its synthetic forms minocycline and doxycycline have potent matrix metalloproteinase inhibitory activity. Studies have demonstrated that tetracyclines can inhibit collagenase as well as gelatinase A both in vitro and in vivo [223, 225-228]. Minocycline was chosen in order to test for inhibitory activity against gelatinase A and B in our enzyme-inhibition assays.

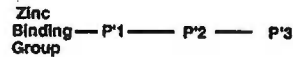
As for the synthetic peptides, small molecule inhibitors of matrix metalloproteinases have been reviewed and the largest group are the collagen substrate analogs [223]. To the extent possible from available information, the design of many of these was intended to mimic transition-state analogs. Most classes contain a zinc-coordinating ligand, such as a thiol [66, 177, 229, 230], hydroxamic acid [66, 68, 224, 231-234], carboxylate [66, 235-237], phosphinate, phosphonate or phosphonamidate group [238-242]. The zinc-coordinating ligand is attached to a peptidic residue containing a hydrophobic side chain recognized by the enzyme's active site. Up to 3 of the amino acid residues in the peptide inhibitors are found on either side of the collagen scissile bond (Fig. 31). The left-hand side inhibitors contain amino acid residues N-terminal to the



Left Hand Side Inhibitors:



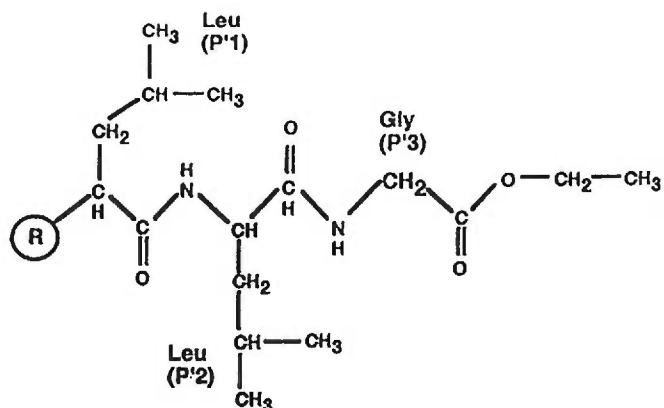
Right Hand Side Inhibitors:



Left and Right Hand Side Inhibitors:



Figure 31: The $\alpha 1$ type I collagen cleavage site. The amino acid sequence around the scissile bond is shown. The "P" sites indicate homologous amino acids used in the design of MMP inhibitors. The relative positions of homologous amino acid residues and zinc-binding moieties are shown for the left-hand side, right-hand side, and left- and right-hand side inhibitors. (from: M. Vincenti, "Using Inhibitors of Metalloproteinases to Treat Arthritis", *Arthr. Rheum.*, 37: 1115, 1994.)

A

Zinc Binding Group (R)

-SH (THIOL)

-CH₂CONHOH (HYDROXAMIC ACID)

-CH₂COOH (CARBOXYALKYL)

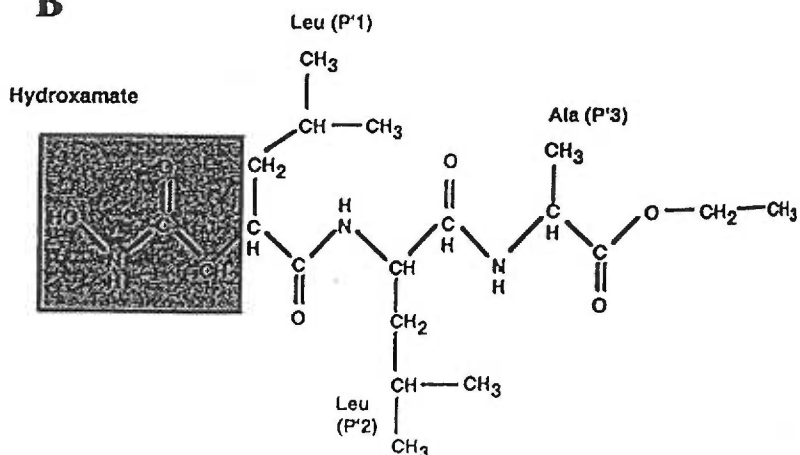
B

Figure 32: Structure of the right-hand side inhibitors (A) and structure of a representative hydroxamate-base peptide inhibitor (B). The "P" sites indicate homologous amino acids used in the design of MMP inhibitors.

(from: M. Vincenti, "Using Inhibitors of Metalloproteinases to Treat Arthritis", *Arthr. Rheum.*, 37: 1115, 1994.)

collagen cleavage site with the zinc-binding molecule at the C-terminus of the peptide, whereas right-hand side inhibitors are in the opposite orientation with the zinc ligand at the N-terminus of the peptide (Fig. 32a). Current theory suggests that these compounds act by chelating the catalytic zinc molecule thereby inactivating the enzyme [223]. Most of the X-ray structures of MMP inhibitor complexes published show a substrate-like binding of the inhibitor along the active site cleft and a zinc-binding group which is in most cases a hydroxamic acid group (Fig. 32b) [68-70, 72, 73, 77, 243]. Most inhibitors in these structures are right-hand-side inhibitors with large hydrophobic P1' residues occupying the S1' pocket of the protein. The crystal structure of neutrophil collagenase complexed to a hydroxamate inhibitor was recently described in which the inhibitor binds to the S1-S2' sites and coordinates to the catalytic zinc via the hydroxyl and carbonyl oxygens of the hydroxamate [244]. The crystal structures of matrilysin complexed to hydroxamate, carboxylate or sulfodiimine inhibitors were also recently determined [66]. Each inhibitor was shown to interact with the active site zinc in a unique manner, the hydroxamate inhibitor being the most potent inhibitor [66]. This emphasizes the dominant role the zinc-coordinating group plays in determining the relative potencies of the various inhibitors, and there is an interplay between zinc coordination and the exact orientation of the other atoms in the inhibitor. Much less is known about the interactions of synthetic inhibitors with the gelatinases since no crystal structures of the catalytic domain of the gelatinases have yet been determined. It is hypothesized that because of overall similarities in the MMP active site, the synthetic inhibitors interact at the gelatinase active site in a similar manner as with collagenase. Based on this information, several

synthetic inhibitors, were selected for studies on their interactions with gelatinase A and B in enzymatic assays.

In addition to the above-mentioned classes of substrate analog MMP inhibitors, peptides that mimic sequences in the conserved region of the propeptide domain of the matrix metalloproteinases have been shown to have inhibitory activity against stromelysin and collagenase, as well as inhibiting tumor cell invasion [245-249]. In these studies it has been suggested that the propeptide binds to the active site and inhibits the enzyme in either a mixed or competitive mode of inhibition [246]. However, recent findings propose that with thermolysin, whose active site interactions differ slightly from the other MMPs [71], the prosequence may interact with enzyme at a region distinct from the active site in a noncompetitive mode of inhibition [249]. Propeptides were synthesized and used for analysis in the enzymatic assays with gelatinase A and B.

Therefore, of the various inhibitors mentioned above several, including minocycline, tryptophan-hydroxamate, a collagenase inhibitor, and a propeptide inhibitor were analyzed to determine their mechanisms of inhibition of, and specificity for, gelatinase A and B in the protein and peptide substrate enzymatic assays.

In addition to their roles in various connective tissue disorders and in tumor invasion and metastasis, the MMPs have been proposed to play a role in the development of primary open angle glaucoma [250]. Primary open angle glaucoma (POAG) is a major blinding disease and the incidence increases dramatically with aging. The primary risk factor for glaucoma is increased intraocular pressure [251]. Aqueous humor is made by the ciliary body and flows into the anterior chamber of the eye where it bathes the lens, iris

and cornea (Fig. 33). It exits the eye through a porous filtering tissue called the trabecular meshwork (TM) and then flows out into Schlemm's canal where it enters the venous drainage system (Fig. 34). In glaucoma the aqueous humor outflow is typically reduced, while aqueous humor production by the ciliary body is nearly normal. Resistance to aqueous outflow through the TM is increased causing a subsequent increase in the intraocular pressure. Ultimately, it's the increased intraocular pressure which causes irreparable damage to the optic nerve producing loss of vision. The cause of the obstruction of the TM has not been determined, although outflow pathway ECM has been implicated as a major component of the normal aqueous humor outflow resistance [252, 253]. The normal turnover and replacement of outflow pathway proteoglycan side-chains, glycosaminoglycans, by TM cells is 1.5 days as compared with 10-14 days in the cornea or sclera [254].

Trabecular ECM turnover is initiated by members of the MMP family, and the MMP activity has been shown to be tightly controlled by the inhibitory action of the TIMPs in many other systems [2, 252, 253]. Disruption of the normal ECM turnover by these MMPs, possibly caused by an imbalance in the MMP-TIMP net activity, within the aqueous humor outflow pathway is hypothesized to be a primary cause of the elevated intraocular pressure observed in POAG [250].

In order to test this hypothesis, it has been necessary to manipulate the outflow pathway MMP activity and determine the effects in a perfused human anterior segment organ culture system, which has been described previously [250, 255-257]. Thus, increasing metalloproteinase activity, for example by the addition of purified

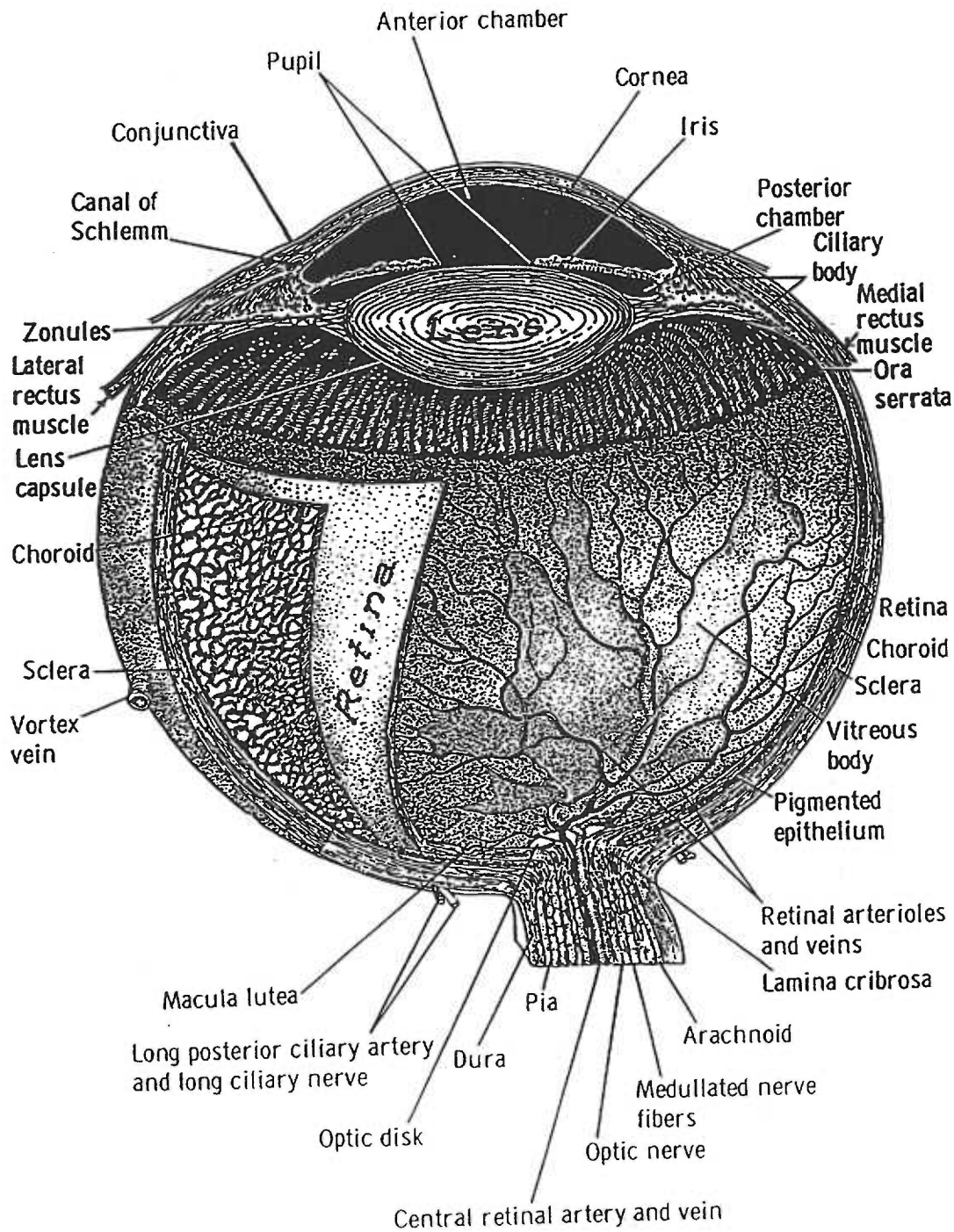


Figure 33: Anatomical Structure of the Eye.
 (from: D. Vaughan, General Ophthalmology, Chapter 1, First Edition, Lange Medical Publication, 1968.)

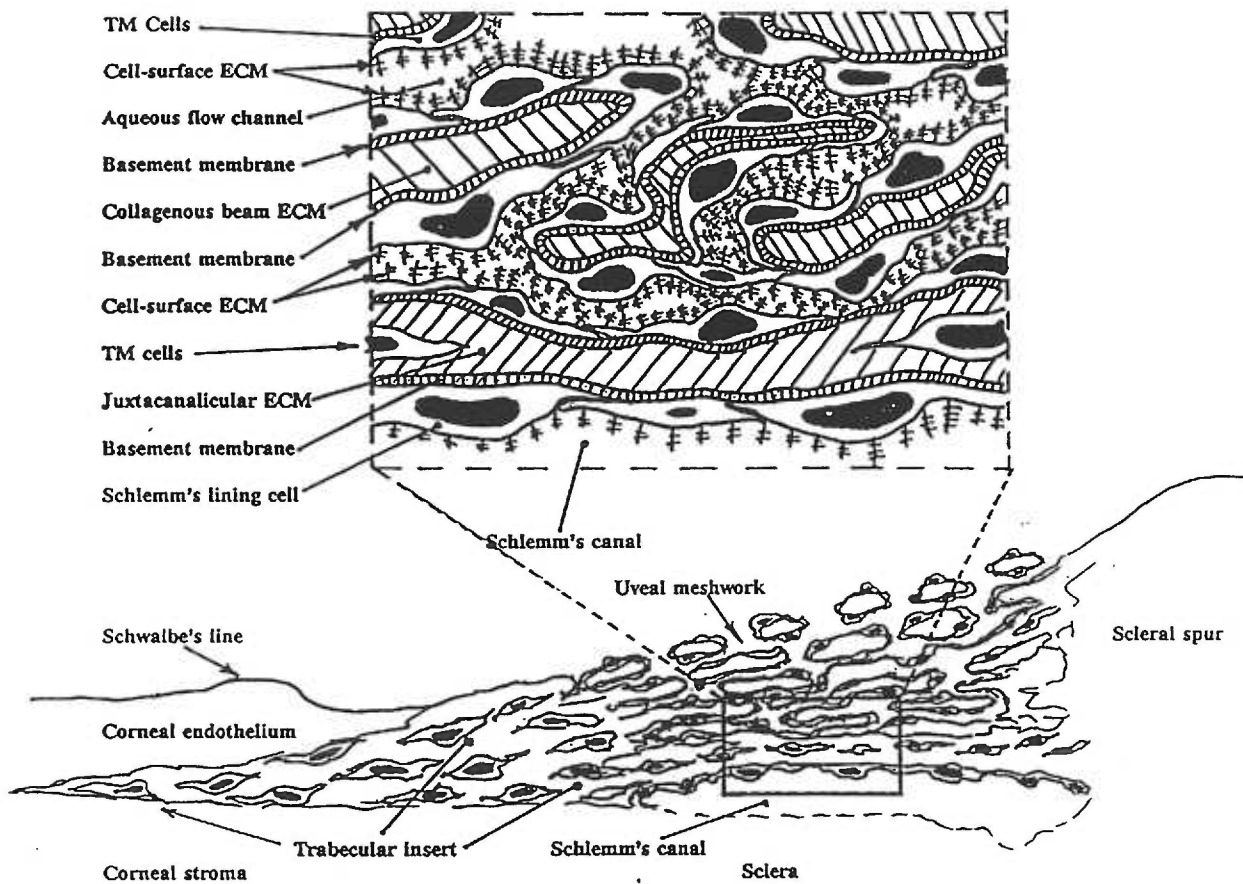


Figure 34: Diagrammatic view of the ECMs of the human trabecular meshwork. (from: T. Acott, "Biochemistry of Aqueous Outflow" in Textbook of Ophthalmology , Podos and Janoff, eds. Gower Medical Publishing, 1992.)

metalloproteinases to the outflow system, should increase the outflow rates causing the opposite of glaucoma. Moreover, decreasing the metalloproteinase activity, for example by treating with specific inhibitors of metalloproteinases, should reduce outflow rates producing glaucoma. Therefore, in order to test the hypothesis that an imbalance in the overall MMP-TIMP activity leads to glaucoma, or its opposite, and in conjunction with the enzyme inhibitor and gelatinase A and B activity assays, the same inhibitors (described above) were tested in the perfused anterior segment organ culture system.

B. Materials and Methods

Kinetic Assays - Purified enzymes (gelatinase A and B) were activated prior to their kinetic analysis in enzymatic assays. Gelatinase A was activated with 1 mM amino phenyl mercuric acetate (APMA from Sigma) for 2 hours at 37°C in 150 mM NaCl, 50 mM Tris, pH 7.5, 10 mM CaCl₂. Gelatinase B was activated for kinetic studies with 1 mM APMA for 18 hours at 37°C in the same buffer.

The FITC-gelatin assays to study enzyme and enzyme inhibition utilized fluorescein isothiocyanate (FITC) conjugated to gelatin as a protein substrate for the gelatinases [258, 259]. FITC was conjugated to gelatin by first adding 1 gram of gelatin (Sigma) to 100 mls 50 mM sodium bicarbonate, pH 9.5 and 150 mM NaCl. The gelatin was dissolved by warming the mix and stirring. Then 40 mg of FITC (Sigma) was added to the gelatin, mixed together, and incubated for 1 hour in the dark. At 1 hour, Tris base was added (to a final concentration of 50 mM) to stop the reaction. The FITC-gelatin was

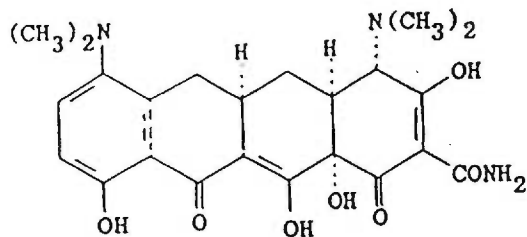
then dialyzed extensively against 50 mM Tris, pH 8.5 in the dark for 18 hours, followed by dialysis against 50 mM Tris, pH 7.2 for another 18 hours in the dark. The dialysis buffers were changed frequently. To check if the dialysis was complete, a small aliquot was removed and precipitated with 10% trichloroacetic acid (TCA). After it was centrifuged, absorbance readings were taken of the supernatant to measure background. When the background levels were low, the FITC-gelatin was used as the substrate in the following kinetic assays. In brief, the enzyme was incubated with the FITC-labeled gelatin at 37°C for various time points in the following buffer: 150 mM NaCl, 50 mM Tris-Cl, pH 7.5, 10 mM CaCl₂, and 100 μM ZnCl₂. The reaction was stopped by adding an equal volume of 10 %TCA and incubated from 3-18 hours at 4°C. The reaction was then centrifuged at 4°C for 20 minutes at 12,000 x g. The supernatant was removed to a fresh tube and the pH was adjusted to >8 by adding NaOH from a 5 N stock solution. The absorbance was then measured at a wavelength of 494 nm, thereby giving a measure of cleaved product. Standard kinetic curves were generated from the data and optimum reaction times, enzyme concentrations and substrate concentration ranges were established for subsequent inhibition reactions. Gelatinase A and B were determined to be in the linear range when used at concentrations between 100 pM and 1 nM. When reactions were performed in the presence of various inhibitors, enzyme was combined in the reaction buffer (described above) with the inhibitor and they were preincubated for 15 minutes at 37°C before adding substrate and starting the reaction. Data was collected and analyzed by graphic analysis as described above. The peptide inhibitors analyzed for their inhibitory activity against gelatinase A and B included: Minocycline (Sigma), L-Tryptophan-Hydroxamate

(Sigma), p-Hydroxyl benzoyl-Alanine-Phenylalanine (Sigma), a collagenase inhibitor, (2R)-2-Mercaptomethyl-4-Methylpentanol L-Phenylalanyl-L-Alanine Amide (Peptides International), and the propeptides Ac-RCGVP-, -RCGVDP-, and -RCGNPD-NH₂ (synthesized and hplc-purified by members in the Acott lab). Figures of the inhibitors studied in the enzymatic assays and outflow system are shown in Fig. 35a-c and Fig. 36a-b.

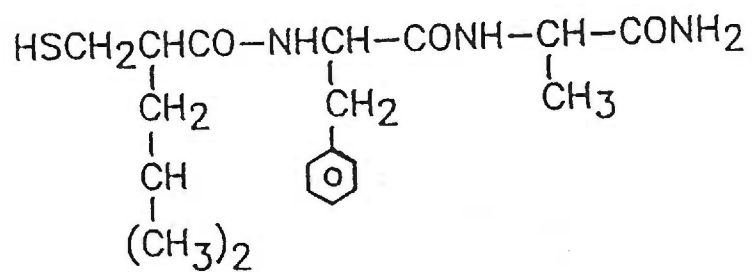
In addition to the protein substrate assays, continuously-recording fluorescent peptide assays were also used for kinetic analysis of gelatinase A and B activity and their inhibition. Gelatinases were activated as described above. A methoxycoumarin-labeled peptide substrate, Mca-Pro-Leu-Gly-Leu-Dpa-Ala-Arg-NH₂, available from Peninsula Labs, was utilized in the kinetic assays and has been described previously as a substrate for stromelysin and collagenase [220, 260]. Progelatinases for the peptide substrate assays were purchased from Biogenesis. Analysis of the proenzymes and the activated enzymes by gelatin zymography was performed prior to the enzymatic assays. The enzymes were activated with APMA as previously described, or gelatinase B was activated with the active form of stromelysin in a 1:40 ratio, respectively, for two hours at 37°C [38]. The active or proforms of the gelatinases were electrophoresed on a 10 % SDS-PAGE gel containing 0.1 mg/ml gelatin as a substrate. The gel was incubated overnight in reaction buffer and then stained with Coomassie blue stain, as has been described in the previous chapter .

For the purpose of their kinetic analysis in enzyme assays, active gelatinase A or B was incubated in the following reaction buffer: 150 mM NaCl, 50 mM Tris-Cl, 10 mM CaCl₂, and 0.01 % Brij, pH 7.5 at 37°C for 15 minutes prior to adding the peptide

A



B

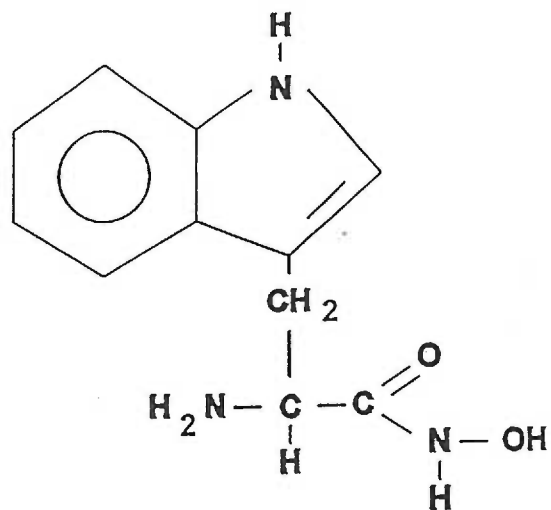


C



Figure 35: Structures of Matrix Metalloproteinase Inhibitors.
(A) Minocycline, (B) Collagenase Inhibitor, (C) Propeptides.

A



B

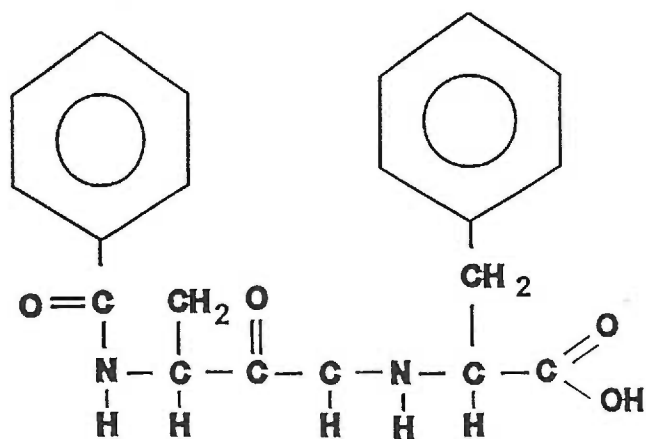


Figure 36: Structures of Matrix Metalloproteinase Inhibitors.
(A) Tryptophan-Hydroxamate, (B) p-Hydroxyl benzoyl-Ala-Phe.

substrate. The peptide substrate was solubilized in 100 % DMSO and then diluted ≥ 2000 -fold in reaction buffer prior to use in the enzyme reactions. The initial rate of cleavage of the enzyme was then measured in a continuously-recording assay using a Perkin-Elmer Luminescence Spectrometer LS50B. The peptide substrate Mca-Pro-Leu-Gly-Leu-Dpa-Ala-Arg-NH₂ has an excitation wavelength of 328 nm and an emission wavelength of 393 nm. A known concentration of the product peptide Mca-Pro-Leu (Peninsula Labs), solubilized in 100 % DMSO and diluted 1000-fold, was used to quantitate units of fluorescence. When enzyme inhibition was being analyzed, the selected inhibitor was incubated in the presence of the enzyme in the same reaction buffer for 30-60 minutes at 37°C prior to adding substrate and starting the reaction. Data was recorded as was described for the enzyme assays.

Data Analysis -The data, from both the protein-substrate and peptide substrate enzyme assays, were corrected for background fluorescence and then converted to units of product (nM) per second. The resulting data were then analyzed using the Grafit software (3.03 version from Erithacus Software Ltd., 1989-1994). Linear fits and subsequent kinetic constants were obtained for the individual enzyme assays in the absence, as well as in the presence of various selected inhibitors. The equations used for the linear fits are described in detail in the results section of this manuscript. The different types of inhibition, to be discussed below, have characteristic effects on plots of $[S]/v$ versus $[S]$ or $1/V$ versus $1/[S]$ (Fig. 37) and these criteria, as well as the linear fits and subsequent kinetic inhibition constants, were used to determine the type of inhibition for each inhibitor on the gelatinases.

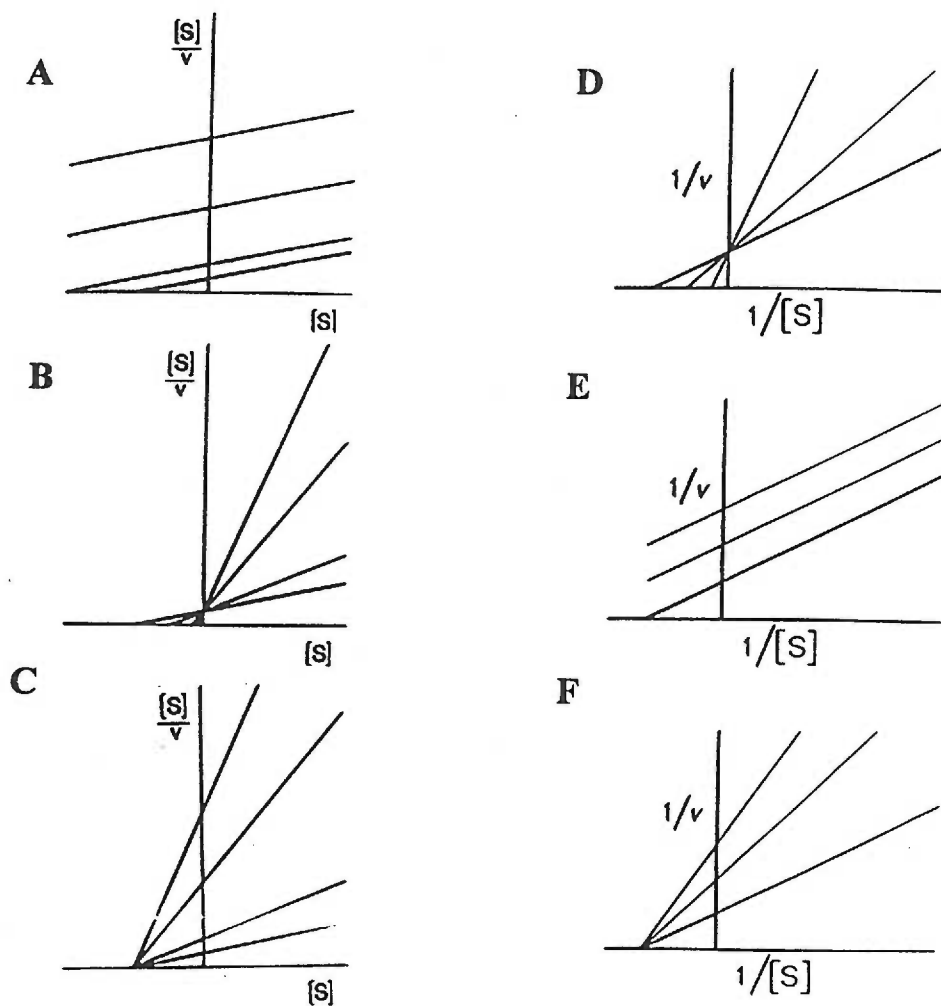


Figure 37: Hanes (A-C) or Lineweaver Burk (D-F) plots for various mechanisms of inhibition. (A, D) Competitive, (B, E) uncompetitive, and (C, F) noncompetitive inhibition. (from: C. Knight, "The Characterization of Enzyme Inhibition" in Proteinase Inhibitors, Barret and Salvesen, eds. Elsevier Science Publishers, 1986; and from: A. Fersht, Enzyme Structure and Mechanism, Second Edition, W. H. Freeman and Company, 1985.)

Outflow System - Human anterior segment explants, including the intact cornea, undisturbed trabecular outflow pathway and a 5010 mm rim of sclera were subjected to stationary organ culture for 48 hours and then perfused organ culture for approximately 5 days until flow rates stabilized. The perfusion apparatus and culture conditions have been described and characterized in detail elsewhere [254-257, 261]. Briefly, explants were mounted on a polycarbonate pedestal and perfused with serum-free Dulbecco's modified Eagle medium (DMEM) with Penicillin G (100 units/ml) and Streptomycin sulfate (100 µg/ml) at 37°C, 100% humidity and 5% CO₂/95% air (Fig. 38). Perfusion fluid has been shown to flow almost exclusively through the normal trabecular outflow pathway at approximately *in vivo* outflow rates (approximately 2.5 µl/min). Morphology, cellular ultrastructure and biosynthetic profiles are essentially identical to those of fresh tissue for at least three weeks in this culture system. Outflow facility was measured gravimetrically to ± 10 µl approximately twice daily and is presented as %Co. C is normalized to the percentage of baseline or pre-treatment facility and calculated from the standard outflow expressions:

$$Q = P/R$$

$$C = Q/P$$

Where Q is the flow rate in µl/min, P is the perfusion head expressed in mm of mercury, R is the flow resistance and C is the outflow facility expressed in (µl/min)/mm Hg.

Average outflow rates stabilize after a few days in culture at approximately 3 µl/min, although individual explants stabilized at flow rates between 1 and 8 µl/min. The average normal *in vivo* flow rate is ~2.4 µl/min. Except as indicated, the experimental

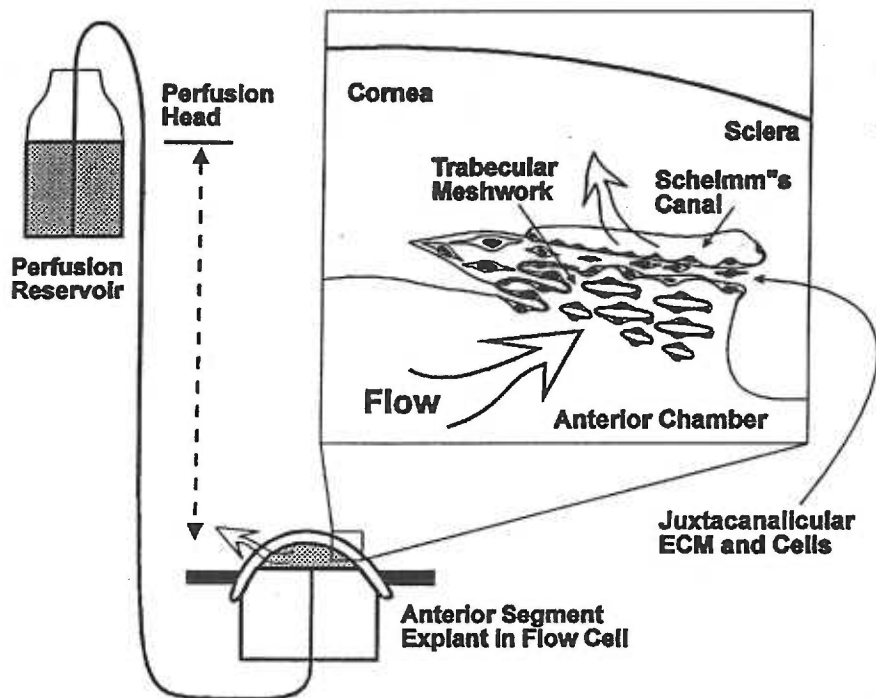


Figure 38: Perfused Anterior Segment Explant Organ Culture. Outflow from the anterior chamber across the trabecular meshwork and out through Schlemm's canal is measured in terms of outflow facility as % C_0 , where outflow facility of untreated explants is defined as 100 % C_0 .

perfusion head was 10 cm of water (7.35 mm Hg), approximating the pressure drop across the trabecular meshwork in vivo. Manipulative agents or control vehicle were added to the perfusion medium providing continuous exposure to the explants for the times indicated in the figures. The inhibitors were dissolved in water or absolute ethanol (at 10,000x) and diluted into culture medium for use. Parallel vehicle controls were analyzed in all cases. Inhibitor concentrations utilized in the outflow apparatus were similar, if not identical to, those utilized in the enzyme assays. In other words, IC_{50} values of the inhibitors were determined on gelatinase A and B in the enzyme inhibitor assays, and inhibitor concentrations close to or equal to those values were selected for the outflow system.

C. Results

FITC-Gelatin Assays and Graphic Data Analysis - Purified gelatinase A or B was activated as described above and the activated products were initially analyzed on a gelatin zymogram to determine the size of the active enzyme species as shown in the previous chapter (Fig. 30a). For the purpose of kinetic analysis of the gelatinases, the active enzymes were then incubated in the appropriate reaction buffer at various concentrations of the FITC-labeled gelatin, as described in the methods section. Cleaved product was determined from the absorbance values of the reactions following the stopping point of the assay. Several assays were run at different time points and at different enzyme concentrations in order to determine the optimal conditions for first

order reaction kinetics. Gelatinase A and B were found to be in the linear range for initial rates of cleavage when used at concentrations of 0.1-1 nM. Optimal reaction time was found to be 30 minutes at 37°C. After establishing those conditions, assays were run at various substrate concentrations and kinetic constants were determined based on graphical representation of the data fits using the Grafit program for fitting kinetic data.

Briefly, enzyme kinetics can usually be described by simple models because the enzyme acts on only one substrate molecule at a time [262]. When the enzyme concentration is kept constant and the substrate concentration [S] is varied, provided that [S] is always greater than the enzyme concentration, the velocity v of the enzyme-catalyzed reaction varies according to the Michaelis and Menten equation:

$$v = V[S]/(K_m + [S])$$

$$\text{or } v = [E]_0[S]k_{\text{cat}}/(K_m + [S])$$

$$\text{where } k_{\text{cat}}[E]_0 = V_{\text{max}}$$

At high substrate concentrations the velocity approaches a limiting maximum value V , whereas at low concentrations the velocity is proportional to [S]. The Michaelis constant K_m is defined as the concentration of substrate at which the velocity is half the maximum value. The kinetic constants V and V/K_m are the basic kinetic parameters that characterize the enzyme and substrate interaction [262-264]. Usually the values of V and K_m may be determined graphically by fitting the data directly to the Michaelis Menten equation, graphed as V versus [S], or by transforming the data and obtaining constants from linear plots of either $1/v$ versus $1/[S]$ (the Lineweaver Burk plot) or of $[S]/v$ versus [S] (the Hanes plot). The k_{cat} constant is a first-order rate constant that refers to the

properties and reactions of the enzyme-substrate, enzyme-intermediate, and enzyme-product complexes. It is often considered to be the turnover number of the enzyme because it represents the maximum number of substrate molecules converted to products per active site per unit time [263]. Finally, the k_{cat}/K_m constant, usually given in the units of $\text{sec}^{-1}\cdot\text{M}^{-1}$, may be referred to as the “specificity constant” because it determines the specificity for competing substrates [262, 263].

For the FITC-gelatin assays, enzyme concentrations were estimated primarily from their absorbance values, as well as from amounts of Coomassie stain per enzyme on SDS-PAGE gels. Their concentrations were confirmed later based on their specific activities as compared to known amounts of the same enzymes. Kinetic constants were averaged from several independent assays, and were determined from the Michaelis Menten plot, as well as from the two linear plots, the Lineweaver Burk, and Hanes plots for gelatinase A (Fig. 39) and for gelatinase B (Fig. 40), as mentioned above, and are summarized in the table (Fig. 41). The K_m and V_{max} values were obtained from the absorbance values of product released as determined by the following equation, where V_{max} is defined as nM product per second:

$$V_{max} = ((OD_{495}/\epsilon_{495} \text{ gelatin } \text{M}^{-1}\cdot\text{cm}^{-1}) * 10^9 \text{ nM/M}) / (4.5 \text{ moles FITC/moles gelatin})(1800 \text{ sec})$$

As shown in the table in Figure 41, kinetic constants determined for gelatinase A averaged from five independent assays were as follows: $K_m = 11.87 \mu\text{M}$, $V_{max} = 82.03 \text{ nM/sec}$, and $k_{cat} = 8.20 \text{ sec}^{-1}$, whereas kinetic constants determined for gelatinase B, averaged from five independent assays, were $K_m = 15.02 \mu\text{M}$, $V_{max} = 97.71 \text{ nM/sec}$

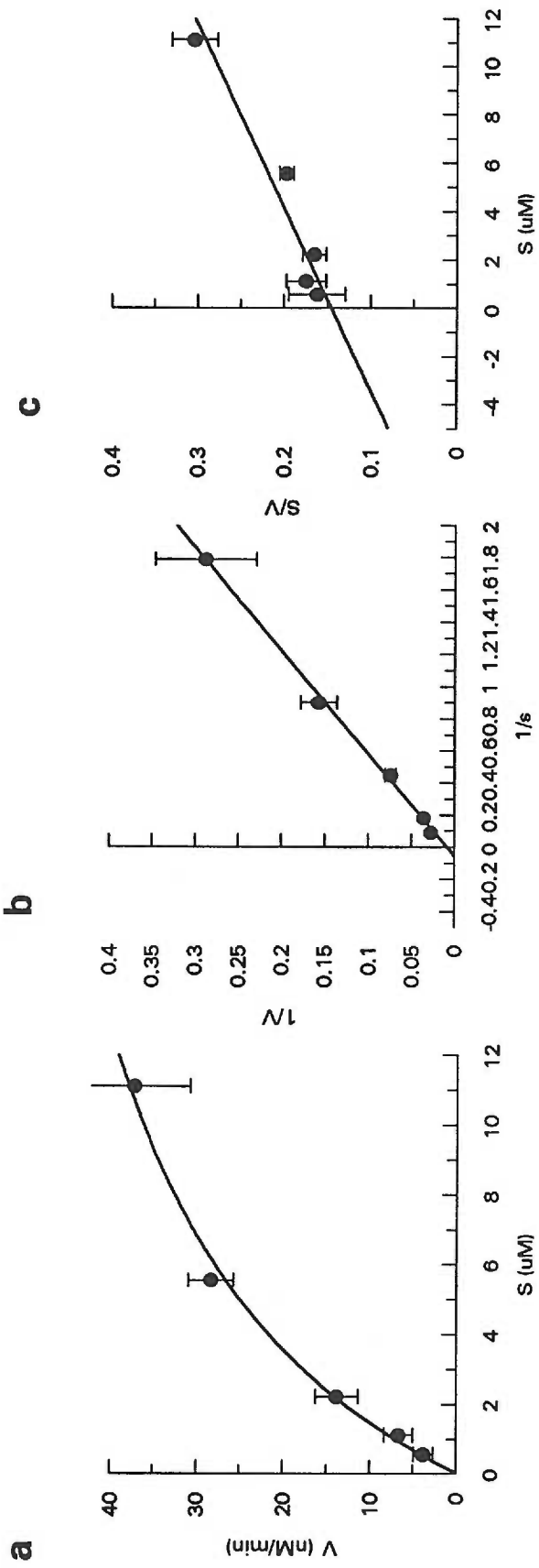


FIGURE 39: 10 nM Gelatinase A on FITC-gelatin substrate; a) Michaelis Menten Plot, b) Lineweaver Burk Plot, c) Hanes Plot

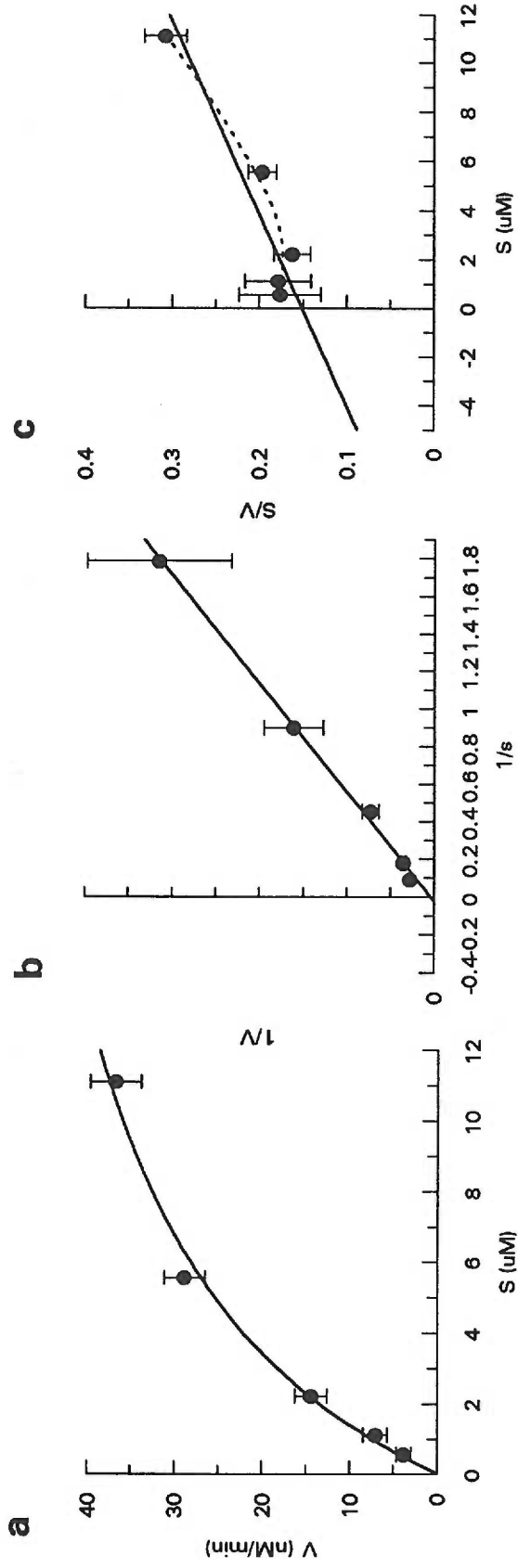


FIGURE 40: 10 nM Gelatinase B on FITC-gelatin substrate; a) Michaelis Menten Plot, b) Lineweaver Burk Plot, c) Hanes Plot

Enzyme	K_m (μM)	V_{max} (nM/sec)	k_{cat} (sec^{-1})	k_{cat}/K_m ($M^{-1} \cdot sec^{-1}$)
Gelatinase A	11.87 \pm 3.5	82.03 \pm 16.9	8.20 \pm 1.7	710,593 \pm 72,800
Gelatinase B	15.02 \pm 8.0	97.71 \pm 39.6	9.78 \pm 3.9	704,323 \pm 98,807

FIGURE 41: Gelatinase activity on the FITC-gelatin protein substrate. These data are from five independent assays and were fit using the Grafit program as described in 'Materials and Methods'. Gelatinase A and gelatinase B concentrations were determined to be 10 nM in each assay.

and $k_{\text{cat}} = 9.78 \text{ sec}^{-1}$. Enzyme concentration was determined to be approximately 10 nM per enzyme per reaction. The kinetic constants of K_m and k_{cat} determined on gelatinase A and B suggest that the gelatinases have similar affinities for the substrate, as well as similar enzymatic activities on the substrate molecule, respectively.

Enzyme-Inhibition Assays - After establishing initial cleavage rates of the reactions and relative binding affinities of the enzymes for the protein substrate, various inhibitors, antibiotics as well as synthetic peptides, were selected for analysis in subsequent enzyme-inhibition assays. Of the antibiotics, tetracycline and its synthetic forms minocycline and doxycycline have potent matrix metalloproteinase inhibitory activity [225, 228]. Minocycline was chosen in order to test for inhibitory activity against gelatinase A and B in the enzyme-inhibition assays. As for the synthetic peptides, synthetic small molecule inhibitors of matrix metalloproteinases contain a zinc-coordinating ligand, such as a thiol, hydroxamic acid, carboxylate, or phosphinate group attached to a short peptide sequence [223]. Based on the available information on potency of MMP inhibitors, a few commercially-available, synthetic peptide inhibitors were chosen to analyze in the enzyme-inhibition assays described above. These were a mercaptopeptide collagenase inhibitor (HS-CH₂-R-CH(CH₂-CH(CH₃)₂)CO-Phe-Ala-NH₂), L-tryptophan-hydroxamate, and p-Hydroxyl benzoyl-alanine-phenylalanine. In addition, peptides that mimic sequences in the conserved region of the propeptide domain of the matrix metalloproteinases have been shown to have inhibitory activity against stromelysin and collagenase [245, 247]. Therefore, three different propeptides, Ac-RCGVP-, -RCGVDP- and -RCGNPD-NH₂, were synthesized and tested for inhibitory activity on gelatinase A and B in the same

enzyme inhibition assays.

For the actual inhibition assays, either activated gelatinase A or activated gelatinase B was preincubated with a specific inhibitor in the reaction buffer at 37°C for up to 60 minutes. The FITC-labeled gelatin substrate was then added to initiate the reaction, as was described for the enzyme alone. In the initial enzyme inhibition assays, enzyme and substrate concentrations were kept constant while inhibition concentration was varied over a range of inhibitor concentrations in order to obtain data for kinetic constants, as well as to determine the IC_{50} value for each inhibitor. The IC_{50} value is the concentration of inhibitor required to decrease the enzyme activity by 50%. The IC_{50} value, however, gives no information on the mechanism of inhibition and the equation for determining an IC_{50} value relative to a K_i changes according to the types of binding and inhibition events that occur. Moreover, the measured IC_{50} value depends on the substrate concentration. In the case of the inhibition assays presented in this text, IC_{50} values were determined in order to estimate an effective range of inhibitor concentrations for the inhibition of the two gelatinases in subsequent assays for determination of kinetic inhibition constants, as well as for their analysis in the explant outflow system, as will be described below. Resulting data was analyzed, graphed, and IC_{50} values were determined for each inhibitor on both gelatinase A (Fig. 42) and gelatinase B (Fig. 43). IC_{50} values for gelatinase A and B are summarized in the tables in Figure 51 and Figure 52, respectively, and will be discussed in combination with the kinetic data.

In order to determine kinetic constants of the gelatinases in the presence of the various inhibitors, the enzyme and inhibitor concentrations were kept constant in the

kinetic assays, whereas the substrate concentrations were varied over a wide range. Resulting data were analyzed, graphed, and fit using the Grafit software program. Michaelis Menten plots, and linear plots, such as the Lineweaver Burk plot and Hanes plot, were used to fit the transformed data. These results helped to determine efficacy and specificity of inhibition on both gelatinase A and B for each inhibitor tested. The types of inhibition were also determined based on the graphical representation of the data, as the different types of inhibition have characteristic effects on the various linear plots [262]. Equations for competitive, as well as uncompetitive and mixed types of inhibition, were used to determine the inhibition constants of the various inhibitors on the gelatinases [262, 264].

Inhibitors may be classified into various types according to whether there is an effect on the apparent values of K_m , k_{cat} , or on both parameters [262, 264]. If an inhibitor binds reversibly to the active site of the enzyme and prevents the substrate from binding, the inhibitor and substrate compete for the active site and the inhibitor is said to be a competitive inhibitor. Competitive inhibition affects the K_m only, with no accompanying effect on the k_{cat} . For a competitive inhibitor K_{ic} is the inhibition constant [262, 263] and the following equations may be written:

$$(K_m/k_{cat})_{inh} = (1 + [I]/K_{ic})/(k_{cat}/K_m)$$

$$K_{ic} = [I] / [(k_{cat}/K_m)(K_m/k_{cat})_{inh} - 1]$$

Some inhibitors are at the other extreme from competitive inhibition decreasing the value of the apparent k_{cat} but leaving the k_{cat}/K_m unaffected. This is considered to be uncompetitive inhibition and the following equations may be written, where K_{iu} is the

uncompetitive inhibition constant:

$$1/(k_{cat})_{inh} = (1 + [I]/K_{iu})/k_{cat}$$

$$K_{iu} = [I]/(k_{cat}/(k_{cat})_{inh} - 1)$$

On the other hand, some inhibitors have both specific and catalytic effects, or, competitive and uncompetitive components, respectively. These are said to be mixed inhibitors, where both the k_{cat}/K_m and k_{cat} values vary with the inhibitor concentration, although the inhibition may be predominantly of one type or the other depending on the relative values of the inhibition constants. (For example the predominant type of inhibition will be the lower value of the two K_i 's determined.) [262, 263, 265]

In summary, from the graph panels, consisting of Michaelis Menten, Lineweaver Burk and Hanes plots of gelatinase A and B uninhibited and inhibited activity (Fig. 44-50), it is apparent that some inhibitors analyzed in these studies were better inhibitors, in general, as well as more specific for either gelatinase A or B. IC_{50} data was represented graphically for gelatinase A (Fig. 42) and gelatinase B (Fig. 43) in order to determine how well the fits correlated with the data. Kinetic constants and IC_{50} values for gelatinase A (Fig. 51) and gelatinase B (Fig. 52) were determined based on graphical analysis and linear fits. Equations used for determining the K_i values were dependent on the type of inhibition each consecutive inhibitor demonstrated on the gelatinases.

Minocycline was one of the first inhibitors tested and had similar IC_{50} values (near 100 μ M) for both gelatinases on the gelatin substrate. In contrast, although it was a mixed inhibitor for both enzymes, the K_i values of minocycline were quite different for gelatinase A, with a K_i of 449 μ M and for gelatinase B, with a K_i of 178 μ M. The

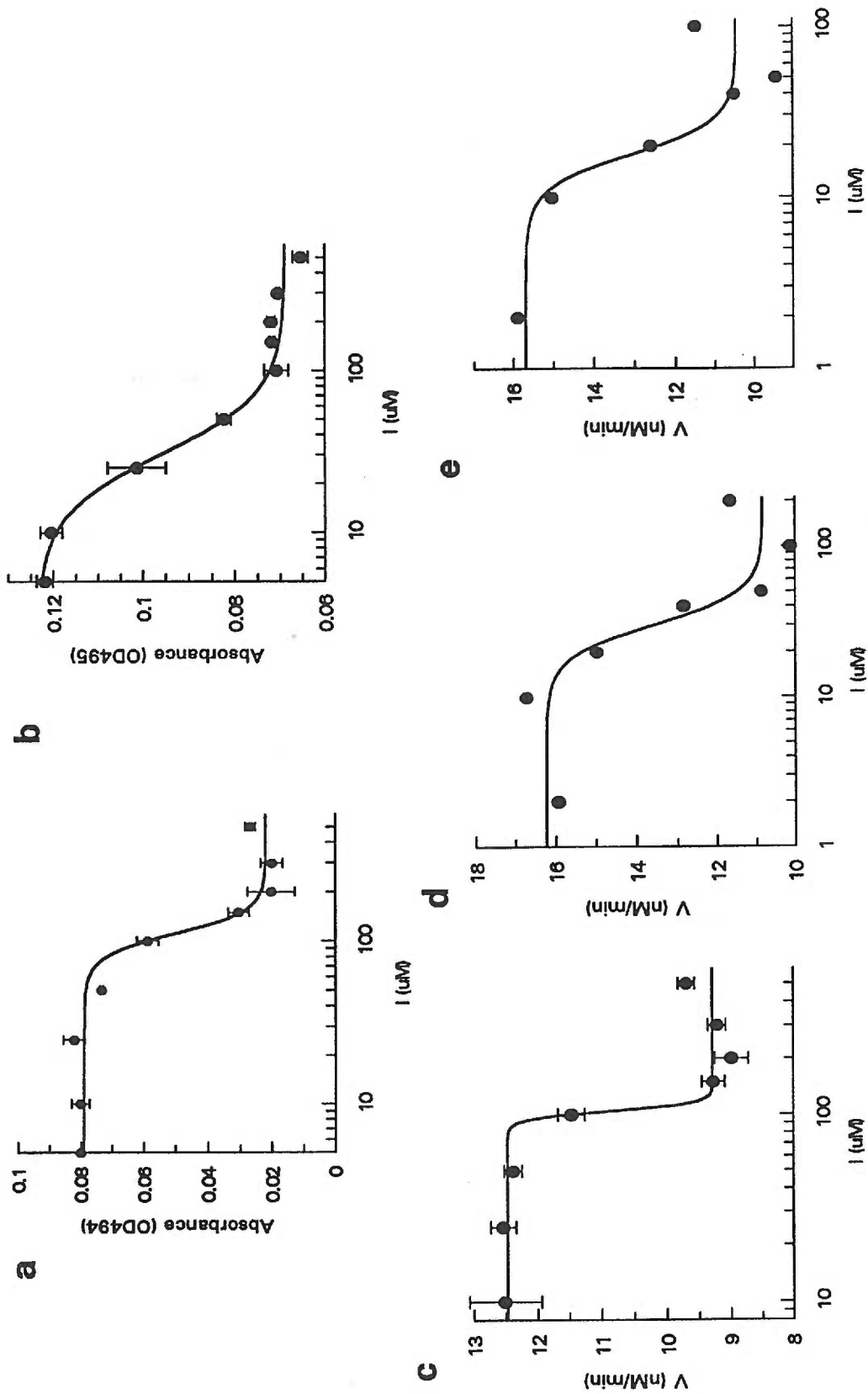


FIGURE 42: IC50 curves of 10 nM gelatinase A with 2.2 μM substrate concentration and a) Minocycline, b) Tryptophan-Hydroxamate, c) RCGVP, d) RCGV, e) RCGNPD

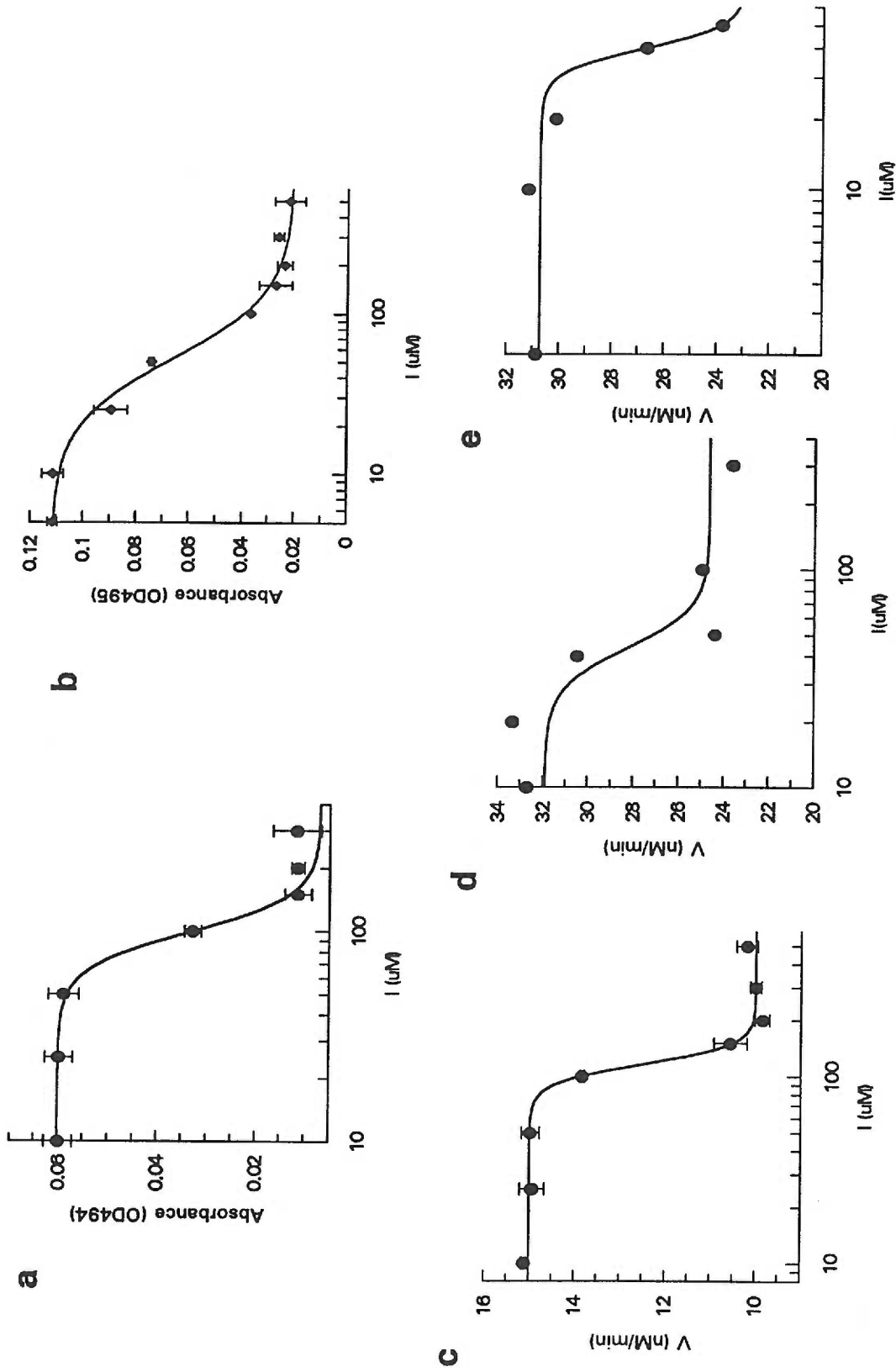


FIGURE 43: IC50 curves of 10 nM Gelatinase B at 2.2 μM substrate concentration and a) Minocycline, b) Tryptophan-Hydroxamate, c) RCGVP, d) RCGVPD, e) RCGNPD

collagenase inhibitor was analyzed for inhibitory activity on either gelatinase in these assays and was found to act as either a competitive or mixed inhibitor based on the linear plots. The K_i values were 129 μM or 264 μM for gelatinase A or B, respectively. The L-tryptophan-hydroxamate inhibitor, which was found to be a competitive inhibitor for gelatinase A with a K_i of 123 μM had an IC_{50} of 30 μM . It was determined to be a mixed inhibitor of gelatinase B with an IC_{50} of 50 μM and a K_i of 586 μM . The synthetic inhibitor, p-Hydroxyl benzoyl-alanine-phenylalanine, was analyzed and found to inhibit gelatinase A as a competitive inhibitor with a K_i of 300 μM , but did not have any inhibitory activity towards gelatinase B in these assays.

Synthetic peptides were synthesized to the propeptide domain of the gelatinases and tested for their inhibitory activity on gelatinase A and B, as has been shown previously for stromelysin [246]. First, a five amino acid peptide, RCGVP, was tested for inhibitory activity. It was found to inhibit gelatinase A with an IC_{50} of 94 μM and gelatinase B with an IC_{50} of 50 μM . The K_i values were significantly higher, when using the equation for a mixed inhibitor as was the apparent mode of inhibition, inhibiting gelatinase A with a K_i of 974 μM and a K_i of 800 μM for gelatinase B. Subsequently, two, distinct six-amino acid peptides were synthesized, RCGVPD and RCGNPD, and analyzed for their mode of inhibition of gelatinase A and B. The valine in the peptide sequence is conserved in the propeptide sequence of all of the matrix metalloproteinases, except in gelatinase A where it is replaced by an asparagine residue. Interestingly, when both inhibitors were tested for inhibitory activity, the RCGVPD peptide inhibited gelatinase A better than gelatinase B with a K_i of 61 μM versus a K_i of 271 μM , respectively. Additionally, the propeptide,

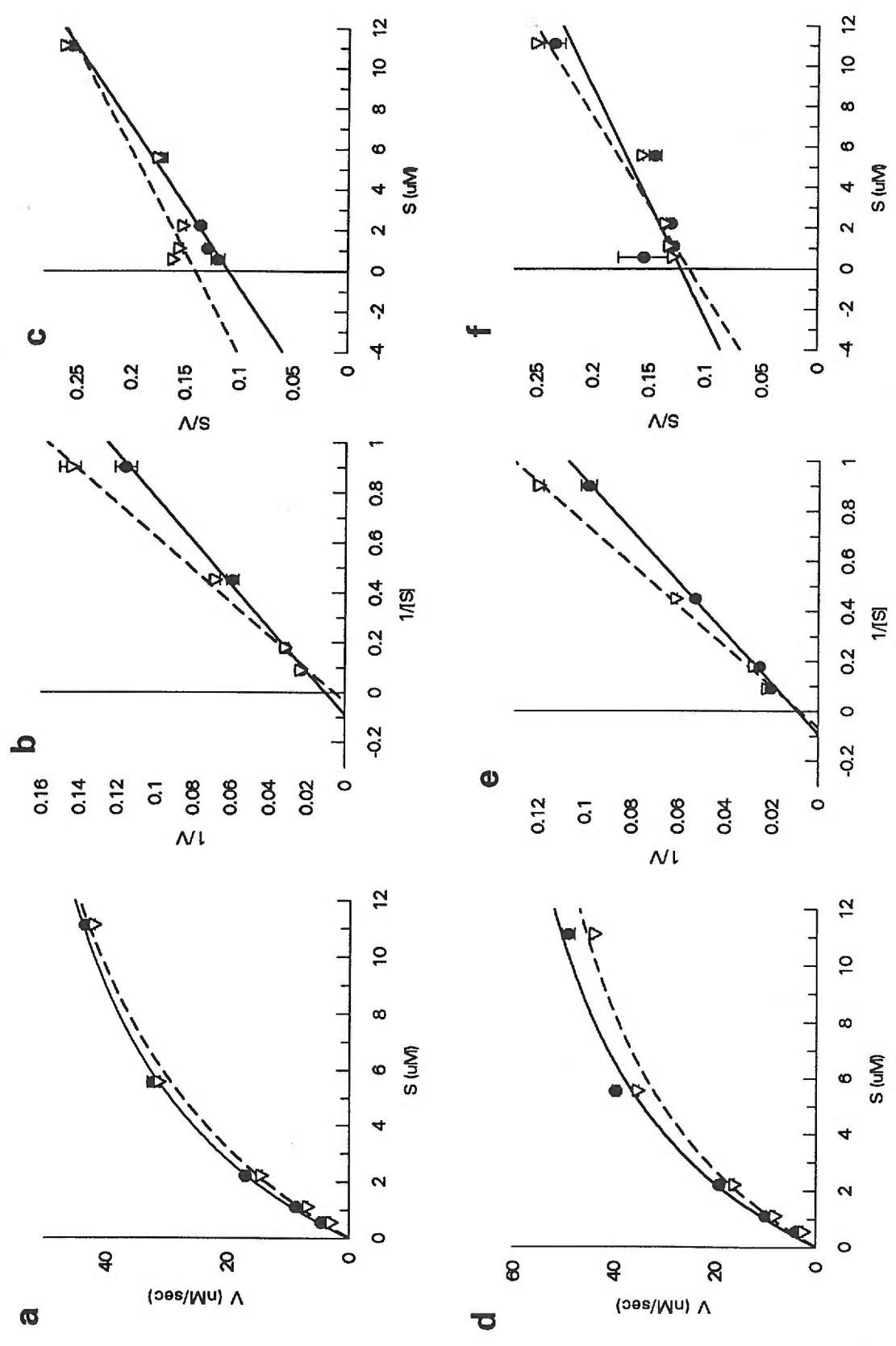


FIGURE 44: 10 nM Gelatinase A (a-c) or 10 nM Gelatinase B (d-f) in the absence (---) or presence (- - -) of 100 μ M Minocycline; a) and d) Michaelis Menten Plot, b) and e) Lineweaver Burk Plot, c) and f) Hanes Plot

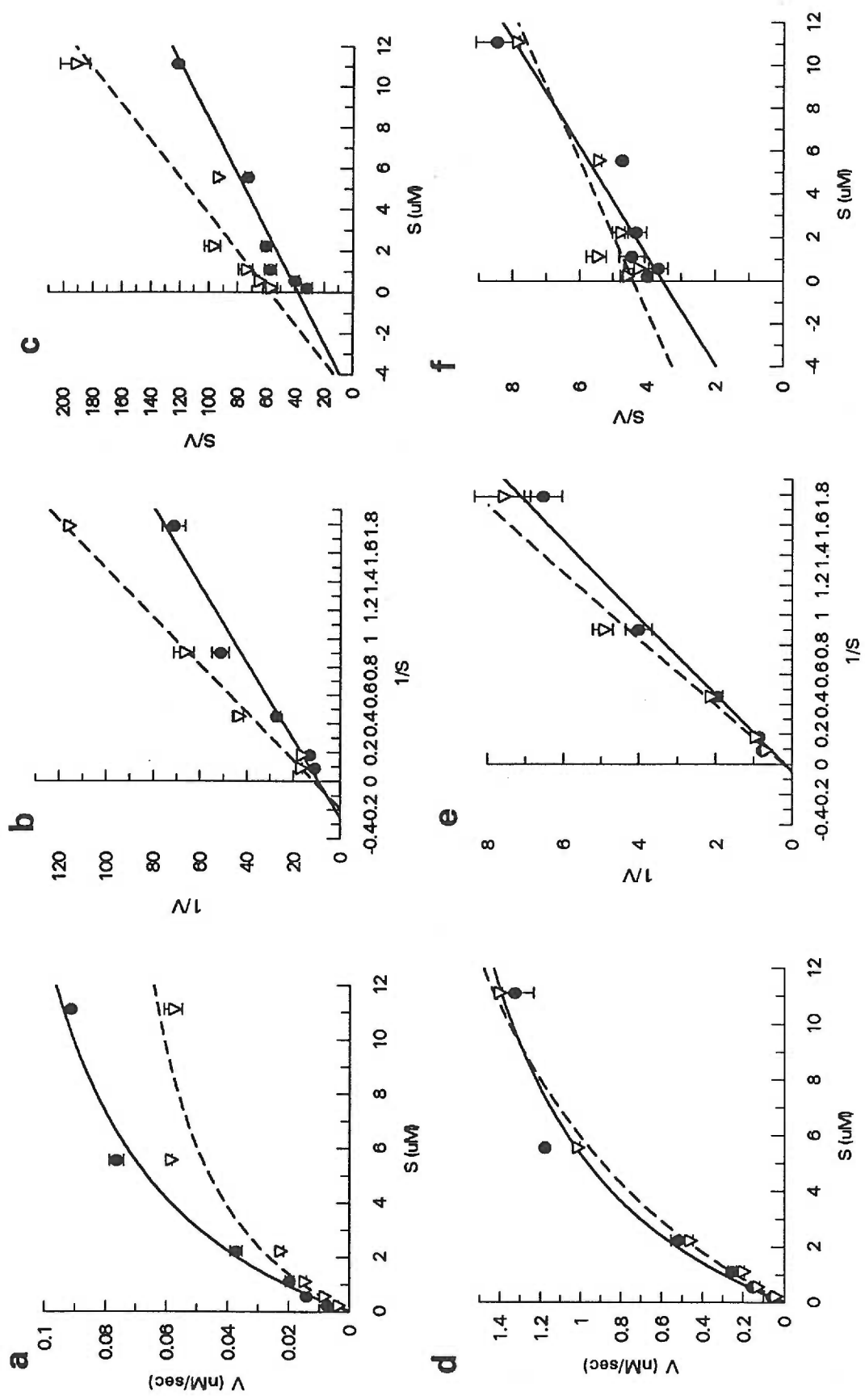


FIGURE 45: 10 nM Gelatinase A (a-c), or 10 nM gelatinase B (d-f), in the absence (---) or presence (- - -) of 100 μ M Tryptophan-Hydroxamate; a) and d) Michaelis Menten Plot, b) and e) Lineweaver Burk Plot, c) and f) Hanes Plot.

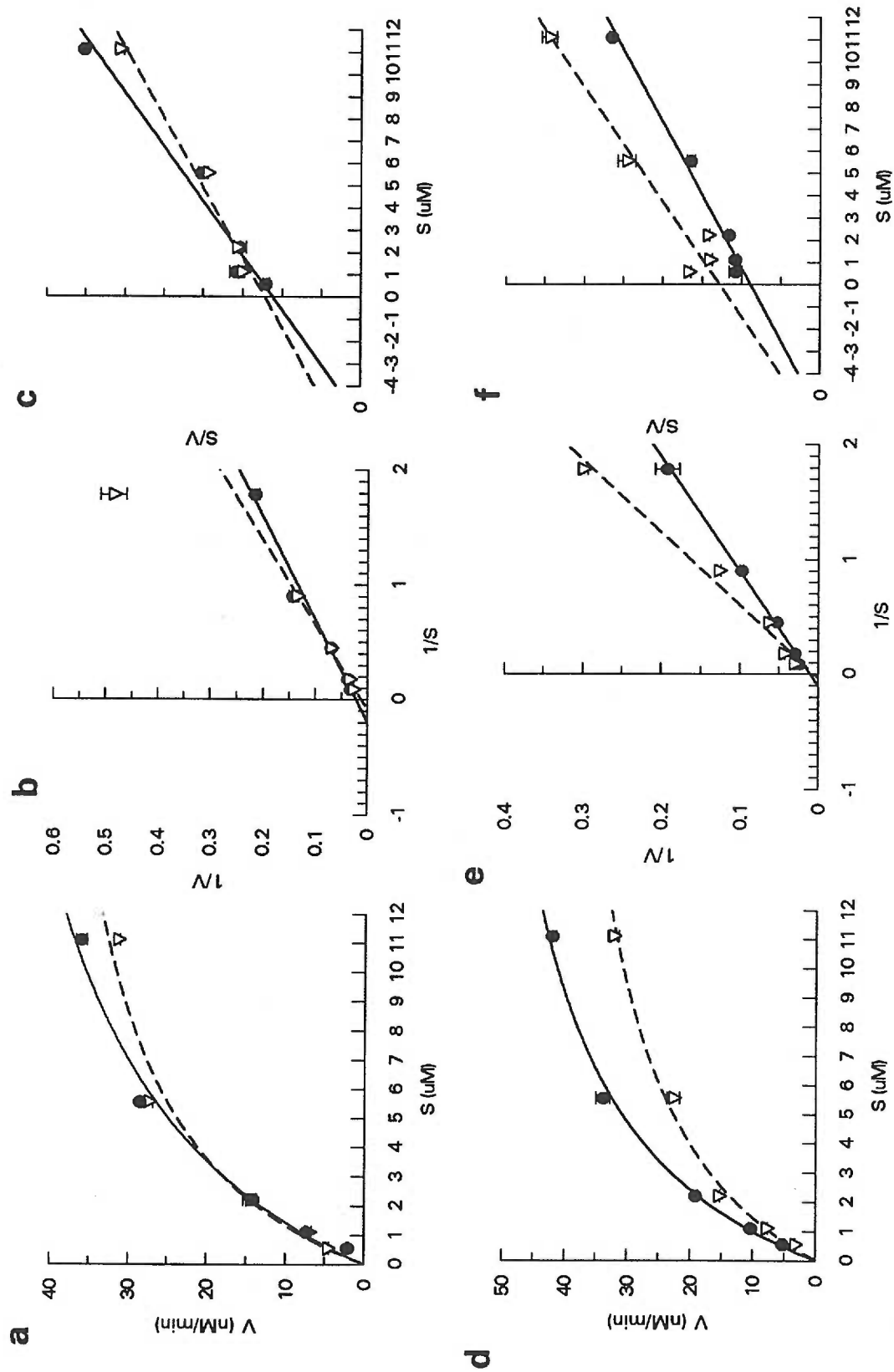


FIGURE 46: 10 nM Gelatinase A (a-c) or 10 nM gelatinase B (d-f) in the absence (---) or presence (- - -) of 150 μ M Collagenase Inhibitor; a) and d) Michaelis Menten Plot, b) and e) Lineweaver Burk Plot, c) and f) Hanes Plot.

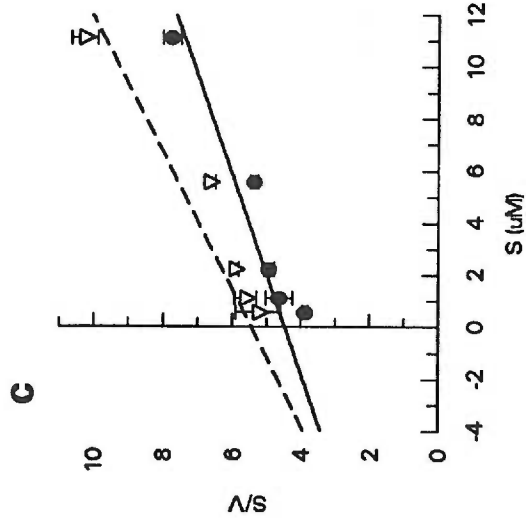
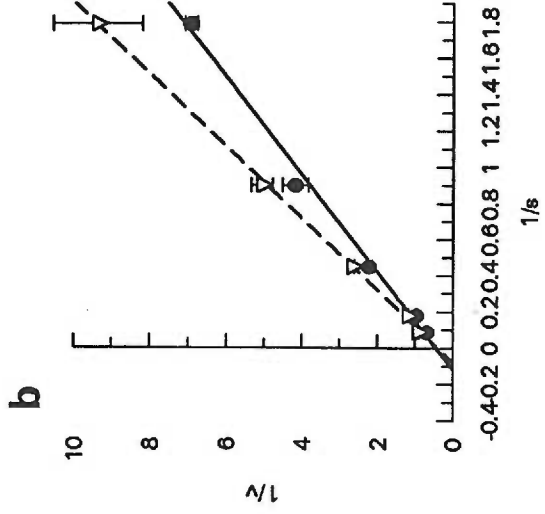
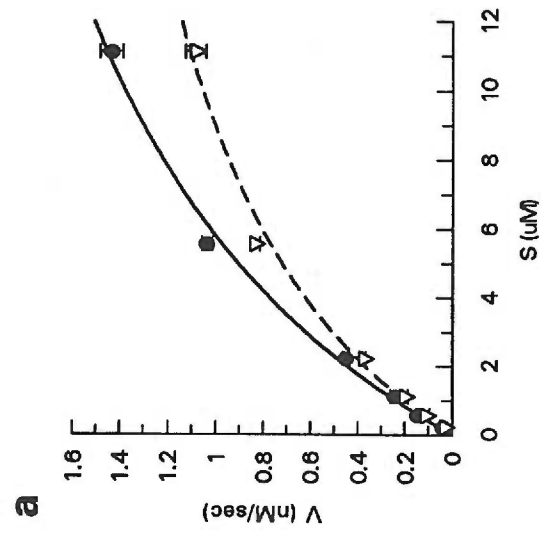


FIGURE 47: 10 nM Gelatinase A in the absence (---) or presence of 100 uM p-Hydroxyl benzoyl-Ala-Phe (- - -); a) Michaelis Menten Plot, b) Lineweaver Burk Plot, c) Hanes Plot.

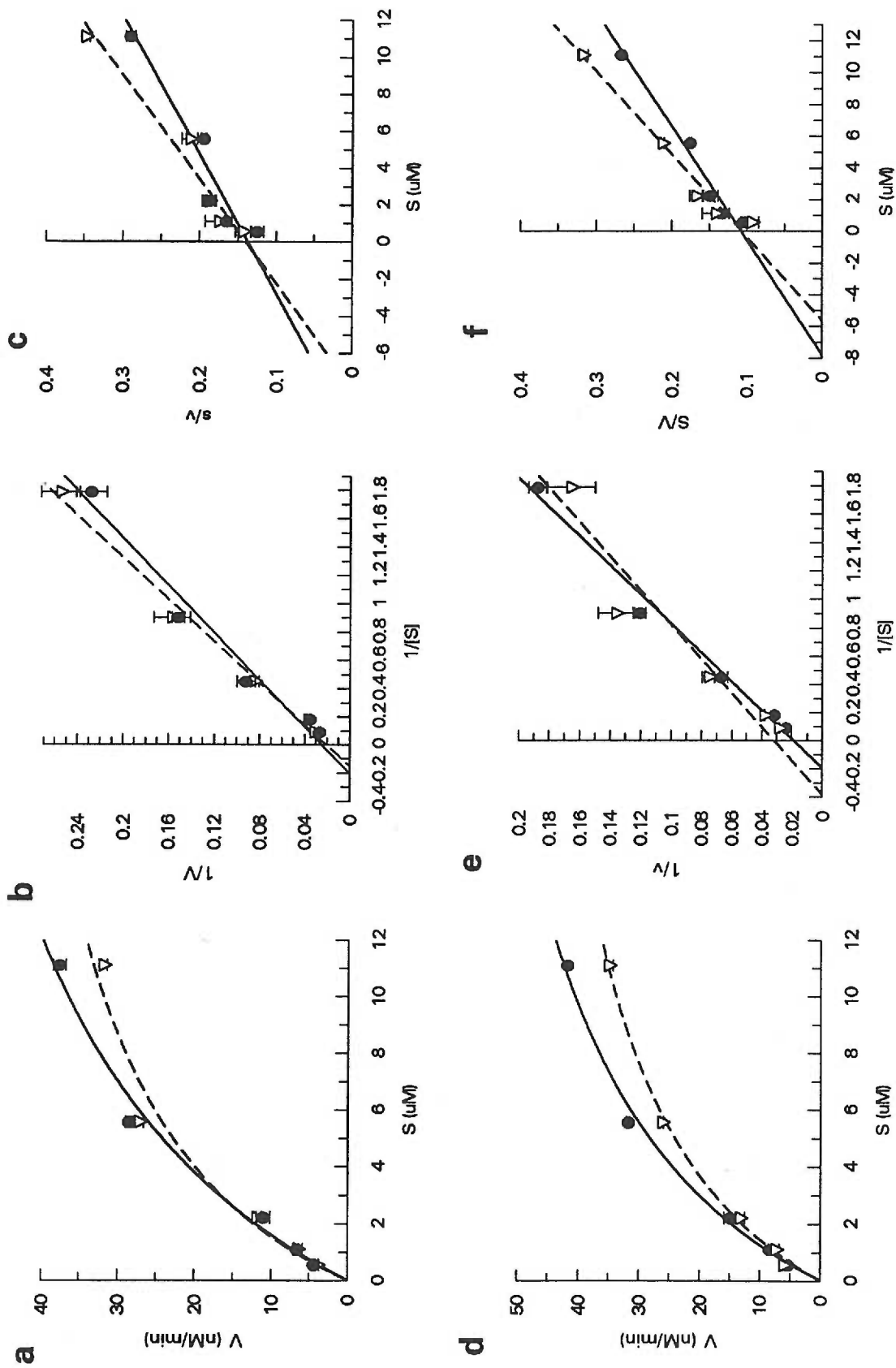


FIGURE 48: 10nM Gelatinase A (a-c) or 10 nM gelatinase B (d-f) in the absence (---) or presence (- - -) of 100 uM RCGVP; a) and d) Michaelis Menten Plot, b) and e) Lineweaver Burk Plot, c) and f) Hanes Plot.

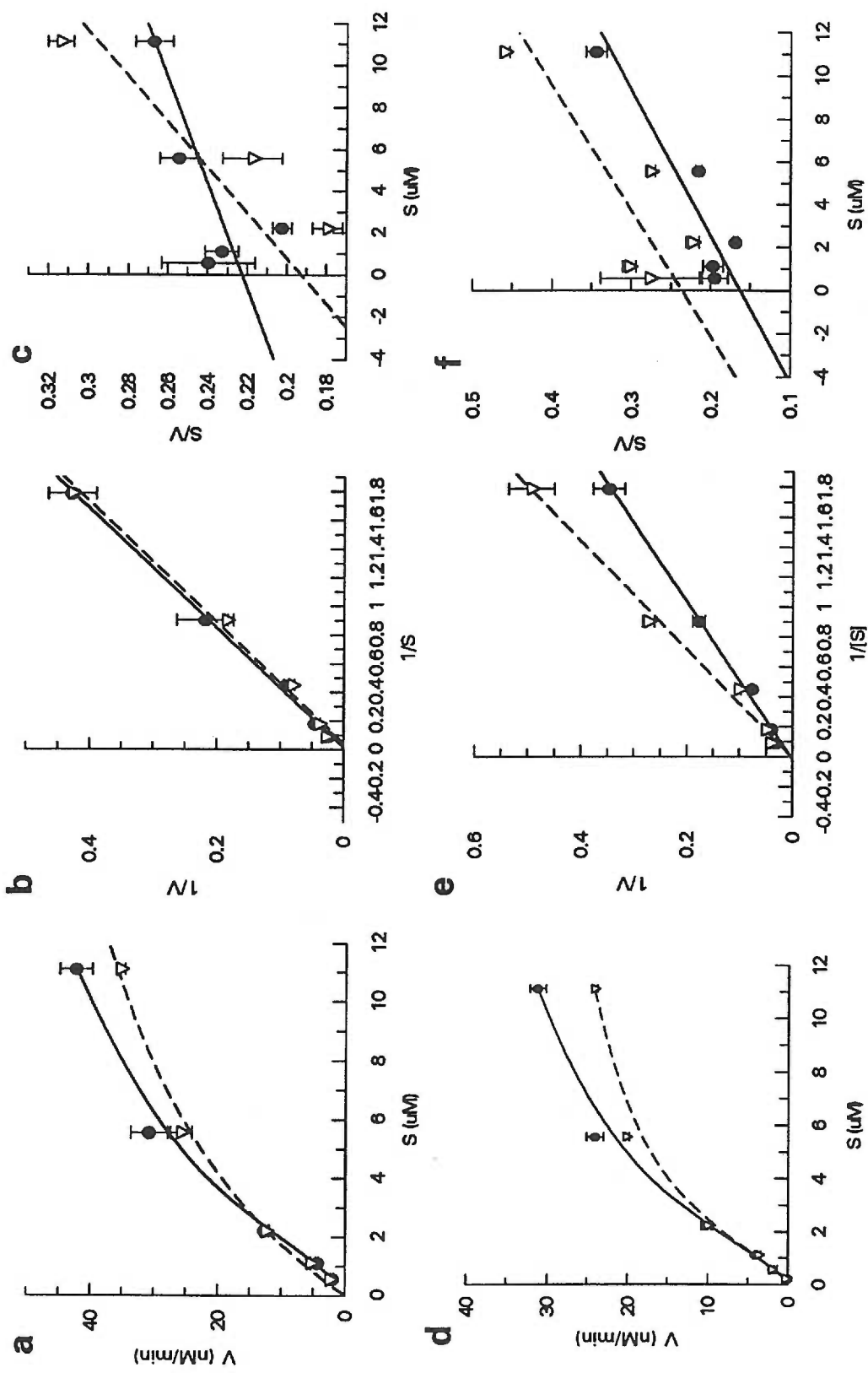


FIGURE 49: 10 nM Gelatinase A (a-c) or 10 nM gelatinase B (d-f) in the absence (---) or presence (- - -) of 35 μ M RCGVPD; a) and d) Michaelis Menten Plot, b) and e) Lineweaver Burk Plot, c) and f) Hanes Plot.

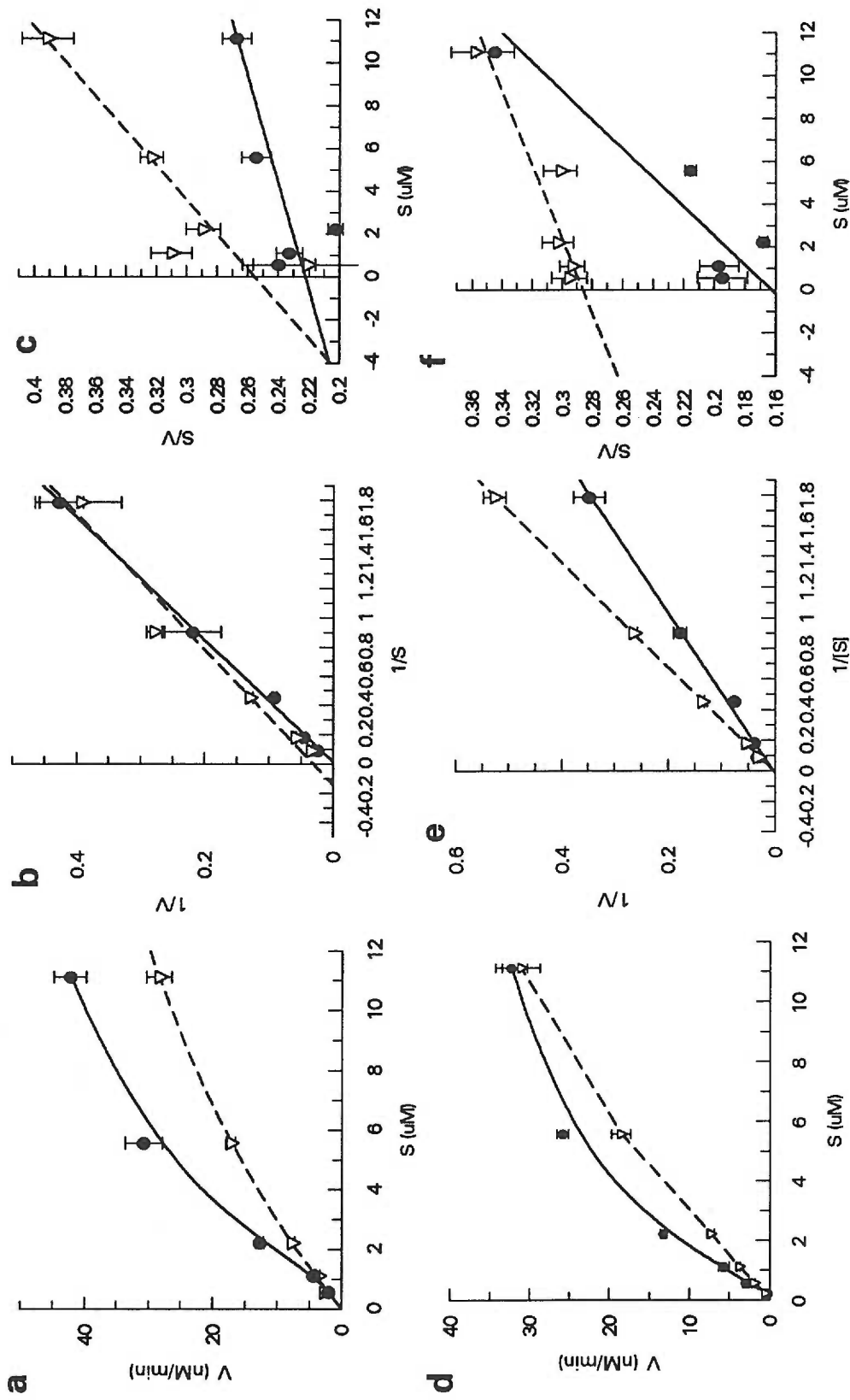


FIGURE 50: 10 nM Gelatinase A (a-c) or 10 nM gelatinase B (d-f) in the absence (---) or presence (- - -) of 35 μM RCGNPD; a) and d) Michaelis Menten Plot, b) and e) Lineweaver Burk Plot, c) and f) Hanes Plot.

Inhibition of Gelatinase A Activity on FITC-Gelatin Substrate			
Inhibitor	IC₅₀ (μM)	K_i (μM)	Inhibition Type
Minocycline	110	449	mixed
Trp-Hydroxamate	30	123	competitive
p-Hydrox.-Ala-Phe	n.d.	300	mixed
Collagenase Inhibitor	n.d.	129*	competitive/mixed
RCGVVP	94	183*	competitive/mixed
RCGVVPD	30	61	mixed
RCGNPD	18	185	mixed

n.d. = not determined

FIGURE 51: Gelatinase A concentration was 10 nM per assay, as was described in 'Materials and Methods'. Inhibitor concentrations, for kinetic assays to determine Ki values, were as follows, 1) Minocycline = 50 μM, 2) Tryptophan-Hydroxamate Inhibitor = 100 μM, 3) p-Hydroxyl benzoyl-Ala-Phe = 100 μM, 4) Collagenase Inhibitor = 150 μM, 4) RCGVP = 10 μM, 5) RCGVVPD = 35 μM and, 6) RCGNPD = 35 μM. Linear fits and equations used to determine Ki values are described in 'Results'; graphical representation of data is in Figures 42-50. The "*" indicates that the equation for a competitive inhibitor was used to determine the kinetic constant.

Inhibition of Gelatinase B Activity on FITC-Gelatin Substrate			
Inhibitor	IC₅₀(μM)	Ki (μM)	Inhibition Type
Minocycline	98	178	Mixed
Trp-Hydroxamate	52	586	Mixed
Collagenase Inhibitor	n.d.	264	Mixed
RCGVP	50	800	Mixed
RCGVDP	43	271	Mixed
RCGNPD	91	47	Mixed/Competitive

n.d. = not determined

FIGURE 52 : Gelatinase B concentration was 10 nM per assay, as was described in 'Materials and Methods'. Inhibitor concentrations, for kinetic assays to determine Ki values, were as follows, 1) Minocycline = 50 μ M, 2) Tryptophan-Hydroxamate Inhibitor = 100 μ M, 3) Collagenase Inhibitor = 150 μ M, 4) RCGVP = 10 μ M, 5) RCGVPD = 35 μ M and, 6) RCGNPD = 35 μ M. Linear fits and equations used to determine Ki values are described in 'Results'; graphical representation of data is in Figures 42-50.

RCGNPD, was a better inhibitor of gelatinase B, with a K_i of 47 μM , than it was of gelatinase A, having a K_i of 185 μM . These results were unexpected as the inhibitors were worse for their corresponding gelatinase than vice versa. However, both peptides acted as mixed inhibitors on both gelatinase A and gelatinase B. The IC_{50} values correlated with the K_i values for both gelatinases and were between 30-90 μM .

Fluorescent-Peptide Substrate Assays and Graphical Data Analysis - Two different sources of enzyme were used in these assays. First, gelatinase A and B, purified from cultured cells as was described for the FITC-gelatin assays, were analyzed for enzymatic activity on a quench-release peptide substrate [260]. Assays were run and analyzed on a LS50B luminescence spectrometer (fluorometer) and kinetic constants were obtained for both enzymes. Gelatinase A, purified from the media from HS27 cells as described previously, had a K_m of 10 μM , a V_{max} of 0.64 nM/sec and a k_{cat} of 0.64 sec^{-1} . These results maybe directly compared with the kinetic results from the gelatin-substrate data because the enzyme source was the same in these sets of assays. The results suggest that although gelatinase A may have a similar affinity for the peptide and protein substrates, as shown by similar K_m values, the actual turnover number of the enzyme (k_{cat}) on the two substrates is quite different, as it prefers the gelatin substrate. In order to determine whether the enzymatic activity was solely due to MMP activity, and not to other nonspecific proteinase activity, assays were run in the presence of the zinc chelating agent, 1,10-O-phenanthroline (Fig. 53a), the serine proteinase inhibitor, PMSF (Fig. 53b), and the chelator, EDTA (Fig. 53c). As expected, the phenanthroline completely abolished the gelatinase activity, the PMSF had no effect on gelatinase activity, and the

EDTA inhibited the gelatinase activity to approximately 10 % of its original activity.

Gelatinase B, purified from cultured cells as described in the previous chapter, was not nearly as active on the same peptide substrate as the gelatinase A and kinetic constants were unable to be determined for gelatinase B from this source.

Gelatinase A and B were subsequently purchased from a commercial source (Biogenesis) as proenzymes and utilized in the remainder of the fluorescent peptide assays in the absence or presence of inhibitors. Both enzymes were initially analyzed by gelatin zymography to determine the sizes of the activated enzyme species, and to determine whether there was any contaminating metalloproteinase activity (Fig. 54). As expected, APMA-activated gelatinase A gave several active enzyme species consisting of a 62 kDa form, a 45 kDa form, and a 38 kDa form on a gelatin zymogram. The APMA-activated gelatinase B existed predominantly as an 82 kDa species, whereas only a minor band was present at approximately 66 kDa. The stromelysin-activated gelatinase B gave an approximate equal ratio of the 82 kDa form and the 66 kDa form. Gelatinase A was used at a final concentration of 100 pM and gelatinase B was used at a final concentration of 1 nM. It is of note that despite the new source of purified enzyme, there was a significant difference in the substrate specificity of gelatinase A and B, the peptide substrate being a better substrate for gelatinase A than it was for gelatinase B. This may explain why different concentrations of gelatinase A and B were necessary in order to obtain similar activities in the enzyme assays.

The enzymes were activated as was described previously for the purified gelatinases. Briefly, gelatinase A and B were incubated with 1 mM APMA at 37°C for 2

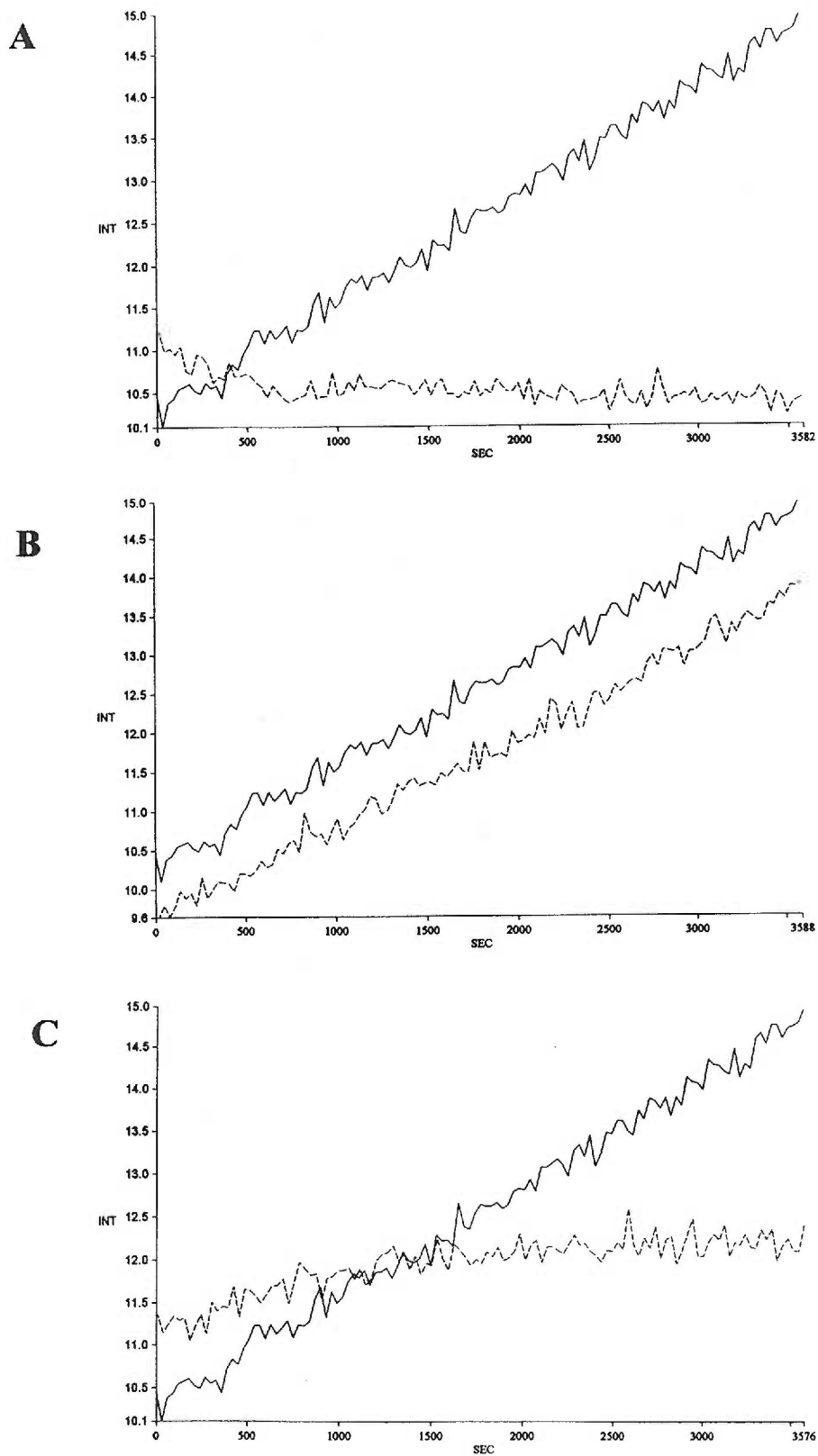


Figure 53: Gelatinase A activity on the peptide substrate measured by intensity of fluorescence versus time in the absence (-) or presence (- - -) of various agents: (A) 10 mM 1,10-Phenanthroline, (B) 10 μ M Phenylmethylsulfonyl fluoride (PMSF), and (C) 10mM EDTA.

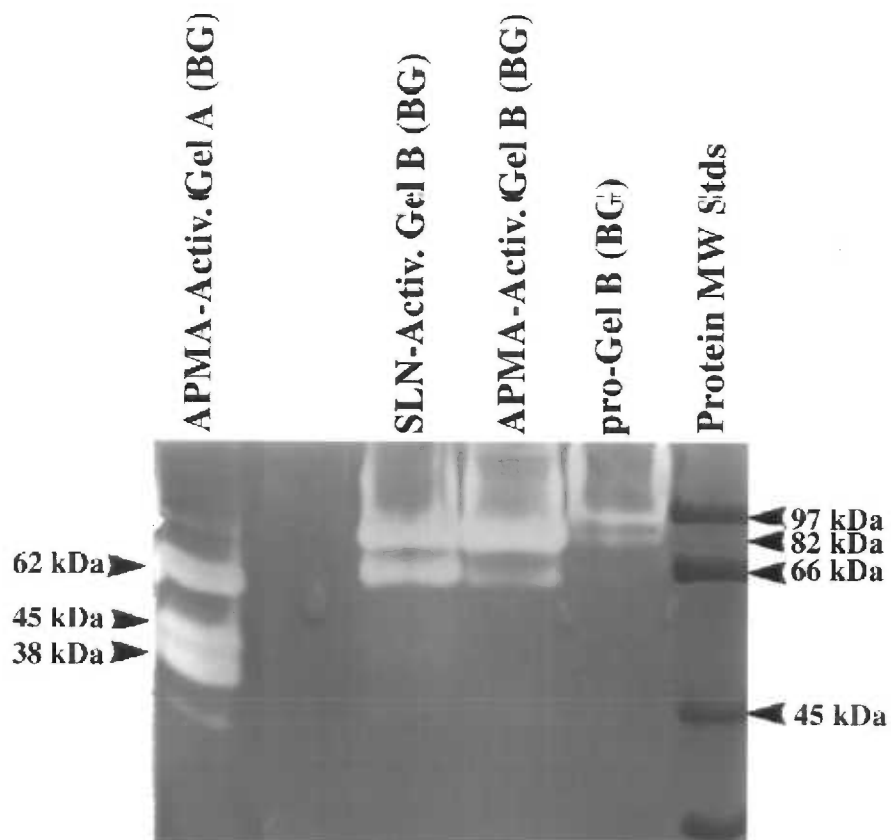


Figure 54: Gelatin zymogram of APMA-activated gelatinase A (lane one) or stromelysin-activated-, APMA-activated-, or pro-form of gelatinase B, as indicated. Enzymes are at approximately 1 nM concentration.

hours and 18 hours, respectively. Active enzymes were run in enzymatic assays where the enzyme concentrations were varied and the substrate concentration was kept constant. Initial rates of cleavage were recorded and data was graphed in order to determine the optimum enzyme concentrations where the resulting cleavage rates are linear (Fig. 55). From these graphs, the optimal concentration of gelatinase A was determined to be 100 pM per assay, and 1 nM per assay for gelatinase B. Kinetic constants were then determined, as shown graphically for gelatinase A (Fig. 56) and gelatinase B (Fig. 57) from several assays ($n = 5$). Gelatinase A was found to have a K_m of 2.8 μM , a V_{max} of 0.24 nM/sec and a k_{cat} of 2.4 sec^{-1} (Fig. 58). Gelatinase B was found to have a K_m of 2.76 μM , a V_{max} of 0.16 nM/sec and a k_{cat} of 0.16 sec^{-1} (Fig. 58).

Enzyme-Inhibition Assays - In order to determine the kinetic inhibition constants for the same inhibitors that had been analyzed in the FITC-gelatin, each inhibitor was preincubated with either active gelatinase A or active gelatinase B prior to beginning the enzymatic cleavage reaction with the peptide substrate and product released was monitored on the fluorometer. Data was analyzed and linear fits were made using the Grafit program, as was described for the FITC-gelatin assays. Kinetic inhibition constants were then determined for each inhibitor on gelatinase A and B from the linear fits of the data, as shown graphically in Figures 59-68 and as summarized in the tables in Figures 69-70. As described for the previous section, IC_{50} data was represented graphically for each inhibitor on gelatinase A (Fig. 59) and gelatinase B (Fig. 60) in order to determine how well the curve was fit to the data.

In summary from the tables (Fig. 69-70), minocycline was found to have a K_i of 55

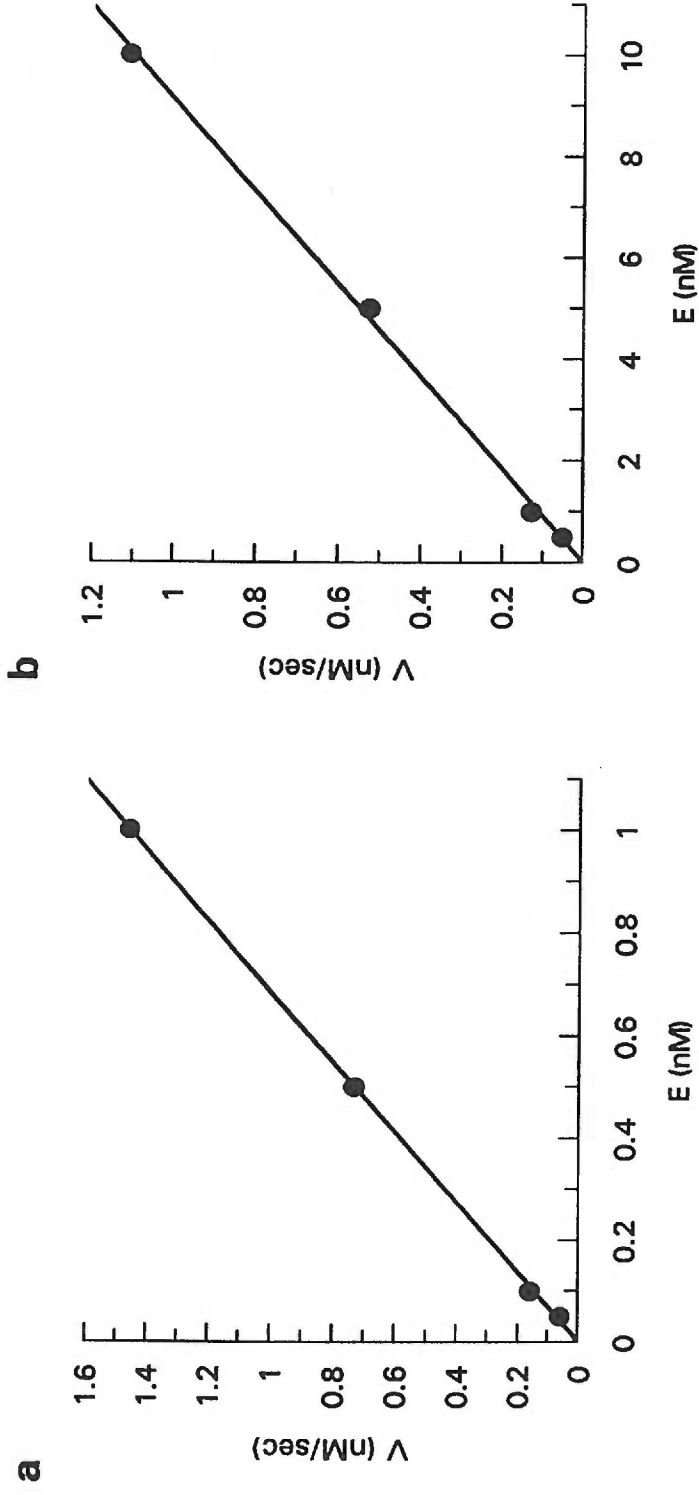


FIGURE 55: Gelatinase A (a) or gelatinase B (b) on 6 μ M Mca-peptide substrate.

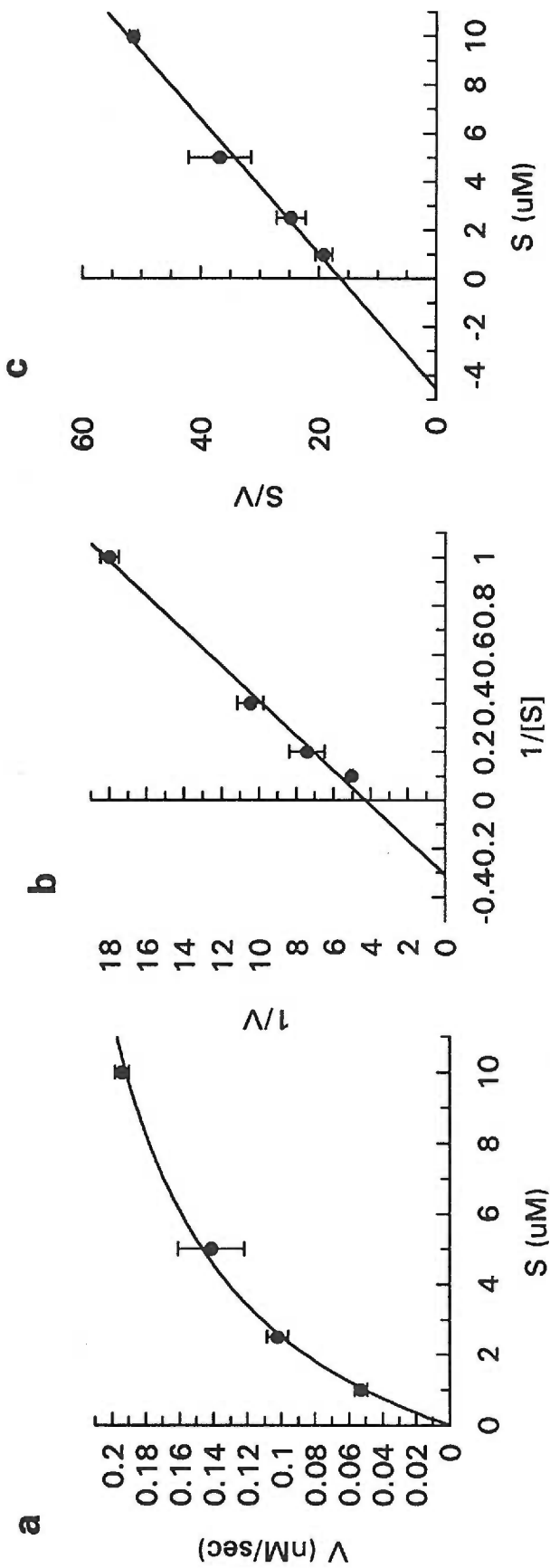


FIGURE 56: 100 pM Gelatinase A on Mca-peptide substrate; a) Michaelis Menten Plot, b) Lineweaver Burke Plot, c) Hanes Plot

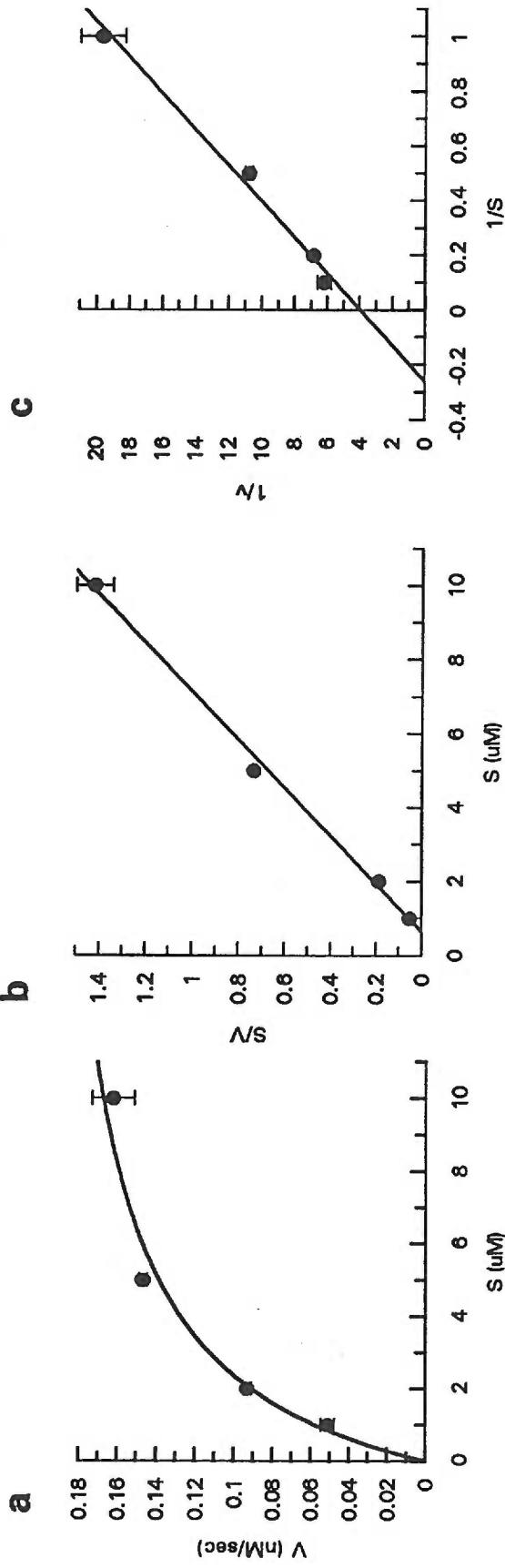


FIGURE 57: 1 nM Gelatinase B on Mca-peptide substrate; a) Michaelis Menten Plot, b) Lineweaver Burk Plot, c) Hanes Plot

Enzyme	K_m (μM)	V_{max} (nM/sec)	k_{cat} (sec^{-1})	k_{cat}/K_m ($\text{M}^{-1}\cdot\text{sec}^{-1}$)
Gelatinase A	2.8 ± 0.35	0.24 ± 0.02	2.4 ± 0.21	$857,100 \pm 99,000$
Gelatinase B	2.76 ± 0.41	0.16 ± 0.01	0.15 ± 0.01	$56,500 \pm 9,500$

FIGURE 58: Gelatinase activity on the fluorescent peptide substrate Mca-Pro-Leu-Gly-Leu-Dpa-Ala-Arg-NH₂. These data are from five independent assays and were fit using the Grafit program as described in 'Materials and Methods'. Gelatinase A concentration was 100 pM and gelatinase B concentration was 1 nM in each assay.

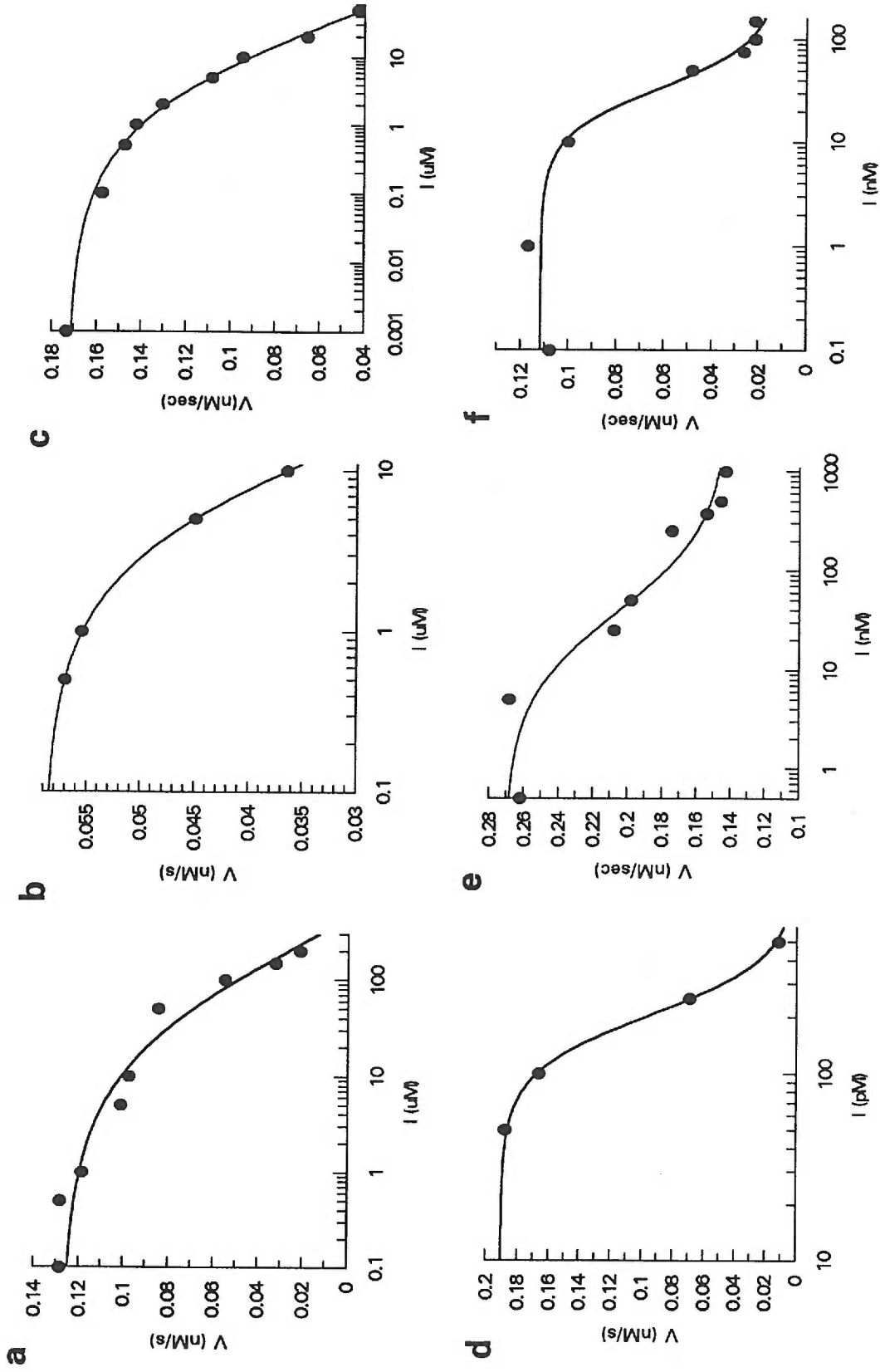


FIGURE 59: IC50 curves on 100 pM Gelatinase A; a) Minocycline, b) Collagenase Inhibitor, c) RCGVPD, d) rhTIMP-1, e) MBP-TIMP-2, f) hTIMP-3

μM and an IC_{50} of $65 \mu\text{M}$ on gelatinase A, and a K_i of $65 \mu\text{M}$ and an IC_{50} of $82 \mu\text{M}$ on gelatinase B (Fig. 61). The graphical representation of the inhibition suggests that it may be acting as a noncompetitive or uncompetitive inhibitor and the data show some differences in the type of inhibition on gelatinase A as compared with gelatinase B. The peptide inhibitor L-tryptophan-hydroxamate was analyzed and found to act as a predominantly competitive inhibitor with a K_i of $217 \mu\text{M}$ for gelatinase A and a K_i of $88 \mu\text{M}$ for gelatinase B (Fig. 62). The collagenase inhibitor was found to have inhibitory activity against both enzymes, with K_i 's of $1.4 \mu\text{M}$ and $0.8 \mu\text{M}$ on gelatinase A and B, respectively, and demonstrated noncompetitive inhibition on both enzymes. (Fig. 63). The IC_{50} 's for both of the enzymes were approximately 5-10 times their K_i values. Finally, the synthetic propeptides RCGVPD and RCGNPD were analyzed for inhibitory activity and found to act as mixed inhibitors (Fig. 64 and Fig. 65). The K_i values were found to be $0.9 \mu\text{M}$ and $2.7 \mu\text{M}$, respectively, on gelatinase A, and $0.71 \mu\text{M}$ and $0.042 \mu\text{M}$, respectively, on gelatinase B.

In addition to the synthetic inhibitors analyzed, the inhibitory activity of the endogenous inhibitors, the tissue inhibitors of matrix metalloproteinases (TIMPs), was tested. Human recombinant TIMP-1 protein, expressed in mammalian cells and purified from the medium by heparin-sepharose chromatography, was a generous gift from the Sakai lab. The TIMP-1 protein concentration was determined by amino acid analysis and the inhibitor was used to titrate the gelatinases to check the accuracy of the concentration of gelatinase utilized in the enzymatic assays (data not shown) [198, 206]. Subsequently, TIMP-1 was analyzed for inhibitory activity against gelatinase A and B as has been shown

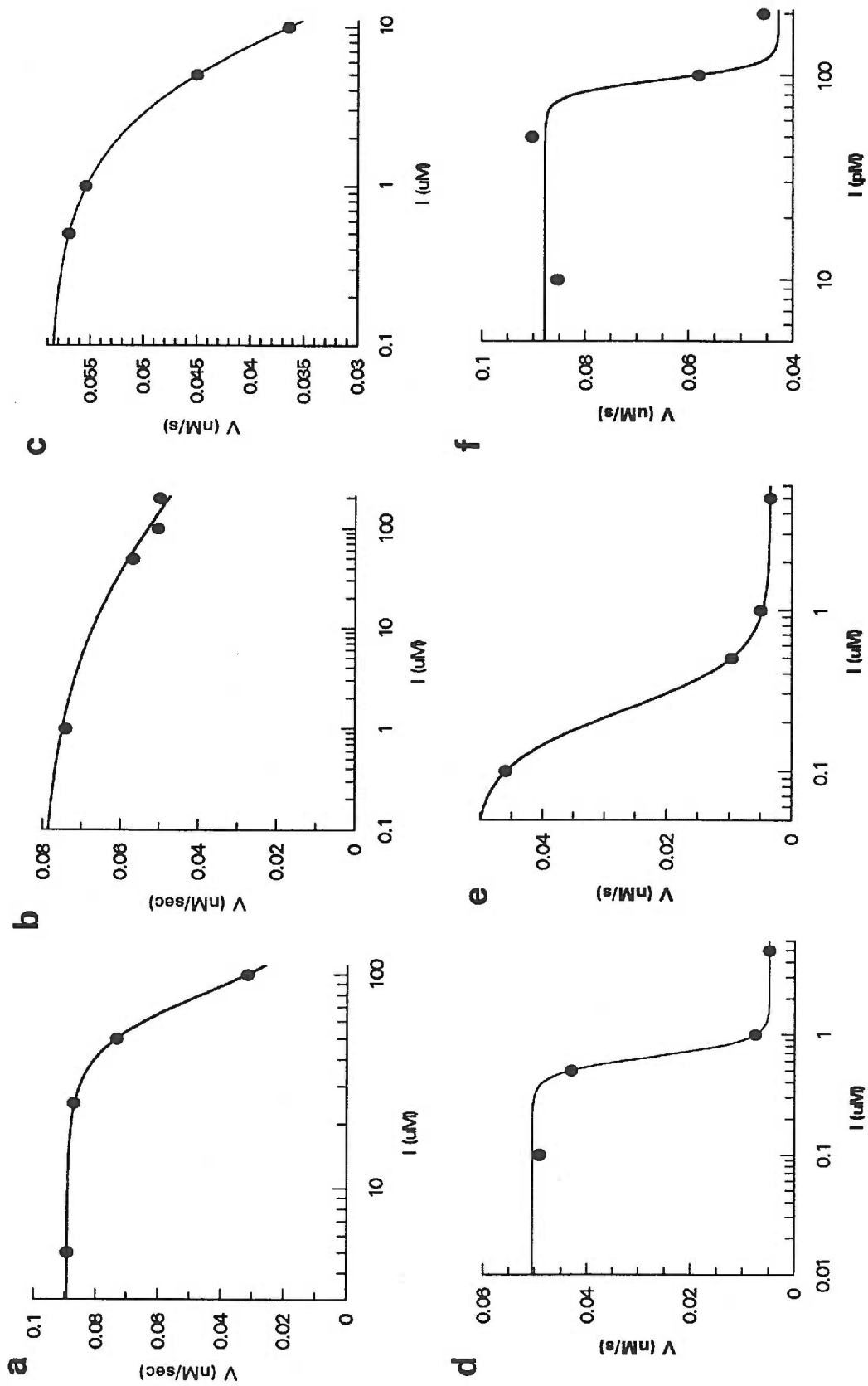


FIGURE 60: IC50 curves of 1 nM Gelatinase B on 5 uM Mca-peptide substrate with a) Minocycline, b) Tryptophan-Hydroxamate, c) Collagenase Inhibitor, d) RCGVPD, e) RCGNPD, f) rhTIMP-1

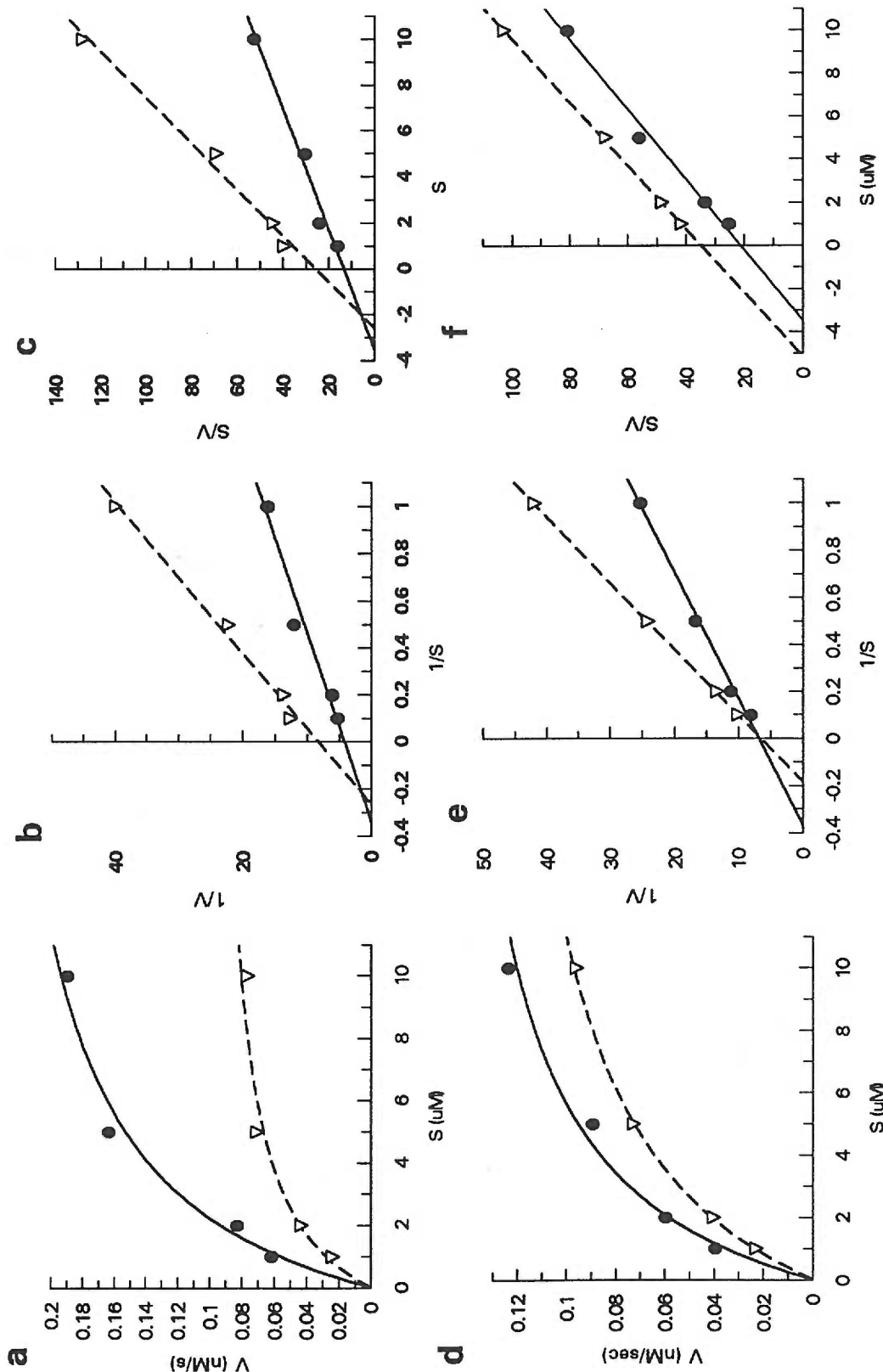


FIGURE 61: 100 pM Gelatinase A (a-c) or 1 nM gelatinase B (d-f) in the absence (---) or presence (- - -) of 50 μ M Minocycline; a) and d) Michaelis Menten Plot, b) and e) Lineweaver Burk Plot, c) and f) Hanes Plot.

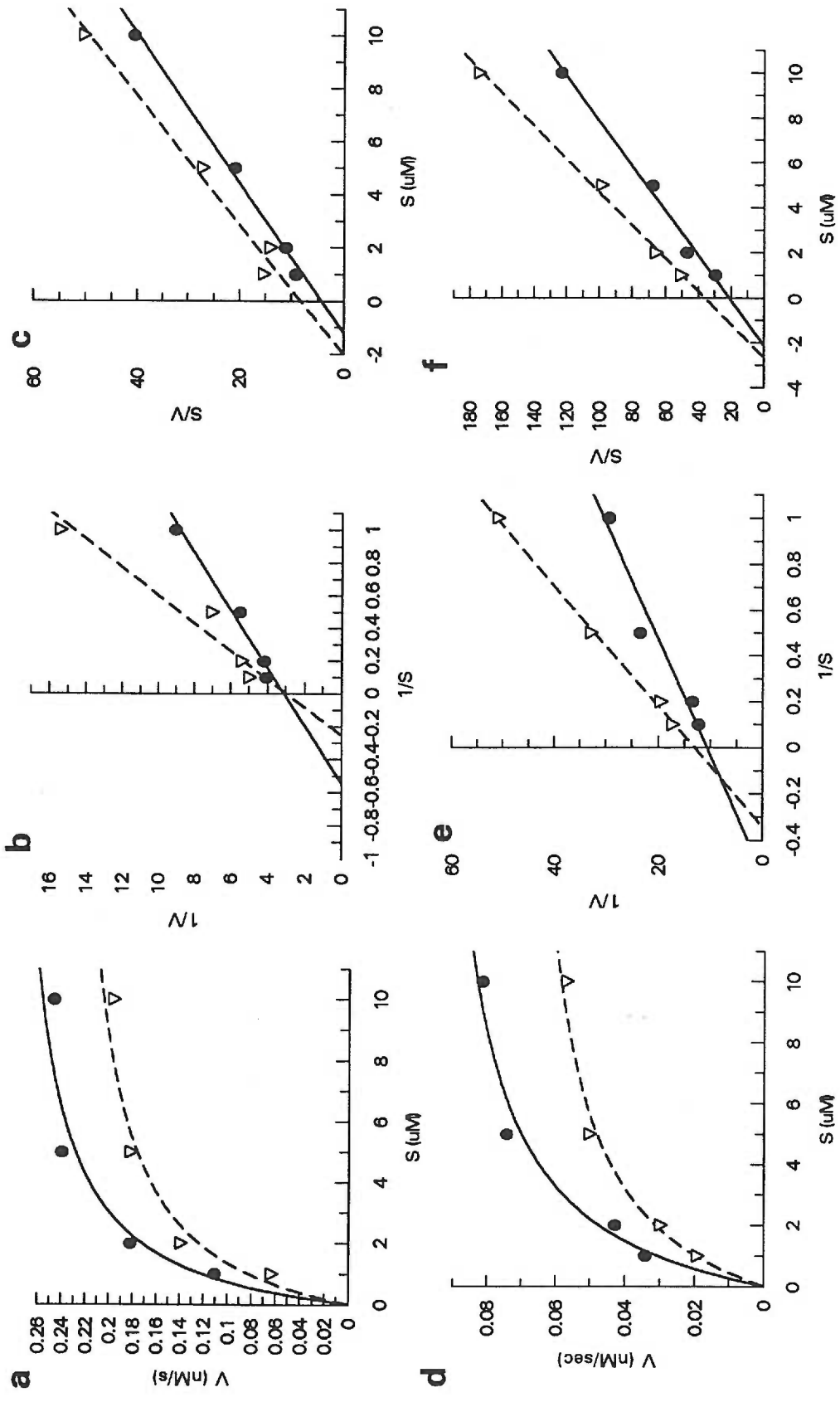


FIGURE 62: 100 pM Gelatinase A (a-c) or 1 nM gelatinase B (d-f) in the absence (---) or presence (- - -) of 200 μ M Tryptophan-Hydroxamate, respectively; a) and d) Michaelis Menten Plot, b) and e) Lineweaver Burk Plot, c) and f) Hanes Plot.

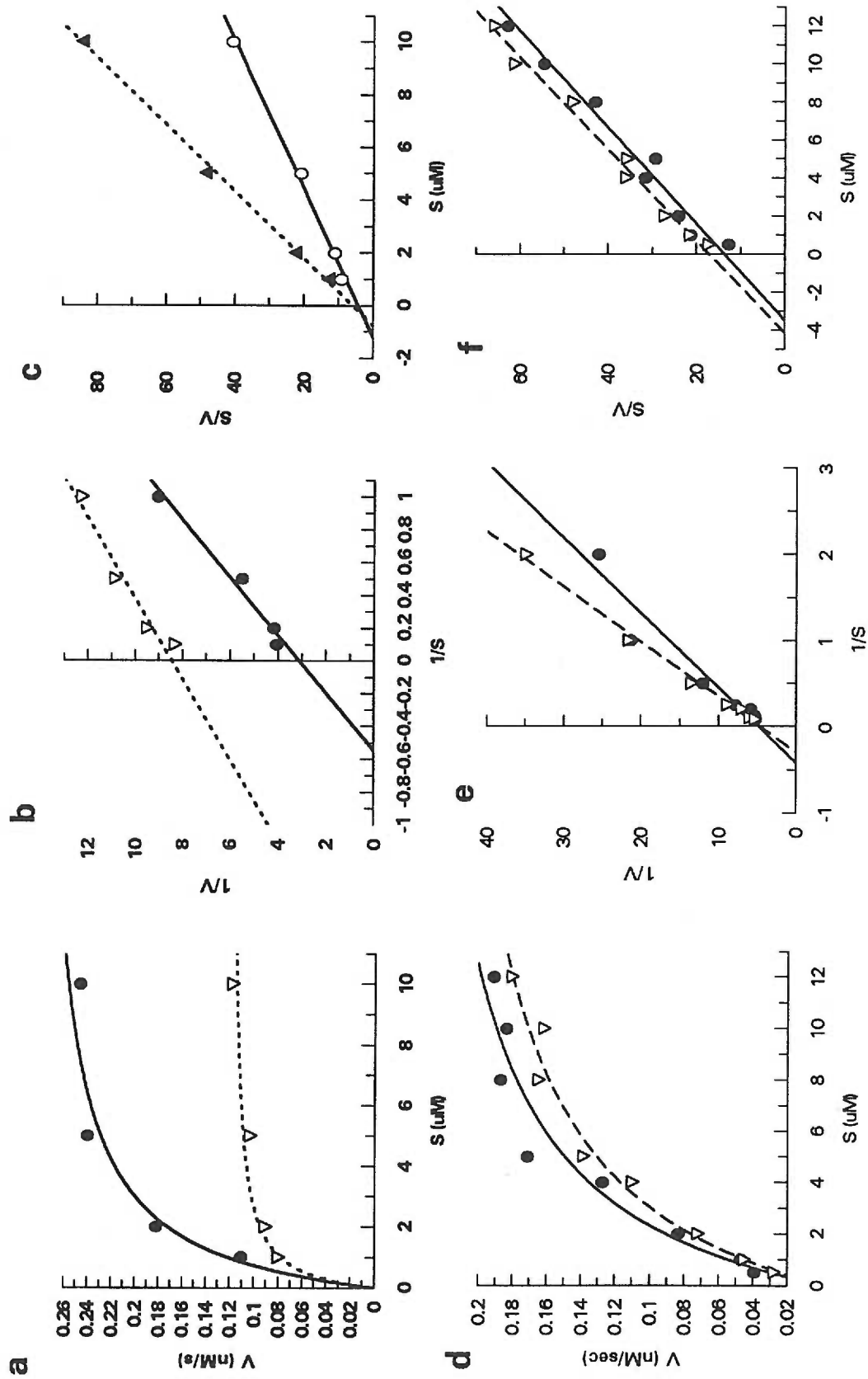


FIGURE 63: 100 pM Gelatinase A (a-c) or 1 nM gelatinase b (d-f) in the absence (---) or presence (- - -) of 500 nM Collagenase Inhibitor; a) and d) Michaelis Menten Plot, b) and e) Lineweaver Burke Plot, c) and f) Hanes Plot.

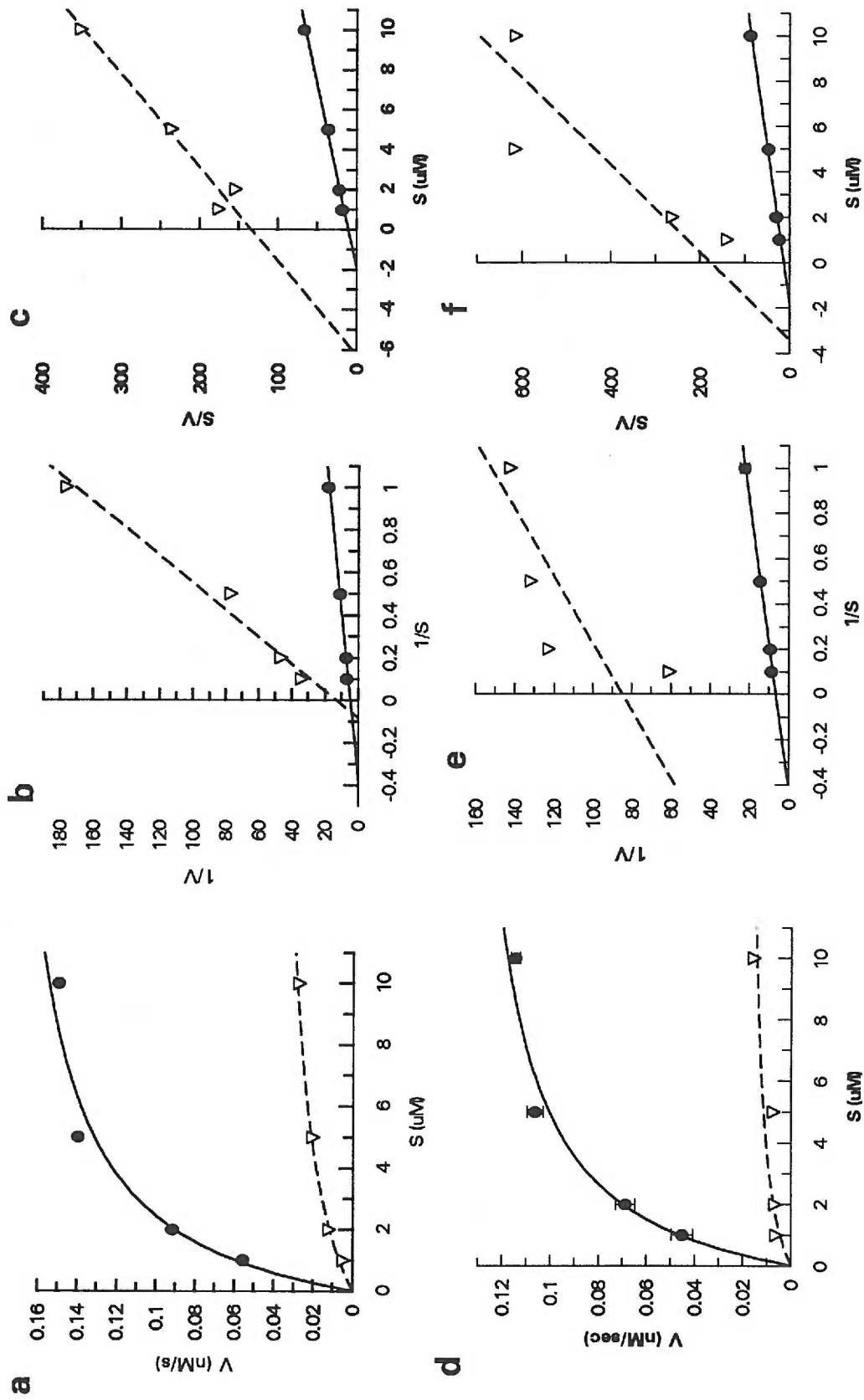


FIGURE 64: 100 pM Gelatinase A or 1 nM gelatinase B in the absence (---) or presence (- - -) of 10 μM or 1 μM RCGVPD, respectively; a) and d) Michaelis-Menten Plot, b) and e) Lineweaver Burk Plot, c) and f) Hanes Plot.

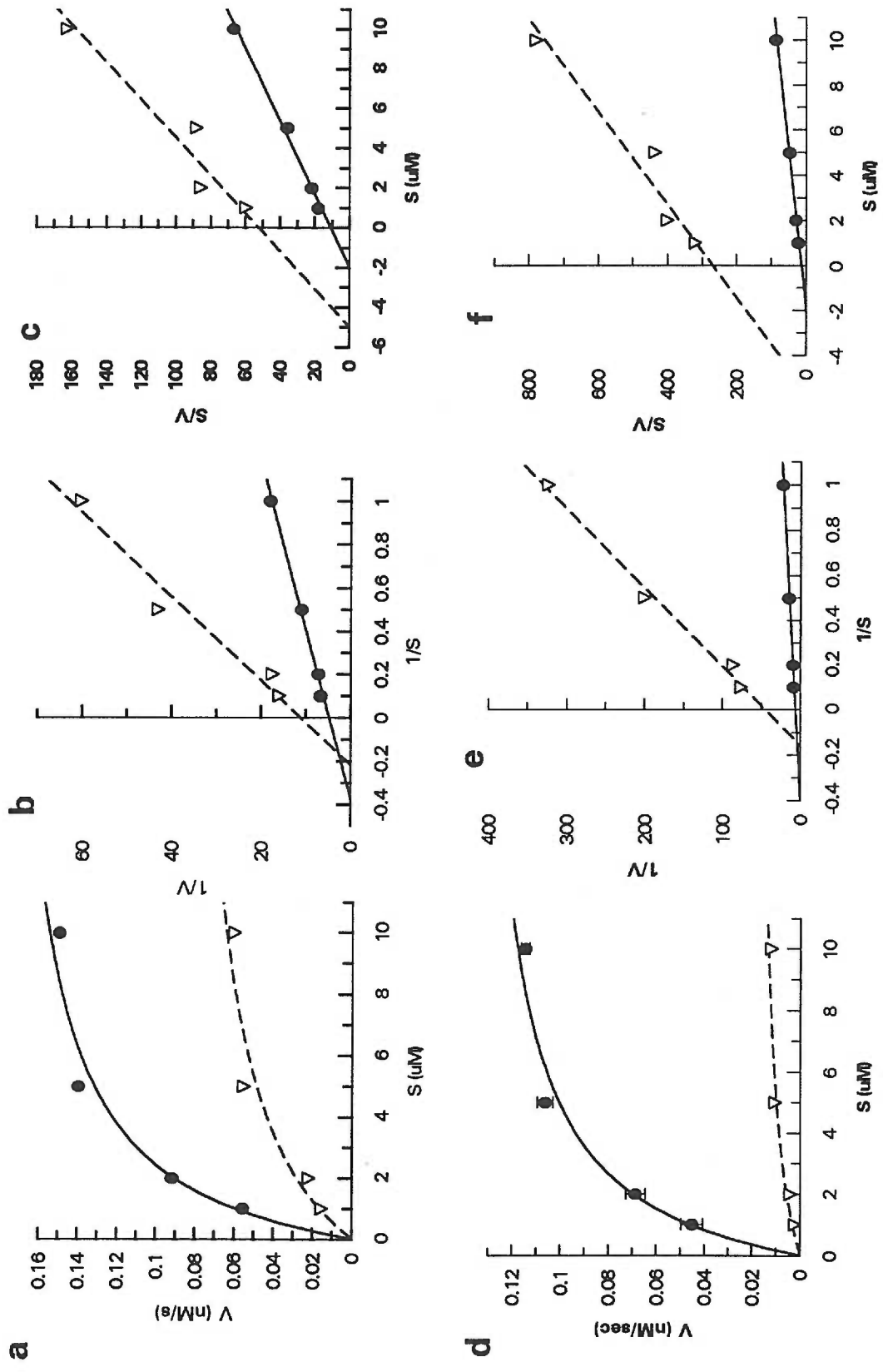


FIGURE 65: 100 pM Gelatinase A (a-c) or 1 nM gelatinase B (d-f) in the absence (---) or presence (- - -) of 10 uM RCGNPD, respectively; a) and d) Michaelis-Menten Plot, b) and e) Lineweaver Burk Plot, c) and f) Hanes Plot.

previously in different enzymatic assays as reviewed [119, 136, 166, 198] . Recently, TIMP-1 has been shown to inhibit collagenase as a slow, tight-binding noncompetitive inhibitor in a two-step process [161]. TIMP-1 was found in these assays to inhibit gelatinase A with a $K_i = 45$ pM and gelatinase B with a $K_i = 184$ pM on the fluorescent peptide substrate. The inhibitor was utilized at a concentration of 200 pM and acted as a noncompetitive inhibitor on both enzymes (Fig. 66).

In addition, TIMP-3 was purified from human placenta (from Xianghong Zhu in the Acott lab) and from mammalian cells expressing recombinant TIMP-3 (purification steps were described in 'Materials and Methods') using carboxymethyl chromatography (unpublished data) and the purified protein was analyzed for inhibitory activity against gelatinase A. Recombinant TIMP-3 had been shown previously to inhibit stromelysin and collagenase with a specific activity similar to that of TIMP-1 [144]. After estimating the purified TIMP-3 protein based on absorbance values, the protein was analyzed and found to inhibit gelatinase A with a K_i of 32 nM as a noncompetitive inhibitor (Fig. 67) suggesting that the different TIMPs may inhibit the metalloproteinases in a similar manner, but may have different affinities for the various MMPs.

Additional linear plots may be utilized to help fit the data in order to determine the mechanism through which the inhibitor is acting. Some inhibitor data, with minocycline or the Trp-hydroxamate inhibitor on gelatinase B activity, was plotted for this purpose in a Dixon plot ($1/V$ vs. $[I]$) or in a Cornish-Bowden plot ($[S]/V$ vs $[I]$) (Fig. 68). In this way, it was possible to observe the effects of increasing the inhibitor concentration on velocity at fixed values of enzyme and substrate [262]. The results confirmed that both

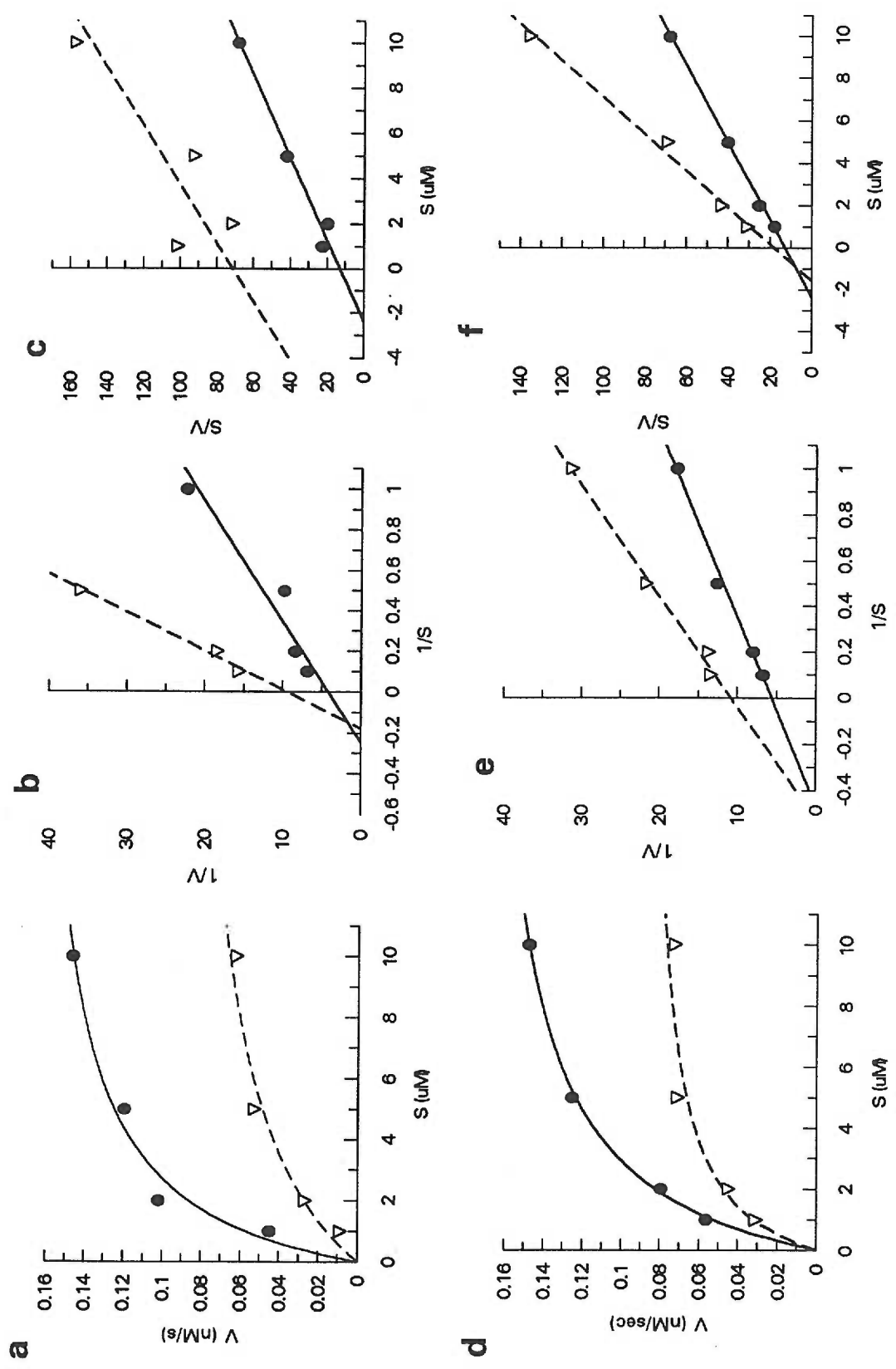


FIGURE 66: 100 pM Gelatinase A (a-c) or 1 nM Gelatinase B (d-f) in the absence (---) or presence (- - -) of 200 pM rTIMP-1; a) and d) Michaelis Menten Plot, b) and e) Lineweaver Burk Plot, c) and f) Hanes Plot.

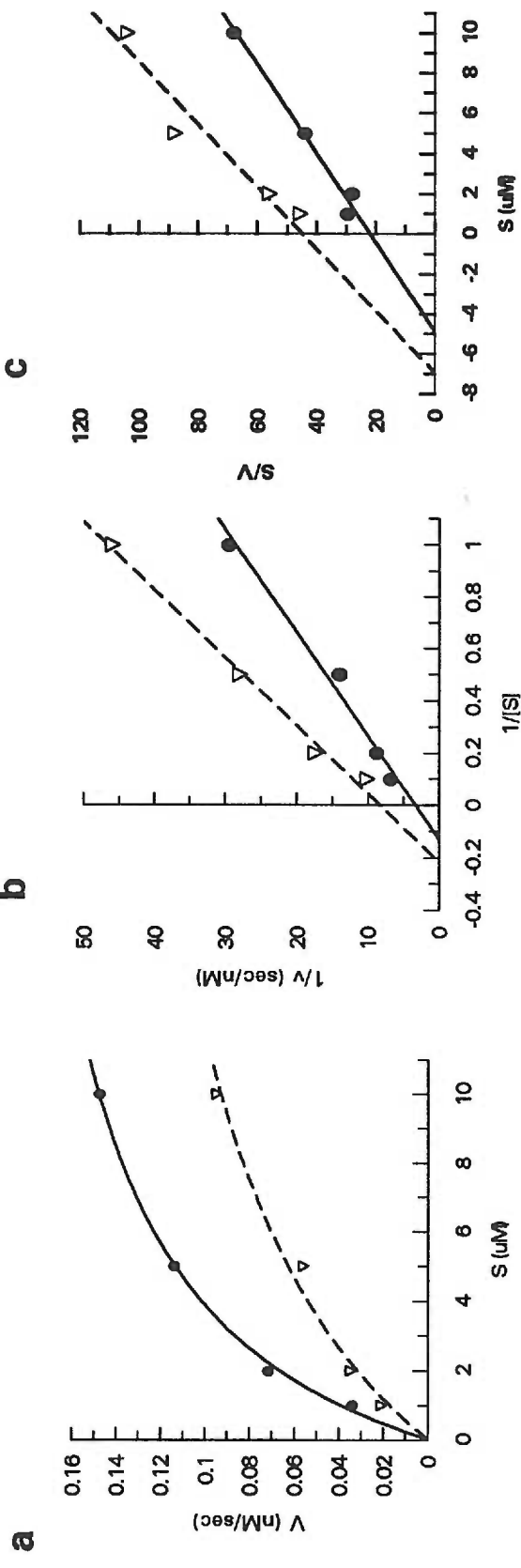


FIGURE 67: 100 pM Gelatinase A in the absence (---) or presence (- - -) of 33 nM TIMP-3; a) Michaelis Menten Plot, b) Lineweaver Burk Plot, c) Hanes Plot

minocycline and tryptophan-hydroxamate are competitive inhibitors of gelatinase B activity on the peptide substrate, as determined by previous fits and summarized in the tables in Figures 69 and 70.

Outflow system - The inhibitors analyzed above in the enzyme-inhibition assays were also analyzed in a glaucoma model system. This was done in order to test the hypothesis that disruption of the normal extracellular matrix turnover by the matrix metalloproteinases within the aqueous humor outflow pathway may cause the increase in intraocular pressure observed in primary open-angle glaucoma. Outflow rates change in response to changes in perfusion head, as has been described previously [255-257]. Perfusion head pressure was maintained for several days, and outflow rate per mm Hg perfusion head was found to be constant. Stable outflow rate and normal morphology were maintained for several weeks in this culture system. This outflow model system was set up and tested by members of the Acott lab. The following inhibitor data was also performed by the same members of the Acott lab [250].

Flow rate was normalized to the 7.35 mm Hg flow value (Fig. 71a). A mixture of purified matrix metalloproteinases containing a 1:1:1 ratio of stromelysin, gelatinase A and gelatinase B was added to the perfusion medium and the outflow rates over time were evaluated (71b). The outflow was found to increase gradually to a plateau by around three days. Perfusion with no additions or with bovine serum albumin produced no significant changes in outflow (Fig. 71b). Recombinant human IL-1 α was added to the perfusion medium at time = 0 and outflow rate increased gradually over time, as expected (Fig. 71c). Various inhibitors were then added to the perfusion medium on stabilized

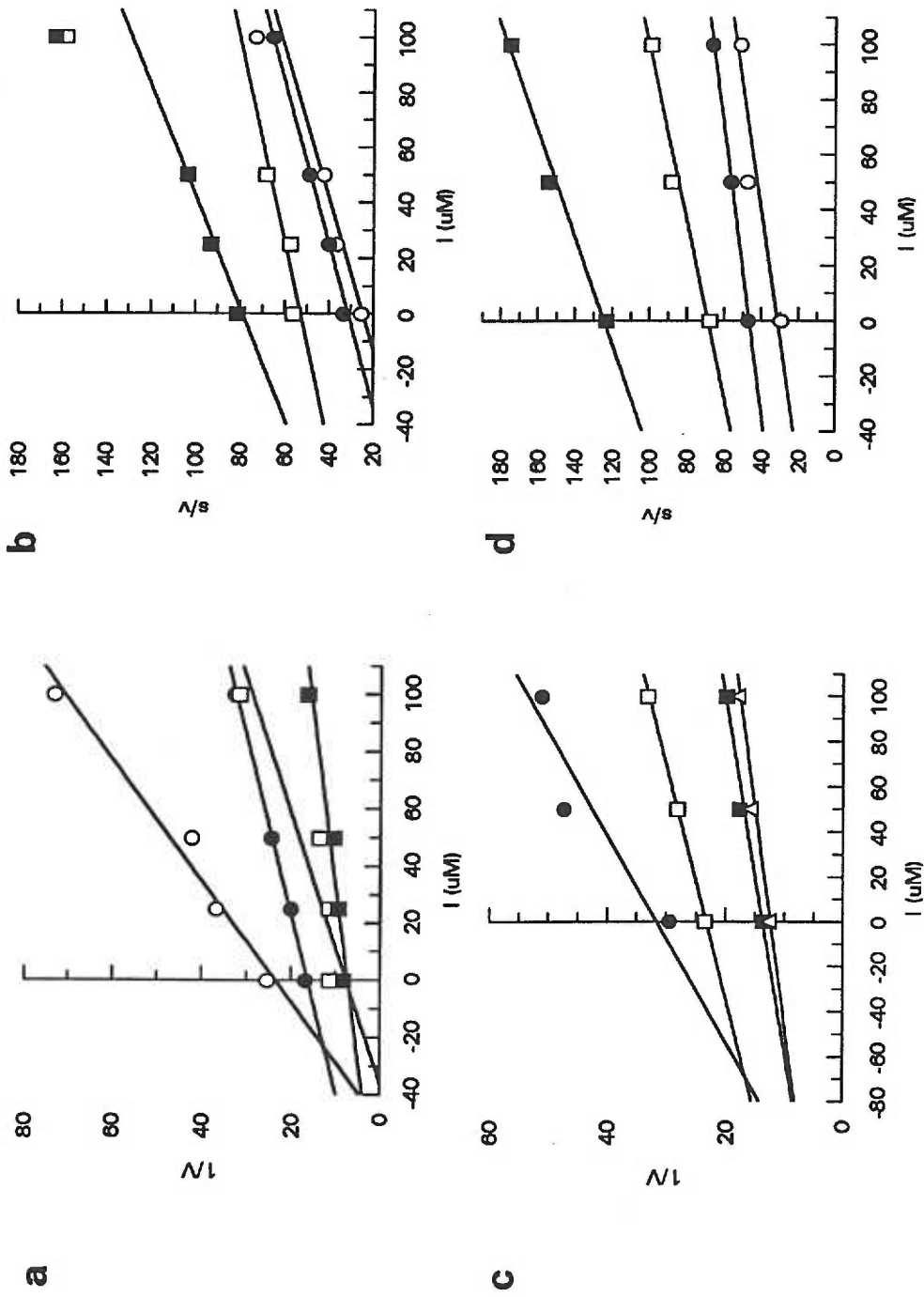


FIGURE 68: 1 nM Gelatinase B and either Minocycline (a-b) or Tryptophan-Hydroxamate (c-d) at 0-100 μM concentrations and at substrate concentrations between 1-10 μM ; a) and c) Dixon Plot, b) and d) Cornish-Bowden Plot

Inhibition of Gelatinase A Activity on Mca- Peptide Substrate			
Inhibitor	IC₅₀ (μM)	K_i (μM)	Inhibition Type
Minocycline	64	55	Noncompetitive
Trp-Hydroxamate	n.d	217	Competitive
Collagenase Inhibitor	6	1.4	Noncompetitive
RCGVDP	1.2	0.9	Noncompetitive
RCGNPD	2.7	2.7	Noncompetitive
rhTIMP-1	2.03 x 10 ⁻⁴	45 x 10 ⁻⁶	Noncompetitive
hTIMP-3	0.032	0.033	Noncompetitive
MBP-rTIMP-2	0.038	n.d.	n.d.

n.d. = not determined

FIGURE 69: Gelatinase A concentration was 100 pM per assay, as was described in 'Materials and Methods'. Inhibitor concentrations, for kinetic assays to determine Ki values, were as follows, 1) Minocycline = 50 μM, 2) Tryptophan-Hydroxamate Inhibitor = 100 μM, 3) Collagenase Inhibitor = 2 μM, 4) RCGVDP = 10 μM, 5) RCGNPD = 10 μM and, 6) recombinant human TIMP-1 = 100 pM, 8) hTIMP-3 = 33 nM. Linear fits and equations used to determine Ki values are described in 'Results'; graphical representations of data are in Figures 59-68.

Inhibition of Gelatinase B Activity on Mca- Peptide Substrate			
Inhibitor	IC₅₀(μM)	K_i (μM)	Inhibition Type
Minocycline	82	65	Competitive
Trp-Hydroxamate	48	88	Competitive
Collagenase Inhibitor	16	0.8	Noncompetitive/mix.
RCGVDP	0.65	0.71	Noncompetitive
RCGNPD	0.023	0.0042	Noncompetitive
rhTIMP-1	1.84×10^{-4}	0.95×10^{-4}	Noncompetitive/mix

FIGURE 70: Gelatinase B concentration was 1 nM per assay, as was described in 'Materials and Methods'. Inhibitor concentrations, for kinetic assays to determine Ki values, were as follows, 1) Minocycline = 50 μ M, 2) Tryptophan-Hydroxamate Inhibitor = 100 μ M, 3) Collagenase Inhibitor = 2 μ M, 4) RCGVPD = 1 μ M, 5) RCGNPD = 1 μ M and, 6) recombinant human TIMP-1 = 100 pM. Linear fits and equations used to determine Ki values are described in 'Results'; graphical representations of data are in Figures 59-68.

explants and outflow rates were evaluated for each inhibitor. Minocycline added to the perfusion medium (to a final concentration of 100 μM) produced a significant decrease in outflow facility by 24 hours (Fig. 72a). Addition of L-tryptophan hydroxamate (to a final concentration of 50 μM) to the perfusion medium produces a gradual and sustained depression in outflow facility over several days following treatment (Fig. 72b). Addition of IL-1 reverses the outflow depression. In addition, the small pro-peptide inhibitor, Ac-RCGVP-NH₂, was added to the perfusion medium, at a final concentration of 200 μM , and was found to depress outflow facility in a fairly rapid and reversible manner (Fig. 72c). Purified human TIMP-2 (50 nM) was added to perfusion medium and outflow was monitored for 120 hours. Medium was then replaced with TIMP-2-free medium and outflow monitored until recovery to pre-treatment levels (Fig. 72d). In separate studies, IL-1 and TIMP-2 were added together to stabilized explant perfusion medium and outflow was measured over time (Fig. 72d).

D. Discussion

The data and results presented above demonstrate that the enzymatic activities of gelatinase A and B are somewhat different from each other and vary according to the substrate selected for enzymatic cleavage. The gelatinases had similar affinities for the protein and peptide substrates, as shown by their similar K_m values. However, their rates of proteolysis were different by a factor of approximately 100 as the rate of the enzymatic cleavage of the gelatin substrate, or k_{cat} , was much faster than that for the peptide

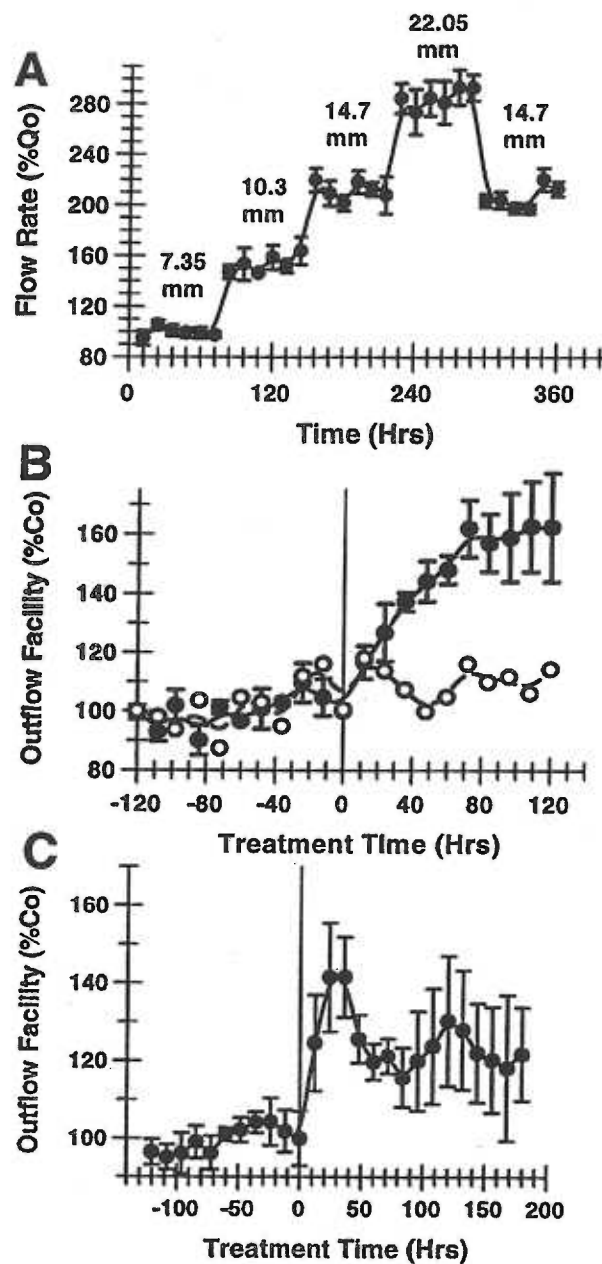


Figure 71: Graphical representation of outflow rate changes in response to various modulators; work represented here was performed and the data were collected and analyzed by John Bradley and Ted Acott in the Acott Lab. (A) Flow rate (Q_0) was normalized to the 7.35 mm Hg flow value. Points are mean \pm SEM for $n = 4-8$ experiments. (B) After outflow had stabilized, 20 μ g of purified metalloproteinases (1:1:1 of gelatinase A, B, and stromelysin) (solid circles) or of bovine serum albumin (solid squares) were added per ml of perfusion medium. Values are mean outflow facility \pm ranges for two explants; $P < 0.0001$, comparing pre- and post-treatment values by student's t analysis. (C) Recombinant human IL-1 α (40 U/ml) was added to the perfusion medium at time = 0. Values are mean $\%Co \pm$ SEM of four explants; $P < 0.0001$ comparing pre- and post-treatment values via student's t -test.

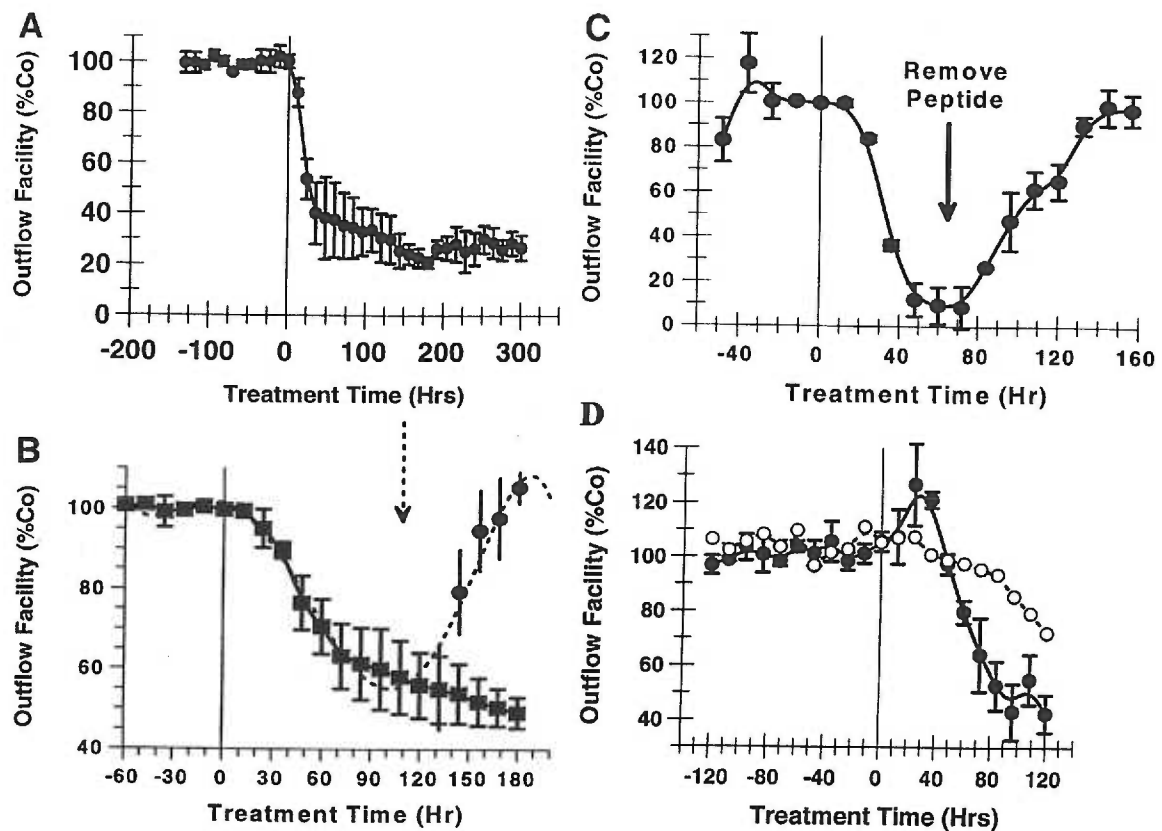


Figure 72: Graphical representation of outflow rate changes in response to various modulators; work presented here performed by John Bradley and Ted Acott. (A) Stabilized explants were treated with minocycline (100 μ M) and outflow facility measured. Mean %Co \pm SEM is shown for four explants; $P < 0.0001$ for pre- compared to post-treatment explant outflow facility. (B) Stabilized explants were treated with tryptophan hydroxamate (50 μ M) and outflow facility was measured (solid squares). Mean %Co \pm SEM is shown for three explants; $P < 0.001$ for pre- compared to post-treatment explant outflow facility. In additional experiments, IL-1 α (50 U/ml) was added to the perfusion medium without removal of the hydroxamate (solid triangles, $n = 1$ added as marked by the dashed arrow or solid circles, $n = 3$ with vertical bars showing \pm SEM, added as marked by the dotted arrow). Addition of IL-1 reverses the outflow depression. (C) Stabilized explants were treated with a short peptide (Ac-RCGVP-NH₂; 200 μ M) from the pro-peptide sequence of the MMPs and outflow facility measured; after 60 hours, media without the inhibitory peptide was perfused to evaluate recovery from the inhibition (arrow). Mean %Co \pm SEM is shown for three explants. (D) Purified human TIMP-2 (50 nM) was added to perfusion medium and outflow was monitored for 120 hours (solid circles). Medium was then replaced with TIMP-2-free medium and outflow monitored until recovery to pre-treatment levels (approximately 100 hours; data not shown). In separate studies, 50 U/ml of IL-1 α and 14 nM TIMP-2 were added together to stabilized explant perfusion medium and outflow measure for 120 hours (open circles). Inhibitors were dissolved in water or absolute ethanol (at 10,000 \times) and diluted into culture medium; parallel vehicle controls were analyzed in all cases.

substrate. It was also of note that the gelatinases had very similar activities on the gelatin substrate, whereas the peptide substrate was clearly a better substrate for gelatinase A than it was for gelatinase B, as determined by their respective k_{cat}/K_m values.

Additionally, several inhibitors of different classes were selected and analyzed for their inhibitory activity against gelatinase A and B in assays with the gelatin substrate and also in the fluorescent peptide substrate assays. Many studies have been devoted to the analysis of the inhibitory activity of MMP inhibitors in the search for more potent inhibitors that may have possible therapeutic value in the treatment of clinical disease as reviewed [223]. In addition to improving our understanding of the general mechanism of action of the gelatinases, understanding the modes of inhibition of not only the TIMP activity on the gelatinases, but also of various synthetic inhibitors, may help in the future to develop more potent MMP inhibitors.

Several different classes of inhibitors have been developed based on different strategies. Some chemotherapeutic agents, antibiotics, and synthetic peptides have been found to inhibit the MMP activity [223, 225, 228]. Some of the inhibitors have been developed as substrate analogs [230, 231, 243]. Other inhibitors have been developed based on the propeptide domain of the MMPs [245-248]. Inhibition of gelatinase A and B activity was achieved with the following compounds, 1) minocycline, a tetracycline derivative, 2) L-tryptophan-hydroxamate, 3) p-hydroxyl benzoyl-Ala-Phe, a substrate analog, 4) a collagenase inhibitor, 5) the propeptide sequences RCGVP, RCGVPD, and RCGNPD. TIMP-1, TIMP-2 and TIMP-3 were expressed and/or purified from various sources and their inhibitory activities against gelatinase A and B were also evaluated in the

same assays. When FITC-gelatin was selected as the substrate, the most potent inhibitor of gelatinase A was the propeptide inhibitor, RCGVPD, which appeared to inhibit as a mixed inhibitor. The most potent inhibitor of gelatinase B was the propeptide, RCGNPD, which also acted as a mixed inhibitor. These results are interesting considering the propeptide sequences of the respective gelatinases: gelatinase A has an Asn residue at the fourth position of the peptide, whereas gelatinase B has a Val residue in the same position. These results were consistent with those found in the peptide substrate assays and demonstrate the preferences of the propeptides for the two gelatinases. The significance of these results may be that in vivo the proenzyme with its respective propeptide is more easily activated than it would otherwise be with a more tightly associated propeptide. It is thus likely that chimeric forms of the enzymes with the switched propeptides would be difficult to activate. Presumably these natural sequence differences give a selective physiological advantage.

Of the other inhibitors analyzed in the protein substrate assays, minocycline was also one of the more potent inhibitors against gelatinase A and B and acted as a mixed inhibitor in both cases. In contrast, Trp-hydroxamate appeared to be a competitive inhibitor against gelatinase A and had better inhibition on gelatinase A than gelatinase B.

It is important to note that despite the linear fits of the enzymatic activity of the gelatinases on the gelatin substrate in the absence or the presence of inhibitors, the data were not always linear indicating the possibility of a more complex mechanism of action than previously described. Since the mechanism of action of the gelatinases is as yet undetermined, it is possible that a higher than first order reaction may be occurring during

the proteolysis of protein substrates. Another possible reason for the nonlinearity in the linear plots may be that insufficient data points were collected and the variance from a straight line may be within the standard error of the data. This could be addressed by additional replicates of the assays and more substrate concentrations tested within the range studied.

The inhibition results from the peptide substrate assays demonstrate that the same inhibitors that were analyzed in the protein substrate assays had lower K_i values, and therefore better inhibitory activity in general against the gelatinases in the peptide substrate assays. It follows that the interactions of a peptide substrate with the enzyme's active site may be easier to disrupt than the interactions of a protein substrate and the active site of the enzyme. As for the specificity and type of inhibition against gelatinase A or B, there were occasional differences in the peptide substrate data. The most potent inhibitor of gelatinase A, excluding the full length TIMP proteins, was the propeptide RCGVPD, whereas for gelatinase B it was the propeptide RCGNPD, and both inhibitors acted as noncompetitive inhibitors on the gelatinases. These results were the same as those for the protein substrate data and the significance was discussed above. The collagenase inhibitor was one of the better inhibitors as it was shown to be a noncompetitive inhibitor of gelatinase A and B with a K_i of 1 μ M in the peptide substrate data. Minocycline was a decent inhibitor and had approximately equal effectiveness on gelatinase A and B, although higher concentrations of inhibitor were necessary to inhibit the gelatinases. It appeared to act as a competitive inhibitor against gelatinase B in the peptide substrate assays.

These results are similar to those discussed above. However as compared with the protein substrate data, in most cases the data from the peptide substrate assays fit well with the linear fits. This implies first order reaction kinetics of the gelatinases on the peptide substrate. In the presence of the inhibitors, the data tended to become somewhat more nonlinear in the linear fits indicating a possibly more complex mode of inhibition than previously discussed. However, as mentioned above, the nonlinearity may also result from standard error incorporated into the assays and/or insufficient data points within the range of substrate and inhibitor concentrations analyzed.

Finally, recombinant TIMP-1 was analyzed in the peptide substrate assays in order to correlate determined K_i values on gelatinase A and B with those that had been published previously [3, 119]. As expected, the TIMP-1 had a K_i in the subnanomolar range and inhibited active gelatinase A and B with approximately equal effectiveness. Additionally, a purified recombinant TIMP-2 fusion protein was shown to have good inhibitory activity against gelatinase A. Purified TIMP-3 was also shown to have inhibitory activity against gelatinase A with a K_i in the nanomolar range and acted as a noncompetitive inhibitor.

The variety of types of inhibition demonstrated in this study, from competitive to noncompetitive to mixed, suggest complexities in the modes of inhibition of structurally different inhibitors, and even possible differences in the mechanism of action of the gelatinases on different substrates. A recent finding has shown that three peptide inhibitors, all containing different functional groups, interacted with different residues at the active site of matrilysin [66]. There are subtle differences that exist in the structures of

not only gelatinase A and B, but also of the other MMP family members. How the family of TIMP proteins interacts with the gelatinases is still ambiguous, although more biochemical and kinetic data will help to address these concerns. The study recently published on the mechanism of TIMP-1 inhibition of collagenase activity on a peptide substrate suggests that TIMP-1 binds to the free enzyme and to the enzyme-substrate complex in a noncompetitive manner when a peptide substrate is used [161]. It is possible that the physiological substrates of the enzyme might compete more effectively with TIMP-1 binding and that this may affect the mode of inhibitor binding.

A glaucoma model system, in the form of a perfused anterior segment explant organ culture was recently constructed and tested by members of the Acott lab and has been described previously [250]. Obstruction of the normal aqueous humor outflow pathway is thought to be a primary cause of the increase in intraocular pressure seen in glaucoma. This model system was utilized in order to test the following hypothesis: an imbalance in the net MMP/TIMP activity in the ECM of the trabecular meshwork or in the aqueous outflow pathway may cause a change in the intraocular pressure as observed in primary open-angle glaucoma. Outflow rates have been shown to change in response to changes in perfusion head pressure [254, 256, 257]. Outflow rate was found to be constant in the system when perfusion head pressure was maintained, and stable rates of outflow and normal morphology were maintained in this culture system for several weeks.

For the purpose of testing the hypothesis stated above, a mixture of purified MMPs was added to the perfusion medium and the resulting outflow rates were evaluated. As expected, the rates increased gradually over time demonstrating that MMP activity has

a definite effect on the outflow rate. To further determine the involvement of specific MMPs in the system, the inhibitors that had been analyzed in the kinetic assays were analyzed in the outflow system at similar concentrations. The inhibitors were shown to decrease the outflow rate in general, causing a 'glaucomatous state' in the explant system. The different inhibitors had varying effects on the outflow rates and the propeptide inhibitor, RCGVP seemed to be the most effective inhibitor tested. Its effects were reversible as it could be removed from the system and the normal outflow rates were regained. These inhibitor results help demonstrate the direct involvement of specific members of the MMPs in the outflow pathway, and therefore, as stated in the hypothesis, in primary open angle glaucoma, as observed in the explant outflow organ culture system described here. All studies undertaken and data collected from the outflow system were performed by other members of the Acott lab.

IV. Patterns of Expression of human TIMP-3

A. Introduction

The macular dystrophies represent a large group of disorders that affect central vision. Age-related macular degeneration (AMD) is a leading cause of blindness and has an estimated prevalence of 20 % for individuals over 65 years of age in developed countries [266, 267]. Although a strong genetic component exists, AMD gene defects have yet to be identified. Sorsby's fundus dystrophy (SFD) is less common than AMD, has an earlier age of onset, is an autosomal dominant disorder, and shares most of the clinical and pathophysiological features of AMD [268]. Early manifestations of both AMD and SFD include Bruch's membrane thickening and the formation of extracellular matrix- and lipid-containing deposits [269], and subsequent neovascularization and atrophy of the choroid, retinal pigment epithelium (RPE), and retina [270]. Cause-and-effect has not been established, although these deposits are thought to impair the normal functions of the choriocapillaris and RPE. In both diseases, subretinal neovascularization and atrophy of the choriocapillaris, RPE and photoreceptors can ultimately result in central vision loss [267].

Bruch's membrane is a multi-layered structure located between the single layer of RPE and the choroidal microvasculature (Fig. 73) [271, 272]. Photoreceptor nutrients, including retinol, and retinal cellular wastes, both of which are processed by the RPE, must traverse Bruch's membrane going from or to the choriocapillaris. This ECM

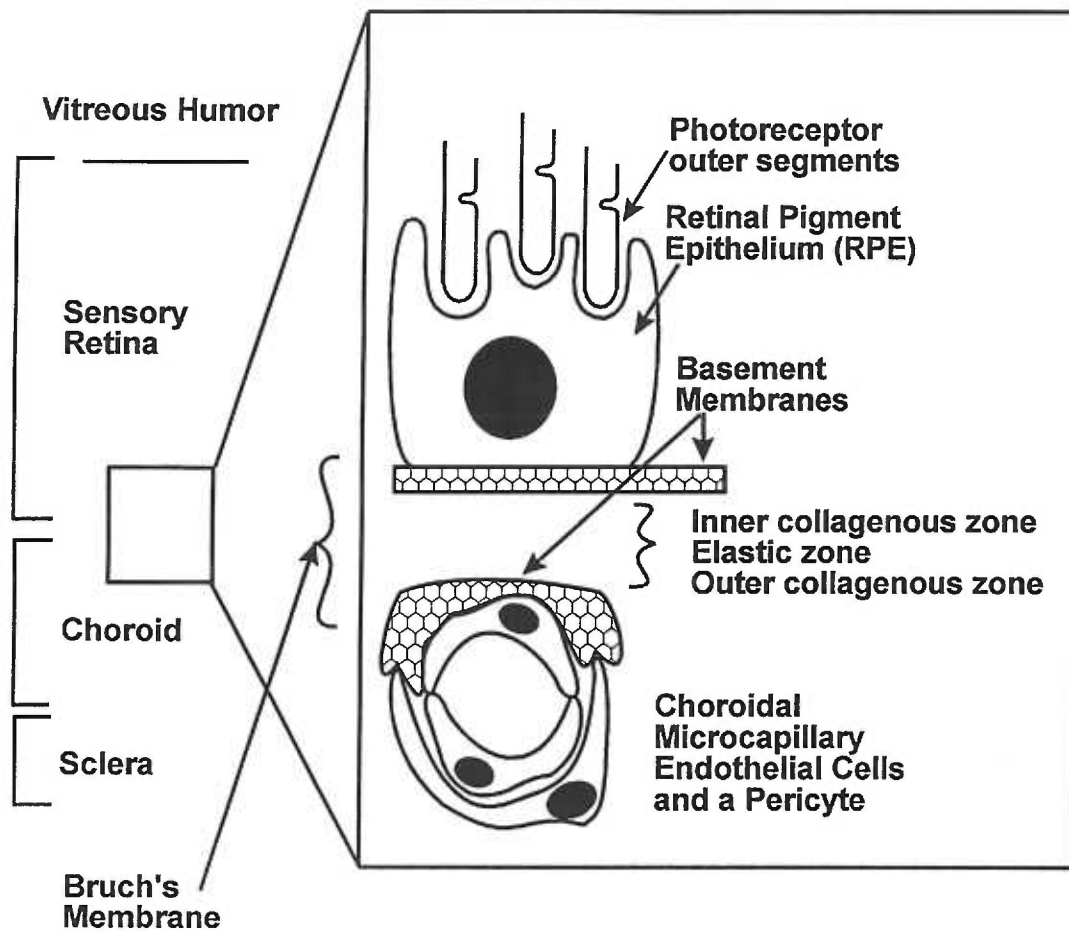


Figure 73: Schematic of Human Retina.
 Bruch's membrane is bordered on either side by the single layer of RPE cells and the choriocapillaris.

structure is composed of a variety of basement membrane and stromal ECM proteins, such as collagens, fibronectin, laminin and proteoglycans. Remodeling of the ECM is critical for normal development and is a continuous process of degradation and replacement biosynthesis of ECM molecules in normal adult tissues. This process of remodeling requires the tightly regulated activity of the MMPs, as described previously. The complex regulation of the MMPs occurs at the levels of transcriptional regulation, activation of the latent proenzymes, and constraint of activity by their interactions with the TIMP, as described earlier [2-4, 136, 273]. It has been shown that the disruption of normal homeostatic ECM remodeling also plays a role in the etiology of several diseases, including cancer and arthritis [15, 162, 163, 166, 274].

TIMP-1 and TIMP-2 have been relatively well characterized, as reviewed [119, 136, 166]. All of the TIMPs bind to and inhibit the activated MMPs with a 1:1 molar stoichiometry and subnanomolar K_i values [144, 148]. The C-terminus or putative 'regulatory' domain of TIMP-1 and -2 also bind to the C-terminal domains of gelatinase B and A, respectively, as has been described previously. Recently, the sequences for mouse and human TIMP-3 have been reported [124, 126, 275]. Less is known about TIMP-3 than the other members of the TIMP family. However, it is unique in having a strong affinity for the ECM, while the other two TIMPs are found predominantly in the media from cultured cells [143, 276]. TIMP-3 shares considerable sequence homology with the other TIMPs, but the regulation of each is different [143, 144, 277].

In humans, TIMP-3 was mapped to chromosome 22q13 [124], as was the Sorsby's fundus dystrophy (SFD) locus [278]. Patients with SFD have been shown to

have specific mutations in TIMP-3 [278, 279]. Several similar, but distinct point mutations have been identified in exon 5 in different families, for example a serine or tyrosine to a cysteine mutation has been observed near the carboxyl terminal of this protein [278, 279]. Recently, another similar mutation, a glycine to a cysteine mutation, has been identified in another family [280, 281]. These TIMP-3 mutations in SFD demonstrate a critical role for TIMP-3 in the retina, although the functional details remain to be determined.

The TIMPs share 12 conserved cysteine residues, which are involved in 6 disulfide bonds [169]. The TIMP-3 mutations seen in patients with SFD are near the C-terminus in the 'regulatory' domain. The mutations all result in an extra cysteine, which may disrupt the tertiary structure of the protein by introducing new, incorrectly formed disulfide bridges during folding of the protein. They may also change the ECM binding properties of the TIMP-3 protein, or possibly affect some other function of the protein.

Since little is known about TIMP-3 expression in the retina or choroid, studies were undertaken to examine TIMP-3 expression at both the transcriptional and protein levels and localization of TIMP-1, -2 and TIMP-3 proteins to specific cellular layers in the human eye [282]. The questions to be addressed in performing these studies were: 1) what is the normal function of TIMP-3 versus that of TIMP-1 and -2 in the eye tissues surrounding Bruch's membrane, and 2) why might particular cysteine mutations in TIMP-3 cause the pathological features seen in patients with SFD. Further confocal microscopy studies were performed to compare the patterns of expression of TIMP-3 from normal cell lines versus the TIMP-3 expression in cell lines from SFD patients with a mutant TIMP-3.

B. Materials and Methods

Tissue and Cell Culture - Human RPE and choroidal microvascular pericytes and endothelial cells were cultured as previously described [283]. For preparation of RNA, these cells were grown to confluence in 75-cm² culture flasks in Dulbecco's modified Eagle medium (DMEM) supplemented with 10% fetal calf serum. For analysis of the basal levels of TIMP-1, 2 and 3 and glyceraldehyde-3-phosphate dehydrogenase (GAPD) transcripts in these cells, they were used at confluence without prior serum-free culture. For the treatments, the cells were rendered quiescent by incubation in serum-free DMEM for 18-24 hrs and then treated with the phorbol mitogen, 12-O-tetradecanoylphorbol-13-acetate (TPA) (1 μ M, Sigma, St Louis, MO), bFGF (10 ng/ml; R&D Systems, Minneapolis, MN), both TPA and bFGF together, serum (10%), all-trans retinol (200 ng/ml; Hoffmann-LaRoche, Nutley, NJ), or vehicle, all in fresh medium, for various times prior to isolation of total RNA as detailed below. Tissues for similar transcript analysis were simply dissected from whole human donor eyes by rinsing the vitreous from the bisected globes, teasing the retina from the choroid, dissecting the choroid and isolating the total RNA from each as detailed below. For protein studies, cells were grown to confluence in DMEM with 10% FCS, maintained serum-free in DMEM for 24 h, and then exposed to similar treatments (see above) for 36 hrs. Media was removed and frozen until use for TIMP-1 or TIMP-2 analysis and TIMP-3 was extracted from ECMs as detailed below.

RNA preparation, RT-PCR and Northern Analysis - Total cellular RNA was isolated and prepared from dissected retinal tissues and from cultured cells as described previously [189, 195]. In brief, cells or tissue were rinsed in PBS. In order to lyse the cells, a stock solution of 4 M guanidinium isothiocyanate was added and the cells were incubated at room temperature for 5 minutes. The tissue was sonicated at this stage in short 2 second bursts for a total of 60 seconds. Then β -mercaptoethanol was added to the lysed cells or tissue and finally a solution of 2 M Na Acetate, pH 4.0 was added. The tubes were vortexed and the nucleic acids extracted by adding an equal volume of a 1:1 phenol:chloroform. The tubes were vortexed for 10 seconds and then incubated on ice for 15 minutes. They were then centrifuged at 12,000 x g for 20 minutes at 4°C and the aqueous phase was removed to a clean tube. The RNA was precipitated by adding an equal volume of 100% isopropanol and incubation at -20°C overnight. The RNA was pelleted by centrifugation at 12,000 x g for 20 minutes at 4°C and the pellet was washed with 70 % EtOH.

For the RT-PCR experiments, the RNA was reverse transcribed to cDNA for 90 min at 37°C with M-MLV reverse transcriptase (1 Unit in 20 μ l; GIBCO/BRL, Grand Island, NY) and 0.25 μ g oligo-dT in 50 mM Tris-HCl (pH 8.3), 75 mM KCl, 10 mM dithiothreitol (DTT), 3 mM MgCl₂, and 0.5 mM of each dNTP. Aliquots of these cDNAs (2 μ l) were amplified by PCR using Tfl DNA polymerase (2 Units in 100 μ l; Epicentre, Madison, WI), but with the following changes: 125 nM of each (sense and antisense) PCR primer, 0.2 mM each dNTP, 50 mM Tris (pH 9.0), 2 mM (NH₄)₂SO₄ and 1.75 mM MgCl₂ were used. Thirty-five PCR cycles (95°C, 15 sec ; 55°C, 1 min; 72°C, 2 min)

were used with a final extension of 5 minutes at 72°C. PCR products were electrophoresed on 3% agarose gels in TAE buffer (40 mM Tris-acetate, 1 mM EDTA, pH 8) with ethidium bromide staining and using a 123 bp DNA ladder for size standards (GIBCO/BRL). TIMP-3 PCR product bands were excised from the gel and cleaned (Gene Clean; Bio101, La Jolla, CA) prior to restriction digestion. The DNA was then digested with Pst I, Bbv I or Nsi I (Boehringer Mannheim, Indianapolis, IN) overnight at 37°C and the fragments were electrophoresed on 3% agarose gels in TAE buffer and photographed. For all semi-quantitative comparisons of transcript levels, dilution curves (of both RNA and cDNA) were used to determine the linearity ranges of the methods. Glyceraldehyde 3-phosphate dehydrogenase (GAPD) primers were used as a “housekeeping” gene for comparison of RNA levels.

Northern analysis of RNA from cell cultures and from tissue samples was performed using 10 µg of total RNA electrophoresed on 1 % agarose gels containing 0.4 M formaldehyde, followed by transfer to positively charged nylon membranes (Boehringer Mannheim) [189]. The TIMP-3 cDNA probe was amplified by PCR from human cDNA using a 36-mer sense and a 36-mer antisense primer specific for the human TIMP-3 sequence. The PCR product was cleaned (Gene Clean) and then subjected to random-primed radiolabeling using ³²P-dATP (kit from Boehringer Mannheim) to a specific activity of > 10⁷ CPM/µg [189]. The blot membranes were prehybridized in a buffer containing 50 % formamide, 5x Denhardt's solution, 5x SSC, 25 mM potassium phosphate and 50 µg/ml salmon sperm DNA for 2 hr. at 42°C. TIMP-3 probe was then added to the prehybridization mix and hybridized at 42°C overnight. Membranes were washed twice in

1x SSC, 0.1% SDS at room temperature for 15 minutes, and then twice in 0.2x SSC and 0.05% SDS for 10 minutes at room temperature. Membranes were then sealed in plastic and autoradiographed for 24-48 hr. Some membranes were then stripped and reprobed with similar specific TIMP-1, TIMP-2 or GAPD cDNA probes.

Protein Isolation and Purification - For TIMP-3 analysis, RPE cells that had been treated as detailed above, were washed twice in PBS with 5 mM EDTA, 5 mM EGTA and were then incubated at 37°C until they were released from the flask [197, 276]. Residual cells were removed by rinsing again in PBS. Flasks were then rinsed with deionized water, and the extracellular matrix was extracted with SDS sample buffer. The samples were then boiled for 10 minutes under reducing conditions (ie, in the presence of 10 mM DTT), and subjected to SDS-PAGE and Western analysis using a polyclonal rabbit antibody made to TIMP-3 (Triple Point Biologics). TIMP-3 protein standards were purified from human placenta or were purified recombinant mouse TIMP-3 obtained from UTI (Calgary, Canada). TIMP-1 and 2 were analyzed directly in culture medium conditioned by the cultured cells.

Immunoblots of Western transfers - Media or ECM extracts (see above) were electrophoresed on SDS-PAGE (12% or 15% acrylamide gels) and proteins were electro-transferred to nitrocellulose (Schleicher and Schuell). Filters were blocked in 2 % non-fat skimmed milk and probed with primary antibodies to TIMP-1, 2 or 3 overnight at 4°C with shaking. The blots were then washed four times for 15 mins at room temperature with 1x PBS and incubated for 2 hrs at room temperature with goat anti-rabbit secondary antibody conjugated to alkaline phosphatase (Sigma). The immunoblot was washed four

times in PBS for 15 minutes at room temperature and developed by addition of 5-bromo-4-chloro-3-indolylphosphate/nitroblue tetrazolium substrate for alkaline phosphatase as recommended by the manufacturers (Sigma).

Reverse Zymogram of TIMPs - Reverse zymography was used to analyze TIMP-1, 2 and 3 activities from culture medium or extracted from the cellular ECM. SDS-PAGE gels were prepared with the incorporation of purified matrix metalloproteinases and substrate (gelatin) into the acrylamide matrix of the gel [197, 198]. SDS (0.1%), 12% polyacrylamide gels were prepared, except that the metalloproteinases were also added into the acrylamide mix and the water volume was reduced accordingly. Gelatin substrate was added to a final concentration of 0.1 mg/ml prior to polymerization of the gels. Samples were electrophoresed at 4°C, gels were washed in 2.5% Triton X-100, 50 mM Tris-HCl (pH 7.5), and 5 mM CaCl₂ once for 15 min and then again overnight at room temperature with shaking. Gels were then rinsed three times in deionized H₂O, incubated in 50 mM Tris-HCl (pH 7.5) and 5 mM CaCl₂, 10 μM ZnCl₂ for 24 hrs at 37°C with shaking and then stained with Coomassie blue.

Immunohistochemistry - All immunohistochemistry experiments were performed by Elaine Johnson, Ph. D., and the Morrison lab. Donor human eyes were dissected, immersed in O.C.T., frozen in 2-methyl butane chilled in liquid nitrogen and stored at -70°C. The eyes that were analyzed were from nine different individuals, 4 female and 5 male, ranging in age from 55 to 89 years of age; death to enucleation ranged from 2 to 14 hours, and storage at 4°C at the eye bank before fixation ranged from 4 to 10 hours. Longitudinal- and cross-sections (3 μm) were cut on a cryostat and placed on γ-

aminopropyl triethoxysilane-coated glass slides. Primary antibodies were produced in rabbits against unique 15 or 16 amino acid peptides synthesized from unique sequences for human TIMP-1, 2 or 3 (Triple Point Biologics, Forest Grove, OR). Antibodies were peptide-affinity purified and have been described previously. Sections were washed in phosphate-buffered saline (PBS), fixed in 4°C methanol for 5 min, washed in PBS, blocked with 20% normal goat serum in PBS with 1% bovine serum albumin (BSA) for 30 min, and incubated overnight with primary antibody (2 mg/ml stock solutions were diluted 1/1000 for TIMP-1, 1/2500 for TIMP-2, or 1/1000 or 1/2500 for TIMP-3 in PBS/BSA) at 4°C. Sections were then washed in PBS containing 0.01% Triton X-100, incubated for 30 min with biotinylated secondary antibody (diluted 1/200; Vector Labs, Burlingame, CA), washed in PBS/BSA for 45 min, and developed in 0.05% 3,3-diaminobenzidine with 0.03% H₂O₂ in Tris-buffered saline (pH 7.2) for 3 min. Sections were then rinsed in deionized water and nuclei were counterstained with 50% Gill #3 hematoxylin (Sigma, St. Louis, MO). Sections were dehydrated in ascending concentrations of ethanol, cleared in xylene and coverslipped for photography. Controls included substitution of pre-immune rabbit antibody for primary antibody and pre-absorption with the peptide antigens (0.5 mg/ml).

Confocal Microscopy - Cultured cells (either RPE or skin fibroblasts) were seeded on 2- or 4-well chamber slides (Nunc) and grown in DMEM and 10 % fetal calf serum to confluency. Cells were rinsed in PBS and then incubated in 4% paraformaldehyde (in 100 mM sodium phosphate buffer, pH 7.4) for 1 hour at room temperature to fix the cells. The cells were washed three times for five minutes in 100

mM Tris buffer, pH 7.6. They were then digested with 0.3 Units/ml hyaluronidase (Sigma) at 37°C for 15 minutes. Cells were washed three times in 100 mM Tris buffer, pH 7.6 and 0.1% Triton X-100 and then blocked in 2% goat serum for 15 minutes. The primary antibody (of either TIMP-3 or Fibronectin) was then added at a dilution of 1/100 (from a 2 mg/ml stock concentration) and the cells were incubated overnight at 4°C with shaking. The cells were then washed in 100 mM Tris buffer, pH 7.6 three times, followed by incubation with 2% goat serum for 10 minutes. The secondary antibody, with a conjugated FITC label, was then added at a dilution of 1/25 (goat anti-rabbit Ig G) and incubated for 30 minutes. The cells were washed again three times in 100 mM Tris buffer, pH 7.6. Propidium iodide, a nuclear staining agent, was then added to the RPE cells at a concentration of 2 mg/ml and incubated for 10 minutes. Finally, the cells were washed several times in 100 mM Tris buffer, pH 7.6, equilibrated in Slow Fade buffer (from Molecular Probes, Inc.), and covered with a coverslip in Slow fade buffer with glycerol.

Tissue or cell specimens were viewed using a Leica 900 confocal laser scanning microscope (New Jersey) and analysis system consisting of an inverted Leitz fluovert-FU microscope, a krypton-argon laser, a simultaneous dual channel (PMT) detector and a 24 bit imaging system. Appropriate filter sets were used to distinguish between fluorescein (FITC) and propidium iodide (PI) light emissions. The two data sets were merged using Leica Scanware software function. A 63x - 1.3 NA oil objective lens was used and pinhole settings were maintained at optimal levels for minimal slice thickness resolution. For the optical z-series, slices were taken every 1-2 microns over 6 microns of thickness and transferred to an IBM computer and recorded on Kodak ektachrome 100 film before

being stored on a WORM drive. Settings were optimized using the positive tissue and maintained during scanning of the control tissue to utilize relative brightness as an indication of increased production of the target protein. The excitation wavelength of the FITC-labeled antibody was 496nm and the emission wavelength of the FITC label was 518 nm. One- and two-color confocal images were obtained using the image manipulation program, Adobe Photoshop (Adobe Systems, Inc., 1993). Samples viewed on the confocal microscope were also viewed at lower magnification and acquired as fluorescent photomicrographs using a Zeiss Axioskop microscope.

C. Results

RT-PCR and Northern Analysis - TIMP-1, -2 and -3 mRNA levels were analyzed in human retinal and choroidal tissue and in cultured RPE and choroidal microvascular pericytes and endothelial cells by RT-PCR (Fig. 74). The three transcripts were found to be expressed differentially at varying levels in different tissues. TIMP-1 transcript levels were highest, using equal amounts of total RNA, in retinal extracts and pericyte cell cultures, and at slightly lower levels in the cultured RPE cells. Very little TIMP-1 was detected in the capillary endothelial cells (data not shown). Although present at lower levels than the faster-migrating artifact band, the authentic TIMP-1 PCR product is present in the choroid. TIMP-2 transcripts were present predominantly in RPE cells, with much lower levels being expressed in the neural retina, pericytes, and capillary endothelial cells. TIMP-3 transcripts were present at moderately high levels in the RPE,

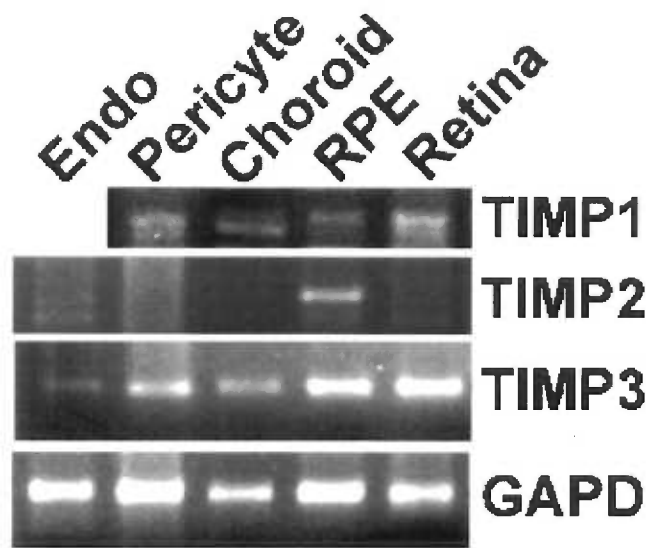


Figure 74: RT-PCR of TIMP mRNA expression by retinal cells and tissues. RT-PCR products were amplified from untreated tissue or cells, with the primer pairs for TIMP-1, -2, -3, or GAPD. Sources of RNA are indicated above the lanes. Choroid and retina were extracted from human tissue after dissection by John Bradley as described in the "Methods" section.

neural retina and pericytes. Moderate levels were also detected in the choroid and TIMP3 mRNA levels were the lowest in the capillary endothelial cells. Total RNA from the choroid, RPE cells, and the capillary endothelial cells was also analyzed by northern analysis using cDNA probes to TIMP-1, TIMP-2 and TIMP-3 (Fig. 75). TIMP-1 mRNA was detected as a 0.9 kb band in moderate levels in the choroid and RPE, and at very low levels in the capillary endothelial cells. Two TIMP-2 transcripts were present at 3.5 and 1 kb, at moderate levels in the RPE and at faintly-detectable levels in the choroid. Several TIMP-3 transcripts were detected at moderate levels in the RPE and choroid, however, the predominant band was at the size of 4.5 kb. The other faintly detectable bands were seen in the RPE at 2 and 2.3 kb, and may represent alternatively-spliced TIMP-3 transcripts (data not shown). GAPD transcripts were also analyzed in both the RT-PCR and the northern blots as a housekeeping gene in order to verify that the cDNA or RNA was loaded in equal amounts.

Restriction digestion analysis of the TIMP-3 PCR products, extracted from the gels, showed that Pst I and Bbv I were able to cleave the cDNA, as expected according to the published TIMP-3 DNA sequence [144]. Pst I cleaved the TIMP-3 PCR band of 236 bp once into fragments of 158 bp and 78 bp (Fig. 76a). BbvI cleaved the TIMP-3 PCR product into two fragments of 169 bp and 67 bp (Fig. 76b). These results verified that the PCR product using the TIMP-3 primers was the authentic TIMP-3 product.

Human RPE cultured cells were stimulated with various typical modulators and mRNA levels of the TIMPs were evaluated by RT-PCR (Fig. 77). As expected, TIMP-1

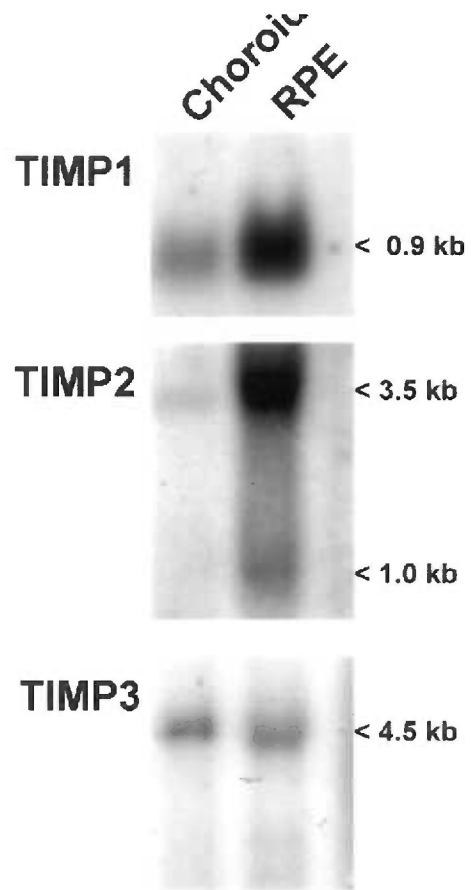


Figure 75: Northern analysis of TIMP mRNA expression by retinal cells and tissues. RPE cell cultures or dissected choroid tissue extracts are indicated. Total RNA (10 ug) was loaded per lane.

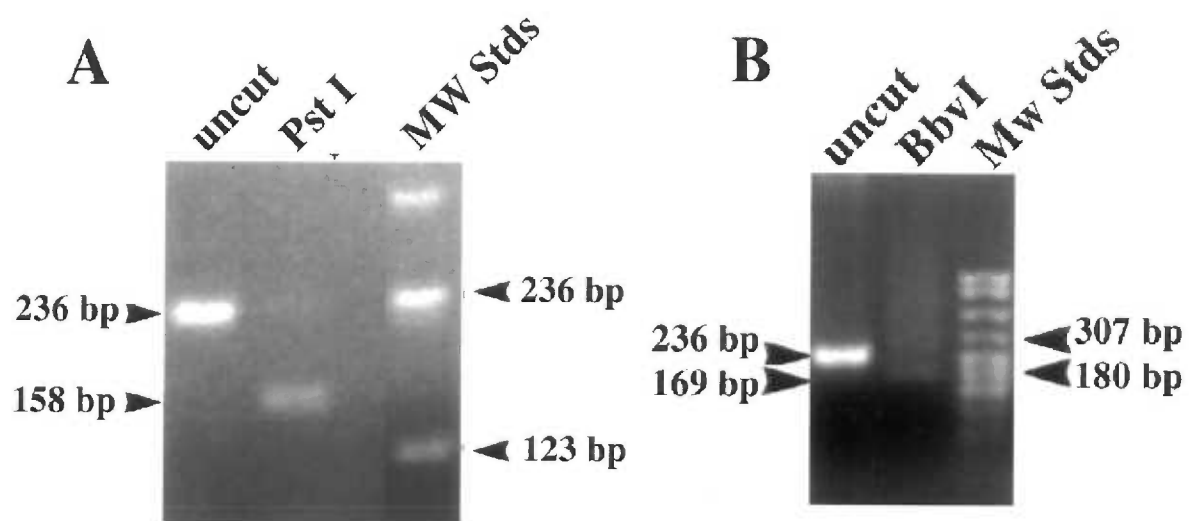


Figure 76: Restriction digestion of the TIMP-3 PCR product from human cells. The 236 bp PCR product was digested with Pst I (A) or Bbv I (B) and loaded adjacent to the uncut PCR product in both panels.

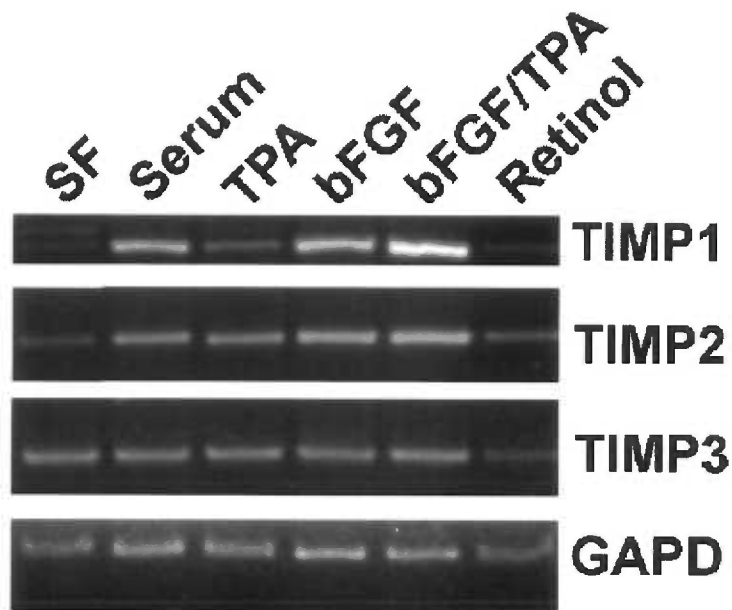


Figure 77: RT-PCR of mRNA from cultured RPE cells that were treated with various modulators (as indicated) and TIMP-1, -2, -3, or GAPD primer pairs were selected for the PCR. Cells were serum-free prior to treatments, which were conducted for 5 hours; serum was added at 10%, bFGF was added at 10 ng/ml, TPA was added at 1 uM and retinol was added at 200 ng/ml.

transcripts are low in untreated cells and increased by the treatment with phorbol esters(TPA), basic fibroblast growth factor (bFGF) and by serum. TIMP-2 transcript levels are higher initially and less affected overall by any of these treatments. TIMP-3 transcript levels appear to be slightly stimulated by the various treatments, but levels in untreated cells are high. Repeated experiments confirmed that TIMP-3 transcripts were only mildly affected by various typical modulators, suggesting a more constitutive pattern of expression.

Immunohistochemistry and Confocal Microscopy - TIMP-1, -2 and -3 proteins were localized in human retina/choroid cryo-sections by immunohistochemistry using antibodies made to unique peptide sequences from these proteins. Immunohistochemistry experiments (in Fig. 78) were performed by Dr. Elaine Johnson and the Morrison lab. TIMP-1 immunostaining is pronounced in the optic nerve (data not shown), but is not detectable in Bruch's membrane or consistently present in other regions of the retina or choroid (Fig. 78a). Some TIMP-2 immunostaining is found in Bruch's membrane (Fig. 78b). This immunostaining is uneven, somewhat punctate and appears to be more in the center of Bruch's membrane rather than in the presumed basement membranes near the cellular surfaces. TIMP-2 immunostaining is associated with a few cells of the choroid and of the sensory retina, perhaps including some of the photoreceptor nuclei.

In contrast, TIMP-3 stains Bruch's membrane very intensely (Fig. 78c). This staining appears to be more intense at the margin of Bruch's membrane, presumably where the RPE and endothelial cell basement membranes are than in the central layers of Bruch's membrane, as seen at higher magnification (Fig. 78d). The presence or absence of TIMP

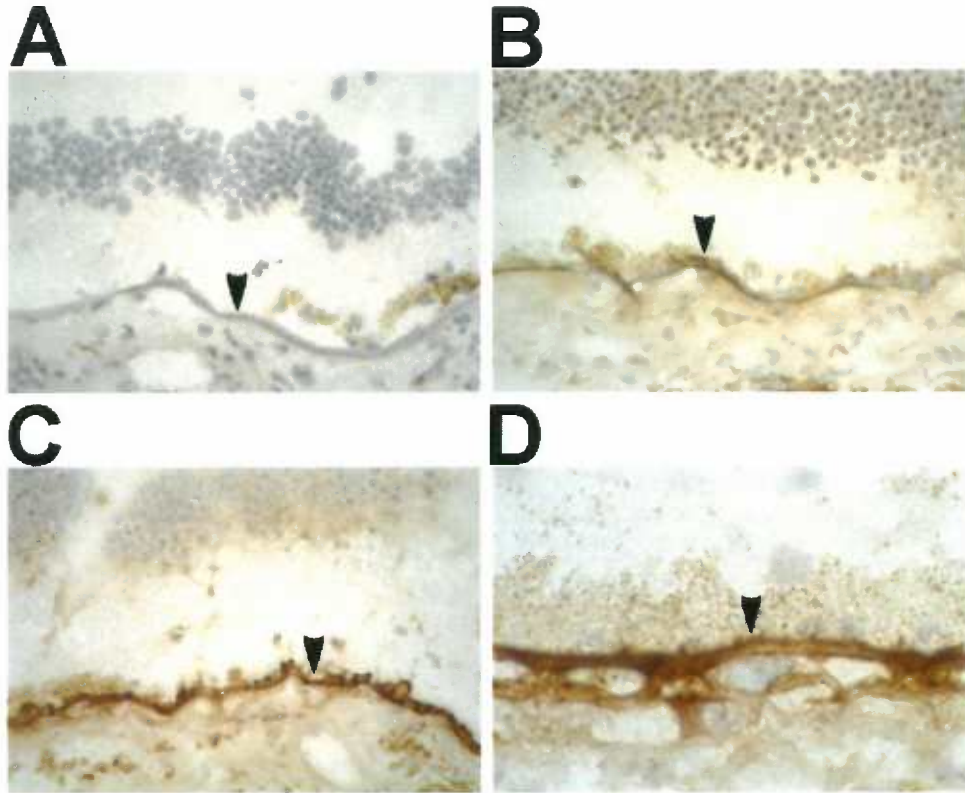


Figure 78: Immunohistochemical localization of TIMPs in the human retina and choroid. All data was collected by Dr. Elaine Johnson. Cryosections of human posterior segments of the eye were immunostained with antibodies to TIMP-1 (A), TIMP-2 (B), or TIMP-3 (C and D). A portion of the sensory retina, including the outer nuclear layer, is seen in the upper portions of A, B and C with Bruch's membrane (indicated by the arrowheads) and the choroid in the lower portion. (D) TIMP-3 staining at higher magnification. The RPE can be seen above Bruch's membrane although it has pulled away in several places during processing, and the choroidal microcapillaries can be seen below Bruch's membrane. TIMP immunostaining is brown.

immunostaining in the interphotoreceptor matrix, was difficult to determine in the cryosections, which are not optimum for this task. A portion of the larger choroidal blood vessels, perhaps one in ten, also stain intensely for TIMP-3, but the other vessels of the choroid do not (data not shown). However, this TIMP-3 choroidal immunostaining could not necessarily be associated with any specific type of blood vessel. Some immunostaining for TIMP-3 in the sensory retina can not be ruled out, but no appreciable retinal blood vessel immunostaining for TIMP-3 was apparent. The controls for these antibodies show minimal non-specific tissue staining (data not shown). The three TIMPs clearly show very different retinal/choroidal distribution patterns.

Confocal microscopy was performed on cultured RPE cells using the same TIMP-1, -2, and -3 primary antibodies. The secondary antibodies were labeled with FITC and proteins were detectable by confocal microscopy. As a control the secondary antibody was reacted with the cells in the absence of the primary antibody and there was no detectable signal. Target proteins were detected by FITC-staining (green stain), whereas nuclei were detected by propidium iodide staining (red stain). As expected from the immunohistochemistry data, the TIMP expression levels varied among the TIMP members. TIMP-1 protein expression was not detectable in the RPE cells (Fig. 79a). TIMP-2 protein was strongly detected in the cytoplasm of the RPE cells, but not detectable in the nucleus (Fig. 79b). TIMP-3 was also detected in the cytoplasm of the cells, and in contrast to TIMP-2, appeared to be localized to the nucleus as well (Fig. 79c). These results appear to support the immunohistochemistry data in terms of detection of the TIMPs in the RPE. In order to determine whether the ECM of the RPE

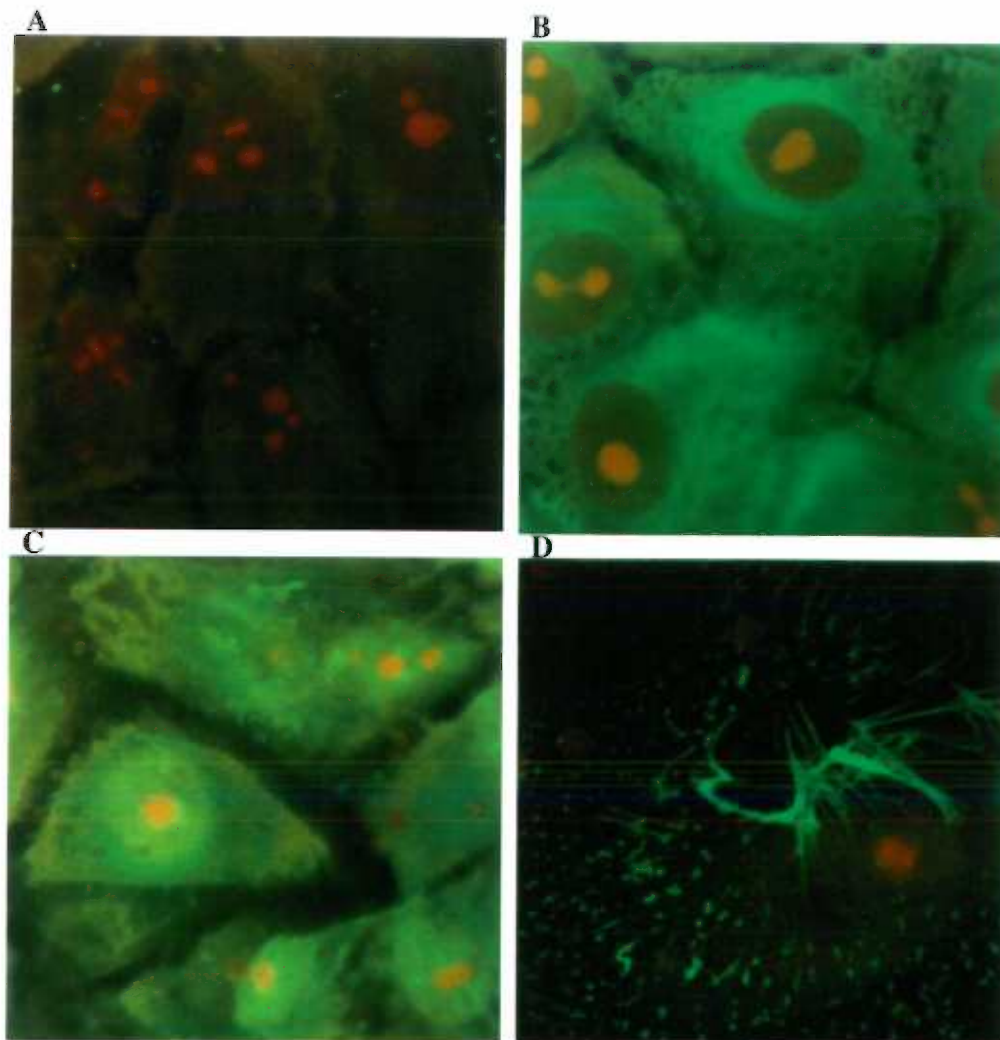


Figure 79: Confocal microscopy of unstimulated, cultured RPE cells with antibodies for TIMP-1 (A), TIMP-2 (B), TIMP-3 (C), and fibronectin (D). The target protein are detected by FITC staining (green stain) and the nuclei are stained with propidium iodide (red stain).

cells could be visualized using this technique, fibronectin was stained for in the RPE cells grown under the same conditions as for TIMP detection. As expected, some fibronectin staining was detected on the basal side of the cells in a combination of a filamentous and punctate form (Fig. 79d) and is thought to be predominantly extracellular. An additional experiment was performed to detect TIMP-3 in RPE cells that were seeded very densely and subsequently grown beyond confluence prior to treatment with the TIMP-3 antibody. These cells show a very distinct pattern of TIMP-3 expression and localization where most of the protein is localized to the ECM on the basal side of the cells (Fig. 80). The panels in Fig. 80 represent laser scans at approximately 1 μ m apart as the laser moves directionally from the apical side to the basal side of the cells.

Immunoblot and Reverse Zymogram Analysis of TIMP Proteins - TIMP-3

protein was purified from the extracellular matrix or from the medium of RPE cultured cells and then analyzed by SDS-PAGE and immunoblotting of Western transfers utilizing the same TIMP-3 antibody as was used for the immunohistochemistry and confocal microscopy. TIMP-3 protein was present in the extracellular matrix extract of RPE cells but could not be detected in the culture medium from the same cells by Western immunoblot analysis, even with 20x concentration (Fig. 81a). Localization of TIMP-3 to the extracellular matrix has been shown previously [143, Staskus, 1991 #224]. TIMP-1 and TIMP-2 proteins could be detected in concentrated culture medium, as expected, but not in the concentrated extracellular matrix extracts (data not shown). Reverse zymography was also performed with the extracellular matrix extracts or with media samples from the RPE cells in order to determine whether TIMP proteins found in either

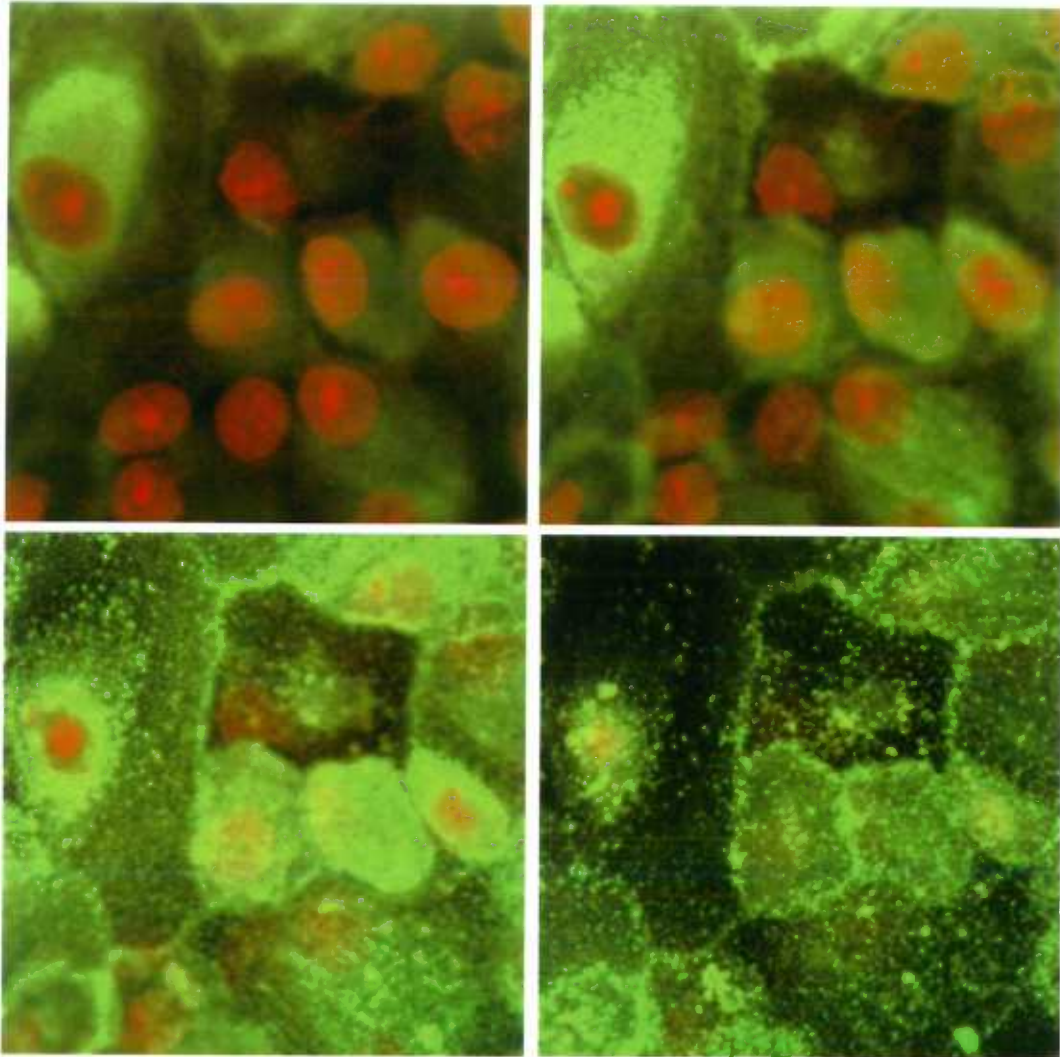


Figure 80: Confocal microscopy of TIMP-3 protein in unstimulated, densely-confluent human RPE cells. TIMP-3 was detected by the FITC staining (green stain) in the cytoplasm and in the ECM of the cells. Nuclei were detected by propidium iodide staining (red stain). The four panels (beginning at the upper left corner and moving clockwise) represent optical slices taken 1μm apart through the whole cell, from the apical to the basal side of the RPE cells.

sample had inhibitory activity. TIMP-1 and -2 from the concentrated culture medium and TIMP-3 from the extracellular matrix all had inhibitory activity (data not shown). TIMP-1, -2 and -3 proteins migrated at apparent molecular weights of approximately 29, 20 and 24 kDa for the nonglycosylated TIMP-3, respectively.

Treatment of RPE cells for 36 hours with TPA, bFGF, or serum, had minimal effects on media TIMP-2 or ECM TIMP-3 protein levels (Fig. 81b). Media TIMP-1 protein levels were increased with TPA or TPA/bFGF treatment, but were not appreciably affected by bFGF treatment alone (Fig. 81b).

Analysis of mutant TIMP-3 - It has recently been shown that at least four distinct point mutations in TIMP-3 are in affected members of separate families with Sorsby's Fundus Dystrophy [279, 284]. These mutations suggest that heterozygous mutations in TIMP-3 are causally responsible for the SFD phenotype. All of the mutations found to date are mutations to a cysteine and are near the carboxy terminus of the protein in the "regulatory domain" of the TIMPs. One of the mutations in TIMP-3, a Gly167 to a Cys, creates a new Bbv I restriction site in the DNA.

Skin fibroblast cell lines were obtained from affected individuals with the Gly167Cys mutation. Total RNA was prepared from the cells and RT-PCR analysis and restriction digestion was performed on the PCR band excised from the gel in order to verify the creation of the new Bbv I restriction site (Fig. 82). The normal PCR product is only cut once to give two fragments of 169 bp and 67 bp. The mutant TIMP-3 PCR product has two BbvI sites producing three fragments of 135bp, 67 bp and 34 bp. Similar analysis was done on skin fibroblasts from unaffected patients as a control (data not

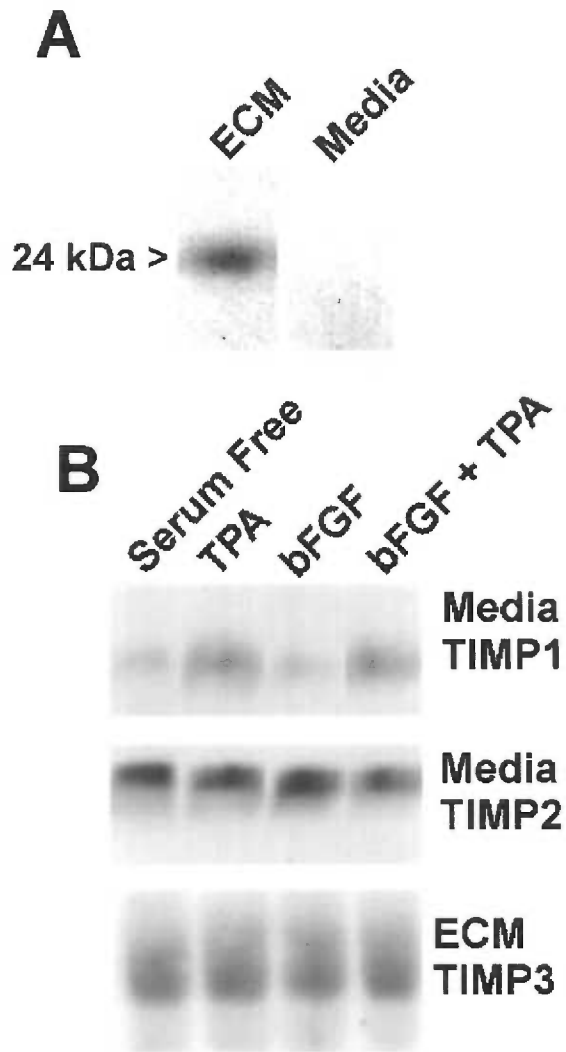


Figure 81: Western immunoblot analysis of TIMP expression by cultured human RPE cells. (A) RPE cell ECM extract and culture medium probed with a TIMP-3 antibody. (B) RPE cell media or ECM extract, as indicated, probed with antibodies to TIMP-1, -2, or -3. Cells were serum-free for 24 hrs prior to a 36-hr treatment, as indicated, with the same concentrations of modulators as described in Figure 77.

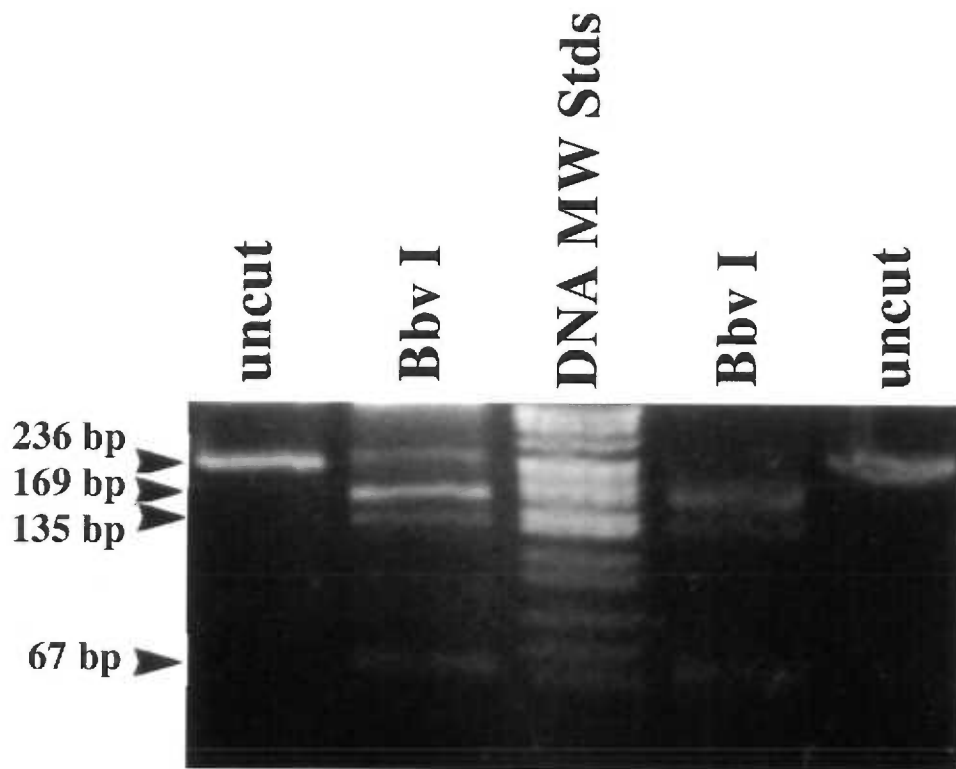


Figure 82: Restriction digestions of TIMP-3 PCR product from the RNA of mutant cells. RT-PCR was performed on RNA extracted from skin cells originally obtained from patients with Sorsby's fundus dystrophy. PCR products were analyzed for a mutation creating a novel Bbv I restriction site. The normal 236 bp TIMP-3 PCR product is cut once to give two fragments of 169bp and 67bp. The mutant TIMP-3 is cut twice yielding three fragments of 135bp, 67bp, and 34bp. Samples were from two different mutant cell lines with the same TIMP-3 mutation.

shown). After the mutation was verified by restriction digestion, the cells were analyzed for TIMP-3 protein expression levels in both the extracellular matrix of the cells and in the medium from the cells by immunoblotting (Fig. 83) and by reverse zymography (data not shown). TIMP-3 protein was localized to the extracellular matrix of the cells from SFD-affected patients (with the Gly167Cys), as it was in the normal cells. Moreover the levels of protein expression did not appear to be different between the mutant and the normal cells, although detection of minor differences may be beyond the limitations of this method. From the reverse zymography it was apparent that the TIMP-3 expressed from the mutant cells had inhibitory activity similar to that of the normal cells. Additionally, the medium from the mutant cell lines was analyzed for possible TIMP-3 activity, but all expressed TIMP-3 protein was found localized to the ECM of the cells. Attempts were made to identify whether mutant TIMP-3 protein existed as some fraction of the total detected TIMP-3 protein in the ECM from the mutant cell lines. However, levels of expressed protein were too low to purify in significant quantities to detect any differences.

In order to determine whether differences in TIMP-3 protein expression levels or localization could be detected in the mutant cell lines versus the normal cell lines, confocal microscopy or immunostaining was performed on slides of monolayers of cultured cells. TIMP-3 staining appeared to be approximately of equal intensity when comparing the normal cell line with the mutant cell line at two different magnifications (Fig. 84, 85). The staining appeared to be both cytoplasmic and also possibly localized to the extracellular matrix of the cells with a somewhat punctate pattern of staining not apparent at lower magnifications. TIMP-3 protein was also localized to the nucleus, although it is possible

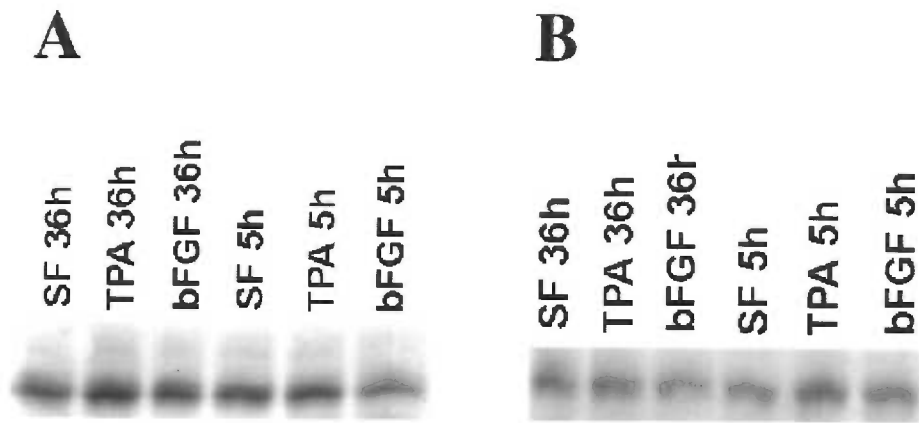


Figure 83: Western immunoblots using an antibody to TIMP-3 on the ECM from normal fibroblasts (A) and mutant fibroblasts (B). Cells were treated with various modulators, as described in Figure 77, but for the times indicated above the lanes.

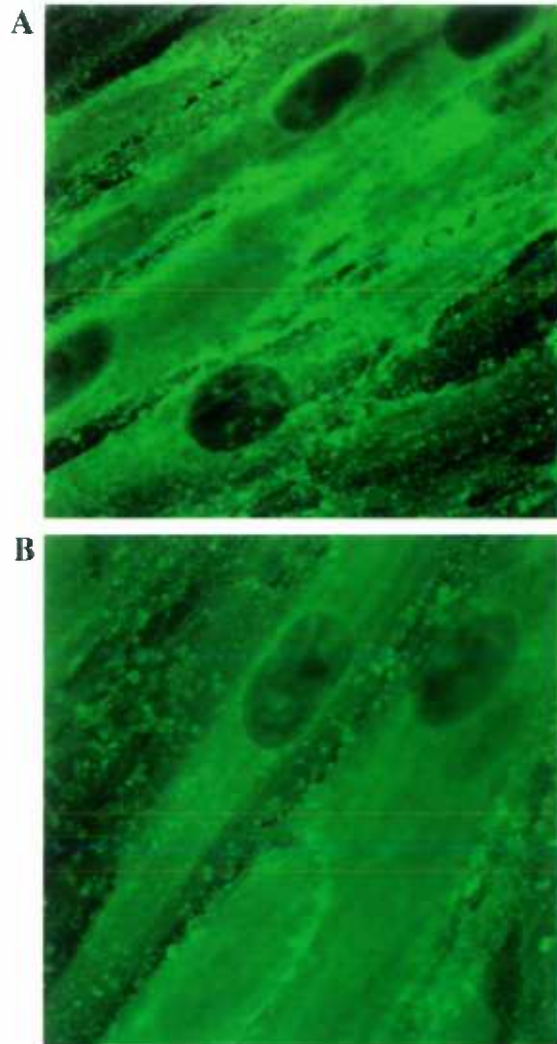


Figure 84: Confocal microscopy of TIMP-3 protein in normal (A) and mutant (B) skin fibroblasts. TIMP-3 protein was detected by FITC staining (green stain) in the cytoplasm and in the ECM of the cells. TIMP-3 staining appears to be slightly more intense in the normal cells (A) as compared with the mutant cells, however, no other significant differences are apparent. Punctate TIMP-3 staining appears to be predominantly ECM-localized.

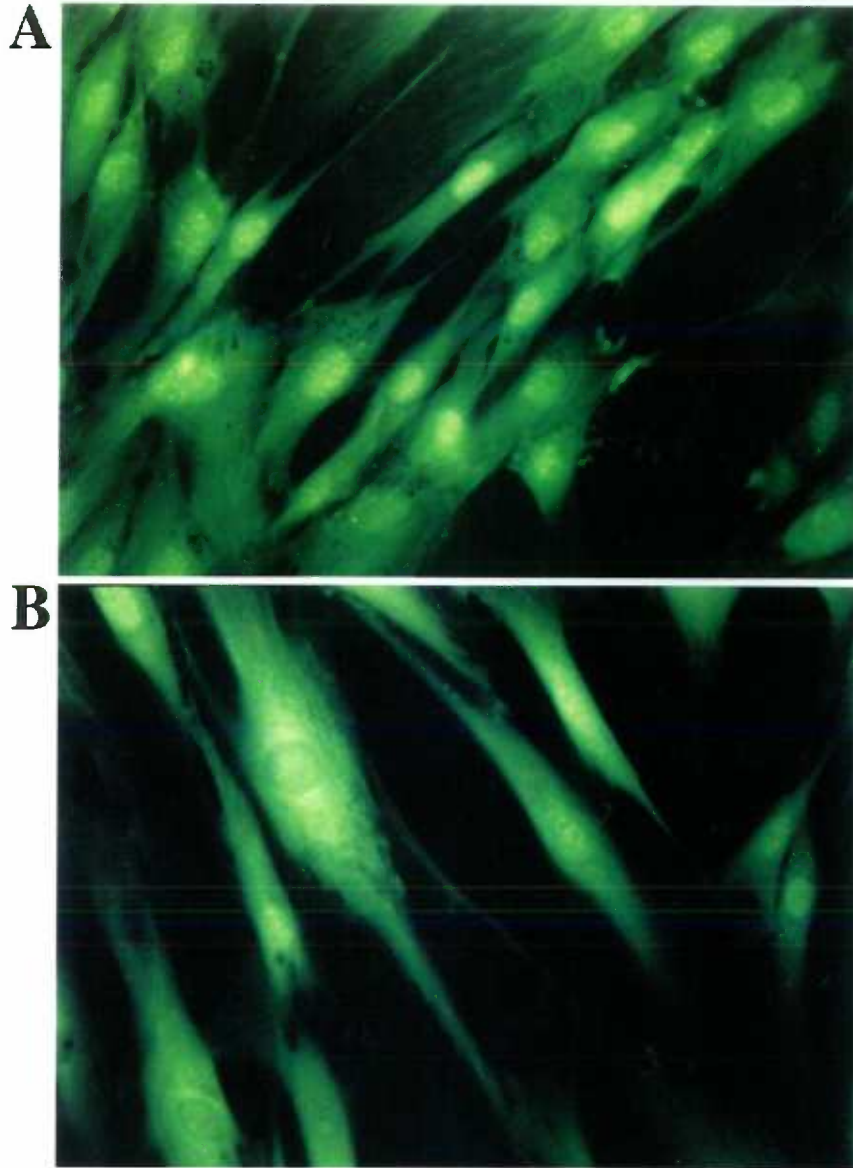


Figure 85: Photomicrograph of TIMP-3 staining in monolayers of normal (A) and mutant (B) skin fibroblasts. Samples that had been analyzed by confocal microscopy were visualized at lower magnification using a Zeiss Axioskop microscope and photographed, as shown here. TIMP-3 protein was detected by FITC staining (green stain) in the cytoplasm, the nucleus, and at lower levels in the ECM of the cells. The intensity of TIMP-3 staining was similar in the normal (A) and (B) mutant skin fibroblasts.

that some of the staining was nonspecific.

In addition to the monolayers of stained cells, cells were seeded at much higher densities and grown as a multilayer for two days prior to treating and staining as previously described. The resulting patterns of TIMP-3 expression were similar to the monolayers except more fibrous, as is seen with some extracellular matrix proteins such as fibronectin. This data did not reveal any significant differences between the normal (Fig. 86a) and the mutant cells (Fig. 86b) when grown in a multilayered form. The same cells were analyzed at higher magnifications by confocal microscopy, but no apparent differences in the TIMP-3 staining were apparent (Fig. 87a, b). In order to visualize fibronectin, an extracellular matrix protein using confocal microscopy, an antibody to fibronectin was utilized. As expected, the fibronectin staining was very fibrous and apparently not associated with the cytoplasm of the cells grown in multilayers (Fig. 87c).

In spite of the strong expression levels and staining of TIMP-3 with both the RPE and fibroblast cells, there were difficulties in determining which stained proteins were considered to be cytoplasmic versus those that were distinctly extracellular. For the purpose of determining whether there was TIMP-3 staining in the ECM, and to distinguish it from the cytoplasmic staining, the cells were seeded in monolayers, grown, and treated as before except the fixative step was omitted. This was intended to avoid permeabilizing the cells such that the TIMP-3 antibody had no access to intracellularly expressed proteins. Although most of the cells were lost during the procedure, of the cells that remained TIMP-3 protein was faintly detectable in a punctate pattern associated with the outside of the cells (Figs. 88).

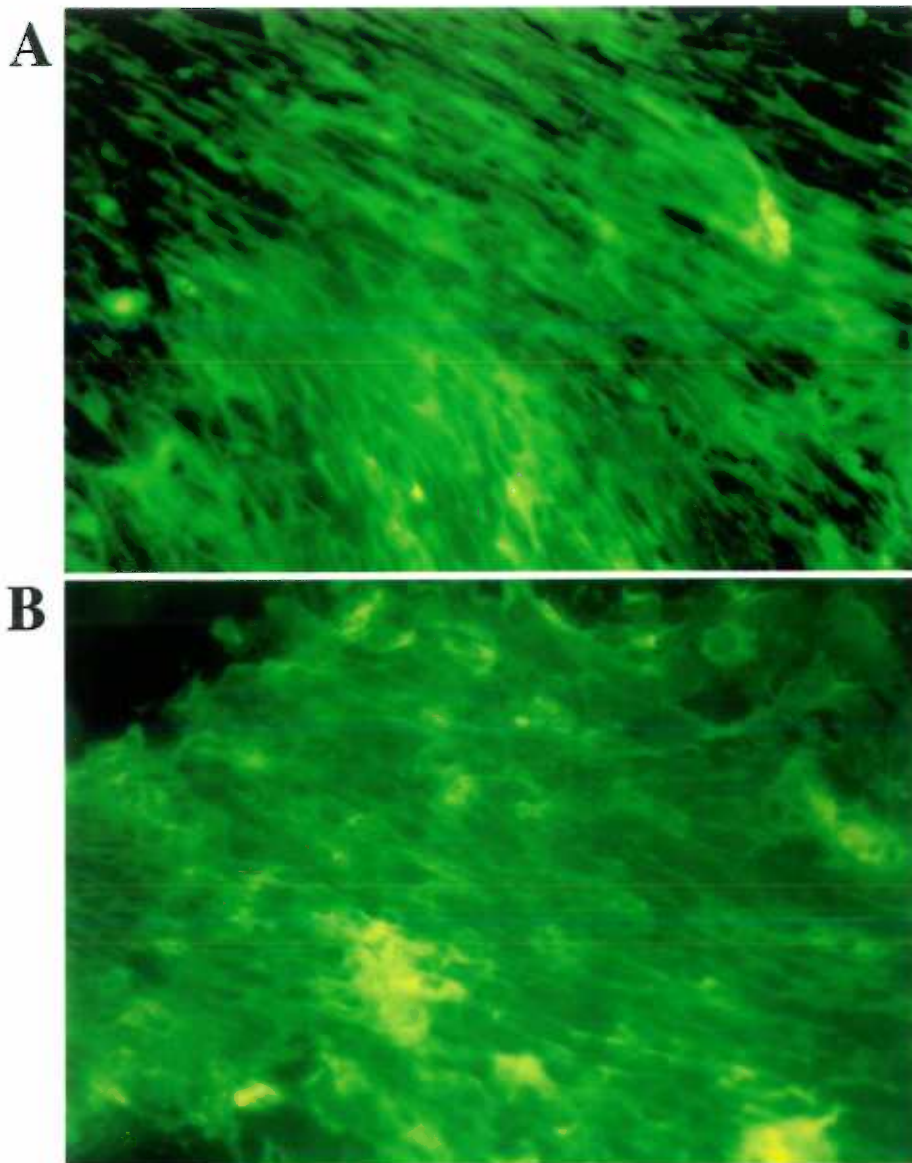


Figure 86: Photomicrograph of TIMP-3 staining in normal (A) and mutant (B) skin fibroblasts grown in multilayers. TIMP-3 protein is detected by FITC staining (green stain) in cells that had been densely seeded and cultured as described in the "Materials" section. Normal (A) and mutant (B) cells show similar TIMP-3 staining patterns as the protein is clearly localized to the ECM of the cells in long fibrils, as well as localized to the cytoplasm of the cells. The morphology of the cells was affected by processing.

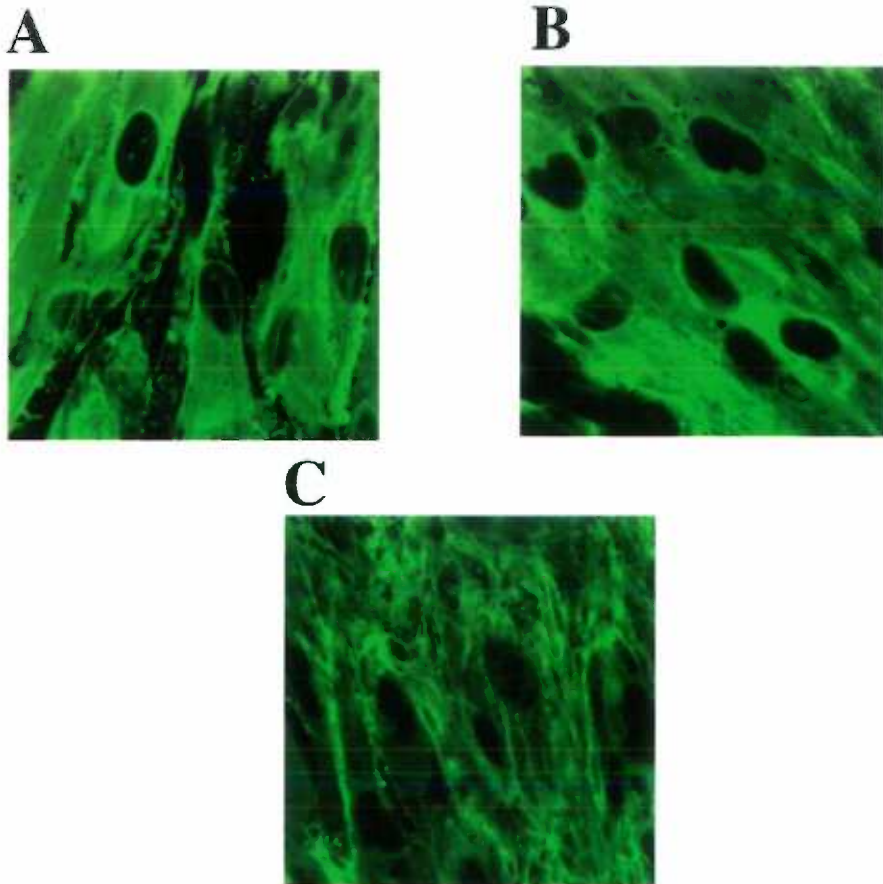


Figure 87: Confocal microscopy of TIMP-3 staining in normal (A) and mutant (B and C) cells grown in multilayers. The samples shown in Figure 86 are the same shown here, but at higher magnification. No significant differences are apparent in the TIMP-3 staining from the normal (A) versus the mutant (B) cells. Fibronectin (C) was stained as a representative ECM protein. TIMP-3 or fibronectin is detected by FITC staining (green stain).

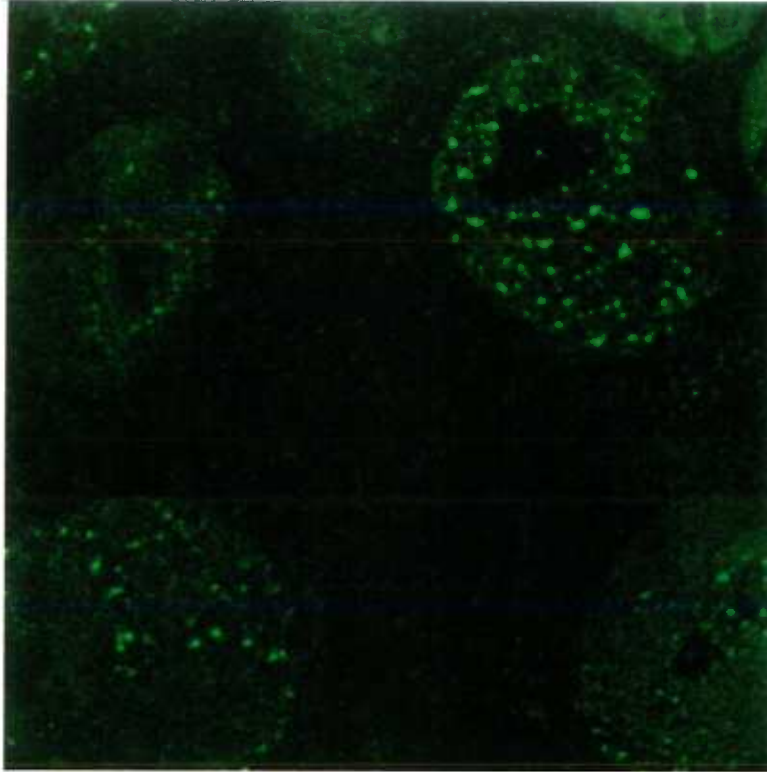


Figure 88: Confocal microscopy of TIMP-3 protein staining in monolayers of unfixed fibroblasts. Fibroblasts were grown under identical conditions as described for the cells in Figure 84, however they were not fixed prior to incubation with the primary antibody. The purpose was to avoid permeabilization of the cells. Cells were lysed at the coverslip-stage of the procedure with glycerol and resultant "ghosts" were analyzed. Extracellular TIMP-3 protein was detected at low levels by FITC staining (green stain) in a distinct punctate pattern associated with the cells.

D. Discussion

TIMP-3 is found predominantly in Bruch's membrane and is expressed by cultured RPE and to a lesser extent by choroidal microvascular pericytes and endothelial cells. The data shown above, using immunohistochemistry, RT-PCR and Northern analysis of mRNA, and immunoblots of Westerns, are in general agreement. More TIMP-3 mRNA is seen in isolated retina than expected, based on the other observations mentioned earlier. A similar observation was recently reported [285]. TIMP-1 is expressed at low levels by the RPE cells, when unstimulated, and is found only occasionally within most of the retina or choroid. TIMP-2 is found at moderate levels in Bruch's membrane and is expressed primarily by RPE. Both TIMP-1 and TIMP-2 exhibit dense immunostaining in the optic nerve (data not shown), suggesting important roles in these tissues and some TIMP-2 immunostaining may be present in the photoreceptor nuclei. Thus, the distribution and expression of the three TIMPs is discrete within the retina and choroid. Confocal microscopy and immunostaining experiments have shown that TIMP-3 can be localized to the ECM of densely confluent RPE cells, although its distribution pattern in less confluent RPE cells is not so distinct, as it is found in the cytoplasm, the nucleus and the ECM. The patterns of expression of TIMP-1, -2, and -3 are distinct from each other in RPE cells, as well as in skin fibroblasts and this is in agreement with earlier findings. In fibroblast cells, shown to express mutant TIMP-3, from SFD patients, the TIMP-3 protein staining does not appear to be significantly different than from that in normal cells.

SFD and AMD share several characteristics. Increases in lipid and ECM deposits

and thickening of Bruch's membrane are early events in both SFD and AMD [269, 271, 272]. Bruch's membrane is composed of basement membrane and stromal ECM elements. As in other tissues, these ECM associated with these tissues likely undergo a continuous homeostatic cycle of degradation and biosynthetic replacement. The activated MMPs initiate ECM turnover and TIMP-3, perhaps with help from the other TIMPs, restrains and provides one level of regulation of this degradation. The relatively high TIMP-3 levels in Bruch's membrane, particularly in what appears to be the two basement membranes suggests that ECM turnover in this region may be normally very limited or occurs via a carefully-regulated mechanism. The recent identification of TIMP-3 mutations in patients with Sorsby's fundus dystrophy and our observations on TIMP distribution within the retina and choroid coincide and provide the first step in explaining the pathophysiology of this disease.

Beyond the observation that TIMP-3 activity must be crucial for the normal maintenance and/or function of Bruch's membrane, the molecular explanation for how the identified TIMP-3 mutations cause the SFD pathophysiology is unclear. SFD normally requires approximately 40 years to develop. Since the SFD defect exhibits autosomal dominant inheritance, both normal and mutant TIMP-3 should be expressed in patients with SFD. Bruch's membrane thickening in SFD suggests that there may be too little MMP activity, rather than a defective metalloproteinase inhibitor, although how these tissues may respond to various external stimuli is unknown.

Since the reported mutations in TIMP-3 result in an extra cyteine, the simplest conclusion is that the mutant TIMP-3 folds incorrectly and may form incorrect disulfide

bonds. This could alter the secondary and/or tertiary structure of this protein and affect some aspect of its inhibitory activity, or possibly some other function of the protein. Another possibility is that TIMP-3 protein is synthesized, but due to the misfolding is degraded instead of being secreted, or is secreted but is less stable extracellularly and thus its extracellular half-life is reduced. Alternatively, the extra unpaired cysteine residue in the mutant could be affecting the protein's folding state or 3-D structure. Dominant negative effects, which can not be ruled out, usually occur because the mutant protein interferes, often by complexing with, the activity of the normal form. Little evidence for TIMP homo-dimerization has been presented, however this possibility can not be excluded.

If the mutant TIMP-3 is secreted and does not interfere directly with the activity of the normal TIMP-3, these mutations could produce SFD in several ways. Mutant TIMP-3 could be less active as an inhibitor, thereby allowing excessive MMP activity. This could disrupt the structural organization of Bruch's membrane. By inference from other cells and their ECMs, Bruch's membrane is probably highly organized at the supramolecular level and its functions and those of the RPE and choroidal microcapillary endothelium are most likely dependent on such organization. It seems probable that a complex regulatory mechanism controls ECM turnover and biosynthetic replacement and thus maintains the structure of Bruch's membrane. A TIMP-3 defect could disrupt this homeostatic balance and thus allow a slow thickening of Bruch's membrane, even in the presence of excess ECM turnover.

Mutant TIMP-3 could be active as an inhibitor of the metalloproteinases, but the mutation in the carboxyl-domain could cause a "mislocalization" of TIMP-3 within the

retina. Normally, secreted TIMP-3 localizes to the ECM, putatively binding to some specific, but unidentified ECM molecule (s), and it must be extracted from the ECM in cell culture. In contrast, TIMP-1 and TIMP-2 are found nearly exclusively in cell culture medium, suggesting that they do not bind specifically and with high affinity to ECM components after they are secreted. TIMP-3 association with the ECM may be a unique function of the protein in providing a precise mechanism of localized inhibition. TIMP-3 mislocalization, due to a mutation affecting ECM binding, could result in SFD symptoms due to TIMP-3 diffusing away from its normal sites and thus allowing unchecked MMP activity in normally protected areas, for example, perhaps in the basement membranes of Bruch's membrane. Reciprocally, it could allow TIMP-3 to move freely to areas it would normally be excluded from and therefore inhibit MMP activity where it may not otherwise. However, the data shown here does not support this hypothesis. Another possibility is that the C-terminal "regulatory" domain of TIMP-3, which happens to be the site of the mutations, may serve some specific function in regulating MMP activity beyond that of directly inhibiting the activated enzymes. Somewhat similar roles have been proposed for that domain of the other TIMPs, which bind to the "regulatory" domains of the gelatinases and putatively modulate their behavior [3, 80, 136]. Clearly, more detailed studies that address the distinct role of TIMP-3 in Bruch's membrane are necessary.

A secondary point regarding these observations is that the TIMPs have been shown to be strongly anti-angiogenic [286-288]. A later stage of SFD and AMD is choroidal neovascularization. Mutant TIMP-3 in the choroidal vessel walls may allow neovascularization once the initial insults have developed, since this area is not protected

as effectively as in normal eyes. Since the retinal vasculature exhibits minimal TIMP levels, for any of the TIMPs studied, these vessels may be “unprotected”. Lack of TIMPs around the blood vessels may lead to retinal neovascularization. Thus retinal neovascularization, common in proliferative retinopathy, is not increased in SFD, where TIMP-3 mutations exist. Reciprocally, choroidal neovascularization is not common as a consequence of diabetes. It seems likely that TIMPs are stored in regions where MMP activity seldom occurs or must be stringently regulated. In other “unprotected” regions, TIMPs, presumably TIMP-1 primarily, are probably expressed only on demand, when they are specifically needed to modulate MMP activity. While TIMP-1 is modulated by a wide array of cellular regulators, TIMP-2 is much less susceptible to most regulatory modulators [4, 140, 253, 273]. TIMP-3 has not been studied extensively, but is regulated in some tissues by some modulators [143, 289].

When RPE cells were subjected to some potential modulators, TIMP-1 was found to be stimulated by serum, TPA, and bFGF. TIMP-1 mRNA and protein levels show similar responses. Essentially no significant changes were seen in TIMP-3 protein and mRNA levels in response to the few modulators tested.

The details of the molecular events, leading from a mutation in exon 5 of TIMP-3 to the pathophysiology of SFD, still remain to be determined. Presumably, the mutant TIMP-3 is unable to correctly regulate the proteolytic activity of the MMPs in and around Bruch’s membrane and eventually, neovascular growth from the capillary layer of the choroid that occurs later in SFD. The tissue distribution of the TIMPs, particularly TIMP-3, does provide possible hints. Although TIMP-1 and -2 can be expressed by the retina

and choroid, their distributions and expression appear not to be sufficient to compensate for the TIMP-3 mutation and thus to avert progression of this disease. Although SFD is of earlier onset (at approximately 40 years) than AMD (approximately at 60-80 years), this is still a relatively late age of onset. Thus, the consequences of the TIMP-3 mutation are still relatively subtle. The studies presented herein show that no major changes occur and thus are compatible with the clinical progression of the disease.

V. Conclusions

The extracellular matrix acts as a structural and informational support for the tissues and cells with which it is associated by stabilizing the physical structure and modulating the behavior of those tissues, as well as acting as a barrier to maintain the integrity of tissues. The ECM is made up of various macromolecules such as collagen, elastin, proteoglycans, laminin and fibronectin. The ECM is vital in influencing cellular processes such as embryo development, morphogenesis, proliferation, differentiation, migration, and adhesion. The family of matrix metalloproteinases, whose natural substrates are various ECM components, and their tissue inhibitors of metalloproteinases, are key proteins involved in the maintenance and turnover of the extracellular matrix. Therefore, the MMPs are important in processes including wound healing, uterine involution, bone morphogenesis, and angiogenesis, where the ECM is actively undergoing the degradation and resynthesis events that are necessary, as has been described earlier in this text and is reviewed [2-4].

The activity of the MMPs is tightly controlled for the maintenance of tissue integrity and homeostatic balance in tissues. The MMPs are not only transcriptionally regulated, but are also regulated at the level of activation of their secreted, proenzyme forms, and their activity is inhibited by the inhibitory activity of their natural inhibitors, the TIMPs. Although the transcriptional regulation, the enzyme activation processes, and the inhibition by the TIMPs may be of equal importance, the characterization of inhibition on the enzymatic activity of the MMPs was one of the primary aims of this manuscript. The

balance of the enzymatic activity of the MMPs and the inhibitory activity of the TIMPs is important for the continuation of normal physiological processes, as uncontrolled MMP activity has been found to be associated with various pathological processes such as rheumatoid arthritis, osteoarthritis, periodontitis, and cancer cell invasion and metastasis, perhaps as a consequence of a disruption of the balance of MMP/TIMP activity [5, 6, 8-10, 12, 15, 17].

The studies described in this manuscript have been focused primarily on (a) the characterization of inhibition of two members of the MMP family, gelatinase A and B, (b) their involvement in glaucoma using a model system, (c) the characterization of the expression of TIMP-3 in various eye tissues, and (d) its involvement in Sorsby's fundus dystrophy. First, it was necessary to obtain expressed and purified TIMPs and gelatinases for subsequent studies. This was achieved with mixed results, as the TIMPs were expressed at varying levels and purified from prokaryotic and eukaryotic systems. The final purified products, the MBP-TIMP-2 fusion protein and TIMP-3 expressed from mammalian cells, were shown to have inhibitory activity in enzyme assays and on reverse gelatin zymograms and were utilized for later data collection. The gelatinases were purified from cellular sources until they became commercially available and their enzyme activities on either a protein-substrate or peptide-substrate assay were analyzed and compared. The gelatinases preferred the protein substrate over the peptide substrate as presumably there are more interactions that stabilize the protein substrate's interactions with the enzyme.

Gelatinase A and B activities were then analyzed and shown to be inhibited by a

variety of inhibitors, including minocycline, tryptophan-hydroxamate, a collagenase inhibitor, and propeptide inhibitors. Additionally, the purified TIMPs were analyzed for their inhibitory activities in the enzyme assays, as described above. The most effective inhibitors of gelatinase A and B activity appeared to be the propeptide inhibitors. Interestingly, one amino acid difference in the propeptide sequence, RCGXPD, where the 'X' was either Asn, as is found only in the gelatinase A propeptide sequence, or Val, was enough to affect the inhibition efficacy and specificity on gelatinase A or B. Additionally, minocycline appeared to be a good inhibitor of both gelatinases, and the other inhibitors tested also had some inhibitory activity on either or both of the gelatinases.

The same inhibitors were analyzed in a glaucoma model system in order to determine the involvement of the gelatinases in primary open-angle glaucoma. The model system was developed in the Acott lab and the following hypothesis was tested: an imbalance in the net MMP/TIMP activity in the ECM of the trabecular meshwork or in the aqueous outflow pathway may cause a change in the intraocular pressure as observed in primary open-angle glaucoma. The inhibitors were shown to decrease the aqueous outflow in the model system, as predicted by the hypothesis, thus causing a glaucomatous state. These results, and others described above, have served to implicate the MMPs and the TIMPs as key proteins involved in the turnover of the trabecular meshwork ECM and this suggests their possible roles in the development of primary open-angle glaucoma.

The final section of the manuscript describes the characterization of TIMP-3 expression in various eye tissues. Specific TIMP-3 mutations have been found in patients with Sorsby's fundus dystrophy [278, 279], which shares the same clinical features of age-

related macular degeneration, but has an earlier age of onset. Manifestations of both SFD and AMD include the thickening of Bruch's membrane, the formation of ECM- and lipid-containing deposits, and subsequent neovascularization and atrophy of the choroid, RPE, and retina. The individual TIMP-3 mutations result in an additional cysteine, and are located in the C-terminal domain of the protein which is thought to be the "regulatory" domain of the TIMPs. The cause and effect of the TIMP-3 mutations and SFD remain to be determined, however, it has been of interest to identify the role of the TIMPs in the affected eye tissues. These studies demonstrated that the distribution and expression of TIMP-1, -2, and -3 mRNA and protein in the choroid, RPE, the retina, and Bruch's membrane. The basement membranes of Bruch's membrane were stained most strongly with the TIMP-3 protein, suggesting a direct role for TIMP-3 in maintaining the integrity of the ECM structure in that area and providing localized inhibition or "protection" against the MMP activity that occurs during the remodeling of ECM structures. An additional argument in favor of a specifically localized pattern of inhibition is the fact that of the four TIMPs, TIMP-3 is unique in its ability to bind to the ECM of cultured cells. Given the highly-folded structure of the TIMPs and their characteristic six disulfide bonds, one may speculate that an additional cysteine may cause the TIMP-3 protein to fold incorrectly, thereby affecting its ability to interact effectively with an active MMP molecule. Alternatively, the localization of the misfolded protein may be affected, although additional studies described above, with cells expressing a mutant TIMP-3 have shown that the TIMP-3 protein is still localized to the ECM of the cells. Another possibility is that the mutant protein is not secreted from the cells causing lower levels of

normal TIMP-3 protein to be secreted. However, experiments analyzing differences in mutant versus normal cells and their expression of mutant and normal TIMP-3 protein have been unable to identify any significant differences between the normal and mutant cells. The direct consequences of the TIMP-3 mutations may not be immediately realized, since the onset of the disease is relatively late. This is in general agreement with the results described above and with the clinical progression of the disease. The details of the stages, leading from a mutant TIMP-3 to the pathophysiology of SFD, remain unclear, however, these studies show that the TIMPs are specifically localized to various tissues in the eye and the distribution of the other TIMPs may not be sufficient to compensate for the mutant TIMP-3 in this disease.

VI. REFERENCES

1. Werb, Z., Alexander, C.M., Adler, R.R. (1992) Expression and function of matrix metalloproteinases in development. *Matrix Supplement 1*, 337-43.
2. Birkedal-Hansen, H., Moore, W.G., Bodden, M.K., Windsor, L.J., Birkedal-Hansen, B., DeCarlo, A., Engler, J.A. (1993) Matrix metalloproteinases: a review. [Review]. *Critical Reviews in Oral Biology & Medicine 4*, 197-250.
3. Murphy, G., Docherty, A.J. (1992) The matrix metalloproteinases and their inhibitors. [Review]. *American Journal of Respiratory Cell & Molecular Biology 7*, 120-5.
4. Matrisian, L.M. (1992) The matrix-degrading metalloproteinases. [Review]. *Bioessays 14*, 455-463.
5. Okada, Y., Nakanishi, I (1989) Activation of matrix metalloproteinase 3 (stromelysin) and matrix metalloproteinase 2 ('gelatinase') by human neutrophil elastase and cathepsin G. *FEBS Letters 249*, 353-356.
6. Gravallesse, E.M., Darling, J M, Ladd, A L, Katz, J N, Glimcher, L H (1991) In situ hybridisation studies of stromelysin and collagenase messenger RNA expression in rheumatoid synovium. *Arthritis Rheum. 34*, 1076-1084.
7. Okada, Y., Takeuchi, N, Tomita, I, Nakanishi, I, Nagase, H (1989) Immunolocalization of matrix metalloproteinase 3 (stromelysin) in rheumatoid synovioblasts (B cells): correlation with rheumatoid arthritis. *Ann. Rheum. Dis. 48*, 645-653.
8. McCachren, S.S. (1991) Expression metalloproteinase and metalloproteinase inhibitor in human arthritic synovium. *Arthritis and Rheumatism 34*, 1085-1093.
9. Lohmander, L.S., Hoerrner, L A, Lark M W (1993) Metalloproteinases, tissue inhibitor, and proteoglycan fragments in knee synovial fluid in human osteoarthritis. *Arthritis and Rheumatism 36*, 181-189.
10. Villela, B., Cogen, R B, Bartolucci, A A, Birkedal-Hansen, H (1987) Collagenolytic activity in crevicular fluid from patients with chronic adult periodontitis, localized juvenile periodontitis and gingivitis, and from healthy control subjects. *Journal of Periodontal Research 22*, 381-389.
11. Overall, C.M., Sodek, J (1987) Initial characterization of a neutral

- metalloproteinase, active on native 3/4-collagen fragments, synthesized by ROS 17/2.8 osteoblastic cells, periodontal fibroblasts, and identified in gingival crevicular fluid. *Journal of Dental Research* **66**, 1271-1282.
12. Overall, C.M., Sodek, J, McCulloch, A G, Birek, P (1991) Evidence for polymorphonuclear leukocyte collagenase and 92-kilodalton gelatinase in gingival crevicular fluid. *Infect. Immunol.* **59**, 4687-4692.
 13. Birkedal-Hansen, H. (1993) Role of matrix metalloproteinases in human periodontal diseases. [Review]. *Journal of Periodontology* **64**, 474-84.
 14. Makela, M., Salo, T, Uitto, U J, Larjava, H (1994) Matrix metalloproteinase (MMP-2 and MMP-9) of the oral cavity: cellular origin and relationship to periodontal status. *Journal of Dental Research* **73**, 1397-1406.
 15. Liotta, L.A., Steeg, P.S., Stetler-Stevenson, W.G. (1991) Cancer metastasis and angiogenesis: an imbalance of positive and negative regulation. [Review]. *Cell* **64**, 327-36.
 16. Stetler-Stevenson, W.G., Liotta, L.A., Kleiner, D.E.J. (1993) Extracellular matrix 6: role of matrix metalloproteinases in tumor invasion and metastasis. [Review]. *FASEB Journal* **7**, 1434-41.
 17. Mueller, B.M. (1996) Different roles for plasminogen activators and metalloproteinase in melanoma metastasis. *Current Topics in Microbiology and Immunology* **213** (pt.1), 65-80.
 18. Furcht, L.T., Skubitz, A P, Fields, G (1994) Tumoral cell invasion, MMPs, and the dogma. *Laboratory Investigation* **70**, 781-783.
 19. Goldberg, G.I., Wilhelm, S M, Kronberger, A, Bauer, E A, Grant, G E, Eisen, A Z (1986) Human fibroblast collagenase. Complete primary structure and homology to an oncogene transformation-induced rat protein. *Journal of Biological Chemistry* **261**, 6600-6605.
 20. Hasty, K., Pourmotabbed, T F, Goldberg, G I, Thompson, J P, Spinella, D G, Stevens, R M, Mainardi, C L (1990) Human neutrophil collagenase: a distinct gene product with homology to other matrix metalloproteinases. *Journal of Biological Chemistry* **265**, 11421-11424.
 21. Freije, J.M., Diez-Itza, I, Balbin, M, Sanchez, L M, Blasco, R, Tolivia, J, Lopez-Otin, C (1994) Molecular cloning and expression of collagenase 3, a novel human MMP produced by breast carcinomas. *Journal of Biological Chemistry* **269**,

16766-16773.

22. Gunja-Smith, Z.H., Nagase, H, Woessner, J F (1989) Purification of the neutral proteoglycan-degrading metalloproteinase from human articular cartilage tissue and its identification as stromelysin matrix metalloproteinase-3. *Biochemical Journal* **258**, 115-119.
23. Basset, P., Bellocq, J P, Wolf, C, Stoll, I, Hutin, P, Limacher, J M, Podhajcer, O L, Chenard, M P, Rio, M C, Chambon, P (1990) A novel metalloproteinase gene specifically expressed in stromal cells of breast carcinomas. *Nature* **348**, 699-704.
24. Seltzer, J.L., Eisen, A Z, Bauer, E A, Morris, N P, Glanville, R W, Burgeson, R E (1989) Cleavage of type VII collagen by interstitial collagenase and type IV collagenase (gelatinase) derived from human skin. *Journal of Biological Chemistry* **264**, 3822-3826.
25. Collier, I.E., Wilhelm, S M, Eisen, A, Z, Marmer, B L, Grant, G A, Seltzer, J L, Kronberger, A., He, C, Bauer, E A, Goldberg, G I (1988) H-ras oncogene-transformed human bronchial epithelial cells (TBE-1) secrete a single metalloprotease capable of degrading basement membrane collagen. *Journal of Biological Chemistry* **263**, 6579-6587.
26. Wilhelm, S.M., Collier, I E, Marmer, B L, Eisen, A Z, Grant, G A, Goldberg, G I (1989) SV40-transformed human lung fibroblasts secrete a 92 kDa type IV collagenase which is identical to that secreted by normal human macrophages. *Journal of Biological Chemistry* **264**, 17213-17221.
27. Shapiro, S.D., Griffin, G L, Gilbert, D J, Jenkins, N A, Copeland, N G, Welgus, H G, Senior, R M, Ley, T J (1992) Molecular cloning, chromosomal localization, and bacterial expression of a murine macrophage metalloelastase. *Journal of Biological Chemistry* **267**, 4664-4671.
28. Quantin, B., Murphy, G, Breathnach, R (1989) Pump-1 cDNA codes for a protein with characteristics similar to those of classical collagenase family members. *Biochemistry* **28**, 5327-5334.
29. Sato, H., Takino, T, Okada, Y, Cao, J, Shinagawa, A, Yamamoto, E, Seiki, M (1994) A matrix metalloproteinase expressed on the surface of invasive tumour cells. *Nature* **370**, 61-65.
30. Takino, T., Sato, H, Shinagawa, A, Seiki, M (1995) Identification of the second membrane type matrix metalloproteinase (MT-MMP-2) gene from a human placenta cDNA library. *Journal of Biological Chemistry* **270**, 23013-23020.

31. Hasty, K.A., Jeffrey, J J, Hibbs, M S, Welgus, H G (1987) The collagen substrate specificity of human neutrophil collagenase. *Journal of Biological Chemistry* **262**, 10048-10052.
32. Netzel-Arnett, S., Fields, G.B., Birkedal-Hansen, H., Van Wart, H.E., Fields, G.B. (1991) Sequence specificities of human fibroblast and neutrophil collagenases [published erratum appears in J Biol Chem 1991 Nov 5;266(31):21326]. *Journal of Biological Chemistry* **266**, 6747-55.
33. Knauper, V., Lopez-Otin, C, Smith, B, Knight, G, Murphy, G (1996) Biochemical characterization of human collagenase-3. *Journal of Biological Chemistry* **271**, 1544-1550.
34. Whitham, S.E., Murphy, G, Angel, P, Rahmsdorf, H-J, Smith, B J, Lyons, A, Harris, T H, Reynolds, J J, Herrlich, P, Docherty, A J (1986) Comparison of human stromelysin and collagenase by cloning and sequence analysis. *Biochemical Journal* **240**, 913-916.
35. Nicholson, R.G., Murphy, G, Breathnach, R (1989) Human and rat malignant-tumor-associated mRNAs encode stromelysin-like metalloproteinases. *Biochemistry* **28**, 5195-5203.
36. Murphy, C.G., Yun, A.J., Newsome, D.A., Alvarado, J.A. (1987) Localization of extracellular proteins of the human trabecular meshwork by indirect immunofluorescence. *American Journal of Ophthalmology* **104**, 33-43.
37. Ogata, Y., Enghild, J.J., Nagase, H. (1992) Matrix metalloproteinase 3 (stromelysin) activates the precursor for the human matrix metalloproteinase 9. *Journal of Biological Chemistry* **267**, 3581-3584.
38. Shapiro, S.D., Fliszar, C.J., Broekelmann, T.J., Mecham, R.P., Senior, R.M., Welgus, H.G. (1995) - Activation of the 92-kDa gelatinase by stromelysin and. *Journal of Biological Chemistry* **270**, 6351-6.
39. Wilhelm, S.M., Collier, I E, Kronberger, A, Eisen, A Z, Marmer, B L, Grant, G A, Bauer, E A, Goldberg, G I (1987) Human skin fibroblast stromelysin: structure, glycosylation, substrate specificity and differential expression in normal and tumorigenic cells. *Proceedings of the National Academy of Science* **84**, 6725-6729.
40. Breathnach, R., Matrisian, L M, Gesnel, M C, Staub, A, Leroy, P (1987) Sequences coding for part of oncogene-induced transin are highly conserved in a related rat gene. *Nucleic Acids Research* **15**, 1139-1151.

41. Wolf, C., Royer, N, Lutz, Y, Adida, C, Lorient, M, Bellocq, J, Chambon, P, Basset, P (1993) Stromelysin-3 belongs to a subgroup of proteinases expressed in breast carcinoma fibroblastic cells and is possibly implicated in tumor progression. *Proceedings of the National Academy of Science* **90**, 1843-1847.
42. Murphy, G., Segain, J.P., O. Shea, M., Cockett, M., Ioannou, C., Lefebvre, O., Chambon, P., Basset, P. (1993) The 28-kDa N-terminal domain of mouse stromelysin-3 has the general properties of a weak metalloproteinase. *Journal of Biological Chemistry* **268**, 15435-41.
43. Noel, A., Santavicca, M, Stoll, I, L'Hoir, C, Staub, A, Murphy, G, Rio, M, Basset, P (1995) Identification of structural determinants controlling human and mouse stromelysin-3 proteolytic activities. *Journal of Biological Chemistry* **270**, 22866-22872.
44. Anglard, P., Melot, T, Guerin, E, Thomas, G, Basset, P (1995) Structure and promoter characterization of the human stromelysin-3 gene. *Journal of Biological Chemistry* **270**, 20337-20344.
45. Arthur, M.J., Friedman, S L, Roll, R F, Bissell, D M (1989) Lipocytes from normal rat liver release a neutral metalloproteinase that degrades basement membrane (type IV) collagen. *Journal of Clinical Investigation* **84**, 1076-1085.
46. Garbisa, S., Scagliotti, G., Masiero, L., Di Francesco, C., Caenazzo, C., Onisto, M., Micela, M., Stetler-Stevenson, W.G., Liotta, L.A. (1992) Correlation of serum metalloproteinase levels with lung cancer metastasis and response to therapy. *Cancer Research* **52**, 4548-9.
47. Polette, M., Clavel, C, Cockett, M, Girod De Bentzmann, S, Murphy, G, Birembaut, P (1993) Detection and localization of mRNAs encoding matrix metalloproteinases and their tissue inhibitor in human breast pathology. *Invasion Metastasis* **13**, 31-37.
48. Lyons, J.G., Birkedal-Hansen, B, Moore, W G, O'Grady, R L, Birkedal-Hansen, H (1991) Characteristics of a 95-kDa matrix metalloproteinase produced by mammary carcinoma cells. *Biochemistry* **30**, 1449-1456.
49. Nakajima, M., Welch, D, Wynn, D, Tsuruo, T, Nicolson, G (1993) Serum and plasma Mr 92,000 progelatinase levels correlate with spontaneous metastasis of rat 13762NF mammary adenocarcinoma. *Cancer Research* **53**, 5802-5807.
50. Okada, Y., Gonoji, Y, Naka, K, Tomita, K, Nakanishi, I, Iwata, K, Yamashita, K, Hayakawa, T (1992) Matrix metalloproteinase 9 (92-kDa gelatinase/type IV

- collagenase) from HT1080 human fibrosarcoma cells: purification and activation of the precursor and enzymic properties. *Journal of Biological Chemistry* 267, 21712-21719.
51. Seltzer, J.L., Akers, K T, Weingarten, H, Grant, G A, McCourt, D W, Eisen, A Z (1990) Cleavage specificity of human skin type IV collagenase (gelatinase). *Journal of Biological Chemistry* 265, 20409-20413.
 52. Busiek, D.F., Ross, F.P., McDonnell, S., Murphy, G., Matrisian, L.M., Welgus, H.G. (1992) The matrix metalloprotease matrilysin (PUMP) is expressed in developing human mononuclear phagocytes. *Journal of Biological Chemistry* 267, 9087-92.
 53. Soler, D., Nomizu, T, Brown, W, Shibata, Y, Auld, D S (1995) Matrilysin: expression, purification, and characterization. *Journal of Protein Chemistry* 14, 511-520.
 54. Miyazaki, K., Hattori, Y, Umenishi, F, Yasumitsu, H, Umeda, M (1990) Purification and characterization of extracellular matrix-degrading metalloproteinase, matrin (Pump-1) secreted from human rectal carcinoma cell line. *Cancer Research* 50, 7758-7764.
 55. Imai, K., Yokohama, Y, Nakanishi, I, Ohuchi, E, Fuji, Y, Nakai, N, Okada, Y (1995) MMP-7 (matrilysin) from human rectal carcinoma cells: activation of the precursor, interaction with other MMPs and enzymic properties. *Journal of Biological Chemistry* 270, 6691-6697.
 56. Shapiro, S.D., Kobayashi, D K, Ley, T J (1993) Cloning and characterization of a unique elastolytic metalloproteinase produced by human alveolar macrophages. *Journal of Biological Chemistry* 268, 23824-23829.
 57. Okada, A., Bellocq, J P, Royer, N, Chenard, M P, Rio, M C, Chambon, P, Basset, P (1995) Membrane type-matrix metalloproteinase (MT-MMP) gene is expressed in stromal cells of human colon, breast, and head and neck carcinomas. *Proceedings of the National Academy of Science* 92, 2730-2734.
 58. Imai, K., Ohuchi, E, Aoki, T, Nomura, H, Fuji, Y, Sato, H, Seiki, M, Okada, Y (1996) Membrane type-matrix metalloproteinase-1 is a gelatinolytic enzyme and is secreted in a complex with TIMP-2. *Cancer Research* 56, 2707-2710.
 59. Strongin, A.Y., Collier, I., Bannikov, G., Marmer, B.L., Grant, G.A., Goldberg, G.I. (1995) Mechanism of cell surface activation of 72-kDa type IV collagenase. Isolation of the activated form of the membrane metalloprotease. *Journal of*

Biological Chemistry 270, 5331-8.

60. Pei, D., Weiss, J J (1996) Transmembrane-deletion mutants of the MT-MMP-1 process progelatinase A and express intrinsic matrix-degrading activity. *Journal of Biological Chemistry* 271, 9135-9140.
61. Will, H., Atkinson, S J, Butler, G, Smith, B, Murphy, G (1996) The soluble catalytic domain of MT1MMP cleaves the propeptide of progelatinase A and initiates autoproteolytic activation: regulation by TIMP-2 and TIMP-3. *Journal of Biological Chemistry* 271, 17119-17123.
62. Nagase, H., Ogata, Y., Suzuki, K., Enghild, J.J., Salvesen, G. (1991) Substrate specificities and activation mechanisms of matrix metalloproteinases. [Review]. *Biochemical Society Transactions* 19, 715-8.
63. Vallee, B.L., Auld, D S (1990) Zinc coordination, function, and structure of zinc enzymes and other proteins. *Biochemistry* 29, 5647-5659.
64. Salowe, S.P., Marcy, A.I., Cuca, G.C., Smith, C.K., Kopka, I.E., Hagmann, W.K., Hermes, J.D. (1992) Characterization of zinc-binding sites in human stromelysin-1: stoichiometry of the catalytic domain and identification of a cysteine ligand in the proenzyme. *Biochemistry* 31, 4535-40.
65. Koklitis, P.A., Murphy, G., Sutton, C., Angal, S. (1991) Purification of recombinant human prostromelysin. Studies on heat activation to give high-Mr and low-Mr active forms, and a comparison of recombinant with natural stromelysin activities. *Biochemical Journal* 276, 217-21.
66. Browner, M.F., Smith, W W, Castelhana, A L (1995) Matrilysin-inhibitor complexes: common themes among metalloproteases. *Biochemistry* 34, 6602-6610.
67. Gooley, P.R., O'Connell, J F, et al. (1994) The NMR structure of the inhibited catalytic domain of human stromelysin-1. *Structural Biology* 1, 111-118.
68. Borkakoti, N., Winkler, F K, Williams, D H, D'Arcy, A, Broadhurst, M J, Brown, P A, Johnson, W H, Murray, E J (1994) Structure of the catalytic domain of human fibroblast collagenase complexed with an inhibitor. *Structural Biology* 1, 106-110.
69. Lovejoy, B., Cleasby, A, et al. (1994) Structure of the catalytic domain of fibroblast collagenase complexed with an inhibitor. *Science* 263, 375-377.

70. Spurlino, J.C., Smallwood, A M, et al. (1994) 1.56 Å Structure of the mature truncated human fibroblast collagenase. *Proteins: Structure, function, and genetics* **19**, 98-109.
71. Matthews, B. (1988) Structural basis of the action of thermolysin and related zinc peptidases. *Acct. Chem. Res.* **21**, 333-340.
72. Stams, T., Spurlino, J C, Smith, D L, Wahl, R C, Ito, T F, Qoronfleh, M W, Banks, T M, Rubin, B (1994) Structure of human neutrophil collagenase reveals large S1' specificity pocket. *Structural Biology* **1**, 119-123.
73. Bode, W., Reinemer, P, Huber, R, Kleine, T, Schnierer, S, Tschesche, H (1994) The X-ray crystal structure of the catalytic domain of human neutrophil collagenase inhibited by a substrate analogue reveals the essential for catalysis and specificity. *EMBO Journal* **13**, 1263-1269.
74. Bu, C.H., Pourmotabbed, T (1996) Mechanism of Ca²⁺ - dependent activity of human neutrophil gelatinase B. *Journal of Biological Chemistry* **271**, 14308-14315.
75. Lowry, C.L., McGeehan, G, LeVine III, H (1992) Metal ion stabilization of the conformation of a recombinant 19-kDa catalytic fragment of human fibroblast collagenase. *Proteins: Structure, function, and genetics* **12**, 42-48.
76. Sanchez-Lopez, R., Alexander, C.M., Behrendtsen, O., Breathnach, R., Werb, Z. (1993) Role of zinc-binding- and hemopexin domain-encoded sequences in the. *Journal of Biological Chemistry* **268**, 7238-47.
77. Reinemer, P., Grams, Huber, R, Kleine, T, Schnierer, S, Piper, M, Tschesche, H, Bode, W (1994) Structural implications for the role of the N-terminus in the 'superactivation' of collagenases. A crystallographic study. *FEBS Letters* **338**, 227-233.
78. Murphy, G., Allan, J.A., Willenbrock, F., Cockett, M.I., O. Connell, J.P., Docherty, A.J. (1992) The role of the C-terminal domain in collagenase and stromelysin specificity. *Journal of Biological Chemistry* **267**, 9612-8.
79. Allan, J.A., Hembry, R.M., Angal, S., Reynolds, J.J., Murphy, G. (1991) Binding of latent and high Mr active forms of stromelysin to collagen is mediated by the C-terminal domain. *Journal of Cell Science* **99**, 789-95.
80. Murphy, G., Willenbrock, F., Ward, R.V., Cockett, M.I., Eaton, D., Docherty,

- A.J. (1992) The C-terminal domain of 72 kDa gelatinase A is not required for catalysis, but is essential for membrane activation and modulates interactions with tissue inhibitors of metalloproteinases [published erratum appears in *Biochem J* 1992 Jun 15;284(Pt 3):935]. *Biochemical Journal* **283**, 637-41.
81. Fridman, R., Fuerst, T.R., Bird, R.E., Hoyhtya, M., Oelkuct, M., Kraus, S., Komarek, D., Liotta, L.A., Berman, M.L., Stetler-Stevenson, W.G. (1992) Domain structure of human 72-kDa gelatinase/type IV collagenase. Characterization of proteolytic activity and identification of the tissue inhibitor of metalloproteinase-2 (TIMP-2) binding regions. *Journal of Biological Chemistry* **267**, 15398-405.
 82. Kleiner, D.E.J., Unsworth, E.J., Krutzsch, H.C., Stetler-Stevenson, W.G. (1992) Higher-order complex formation between the 72-kilodalton type IV collagenase and tissue inhibitor of metalloproteinases-2. *Biochemistry* **31**, 1665-72.
 83. Nguyen, Q., Willenbrock, F., Cockett, M.I., O. Shea, M., Docherty, A.J., Murphy, G. (1994) Different domain interactions are involved in the binding of tissue inhibitors of metalloproteinases to stromelysin-1 and gelatinase A. *Biochemistry* **33**, 2089-95.
 84. Goldberg, G.I., Strongin, A., Collier, I.E., Genrich, L.T., Marmer, B.L. (1992) Interaction of 92-kDa type IV collagenase with the tissue inhibitor of metalloproteinases prevents dimerization, complex formation with interstitial collagenase, and activation of the proenzyme with stromelysin. *Journal of Biological Chemistry* **267**, 4583-91.
 85. Strongin, A.Y., Marmer, B.L., Grant, G.A., Goldberg, G.I. (1993) Plasma membrane-dependent activation of the 72-kDa type IV collagenase is prevented by complex formation with TIMP-2. *Journal of Biological Chemistry* **268**, 14033-9.
 86. O'Connell, J.P., Willenbrock, F., Docherty, A.J., Eaton, D., Murphy, G. (1994) Analysis of the role of the COOH-terminal domain in the activation, proteolytic activity, and tissue inhibitor of metalloproteinase interactions of gelatinase B. *Journal of Biological Chemistry* **269**, 14967-73.
 87. Brooks, P.C., Stromblad, S., Sanders, L.C., von Schalscha, T.L., Aimes, R.T., Stetler-Stevenson, W.G., Quigley, J.P., Cheresch, D.A. (1996) Localization of matrix metalloproteinase MMP-2 to the surface of invasive cells by interaction with integrin $\alpha v \beta 3$. *Cell* **85**, 683-693.
 88. Strongin, A.Y., Collier, I.E., Krasnov, P.A., Genrich, L.T., Marmer, B.L., Goldberg, G.I. (1993) Human 92 kDa type IV collagenase: functional analysis of

fibronectin and carboxyl-end domains. *Kidney International* **43**, 158-62.

89. Collier, I.E., Krasnov, P.A., Strongin, A.Y., Birkedal-Hansen, H., Goldberg, G.I. (1992) Alanine scanning mutagenesis and functional analysis of the fibronectin-like collagen-binding domain from human 92-kDa type IV collagenase. *Journal of Biological Chemistry* **267**, 6776-81.
90. Murphy, G., Nguyen, Q., Cockett, M.I., Atkinson, S.J., Allan, J.A., Knight, C.G., Willenbrock, F., Docherty, A.J. (1994) Assessment of the role of the fibronectin-like domain of gelatinase A by analysis of a deletion mutant. *Journal of Biological Chemistry* **269**, 6632-6.
91. Steffensen, B., Wallon, U M, Overall, C M (1995) ECM binding properties of recombinant fibronectin type II-like modules of human 72-kDa gelatinase / type IV collagenase. High affinity binding to native type I collagen but not native type IV collagen. *Journal of Biological Chemistry* **270**, 11555-11566.
92. Shipley, J.M., Doyle, G A, Fliszer, C J, Ye, Q-Z, Johnson, L L, Shapiro, S D, Welgus, H G, Senior, R M (1996) The structural basis for the elastolytic activity of the 92-kDa and 72-kDa gelatinases: role of the fibronectin type II-like repeats. *Journal of Biological Chemistry* **271**, 4335-4341.
93. Netzel-Arnett, S., Sang, Q.X., Moore, W.G., Navre, M., Birkedal-Hansen, H., Van Wart, H.E. (1993) Comparative sequence specificities of human 72- and 92-kDa gelatinases (type IV collagenases) and Pump (matrilysin). *Biochemistry* **32**, 6427-32.
94. Mauviel, A. (1993) Cytokine regulation of metalloproteinase gene expression. *Journal of Cellular Biochemistry* **53**, 288-295.
95. Gaire, M., Magbanua, Z., McDonnell, S., McNei, I.L., Lovett, D.H., Matrisian, L.M. (1994) Structure and expression of the human gene for the matrix. *Journal of Biological Chemistry* **269**, 2032-40.
96. Angel, P., Baumann, I, Stein, B, Delius, H, Rahmsdorf, H J, Herrlich, P (1987) TPA induction of the human collagenase gene is mediated by an inducible enhancer element located in the 5'-flanking region. *Molecular and Cellular Biology* **7**, 2256-2266.
97. Gutman, A., Wasyluk, B (1990) The collagenase gene promoter contains a TPA and oncogene-responsive unit encompassing the PEA3 and AP-1 binding sites. *EMBO Journal* **9**, 2241-2246.

98. Mauviel, A., Kahari, V-M, Kurkainen, M, Evans, C H, Uitto, J (1992) Leukoregulin, a T-cell derived cytokine, upregulates stromelysin-1 gene expression in human dermal fibroblasts: evidence for the role of AP-1 in transcriptional activation. *Journal of Cellular Biochemistry* **50**, 53-61.
99. Matrisian, L.M., Ganser, G.L., Kerr, L.D., Pelton, R.W., Wood, L.D. (1992) Negative regulation of gene expression by TGF-beta. [Review]. *Molecular Reproduction & Development* **32**, 111-20.
100. Frisch, S., Morisaki, J H (1990) Positive and negative transcriptional elements of the human type IV collagenase gene. *Molecular and Cellular Biology* **10**, 6524-6532.
101. Unemori, E.N., Hibbs, M S, Amento, E P (1991) Constitutive expression of a 92-kDa gelatinase (type IV) collagenase by rheumatoid synovial fibroblasts and its induction in normal human fibroblasts by inflammatory cytokines. *Journal of Clinical Investigations* **88**, 1656-1662.
102. Nagase, H., Enghild, J.J., Suzuki, K., Salvesen, G. (1990) Stepwise activation mechanisms of the precursor of matrix metalloproteinase 3 (stromelysin) by proteinases and (4-aminophenyl)mercuric acetate. *Biochemistry* **29**, 5783-5789.
103. Van Wart, H.E., Birkedal-Hansen, H. (1990) The cysteine switch: A principle of regulation of metalloproteinase activity with potential applicability to the entire matrix metalloproteinase gene family. *Proceedings National Academy Sciences* **87**, 5578-5582.
104. Holz, R.C., Salowe, S P, Smith, C K, Cuca, G C, Que, L (1992) EXAFS evidence for a "cysteine switch" in the activation of prostromelysin. *J. Am. Chem. Soc.* **114**, 9611-9614.
105. Springman, E.B., Angleton, E.L., Birkedal-Hansen, H., Van Wart, H.E. (1990) Multiple modes of activation of latent human fibroblast collagens: Evidence for the role of a Cys³⁷ active-site zinc complex in latency and a "cysteine switch" mechanism for activation. *Proceedings National Academy Sciences* **87**, 364-368.
106. Woessner, J.F.J. (1991) Matrix metalloproteinases and their inhibitors in connective tissue remodeling. *FASEB Journal* **5**, 2145-2154.
107. Grant, G.A., Eisen, A Z, Marmer, B L, Roswit, W T, Goldberg, G I (1987) The activation of human skin fibroblast procollagenase. *Journal of Biological Chemistry* **262**, 5886-5889.

108. Crabbe, T., Ioannou, C, Docherty, A J (1993) Human progelatinase A can be activated by autolysis at a rate that is concentration-dependent and enhanced by heparin bound to the C-terminal domain. *European Journal of Biochemistry* **218**.
109. Bergmann, U., Tuuttila, A., Stetler-Stevenson, W.G., Tryggvason, K. (1995) Autolytic activation of recombinant human 72 kilodalton type IV collagenase. *Biochemistry* **34**, 2819-25.
110. Park, A.J., Matrisian, L.M., Kells, A.F., Pearson, R., Yuan, Z.Y., Navre, M. (1991) - Mutational analysis of the transin (rat stromelysin) autoinhibitor. *Journal of Biological Chemistry* **266**, 1584-90.
111. Windsor, L.J., Birkedal-Hansen, H., Birkedal-Hansen, B., Engler, J.A. (1991) An internal cysteine plays a role in the maintenance of the latency of human fibroblast collagenase. *Biochemistry* **30**, 641-7.
112. Bu, C.H., Pourmotabbed, T (1995) Mechanism of activation of human neutrophil gelatinase B. Discriminating between the role of Ca²⁺ in activation and catalysis. *Journal of Biological Chemistry* **270**, 18563-18569.
113. Fridman, R., Toth, M, Pena, D, Mobashery, S (1995) Activation of progelatinase B (MMP-9) by gelatinase A (MMP-2). *Cancer Research* **55**, 2548-2555.
114. Itoh, Y., Binner, S, Nagase, H (1995) Steps involved in activation of the complex of pro-MMP2 (progelatinase A) and tissue inhibitor of metalloproteinases (TIMP) - 2 by 4-aminophenylmercuric acetate. *Biochemical Journal* **308**, 645-651.
115. Atkinson, S.J., Crabbe, T, Cowell, S, Ward, R V, Butler, M J, Sato, H, Seiki, M, Reynolds, J J, Murphy, G (1995) Intermolecular autolytic cleavage can contribute to the activation of progelatinase A by cell membranes. *Journal of Biological Chemistry* **270**, 30479-30485.
116. DeClerck, Y.A., Yean, T.D., Lu, H.S., Ting, J., Langley, K.E. (1991) Inhibition of autoproteolytic activation of interstitial procollagenase by recombinant metalloproteinase inhibitor MI/TIMP-2. *Journal of Biological Chemistry* **266**, 3893-9.
117. Murphy, G.J., Murphy, G., Reynolds, J.J. (1991) The origin of matrix metalloproteinases and their familial relationships. *FEBS Letters* **289**, 4-7.
118. Cawston, T.E. (1986) Protein inhibitors of metalloproteinases. In *Proteinase Inhibitors* (A. J. Barrett, Salvesen, G, ed) Elsevier, Amsterdam 589-610.

119. Willenbrock, F., Murphy, G. (1994) Structure-function relationships in the tissue inhibitors of metalloproteinases [published erratum appears in *Am J Respir Crit Care Med* 1995 Mar;151(3 Pt 1):926]. [Review]. *American Journal of Respiratory & Critical Care Medicine* **150**, S165-70.
120. Docherty, A.J., Lyons, A, Smith, B J, Wright, E M, Stephens, P E, Harris, T J, Murphy, G, Reynolds, J J (1985) Sequence of human tissue inhibitor of metalloproteinase and its identity to erythroid-potentiating activity. *Nature* **318**, 66-69.
121. Carmichael, D.F., Sommer, A, Thompson, R C, Anderson, D C, Smith, C G, Welgus, H G, Stricklin, G P (1986) Primary structure and cDNA cloning of human fibroblast collagenase inhibitor. *Proceedings of the National Academy of Science* **83**, 2407-2411.
122. Stetler-Stevenson, W.G., Kruttsch, H C, Liotta, L A (1989) Tissue inhibitor of metalloproteinase (TIMP-2). A new member of the metalloproteinase inhibitor family. *Journal of Biological Chemistry* **264**, 17374-17378.
123. Boone, T.C., Johnson, M.J., De Clerck, Y.A., Langley, K.E. (1990) cDNA cloning and expression of a metalloproteinase inhibitor related to tissue inhibitor of metalloproteinases. *Proceedings National Academy Sciences* **87**, 2800-4.
124. Apte, S.S., Mattei, M.G., Olsen, B.R. (1994) Cloning of the cDNA encoding human tissue inhibitor of metalloproteinases-3 (TIMP-3) and mapping of the TIMP3 gene to chromosome 22. *Genomics* **19**, 86-90.
125. Uria, J.A., Ferrando, A A, Velasco, G, Freije, J M, Lopez-Otin, C (1994) Structure and expression in breast tumors of human TIMP-3, a new member of the metalloproteinase inhibitor family. *Cancer Research* **54**, 2091-2094.
126. Silbiger, S.M., Jacobsen, V.L., Cupples, R.L., Koski, R.A. (1994) Cloning of cDNAs encoding human TIMP-3, a novel member of the tissue inhibitor of metalloproteinase family. *Gene* **141**, 293-7.
127. Greene, J., Wang, M, Liu, Y E, Raymond, L A, Rosen, C, Shi, Y E (1996) Molecular cloning and characterization of human tissue inhibitor of metalloproteinases 4. *Journal of Biological Chemistry* **271**, 30375-30380.
128. Docherty, A.J., Murphy, G (1990) The tissue metalloproteinase family and the inhibitor TIMP: a study using cDNAs and recombinant proteins. *Ann. Rheum. Dis.* **49**, 469-479.

129. Moutsiakis, D., Mancuso, P., Krutzsch, H., Stetler-Stevenson, W., Zucker, S. (1992) Characterization of metalloproteinases and tissue inhibitors of metalloproteinases in human plasma. *Connective Tissue Research* **28**, 213-30.
130. Ando, H., Twining, S.S., Yue, B.Y., Zhou, X., Fini, M.E., Kaiya, T., Higginbotham, E.J., Sugar, J. (1993) MMPs and proteinase inhibitors in the human aqueous humor. *Investigative Ophthalmology & Visual Science* **34**, 3541-8.
131. Welgus, H.G., Campbell, E J, Bar-Shavit, Z, Senior, R M, Teitelbaum, S L (1985) Human alveolar macrophages produce a fibroblast-like collagenase and collagenase inhibitor. *Journal of Clinical Investigation* **76**, 219-224.
132. Welgus, H.G., Bauer, E A, Stricklin, G P (1986) Elevated levels of human collagenase inhibitors in blister fluid of diverse etiology. *Journal of Investigative Dermatology* **87**, 592-596.
133. Hurskainen, T., Hoyhtya, M, Tuuttila, A, Oikarinen, A, Autio-Harmainen, H (1996) mRNA expression of TIMP-1, -2 and -3 and 92-kD type IV collagenase in early human placenta and decidual membrane as studied by in situ hybridization. *Journal of Histochemistry and Cytochemistry* **44**, 1379-1388.
134. Wilde, C.G., Hawkins, P R, Coleman, R T, LeVine, W B, Delegeane, A M, Okamoto, P M, Ito, L,, Y, Scott, R W, Seilhamer, J J (1994) Cloning and characterization of human tissue inhibitor of metalloproteinases-3. *DNA and Cell Biology* **13**, 711-718.
135. Byrne, J.A., Tomasetto, C, Royer, N, Bellocq, J P, Rio, M C, Basset, P (1995) The tissue inhibitor of metalloproteinases-3 gene in breast carcinoma: identification of multiple polyadenylation sites and a stromal pattern of expression. *Molecular Medicine* **1**, 418-427.
136. Denhardt, D.T., Feng, B., Edwards, D.R., Cocuzzi, E.T., Malyankar, U.M. (1993) Tissue inhibitor of metalloproteinases (TIMP, aka EPA): structure, control of expression and biological functions. [Review]. *Pharmacology & Therapeutics* **59**, 329-341.
137. Spurr, N.K., Goodfellow, P N, Docherty, A J (1987) Chromosomal assignment of the gene encoding the human tissue inhibitor of metalloproteinases to Xp11.1 - p11.4. *Ann. Hum. Genet.* **51**, 189-194.
138. Stetler-Stevenson, W.G., Brown, P D, Onisto, M, Levy, A T, Liotta, L A (1990) Tissue inhibitor of metalloproteinases-2 (TIMP-2) mRNA expression in tumor cell lines and human tumor tissues. *Journal of Biological Chemistry* **265**, 13933-

13938.

139. DeClerck, Y.A., Darville, M I, Eeckhout, Y, Rousseau, G G (1994) Characterization of the promoter of the gene encoding human tissue inhibitor of metalloproteinases-2 (TIMP-2). *Gene* **139**, 185-191.
140. Hammani, K., Blakis, A, Morsette, D, Bowcock, A M, Schmutte, C, Henriet, P, DeClerck, Y A (1996) Structure and characterization of the tissue inhibitor of metalloproteinases-2 gene. *Journal of Biological Chemistry* **271**, 25498-25505.
141. DeClerck, Y.A., Perez, N., Shimada, H., Boone, T.C., Langley, K.E., Taylor, S.M. (1992) Inhibition of invasion and metastasis in cells transfected with an inhibitor of metalloproteinases. *Cancer Research* **52**, 701-708.
142. Shapiro, S.D., Kobayashi, D.K., Welgus, H.G. (1992) - Identification of TIMP-2 in human alveolar macrophages. Regulation. *Journal of Biological Chemistry* **267**, 13890-13894.
143. Leco, K.J., Khokha, R., Pavloff, N., Hawkes, S.P., Edwards, D.R. (1994) Tissue inhibitor of metalloproteinases-3 (TIMP-3) is an extracellular matrix-associated protein with a distinctive pattern of expression in mouse cells and tissues. *Journal of Biological Chemistry* **269**, 9352-9360.
144. Apte, S.S., Olsen, B.R., Murphy, G. (1995) The gene structure of tissue inhibitor of metalloproteinases (TIMP)-3 and its inhibitory activities define the distinct TIMP gene family. *Journal Biological Chemistry* **270**, 14313-8.
145. Yang, T.T., Hawkes, S.P. (1992) Role of the 21-kDa protein TIMP-3 in oncogenic transformation of cultured chicken embryo fibroblasts. *Proceedings of the National Academy of Sciences of the United States of America* **89**, 10676-10680.
146. Williamson, R.A., Marston, F A, Angal, S, Koklitis, P, Panico, M, Morris, H R, Carne, A F, Smith, B J, Harris, T J, Freedman, R B (1990) Disulphide bond assignment in human tissue inhibitor of metalloproteinases (TIMP). *Biochemical Journal* **268**, 267-274.
147. Murphy, G., Houbrechts, A., Cockett, M.I., Williamson, R.A., O. Shea, M., Docherty, A.J. (1991) The N-terminal domain of tissue inhibitor of metalloproteinases retains metalloproteinase inhibitory activity. *Biochemistry* **30**, 8097-102.
148. Willenbrock, F., Crabbe, T., Slocombe, P.M., Sutton, C.W., Docherty, A.J.,

- Cockett, M.I., O. Shea, M., Brocklehurst, K., Phillips, I.R., Murphy, G. (1993) The activity of the tissue inhibitors of metalloproteinases is regulated by C-terminal domain interactions: a kinetic analysis of the inhibition of gelatinase A. *Biochemistry* **32**, 4330-7.
149. DeClerck, Y.A., Yean, T.D., Lee, Y., Tomich, J.M., Langley, K.E. (1993) Characterization of the functional domain of tissue inhibitor of metalloproteinases-2 (TIMP-2). *Biochemical Journal* **289**, 65-9.
150. Williamson, R.A., Bartels, H., Murphy, G., Freedman, R.B. (1994) Folding and stability of the active N-terminal domain of tissue inhibitor of metalloproteinases-1 and -2. *Protein Engineering* **7**, 1035-40.
151. O'Shea, M., Willenbrock, F., Williamson, R.A., Cockett, M.I., Freedman, R.B., Reynolds, J.J., Docherty, A.J., Murphy, G. (1992) Site-directed mutations that alter the inhibitory activity of the tissue inhibitor of metalloproteinases-1: importance of the N-terminal region between cysteine 3 and cysteine 13. *Biochemistry* **31**, 10146-52.
152. Williamson, R.A., Martorell, G., Carr, M.D., Murphy, G., Docherty, A.J., Freedman, R.B., Feeney, J. (1994) Solution structure of the active domain of tissue inhibitor of metalloproteinases-2. A new member of the OB fold protein family. *Biochemistry* **33**, 11745-59.
153. Bodden, M.K., Harber, G.J., Birkedal-Hansen, B., Windsor, L.J., Caterina, N.C., Engler, J.A., Birkedal-Hansen, H. (1994) Functional domains of human TIMP-1 (tissue inhibitor of metalloproteinases). *Journal of Biological Chemistry* **269**, 18943-52.
154. Chesler, L., Golde, D W, Bersch, N, Johnson, M D (1995) Metalloproteinase inhibition and erythroid potentiation are independent activities of tissue inhibitor of metalloproteinases-1. *Blood* **86**, 4506-4515.
155. Uchijima, M., Sato, H, Fuji, M, Seiki, M (1994) Tax proteins of human T-cell leukemia virus type 1 and 2 induce expression of the gene encoding erythroid-potentiating activity (tissue inhibitor of metalloproteinases-1, TIMP-1). *Journal of Biological Chemistry* **269**, 14946-14950.
156. Murate, T., Yamashita, K, Ohashi, H, Kagami, Y, Tsushita, K, Kinoshita, T, Hotta, T, Saito, H, Yoshida, S, Mori, K, Hayakawa, T (1993) Erythroid potentiating activity of tissue inhibitor of metalloproteinase on the differentiation of erythropoietin-responsive mouse erythroleukemia cell line, ELM-I-1,-3, is closely related to its cell growth potentiating activity. *Experimental Hematology*

21, 169-176.

157. Hayakawa, T., Yamashita, K, Tanzawa, K, Uchijima, E, Iwata, K (1992) Growth promoting activity of tissue inhibitor of metalloproteinase-1 (TIMP-1) for a wide range of cells: a possible new growth factor in serum. *FEBS Letters* **298**, 29-32.
158. Nemeth, J.A., Rafe, A, Steiner, M, Goolsby, C L (1996) TIMP-2 growth-stimulatory activity: a concentration- and cell type-specific response in the presence of insulin. *Experimental Cell Research* **224**, 110-115.
159. Wick, M., Burger, C., Brusselbach, S., Lucibello, F.C., Muller, R. (1994) A novel member of human tissue inhibitor of metalloproteinases (TIMP) gene family is regulated during G1 progression, mitogenic stimulation, differentiation, and senescence. *Journal of Biological Chemistry* **269**, 18953-18960.
160. Kolkenbrock, H., Hecker-Kia, A, Orgel, D, Ruppitsch, W, Ulbrich, N (1994) Activity of ternary gelatinase A-TIMP2-matrix metalloproteinase complexes. *Biological Chemistry* **375**, 589-595.
161. Taylor, K.B., Windsor, L J, Caterina, N C, Bodden, M K, Engler, J A (1996) The mechanism of inhibition of collagenase by TIMP-1. *Journal of Biological Chemistry* **271**, 23938-23945.
162. Stetler-Stevenson, W.G., Aznavoorian, S., Liotta, L.A. (1993) Tumor cell interactions with the extracellular matrix during invasion and metastasis. [Review]. *Annual Review of Cell Biology* **9**, 541-73.
163. Liotta, L.A., Stetler-Stevenson, W.G. (1991) Tumor invasion and metastasis: an imbalance of positive and negative regulation. [Review]. *Cancer Research* **51**, 5054s-5059s.
164. Alvarez, O.A., Carmichael, D F, DeClerck, Y A (1990) Inhibition of collagenolytic activity and metastasis of tumor cells by a recombinant human tissue inhibitor of metalloproteinases. *Journal of the National Cancer Institute* **82**, 589-595.
165. Alexander, C.M., Werb, Z. (1992) Targeted disruption of the tissue inhibitor of metalloproteinases. *Journal of Cell Biology* **118**, 727-39.
166. Edwards, D.R., Beaudry, P P, Laing, T D, Kowal, V, Leco, K J, Leco, P A, Lim M S (1996) The roles of tissue inhibitors of metalloproteinases in tissue remodelling and cell growth. *International Journal of Obesity* **20**, Supplement 3, S9-S15.

167. Dean, D.D., Martel-Pelletier, J, Pelletier, J, Howell, D S, Woessner, J F (1989) Evidence for metalloproteinase and metalloproteinase inhibitor imbalance in human osetarthritic cartilage. *Journal of Clinical Investigation* **84**, 678-685.
168. Howard, E.W., Bullen, E C, Banda, M J (1991) Preferential inhibition of 72- and 92-kDa gelatinases by tissue inhibitor of metalloproteinases-2. *Journal of Biological Chemistry* **266**, 13070-13075.
169. Williamson, R.A., Smith, B.J., Angal, S., Murphy, G., Freedman, R.B. (1993) Structural analysis of tissue inhibitor of metalloproteinases-1 (TIMP-1) by tryptic peptide mapping. *Biochimica et Biophysica Acta* **1164**, 8-16.
170. Kozak, S.L., Kabat, D (1990) Ping-pong amplification of a retroviral vector achieves high-level gene expression: human growth hormone production. *Journal of Virology* **64**, 3500-3508.
171. Varmus, H. (1988) Retroviruses. *Science* **240**, 1427-1435.
172. Temin, H.M. (1989) Retrovirus vectors: promise and reality. *Science* **246**, 983.
173. Coffin, J.M. (1990) Retroviridae and their replication. In *Virology* (B. N. Fields, Knipe, D M, ed) Raven Press Ltd., New York 1437-1500.
174. Mann, R., Mulligan, R C, Baltimore, D (1983) Construction of a retrovirus packaging mutant and its use to produce helper-free defective retrovirus. *Cell* **33**, 153-159.
175. Miller, A.D., Buttimore, C (1986) Redesign of retrovirus packaging cell lines to avoid recombination leading to helper virus production. *Molecular and Cellular Biology* **6**, 2895-2902.
176. Bestwick, R.K., Kozak, S L, Kabat, D (1988) Overcoming interference to retroviral superinfection results in amplified expression and transmission of cloned genes. *Proceedings of the National Academy of Science* **85**, 5404-5408.
177. Stack, M.S., Gray, R D (1989) Comparison of vertebrate collagenase and gelatinase using a new fluorogenic substrate peptide. *Journal of Biological Chemistry* **264**, 4277-4281.
178. Salo, T., Lyons, J.G., Rahemtulla, F., Birkedal-Hansen, H., Larjava, H. (1991) Transforming growth factor-beta 1 up-regulates type IV collagenase expression in cultured human keratinocytes. *Journal of Biological Chemistry* **266**, 11436-41.

179. Lefebvre, V., Peeters-Joris, C., Vaes, G. (1991) Production of gelatin-degrading matrix metalloproteinases (type IV). *Biochimica et Biophysica Acta* 1094, 8-18.
180. Murphy, G., Ward, R, Hembry, R M, Reynolds, J J, Kuhn, K, Tyrggvason, K (1989) Characterization of gelatinase from pig polymorphonuclear leukocytes. *Biochemical Journal* 258, 463-472.
181. Tournier, J.M., Polette, M., Hinrasky, J., Beck, J., Werb, Z., Basbaum, C. (1994) Expression of gelatinase A, a mediator of extracellular matrix. *Journal of Biological Chemistry* 269, 25454-64.
182. Stearns, M.E., Wang, M (1993) Type IV collagenase (Mr 72,000) expression in human prostate: benign and malignant tissue. *Cancer Research* 53, 878-883.
183. Librach, C.L., Werb, Z., Fitzgerald, M.L., Chiu, K., Corwin, N.M., Esteves, R.A., Grobelny, D., Galardy, R., Damsky, C.H., Fisher, S.J. (1991) 92-kD type IV collagenase mediates invasion of human cytotrophoblasts. *Journal of Cell Biology* 113, 437-449.
184. Watanabe, H., Nakanishi, I, Yamashita, K, Hayakawa, T, Okada, Y (1993) Matrix metalloproteinase-9 (92 kDa gelatinase / type IV collagenase) from U937 monoblastoid cells: correlation with cellular invasion. *Journal of Cell Science* 104, 991-999.
185. Sambrook, J., Fritsch, E.F., Maniatis, T. (1989) *Molecular Cloning: A Laboratory Manual*. Cold Spring Harbor Laboratory Press, Cold Spring Harbor.
186. Ausubel, F.M., Brent, R., Kingston, R.E., Moore, D.D., Seidman, J.G., Smith, J.A., Struhl, K. (1995) *Current Protocols in Molecular Biology*. John Wiley & Sons, Inc., Boston.
187. Wang, L., Voysey, R, Yu, M (1994) Large scale plasmid DNA prep with minimal phenol. *Biotechniques* 17.
188. Zhou, C., Yujan, Y, Jong, A (1990) Mini-prep in Ten Minutes. *Biotechniques* 8, 172-173.
189. Ausubel, F., Brent, R, Kingston, R et al (1992) *Short Protocols in Molecular Biology*. Greene Publishing Associates and John Wiley and Sons, New York 16.4-16.31.
190. Laemmli, U.K. (1970) Cleavage of structural proteins during the assembly of the head of bacteriophage T4. *Nature* 227, 680-685.

191. Coligan, J.E., Dunn, B M, Ploegh, H L, Speicher, D W, Wingfield, P T (1995) Current Protocols in Protein Science. , Volume 1 John Wiley and Sons, Inc., USA 8.1-8.5.
192. Scopes, R.K. (1987) *Protein purification: principles and practice*. Springer-Verlag, New York.
193. Chen, C., Okayama, H (1987) High-efficiency transformation of mammalian cells by plasmid DNA . *Molecular and Cellular Biology* 7, 2745-2752.
194. Murray, E.J. (1991) Calcium phosphate mediated gene transfer into established cell lines. In *Methods in Molecular Biology, Vol. 7: Gene transfer and expression protocols*. (H. Okayama, Chen, C, ed) The Humana Press Inc., Clifton, NJ 15-21.
195. Chomczynski, P., Sacchi, N. (1987) Single-step method for RNA isolation by acid guanidinium thiocyanate-phenol-chloroform extraction. *Analytical Biochemistry* 162, 156-9.
196. Rodriguez, P.L., Carrasco, L (1995) Improved factor Xa cleavage of fusion proteins containing maltose binding protein. *Biotechniques* 18, 238-243.
197. Staskus, P.W., Masiarz, F.R., Pallanck, L.J., Hawkes, S.P. (1991) The 21-kDa protein is a transformation-sensitive metalloproteinase inhibitor of chicken fibroblasts. *Journal of Biological Chemistry* 266, 449-54.
198. Murphy, G., Willenbrock, F (1995) Inhibitors of matrix metalloendopeptidases. *Methods in Enzymology* 248, 496-510.
199. Seltzer, J.L., Adams, S A, Grant, G A, Eisen, A Z (1981) Purification and properties of a gelatin-specific neutral protease from human skin. *Journal of Biological Chemistry* 256, 4662-4668.
200. Sato, H., Kida, Y, Mai, M, Endo, Y, Sasaki, T, Tanaka, J, Seiki, M (1992) Expression of genes encoding type IV collagen-degrading metalloproteinases and tissue inhibitors of metalloproteinases in various human tumor cells. *Oncogene* 7, 77-83.
201. Heussen, C., Dowdle, E B (1980) Electrophoretic analysis of plasminogen activators in polyacrylamide gels containing sodium dodecyl sulfate and copolymerized substrates. *Analytical Biochemistry* 102, 196-202.
202. Herron, G.S., Banda, M J, Clark, E J, Gavrilovic, J, Werb, Z (1986) Secretion of metalloproteinases by stimulated capillary endothelial cells: expression of

- collagenase and stromelysin activities is regulated by endogenous inhibitors. *Journal of Biological Chemistry* **261**, 2814-2818.
203. Kleiner, D.E., Stetler-Stevenson, W.G. (1994) Quantitative zymography: detection of picogram quantities of gelatinases. *Analytical Biochemistry* **218**, 325-9.
204. Agumughan, R.G., et al. (1986) Structures of the asparagine-linked sugar chains of laminin. *Biochimica Biophysica Acta* **883**, 112-126.
205. Olsen, R. (1983) Purification and some properties of myeloperoxidase and eosinophil peroxidase from human blood. *Biochemical Journal* **209**, 781-787.
206. Murphy, G., Crabbe, T (1995) Gelatinases A and B. *Methods in Enzymology* **248**, 470-484.
207. Hayman, M.J., et al. (1973) Purification of virus glycoproteins by affinity chromatography using *lens culinaris* phytohaemagglutinin. *FEBS Letters* **29**, 185-188.
208. Tsujimoto, M., et al. (1989) Purification and characterization of recombinant human interleukin 5 expressed in CHO cells. *Journal of Biochemistry* **106**, 23-28.
209. Kleine, T., Bartsch, S., Blaser, J., Schnierer, S., Triebel, S., Valentin, M., Gote, T., Tschesche, H. (1993) Preparation of active recombinant TIMP-1 from Escherichia coli inclusion bodies and complex formation with the recombinant catalytic domain of PMNL-collagenase. *Biochemistry* **32**, 14125-31.
210. Ogata, Y., Itoh, Y, Nagase, H (1995) Steps involved in activation of pro-matrix metalloproteinase 9 (progelatinase B)-tissue inhibitor of metalloproteinases-1 complex by 4-aminophenylmercuric acetate and proteinases. *Journal of Biological Chemistry* **270**, 18506-18511.
211. Kishnani, N.S., Staskus, P W, Yang, T-T, Masiarz, F R, Hawkes, S P (1994) Identification and characterization of human tissue inhibitor of metalloproteinases-3 and detection of three additional metalloproteinase inhibitor activities in extracellular matrix. *Matrix Biology* **14**, 479-488.
212. Ray, J.M., Stetler-Stevenson, W.G. (1995) Gelatinase A activity directly modulates melanoma cell adhesion and spreading. *EMBO Journal* **14**, 908-17.
213. Netzel-Arnett, S., Mallya, S.K., Nagase, H., Birkedal-Hansen, H., Van Wart, H.E. (1991) Continuously recording fluorescent assays optimized for five human matrix metalloproteinases. *Analytical Biochemistry* **195**, 86-92.

214. McGeehan, G.M., Bickett, D M, Green, M, Kassel, D, Wiseman, J S, Berman, J (1994) Characterization of the peptide substrate specificities of interstitial collagenase and 92-kDa gelatinase. Implications for substrate optimization. *Journal of Biological Chemistry* **269**, 32814-32820.
215. Senior, R.M., Griffin, G L, Fliszar, C J, Shapiro, S D, Goldberg, G I, Welgus, H G (1991) Human 92- and 72-kilodalton type IV collagenases are elastases. *Journal of Biological Chemistry* **266**, 7870-7875.
216. Banyai, L., Patthy, L (1991) Evidence for the involvement of type II domains in collagen binding by 72 kDa type IV procollagenase. *FEBS Letters* **282**, 23-25.
217. Banyai, L., Tordai, H, Patthy, L (1994) The gelatin-binding site of human 72 kDa type IV collagenase (gelatinase A). *Biochemical Journal* **298**, 403-407.
218. Ye, Q.-Z., Johnson, L, Yu, A E, Hupe, D (1995) Reconstructed 19 kDa catalytic domain of gelatinase A is an active proteinase. *Biochemistry* **34**, 4702-4708.
219. Banyai, L.T., H, Patthy, L (1996) Structure and domain-domain interactions of the gelatin-binding site of human 72-kilodalton type IV collagenase (gelatinase A, matrix metalloproteinase 2). *Journal of Biological Chemistry* **271**, 12003-12008.
220. Knight, C.G., Willenbrock, F., Murphy, G. (1992) A novel coumarin-labelled peptide for sensitive continuous assays of the matrix metalloproteinases. *FEBS Letters* **296**, 263-6.
221. Himelstein, B.P., Canete-Soler, R, Bernhard, E J, Dilks, D W, Muschel, R J (1994) Metalloproteinases in tumor progression: the contribution of MMP-9. *Invasion and Metastasis* **14** (1-6), 246-258.
222. MacDougall, J.R., Matrisian, L M (1995) Contributions of tumor and stromal matrix metalloproteinases to tumor progression, invasion and metastasis. *Cancer and Metastasis Reviews* **14**, 351-362.
223. Vincenti, M.P., Clark, I.M., Brinckerhoff, C.E. (1994) Using inhibitors of metalloproteinases to treat arthritis: easier said than done? *Arthritis & Rheumatism* **37**, 1115-26.
224. Lelievre, Y., Boubouton, R, Boiziau, J, Faucher, D, Achard, D, Cartwright, T. (1990) Low molecular weight , sequence based collagenase inhibitors selectively block the interaction between collagenase and TIMP (tissue inhibitor of metalloproteinase). *Matrix* **10**, 292-299.

225. Greenwald, R.A., Moak, S A, Ramamurthy, N S, Golub, L M (1992) Tetracyclines suppress matrix metalloproteinase activity in adjuvant arthritis and in combination with flurbiprofen, ameliorate bone damage. *Journal of Rheumatology* 19, 927-938.
226. Greenwald, R.A., Golub, L M, Lavietes, B, et al. (1987) Minocycline inhibits rheumatoid synovial collagenase in vivo and in vitro. *Journal of Rheumatology* 14, 23-28.
227. Greenwald, R.A. (1990) Tetracyclines, derivatives as potential inhibitors of connective tissue degradation. *Drug News and Perspectives* 3, 161-166.
228. Fife, R.S., Sledge, G W (1995) Effects of doxycycline on in vitro growth, migration, and gelatinase activity of breast carcinoma cells. *Journal of Laboratory and Clinical Medicine* 125, 407-411.
229. Darlak, K., Miller, R B, Stack, M S, Spatola, A F, Gray, R D (1990) Thiol-based inhibitors of mammalian collagenase. *Journal of Biological Chemistry* 265, 5199-5201.
230. Schwartz, M.A., Venkataraman, S., Ghaffari, M.A., Libby, A., Mookhtiar, K.A., Mallya, S.K., Birkedal-Hansen, H., Van Wart, H.E. (1991) Inhibition of human collagenases by sulfur-based substrate analogs. *Biochemical & Biophysical Research Communications* .
231. Grobelny, D., Poncz, L., Galardy, R.E. (1992) Inhibition of human skin fibroblast collagenase, thermolysin, and pseudomonas aeruginosa elastase by peptide hydroxamic acids. *Biochemistry* 31, 7152-7154.
232. Davies, B., Brown, P D, East, N, Crimmin, M J, Balkwill, F R (1993) A synthetic MMP inhibitor decreases tumor burden and prolongs survival of mice bearing human ovarian carcinoma xenografts. *Cancer Research* 53, 2087-2091.
233. Gonnella, N.C., Bohacek, R, Zhang, X, Kolossvary, I, Paris, C G, Melton, R, Winter, C, Hu, S, Ganu, V (1995) Bioactive conformation of stromelysin inhibitors determined by transferred nuclear overhauser effects. *Proceedings of the National Academy of Science* 92, 462-466.
234. Gowravaram, M.R., Tomcznk, B E, Johnson, J S, Delecki, D, Cook, E R, Ghose, A K, Mathiowetz, A M, Spurlino, J C, Rubin, B, Smith, D L, Pulvino, T, Wahl, R C (1995) Inhibition of MMPs by hydroxamates containing heteroatom-based modifications of the P1' group. *Journal of Medicinal Chemistry* 38, 2570-2581.
235. Chapman, K.T., Kopka, I.E., Durette, P.L., Esser, C.K., Lanza, T.J., Izquierdo-

- Martin, M., Niedzwiecki, L., Chang, B., Harrison, R.K., Kuo, D.W., et al. (1993) Inhibition of matrix metalloproteinases by N-carboxyalkyl peptides. *Journal of Medicinal Chemistry* **36**, 4293-4301.
236. Izquierdo-Martin, M., Chapman, K.T., Hagmann, W.K., Stein, R.L. (1994) Studies on the kinetic and chemical mechanism of inhibition of stromelysin by an N-(carboxyalkyl)dipeptide. *Biochemistry* **33**, 1356-65.
237. Brown, F.K., Brown, P J, Bickett, D M, Chambers, C L, Davies, H G, Deaton, D N, Drewry, D, Foley, H, McElroy, A B, Gregson, M, McGeehan, G M, Myers, P L, Norton, D, Salovich, J M, Schoenen, F J, Ward, P (1994) Matrix metalloproteinase inhibitors containing a (carboxyalkyl)amino zinc ligand: modification of the P1 and P2' residues. *Journal of Medicinal Chemistry* **37**, 675-688.
238. Galardy, R.E., Grobelny, D., Kortylewicz, Z.P., Poncz, L. (1992) Inhibition of human skin fibroblast collagenase by phosphorus-containing peptides. *Matrix Supplement* **1**, 259-262.
239. Bird, J., De Mello, R C, Harper, G P, Hunter, D J, Karran, E H, Markwell, R E, Miles-Williams, A J, Rahman, S S, Ward, R W. (1994) Synthesis of novel n-phosphonoalkyl dipeptide inhibitors of human collagenase. *Journal of Medicinal Chemistry* **37**, 158-169.
240. Cuniasse, P., Raynal, I, Lecoq, A, Yiotakis, A, Dive, V (1995) Three-dimensional structure of cyclohexapeptides containing a phosphinic bond in aqueous solution: a template for zinc metalloprotease inhibitors. *Journal of Medicinal Chemistry* **38**, 553-536.
241. Beusen, D.D., McDowell, L M, Slomczynska, U, Schaefer, J (1995) Solid-state nuclear magnetic resonance analysis of the conformation of an inhibitor bound to thermolysin. *Journal of Medicinal Chemistry* **38**, 2742-2747.
242. Grams, F., Dive, V, Yiotakis, A, Yiallourous, I, Vassiliou, S, Zwilling R, Bode, Stocker, W (1996) Structure of astacin with a transition-state analog inhibitor. *Nature Structural Biology* **3**, 671-675.
243. Grams, F., Crimmin, M, Hinnes, L, Huxley, P, Pieper, M, Tschesche, H, Bode, W (1995) Structure determination and analysis of human neutrophil collagenase complexed with a hydroxamate inhibitor. *Biochemistry* **34**, 14012-14020.
244. Grams, F., Reinemer, P., Powers, J.C., Kleine, T., Pieper, M., Tschesche, H., Huber, R., Bode, W. (1995) X-ray structures of human neutrophil collagenase

- complexed with peptide hydroxamate and peptide thiol inhibitors. Implications for substrate binding and rational drug design. *European Journal of Biochemistry* **228**, 830-41.
245. Hanglow, A.C., Lugo, A., Walsky, R., Finch-Arietta, M., Lusch, L., Visnick, M., Fotouhi, N. (1993) Peptides based on the conserved prodomain sequence of matrix metalloproteinases inhibit human stromelysin and collagenase. *Agents & Actions* **39**, C148-50.
246. Fotouhi, N., Lugo, A., Visnick, M., Lusch, L., Walsky, R., Coffey, J.W., Hanglow, A.C. (1994) Potent peptide inhibitors of stromelysin based on the prodomain region of matrix metalloproteinases. *Journal of Biological Chemistry* **269**, 30227-31.
247. Stetler-Stevenson, W.G., Talano, J.A., Gallagher, M.E., Kruttsch, H.C., Liotta, L.A. (1991) Inhibition of human type IV collagenase by a highly conserved peptide sequence derived from its prosegment. [Review]. *American Journal of the Medical Sciences* **302**, 163-70.
248. Melchiori, A., Albin, A., Ray, J.M., Stetler-Stevenson, W.G. (1992) Inhibition of tumor cell invasion by a highly conserved peptide sequence from the MMP enzyme prosegment. *Cancer Research* **52**, 2353-2356.
249. O'Donohue, M.J., Beaumont, A. (1996) The roles of the prosequence of thermolysin in enzyme inhibition and folding in vitro. *Journal of Biological Chemistry* **271**, 26477-26481.
250. Bradley, J.M.B., Vranka, J.A., Colvis, C.M., Conger, D.M., Alexander, J.P., Fisk, A.S., Samples, J.R., Acott, T.S. (1997) Manipulation of outflow rates by matrix metalloproteinases in a glaucoma model. *Journal of Biological Chemistry In Review*.
251. Quigley, H.A. (1993) Open-angle glaucoma. *New England Journal of Medicine* **328**, 1097-1106.
252. Acott, T.S. (1994) Receptor biology and glaucoma - Integrins in the eye. In *Encounters in glaucoma research 1: Receptor biology and glaucoma* (D. R. Anderson and S. M. Drance, eds), Foglizza Editore, Milano 97-135.
253. Acott, T.S. (1992) Trabecular extracellular matrix regulation. In *Pharmacology of Glaucoma* (S. M. Drance, E. M. Van Buskirk and A. H. Neufeld, eds), Williams & Wilkins, Baltimore 125-157.

254. Acott, T.S., Kingsley, P.D., Samples, J.R., Van Buskirk, E.M. (1988) Human trabecular meshwork organ culture: Morphology and glycosaminoglycan synthesis. *Investigative Ophthalmology Visual Science* **29**, 90-100.
255. Erickson-Lamy, K. (1992) The perfused human ocular anterior segment as a model for aqueous outflow physiology. *Journal of Glaucoma* **1**, 44-53.
256. Tschumper, R.C., Johnson, D.H., Bradley, J.M.B., Acott, T.S. (1990) Glycosaminoglycans of human trabecular meshwork in perfusion organ culture. *Current Eye Research* **9**, 363-369.
257. Johnson, D.H., Tschumper, R.C. (1989) The effect of organ culture on human trabecular meshwork. *Experimental Eye Research* **49**, 113-127.
258. Twining, S.S. (1984) Fluorescein isothiocyanate-labeled casein assay for proteolytic enzymes. *Analytical Biochemistry* **143**, 30-34.
259. Harlow, E., Lane, D. (1988) *Antibodies: a laboratory manual*. Cold Spring Harbor Laboratory, New York.
260. Knight, W.B., Maycock, A.L., Green, B.G., Ashe, B.M., Gale, P., Weston, H., Finke, P.E., Hagmann, W.K., Shah, S.K., Doherty, J.B. (1992) Mechanism of inhibition of human leukocyte elastase by two cephalosporin derivatives. *Biochemistry* **31**, 4980-6.
261. Johnson, D.H., Bradley, J.M.B., Acott, T.S. (1990) The effect of dexamethasone on glycosaminoglycans of human trabecular meshwork in perfusion organ culture. *Investigative Ophthalmology & Visual Science* **31**, 2568-2571.
262. Knight, C.G. (1986) The characterization of enzyme inhibition. In *Proteinase Inhibitors* (A. J. Barrett, Salvesen, G, ed) Elsevier Science Publishers BV, Amsterdam 23-51.
263. Fersht, A. (1985) *Enzyme Structure and Mechanism*. W H Freeman and Company, New York.
264. Cornish-Bowden, A. (1995) *Fundamentals of Enzyme Kinetics*. Portland Press Ltd., London.
265. Engel, P.C. (1996) *Enzymology*. Academic Press Inc. and Bios Scientific Publishers Ltd., San Diego and Oxford.
266. Klein, R., Klein, B.E.K., Linton, K.L.P. (1992) Prevalence of age-related

- maculopathy: The Beaver Dam eye study. *Ophthalmology* 99, 933-943.
267. Bressler, N.M., Bressler, S.B., Fine, S.L. (1988) Age-related macular degeneration. *Survey Ophthalmology* 32, 375-413.
 268. Deutman, A.F. (1994) - Macular dystrophies. In *Medical Retina*, Volume 2 (A. P. Schachat and R. B. Murphy, eds), Mosby, St Louis 1186-1240.
 269. Capon, M.R.C., Marshall, J., Krafft, J.I., Alexander, R.A., Hiscott, O.S., Bird, A.C. (1989) Sorsby's fundus dystrophy: a light and electron microscopic study. *Ophthalmology* 96, 1769-77.
 270. Shovlin, C.L. (1996) Inherited diseases of the vasculature. *Annual Reviews in Physiology* 58, 483-507.
 271. Hogan, M.J., Alvarado, J.A., Weddell, J.E. (1971) *Histology of the human eye. An atlas and textbook*. W. B. Saunders Company, Philadelphia.
 272. Zinn, K.M., Marmor, M.F. (1979) The retinal pigment epithelium. Harvard University Press, Cambridge, MA.
 273. Acott, T.S. (1994) Biochemistry of aqueous humor outflow. In *Textbook of Ophthalmology*, Volume 7 (P. L. Kaufman and T. W. Mittag, eds), Mosby, London 1.47-1.78.
 274. Murphy, G., Willenbrock, F., Crabbe, T., O. Shea, M., Ward, R., Atkinson, S., O. Connell, J., Docherty, A. (1994) Regulation of matrix metalloproteinase activity. [Review]. *Annals of the New York Academy of Sciences* 732, 31-41.
 275. Pavloff, N., Staskus, P.W., Kishnani, N.S., Hawkes, S.P. (1992) A new inhibitor of metalloproteinases from chicken: ChIMP-3. A third member of the TIMP family. *Journal of Biological Chemistry* 267, 17321-6.
 276. Blenis, J., Hawkes, S.P. (1983) Transformation-sensitive protein associated with the cell substratum of chicken embryo fibroblasts. *Proceedings National Academy Sciences* 80, 770-774.
 277. Sun, Y., Hegamyer, G., Kim, H., Sithanandam, K., Li, H., Watts, R., Colburn, N.H. (1995) Molecular cloning of mouse tissue inhibitor of metalloproteinases-3 and its promoter. *Journal Biological Chemistry* 270, 19312-9.
 278. Weber, B.H., Vogt, G., Pruett, R.C., Stohr, H., Felbor, U. (1994) Mutations in the tissue inhibitor of metalloproteinases-3 (TIMP3) in patients with Sorsby's fundus

- dystrophy. *Nature Genetics* 8, 352-6.
279. Felbor, U., Stohr, H, Amann, T, Schonherr, U, Apfelstedt-Sylla, E, Weber, B (1996) A second independent Tyr 168 Cys mutation in the tissue inhibitor of metalloproteinases-3 (TIMP-3) in Sorsby's fundus dystrophy. *Journal of Medical Genetics* 33, 233-236.
280. Acott, T.S., Weleber, R.G. (1995) Vitamin A megatherapy for retinal abnormalities. *Nature Medicine* 1, 3-4.
281. Jacobson, S.G., Cideciyan, A.V., Regunath, G., Rodriguez, F.J., Vandenberg, K., Sheffield, V.C., Stone, E.M. (1995) Night blindness in Sorsby's fundus dystrophy reversed by vitamin A. *Nature Genetics* 11, 27-32.
282. Vranka, J.A., Johnson, E., Zhu, X., Shepardson, A., Alexander, J.P., Bradley, J.M.B., Wirtz, M.K., Weleber, R.G., Klein, M.L., Acott, T.S. (1997) Discrete expression and distribution pattern of TIMP-3 in the human retina and choroid. *Current Eye Research* 16, In Press.
283. Schor, A.M., Schor, S L (1986) The isolation and culture of endothelial cells and pericytes from the bovine retinal microvasculature: a comparative study with large vessel vascular cells. *Microvascular Research* 32, 21-38.
284. Weber, B.H.F., Vogt, G., Wolz, W., Ives, E.J., Ewing, C.C. (1994) Sorsby's fundus dystrophy is genetically linked to chromosome 22q13-qter. *Nature Genetics* 7, 158-61.
285. Ruiz, A., Peterson, B., Bok, D. (1996) Localization and quantification of TIMP-3 mRNA in the human retina. *Investive Ophthalmology & Visual Science* 37, S1143.
286. Takigawa, M., Nishida, Y., Suzuki, F., Kishi, J.-I., Yamashita, K., Hayakawa, T. (1990) Inhibition of angiogenesis in chick yolk-sac membrane by polyamines and its inhibition by tissue inhibitors of metalloproteinases (TIMP and TIMP-2). *Biochemistry Biophysics Research Communications* 171, 1264-1271.
287. Moses, M.A., Sudhalter, J., Langer, R. (1990) Identification of an inhibitor of neovascularization from cartilage. *Science* 248, 1408-1410.
288. Moses, M., Langer, R. (1991) A metalloproteinase inhibitor as an inhibitor of neovascularization. *Journal Cellular Biochemistry* 47, 230-235.
289. Leco, K.J., Hayden, L.J., Sharma, R.R., Rocheleau, H., Greenberg, A.H., Edwards, D.R. (1992) Differential regulation of TIMP-1 and TIMP-2 mRNA

expression in normal and Ha-ras-transformed murine fibroblasts. *Gene* 117, 209-17.